PhD Dissertation

Neuroprotective effects of Astaxanthin in preclinical models of Alzheimer's disease

submitted by

Joshua Adekunle Babalola

for the Academic Degree of

Doctor of Philosophy (PhD)

at the

Medical University of Graz, AUSTRIA

D&F Institut für Pathologie

under the supervision of

Univ.Prof. Dr.med.Univ Prof Gerald Hoefler

2023

DECLARATION

I hereby declare that this thesis is my own original work and that I have fully acknowledged by name all of those individuals and organizations that have contributed to the research for this thesis and agreed to publish the data in this thesis. Due acknowledgment has been made in the text to all other material used. Throughout this thesis and in all related publications I followed the “Standards of Good Scientific Practice and Ombuds Committee at the Medical University of Graz”.

The *in vitro* part of investigation presented in this thesis has been summarized and published in:

Babalola JA, Lang M, George M, Stracke A, Tam-Amersdorfer C, Itxaso I, Lucija D, Tadic J, Schilcher I, Loeffler T, Flunkert S, Prokesch M, Leitinger G, Lass A, Hutter-Paier B, Panzenboeck U, Hoefler G. Astaxanthin enhances autophagy, amyloid beta clearance and exerts anti-inflammatory effects in in vitro models of Alzheimer's disease-related blood brain barrier dysfunction and inflammation. Brain Res. 2023 Aug 12; 1819:148518. doi: 10.1016/j.brainres.2023.148518. Epub ahead of print. PMID: 37579986.

List of all co-authors in this publication:

- *D & F Institute of Pathology, Medical University of Graz, Austria*:
  Babalola Joshua Adekunle, Gerald Hoefler (Corresponding author)
- *Division of Immunology and Pathophysiology, Otto Loewi Research Center, Medical University of Graz, Austria*:
  Anika Stracke, Carmen Tam-Amersdorfer, Magdalena Lang and Ute Panzenboeck
- *Department of Obstetrics and Gynaecology, Medical University of Graz, Austria*: Meekha George

- *Division of Cell Biology, Histology and Embryology, Gottfried Schatz Research Center, Medical University of Graz, Austria:*
  Gerd Leitinger
- *Institute of Molecular Biosciences, University of Graz, Graz, Austria*:
  Jelena Tadic, Achim Lass
- *QPS Austria GmbH, Grambach, Austria:*
  Izaskun Itxaso, Domjan Lucija, Irene Schilcher, Tina Loeffler, Stefanie Flunkert, Manuela Prokesch, Birgit Hutter-Paier

Graz, September 2023 Joshua Adekunle Babalola, MSc.

ACKNOWLEDGEMENTS

Foremost, I would like to express my heart felt gratitude to my late supervisor, Professor **Ute Panzenboeck** for recruiting me and her trust in my capacity to succeed as a doctoral student in her group even when I initially turned down the offer. Thank you for the grace of second chance. Although we had few moments of mentor-mentee relationship, her support, supervision, encouragement those moments she was available really meant much to me. May her soul continue to rest in eternal bliss.

I am eternally grateful to Professor **Gerald Hoefler** who took over the supervision of my doctoral studies after Professor Ute's death. I am grateful for the privilege of access, prompt responses to my mails, the mentoring, encouragement and consistent support. At times I wonder how, he is able to do all these alongside the departmental and clinical coordination, student supervisions, DK-MCD oversight duties and demands from other professional caps he wear.

Beside my supervisor, I would like to express my profound gratitude to members of my thesis committee for their invaluable critiques, comments and suggestions that helped bring out the best from my research dissertation. To Professors **Achim Lass** (Institute of Molecular Biosciences, University of Graz) and **Gerd Leitinger** (Division of Cell Biology, Histology and Embryology, Gottfried Schatz Research Center, Medical University of Graz, Austria), I am grateful for the co-supervision right from when Professor Ute was indisposed, your encouragement, assurance and presence when it mattered most. I owe Dr **Birgit Hutter-Paier** (QPS Austria) a lot of gratitude for the invitation to QPS which availed me the opportunity of carrying out the i*n vivo* part of my thesis dissertation there. My utmost thanks to Dr **Jelena Tadic** (Institute of Molecular Biosciences, University of Graz) for the numerous data discussion sessions, immeasurable inputs and words of advice.

I am grateful to my student colleagues (**Meekha George and Magdalena Lang**) at the Institute of immunology and pathophysiology for their constant support. I am also grateful Drs **Martina Zandl-Lang**, **Elham Fanaee-Danesh** and **Chaitanya Chakravarthi Gali**, former students of Professor Ute for the advice, support and help with trouble shooting issues during pBCECs isolation, cultivation and stainings.

My sincere thanks to my colleagues; **Anika Stracke**, **Carmen Tam-Amersdorfer**, Nathalie Meier-Allard, **Christina Passegger**, **Friedwart Johannes**, **Karin Schramke**, **Waltraud Huber**, **Magdolna Mayer** and **Saleb Gertrude** at the Institute of immunology and pathophysiology. Thank you for the support and enabling environment.

I am sincerely grateful to **Anika Stracke** who helped secured accommodation and all my family needed to settle down as a stranger in Graz when I resumed for my studies November, 2019. Thank you, Ma'am, for the help and support in and out of the laboratory.

I am grateful to colleagues at QPS Austria; Drs **Sideromenos Spyridon**, **Irene Schilcher**, **Tina Loeffler**, **Tobias Pendl**, **David Amschl**, **Magdalena Daurer**, **Joerg Neddens**, **Stefanie Flunkert** and **Manuela Prokesch**, **Izaskun Itxaso**, **Domjan Lucija**, **Burcu Ergun**, **Livia Breznik**, **Roland Rabl**, **Marija Mihalj**, **Richard Scheytt** and other colleagues for their support, useful inputs and assistance during my stay at QPS.

I cannot but appreciate the Metabolic and Cardiovascular Disease (DK-MCD) PhD program, Medical University of Graz and FWF (*Fonds zur Förderung der wissenschaftlichen Forschung*) (Grant; W1226) for availing me the privilege to pursue my doctoral studies at Medical University of Graz.

I would like to express my utmost gratitude to **Karin Osibow** (*Project Manager*; DK-MCD) for her invaluable support right from March 2018, when I first sent her a mail of inquiry as a prospective applicant. I am grateful to her for the numerous helps relating to administrative, legal and paper works. I sincerely appreciate her for guidance and support throughout the course of my studies.

I am also grateful to my parents, siblings and friends for their support and motivation all through the journey.

Lastly but most importantly, I would like to express my heartfelt appreciation and love to my wife (**Oluwafisayo**) and my children (**Wisdom and Wealth**) for their perseverance, understanding and constant support during the course of my studies. Your consistent support kept me going during moments I felt like quitting.

ABBREVIATIONS

ABCA1: ATP binding cassette transporter subfamily A member 1

ABCG1: ATP binding cassette transporter subfamily G member 1

AChEI: Acetylcholinesterase inhibitors

AD: Alzheimer's disease

ADAM10: A disintegrin and metalloproteinase domain-containing protein 10

ADH: adult hippocampal neurogenesis

AGE: glycation end-products

AKT: protein kinase B (Akt)

AMPK: AMP-activated protein kinase

apoE: apolipoprotein E

APP: amyloid precursor protein

APP_{SL}: Swedish and London mutations of amyloid precursor protein

APPxhQC: amyloid precursor protein/ human glutaminyl cyclase

Arg 1: Arginase 1

ASX: Astaxanthin

ATG 5: autophagy-related protein 5

ATP: Adenosine Triphosphate

Aβ: amyloid-beta peptide

BACE1: β-site of APP cleaving enzyme, beta-secretase

BAF A1: Bafilomycin A1

BBB: blood-brain barrier

BCA: bicinchoninic acid assay

BCEC: brain capillary endothelial cells

BSA: bovine serum albumin

CAA: cerebral amyloid angiopathy

CAD: Coronary Artery Disease

CD: Control diet

CD31: cluster of differentiation 31

CMA: Chaperone mediated autophagy

CNS: Central Nervous System

CSF: cerebrospinal fluid

CTFs: C-terminal fragments

DEA: diethylamine

DEANB: diethylamine neutralizing buffer

Dexa: dexamethasone

DMEM: Dulbecco's Modified Eagle Medium

DMSO: Dimethyl sulfoxide

EBSS: Earle's Balanced Salt Solution

EDTA: ethylenediaminetetraacetic acid

EGTA: ethylene glycol-bis (2-aminoethylether)-N, N, N′, N ′-tetra acetic acid

EOAD: Early onset Alzheimer’s disease

ER: endoplasmic reticulum

FA: formic acid

FANB: formic acid neutralization buffer

FFAs: Free fatty acids

GAPDH: Glyceraldehyde 3-phosphate dehydrogenase

GFAP: glial fibrillary acidic protein

GSK3: glycogen synthase kinase 3

GW 6471: N-((2S)-2-(((1Z)-1-Methyl-3-oxo-3-(4-(trifluoromethyl) phenyl) prop-1-enyl) amino)-3-(4-(2-(5-methyl-2-phenyl-1,3-oxazol-4-yl) ethoxy) phenyl) propyl) propenamide

HCl: hydrochloric acid

HFD: high-fat diet

HFIP: hexafluoro-2-propanol

HPRT-1: hypoxanthine phosphoribosyl transferase 1

IB: immunoblotting

IBA1: ionized calcium-binding adaptor molecule 1

IDE: insulin-degrading enzyme

IF: immunofluorescent

IGF-1: insulin/insulin-like growth factor 1

IL-10: Interleukin10

IL-1β: Interleukin 1beta

IL-4: Interleukin 4

IL-6: Interleukin 6

ipGTT: Intraperitoneal glucose tolerance test

ipITT: Intraperitoneal insulin tolerance test

IR(s): insulin receptor(s);

IRS-1: insulin receptor substrate 1

IR-β: insulin receptor beta

ITGAM: Integrin Subunit Alpha M

KC-GRO, keratinocyte chemoattractant-growth regulated oncogene

LAMP2A: lysosomal-associated membrane protein 2A

LC3B: microtubule-associated proteins 1A/1B light chain 3B

LOAD: Late onset Alzheimer’s disease

LPS: Lipopolysaccharide

LRP1: low-density lipoprotein receptor-related protein 1

LXR: liver X receptor

MAP2: microtubule-associated protein 2

MAPK: mitogen-activated protein kinase

MCI: Mild Cognitive impairment

MEM: Modified Eagle Medium

mm: mus musculus

mTOR: mammalian target of rapamycin

mTORC1: mammalian target of rapamycin complex 1

mTORC2: mammalian target of rapamycin complex 2

MWM: Morris water maze

Na_2HPO_4: sodium phosphate dibasic

$NaHCO_3$: Sodium bicarbonate

NaN_3: Sodium azide

NC: nitrocellulose

NEP: Neprilysin

NF-κB p65: nuclear factor 'kappa-light-chain-enhancer' of activated B-cells RelA

NTF: neurofibrillary tangles

NTG: non transgenic

OHSC: Organotypic hippocampal slice culture

pBCEC: porcine brain capillary endothelial cells

PBS: Phosphate buffer saline

PDGFRβ: beta-type platelet-derived growth factor receptor

pE: N-terminal pyroglutamate

PECAM/CD31: platelet endothelial cell adhesion molecule

PFA: paraformaldehyde

pGlu: pyroglutamate

PHF: Paired helical filament

PI3-K: phosphoinositide 3-kinase

p-mTOR: phospho-mammalian target of rapamycin

PPAR: peroxisome proliferator-activated receptor

PPARα: peroxisome proliferator-activated receptor-alpha

PPARγ: peroxisome proliferator-activated receptor-gamma

p-S6rp: phospho-S6 ribosomal protein

PSEN1: Presenilin 1

PSEN2: Presenilin 2

PTM: Post translational Modification

QC: glutaminyl cyclase

RAGE: Receptor for advanced glycation end products

RT: room temperature

RXR: retinoid x receptor

S6rp: S6 ribosomal protein

sAPPα: soluble amyloid precursor protein-α

sAPPβ: soluble amyloid precursor protein-β

SF: serum-free

sLRP1: soluble low-density lipoprotein receptor-related protein1

SORL1: Sortilin related receptor 1

SQSTM1/p62: Sequestosome 1

SREBP-1: sterol regulatory element-binding protein-1

ss: sus scrofa

SVD: Small vessel disease

T2D: Type 2 Diabetes

TEER: trans-endothelial electrical resistance

THB: tissue homogenization buffer

TNF-α: tumor necrosis factor-alpha

TREM2: Triggering receptor expressed on myeloid cells 2

UPS, ubiquitin-proteasome system

ZO1: zonula occludens protein-1

β cells: beta cells

TABLE OF CONTENTS

LIST OF FIGURES

LIST OF TABLES

ABSTRACT

Background: Alzheimer's disease (AD) is a multi-factorial degenerative disease of the brain thought to be caused by misfolding of the amyloid beta (Aβ) and tau proteins. Aggregation and misfolding of Aβ and tau proteins are believed to arise from post-translational modification processes like phosphorylation, truncation, racemization, isomerization and pyroglutamylation. Defective degradation and clearance of misfolded Aβ as well as inflammation *per se* are crucial players in the pathology of AD. Blood-brain barrier (BBB) dysfunction causes Aβ accumulation in the brain and this occurs early in the pathophysiology of AD. More recently, a plethora of evidence emerged that links metabolic dysfunctions such as obesity, Type 2 Diabetes (T2D), and dyslipidemia with the pathophysiology of AD. We hypothesized that adding another risk factor, T2D, in addition to pyroglutamylation (hQC) of Aβ might induce a more severe AD pathology and that astaxanthin (ASX) supplementation might confer neuroprotective effects and help to ameliorate the pathophysiological manifestations associated with AD.

Questions addressed: To test our hypothesis *in vitro*, we investigated the Aβ clearance ability of ASX in the presence of exogenous Aβ using primary porcine brain capillary endothelial cells (pBCECs) and its anti-inflammatory potentials in LPS stimulated- organotypic hippocampal slice culture (OHSC). For further validation *in vivo*, we used male and female transgenic AD mice, APPxhQC, expressing human APP751 with the Swedish and the London mutation and human glutaminyl cyclase (hQC) enzyme and their non-transgenic (NTG) littermate. Mice in the control groups were fed 10% kJ fat, 7% sucrose. T2D model groups were fed High-fat Diet (HFD) containing 95% (60KJ% Fat) + 5 % Maltodextrin Placebo diet with 3 doses of 40mg/kg streptozocin injection while the intervention groups were given HFD containing 95% (60KJ% Fat) + 5% NOVASTA alongside 3 doses of 40mg/kg streptozocin injection for 13 weeks starting from 11-12 months of age. We investigated the effect of T2D mimicking diet on glycemic indices, Aβ metabolism, cognitive function and nutrient-sensing pathways (autophagy, insulin, MAPKinase and mTORC1 signalling). Genes involved in lipid biogenesis and markers of nutrient-sensing pathways were evaluated at protein and mRNA levels. Expressions of lipid and liver function parameters were assessed using ELISA-based assays. Deposition of soluble and insoluble Aβ isoforms in brains were determined using ELISA, MSD-

based assays and histological staining. Hippocampal-dependent cognitive impairment was assessed using the Morris Water Maze (MWM).

Results: ASX enhances clearance of misfolded proteins, promotes autophagy, and alters the Aβ processing pathway *in vitro*. T2D mimicking diet caused a progressive shift from soluble to insoluble Aβ pools in APPxhQC male mice. The increased deposition of soluble and insoluble pGlu-3 $A\beta_{42}$ was more pronounced in APPxhQC female mice. T2D mimicking diet impaired memory function in APPxhQC T2D model female and NTG male mice. The T2D phenotype was more pronounced in T2D model NTG female mice. ASX supplementation reduced Aβ deposition and might be a hQC inhibitor. ASX supplementation ameliorated T2D-induced memory dysfunction in male T2D model NTG mice possibly by enhancing NTG Aβ clearance and degradation via autophagy and improving nutrient signalling (autophagy, insulin and inflammatory signaling pathways) in both brain and liver.

Conclusion: We demonstrated ASX's potential in addressing AD-related blood-brain barrier challenges and inflammation *in vitro.* Furthermore, we showed that T2D poses an additional risk to AD pathophysiology and could lead to cognitive impairment induced by metabolic dysfunction. In addition, T2D influences Aβ metabolism and cognitive impairment with sex and genotype playing different roles. ASX might inhibit hQC but supplementation alone is not effective in presence of comorbidities and in late-stage AD.

KURZFASSUNG

Hintergrund: Die Alzheimer-Krankheit (AD) ist eine multifaktorielle degenerative Erkrankung des Gehirns, die vermutlich durch die Fehlfaltung der Amyloid-Beta- (Aβ) und Tau-Proteine verursacht wird. Es wird angenommen, dass die Aggregation und Fehlfaltung der Aβ und Tau-Proteine durch posttranslationale Modifikationsprozesse wie Phosphorylierung, Trunkierung, Racemisierung, Isomerisierung und Pyroglutamylierung entstehen. Defekte Degradation und Clearance von fehlgefaltetem Aβ sowie Entzündungen an sich sind entscheidende Faktoren in der Pathologie von Alzheimer. Eine Störung der Blut-Hirn-Schranke (BHS) ist ursächlich für die Anhäufung von Aβ im Gehirn und tritt schon früh in der Pathophysiologie von Alzheimer auf. In jüngster Zeit ist eine Fülle von Beweisen aufgetaucht, die Stoffwechselstörungen wie Adipositas, Typ-2-Diabetes (T2D) und Dyslipidämie mit der Pathophysiologie von Alzheimer in Verbindung bringen. Wir stellten die Hypothese auf, dass die Hinzufügung eines weiteren Risikofaktors (T2D) neben der Pyroglutamylierung (hQC) von Amyloid-Beta eine schwerwiegendere Alzheimer-Pathologie verursachen könnte und dass eine Astaxanthin (ASX)-Supplementierung neuroprotektive Wirkungen haben und dazu beitragen könnte, die mit Alzheimer verbundenen pathophysiologischen Manifestationen zu verbessern.

Angesprochene Fragen: Um unsere Hypothese *in vitro* zu testen, untersuchten wir die Aβ-Clearance-Fähigkeit von ASX in Gegenwart von exogenem Aβ unter Verwendung von primären Schweine-Hirnkapillarendothelzellen (pBCECs) und seine entzündungshemmenden Potenziale in LPS-stimulierten organotypischen Hippocampus-Scheibenkulturen (OHSC). Zur weiteren Validierung *in vivo* verwendeten wir männliche und weibliche transgene AD-Mäuse, APPxhQC, die menschliches APP751 mit der schwedischen und der Londoner Mutation und menschliches Glutaminylcyclase (hQC)-Enzym exprimieren, sowie ihre nicht-transgenen (NTG) Wurfgeschwister. Die Mäuse in den Kontrollgruppen wurden mit 10% kJ Fett und 7% Saccharose gefüttert. Die Diabetikergruppen erhielten eine fettreiche Diät (HFD) mit 95 % (60 KJ% Fett) + 5 % Maltodextrin-Placebo-Diät mit 3 Dosen 40 mg/kg Streptozocin-Injektion, während die Interventionsgruppen 13 Wochen lang HFD mit 95 % (60 KJ% Fett) + 5 % NOVASTA zusammen mit 3 Dosen 40 mg/kg Streptozocin-Injektion erhielten, beginnend im Alter von 11-12 Monaten. Wir untersuchten die Auswirkungen von T2D auf die glykämischen Indizes, den Aβ-

Stoffwechsel, die kognitive Funktion und die Nährstoffsensorik (Autophagie, Insulin, MAPKinase und mTORC1-Signalisierung). Gene, die an der Lipidbiogenese beteiligt sind und Marker der Nährstoffsensorwege, wurden auf Protein- und mRNA-Ebene analysiert. Die Ausprägung von Lipid- und Leberfunktionsparametern wurde mit ELISA-basierten Assays bewertet. Die Ablagerung von löslichen und unlöslichen Amyloid-beta-Isoformen im Gehirn wurde mit ELISA, MSD-basierten Assays und histologischen Färbungen bestimmt. Die vom Hippocampus abhängige kognitive Beeinträchtigung wurde anhand des Morris-Wasserlabyrinths (MWM) bewertet.

Ergebnisse: ASX erhöht die Clearance von fehlgefaltetem Protein, fördert die Autophagie und verändert den Aβ-Verarbeitungsweg in vitro. T2D führte zu einer progressiven Verschiebung von löslichen zu unlöslichen Aβ-Pools in männlichen APPxhQC-Mäusen. Die erhöhte Ablagerung von löslichem und unlöslichem pGlu-3 Aβ42 war bei weiblichen APPxhQC-Mäusen stärker ausgeprägt. T2D beeinträchtigte die Gedächtnisfunktion in APPxhQC diabetischen weiblichen und männlichen NTG-Mäusen. Der T2D-Phänotyp war bei diabetischen weiblichen NTG-Mäusen stärker ausgeprägt. ASX-Supplementierung reduzierte die Aβ-Ablagerung und könnte ein hQC-Inhibitor sein. ASX-Supplementierung verbesserte T2D-induzierte Gedächtnisstörungen in männlichen diabetischen NTG-Mäusen möglicherweise durch die Verbesserung der NTG-Aβ-Clearance und Abbau über Autophagie und Verbesserung der Nährstoff-Signalwege (Autophagie, Insulin und entzündliche Signalwege) in Gehirn und Leber.

Schlussfolgerung: Wir haben das Potenzial von ASX bei der Bewältigung der mit der Alzheimer-Krankheit verbundenen Probleme der Blut-Hirn-Schranke und der Entzündung *in vitro* nachgewiesen. Darüber hinaus zeigten wir, dass T2D ein zusätzliches Risiko für die AD-Pathophysiologie darstellt und zu kognitiven Beeinträchtigungen durch metabolische Dysfunktion führen könnte. Darüber hinaus beeinflusst T2D den Aβ-Stoffwechsel und die kognitiven Fähigkeiten, wobei Geschlecht und Genotyp eine unterschiedliche Rolle spielen. ASX könnte hQC hemmen, aber eine Supplementierung allein ist bei Vorhandensein von Komorbiditäten und bei AD im Spätstadium nicht wirksam.

1.0 INTRODUCTION

1.1 Alzheimer's disease (AD)

Alzheimer's disease (AD) is a multi-factorial degenerative disease of the brain that is strongly characterized by pathophysiological manifestations such as dysfunction of the neurovascular units-leaky blood brain barrier (BBB) (Zlokovic,2005; 2010; de la Torre, 2010; Marchesi, 2011), loss of memory function (Cummings, 2004), aggregation of Aβ (Querfurth and LaFerla, 2010) and tau-related lesions in neurons termed neurofibrillary tangles (Ballatore et al., 2007; Ittner and Gotz, 2011), synaptic degeneration (Terry et al.,1991; Selkoe, 2002), neuroinflammation (McGeer, 2001; 2002a; 2002b; McGeer and Rogers, 1992), and neuronal cell death (Niikura et al.,2006). The hallmarks of neurodegeneration include oxidative stress, neuro-immune alterations, proteasome impairment, mitochondrial dysfunction and accumulation of abnormal protein aggregates as well as metabolic alterations (Yang et al., 2013; Bloomingdale et al., 2022).

1.2 Brain changes accompanying AD

Changes to the brain often associated with AD include the accumulation of the abnormal and phosphorylated tau proteins, as well as the degeneration of neurons. In AD, the neurons that are first damaged are those in the brain parts responsible for memory, language and thinking. The brain changes that result in these damages are thought to begin about 20 years prior to the manifestation of noticeable symptoms (Villemagne et al., 2013; Reiman et al., 2012; Jack et al., 2009; Bateman et al., 2012; Gordon et al., 2018; Braak et al., 2011; Quiroz et al., 2020; Barthelemy et al., 2020).

AD is a progressive disease that worsens with time. The disease time course and progression differ between individuals. As time progresses, more neurons are damaged and additional brain parts are affected. Studies have shown that people age 65 and older have a disease course of 4-8 years after the first diagnosis, although some live as long as 20 years after their first diagnosis (Tom et al., 2015; Ganguli et al., 2005; Waring et al., 2005; Brookmeyer et al., 2002; Larson et al., 2004, Helzner et al., 2008; Xie et al., 2008; Brodaty et al., 2012; Todd et al., 2013). The aggregation of Aβ into plaques outside the neurons and tau into tangles inside neurons are two of the numerous changes associated with AD. The changes are

followed destruction of neurons that leads to neurodegeneration. Neurodegeneration (N) alongside Aβ (A) and tau (T) accumulation is referred to as the AT(N) framework for AD (Alzheimer's Dement, 2023). Aggregation of Aβ and tau have been suggested to damage neurons by interfering with neuron-to-neuron communication at synapses. Inside the neurons, tau tangles block the transportation of nutrients and other molecules essential for the normal function and survival of neurons (Alzheimer's Dement, 2019).

A healthy brain consists of billions of neurons, each with long branching extensions. These extensions are called synapses and allows for information flow by tiny bursts of chemicals that are released by one neuron and taken up by another neuron. The human brain contains trillions of synapses that allows signals to travel rapidly through the brain, creating the cellular basis of memories, thoughts, sensations, emotions, movements and skills (Alzheimer's Dement, 2023). Loss of synapses is another brain change associated with AD. Synaptic loss is an early event in AD, and it has been reported to precede neuronal death (Selkoe, 2002). In experimental models of AD, synaptic impairments were found to appear before the onset of memory deficit (Terry et al.,1991). Results from experimental animal models showed that the synapse is a target of both misfolded Aβ and tau (Spires-Jones and Hyman, 2014). Loss of neurons is the basic and fundamental feature in the pathophysiology of AD even preceding the manifestation of neuropathological hallmarks of the disease (Coleman and Flood, 1987; Hof et al., 1990; Gomez-Isla et al., 1996). Especially in the CA1 region of the hippocampus and entorhinal cortex, loss of neurons had been reported to correspond to the severity of memory deficits (Giannakopoulos et al., 2003; Simic et al., 1997; West et al., 1994).

1.3 Symptoms of AD

Some of the symptoms reported in people living with AD include; Memory loss that disrupts daily life, challenges in planning or solving problems, difficulty in completing familiar tasks, confusion with time or place. People suffering from AD do have trouble understanding visual images and spatial relationships. Also, they are prone to misplacing things. Likelihood of experiencing changes in judgment or decision-making and mood changes are other symptoms associated with AD. Difficulty walking, speaking and swallowing have also been reported to be common at the late

stage of the disease. Comprehensive symptoms associated with AD are listed in Table 1 (Alzheimer's Dement, 2023).

Table 1: Signs of Alzheimer's dementia compared with typical age-related changes

Signs of Alzheimer's dementia	Typical age-related changes
Memory loss that disrupts daily life: One of the most common signs of Alzheimer's dementia, especially in the early stage, is forgetting recently learned information. Others include asking the same questions over and over, and increasingly needing to rely on memory aids (for example, reminder notes or electronic devices) or family members for things that used to be handled on one's own.	Sometimes forgetting names or appointments, but remembering them later.
Challenges in planning or solving problems: Some people experience changes in their ability to develop and follow a plan or work with numbers. They may have trouble following a familiar recipe or keeping track of monthly bills. They may have difficulty concentrating and take much longer to do things than they did before.	Making occasional errors when managing finances or household bills.
Difficulty completing familiar tasks: People with Alzheimer's often find it hard to complete daily tasks. Sometimes, people have trouble driving to a familiar location, organizing a grocery list or remembering the rules of a favorite game.	Occasionally needing help to use microwave settings or record a television show.
Confusion with time or place: People living with Alzheimer's can lose track of dates, seasons and the passage of time. They may have trouble understanding something if it is not happening immediately. Sometimes they forget where they are or how they got there.	Getting confused about the day of the week but figuring it out later.
Trouble understanding visual images and spatial relationships: For some people, having vision problems is a sign of Alzheimer's. They may also have problems judging distance and determining color and contrast, causing issues with driving.	Vision changes related to cataracts.
New problems with words in speaking or writing: People living with Alzheimer's may have trouble following or joining a conversation. They may stop in the middle of a conversation and have no idea how to continue or they may repeat themselves. They may struggle with vocabulary, have trouble naming a familiar object or use the wrong name (e.g., calling a watch a "hand clock").	Sometimes having trouble finding the right word.
Misplacing things and losing the ability to retrace steps: People living with Alzheimer's may put things in unusual places. They may lose things and be unable to go back over their steps to find them. They may accuse others of stealing, especially as the disease progresses.	Misplacing things from time to time and retracing steps to find them.
Decreased or poor judgment: Individuals may experience changes in judgment or decision-making. For example, they may use poor judgment when dealing with money or pay less attention to grooming or keeping themselves clean.	Making a bad decision or mistake once in a while.
Withdrawal from work or social activities: People living with Alzheimer's disease may experience changes in the ability to hold or follow a conversation. As a result, they may withdraw from hobbies, social activities or other engagements. They may have trouble keeping up with a favorite sports team or activity.	Sometimes feeling uninterested in family and social obligations.
Changes in mood, personality and behavior: The mood and personalities of people living with Alzheimer's can change. They can become confused, suspicious, depressed, fearful or anxious. They may be easily upset at home, at work, with friends or when out of their comfort zones.	Developing very specific ways of doing things and becoming irritable when a routine is disrupted.

1.4 Predisposing Risk factors for AD

Even though, age is the greatest pre-disposing risk factor to AD (van der Flier and Scheltens, 2005), nonetheless, certain genetic and life style factors have been reported to increase the risk of developing AD. These risks are divided into genetic risk factors and modifiable life style factors. The genetic risk factors include variations in genes such as APOE, PSEN1, PSEN2, SORL1, APP, TREM and many other genes (Gao et al., 2019; Cacace et al., 2016; Calero et al., 2015; Alzgene 2010; Corbo and Scacchi 1999; Cho et al., 2020; Farrer et al., 1997; Karch and Goate 2015; Rogaeva et al., 2007; Campion et al., 2019; Cuccaro et al., 2016; Reitz et al.,

2011; Korvatska et al., 2015: Ma et al., 2016; Nguyen et al., 2020; Guerreiro et al., 2013; Jonsson et al., 2013; Allcock et al., 2003; Wang et al., 2015; Ulrich et al., 2014; Meilandt et al., 2020; Jay et al., 2015; Ulland et al., 2017) (Figure 1).

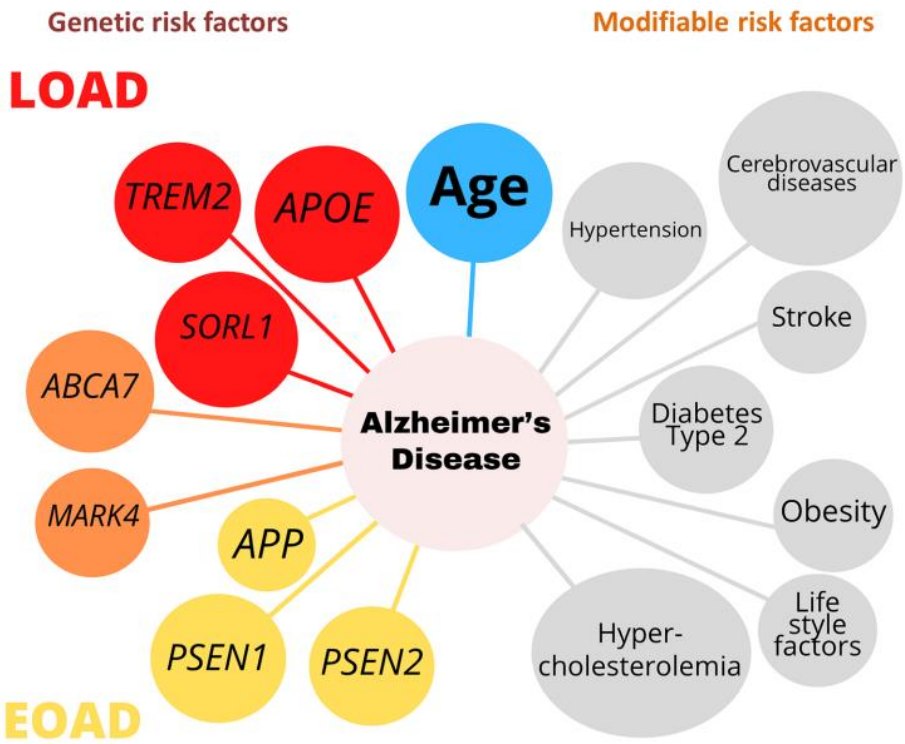

Figure 1: Genetic and lifestyle factors responsible for both early onset and late onset of AD (Adapted from Pradhan et al., 2022 with permission)

Livingston and colleagues in their 2020 landmark Lancet Report (Livingston et al., 2020) suggested that 40 percent of all cases of AD and other related dementias can be prevented or delayed if 12 lifestyle related risk factors are modified. These life style factors include; less education, hypertension, hearing impairment, smoking, obesity, depression, physical inactivity, diabetes, low numbers of social contacts, excessive alcohol consumption, traumatic brain injury, and air pollution (Figure 2). Several epidemiological and longitudinal studies have implicated T2D (Moran et al., 2019; Crane et al., 2013; Biessels et al., 2006; Luchsinger et al., 2007; Knopman and Roberts, 2010), obesity (Whitmer et al., 2008; Tsai et al., 2019), hypertension (Ladecola and Davisson, 2008; Kruyer et al., 2015; Kennelly and Collins, 2012; de

Heus et al., 2019), cerebrovascular diseases (Liu et al., 2015; Kling et al., 2013; Raz et al., 2016), stress, (Machado et al., 2014) and other risk factors for developing AD.

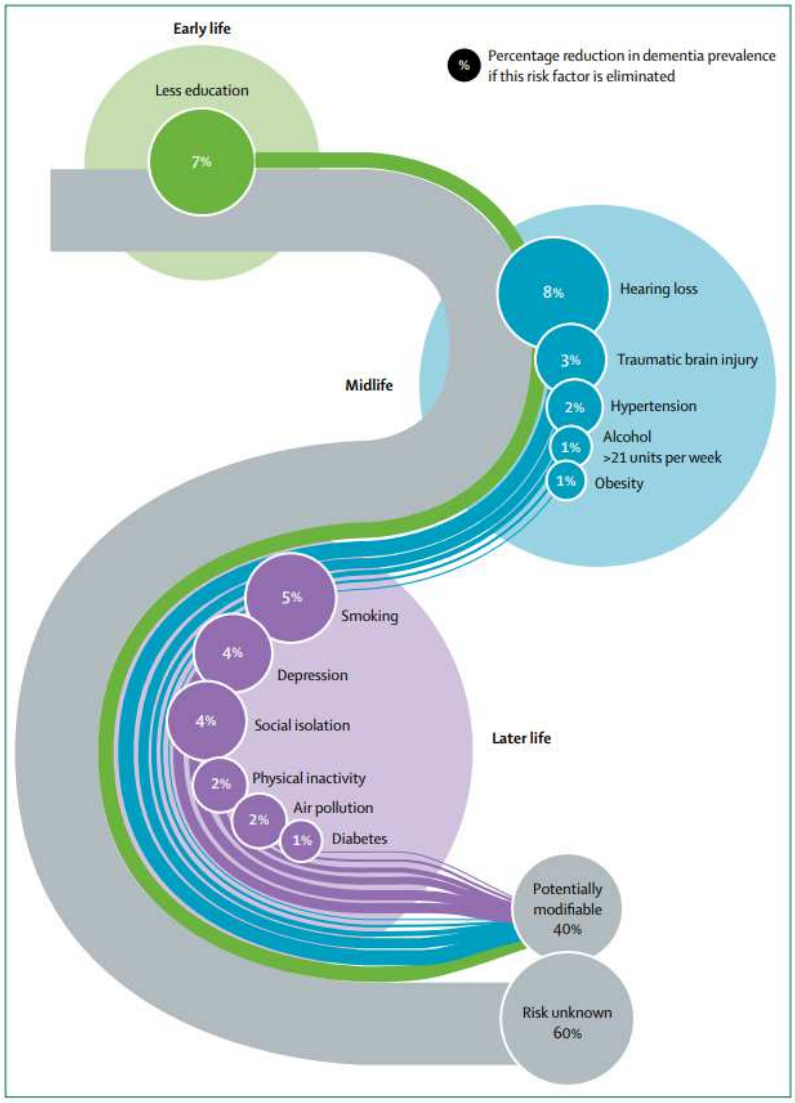

Figure 2: Population attributable fraction of potentially modifiable risk factors for dementia (Adapted with permission from Livingston et al., 2020)

1.5 AD Classification

AD, a degenerative disease of the brain is usually classified into familial cases with Mendelian inheritance (Familial AD, FAD) and sporadic cases with no familial aggregation. Familial cases are predominantly early-onset (younger than 65 years, early- onset familial AD; EOFAD), but also late onset cases (LOFAD) have been described. More than 90% of AD patients appear to be sporadic and usually with a late onset age (older than 65 years, LOAD), while early-onset AD (EOAD) accounts for approximately 1% to 5% of all cases and age at onset ranges from 30 years to 65

years (Dubois et al., 2015). The sporadic form of the disease is complex and thought to be a result of interactions between genetics and life style factors. The familial form is due to mutations in three major genes (amyloid precursor protein (APP) gene, presenilin1 (PSEN1) gene and presenilin 2 (PSEN2) gene) (Piaceri et al., 2013, Lanoiselée et al., 2017) (Figure 3). Presenilin form part of the γ-secretase complex that is required for the production of Aβ from APP (Bekris et al., 2020). Apolipoprotein E (APOE) genotype is the major genetic risk factor for AD (Di Battista et al., 2016). APOE exists in three major polymorphic forms (ε2, ε3 and ε4). The ε4 allele increases risk and the ε2 allele is protective (Liu et al., 2013). One copy of ε4 allele increases the risk by about 3-fold, two copies by nearly 15-fold) (Saddiki et al., 2020).

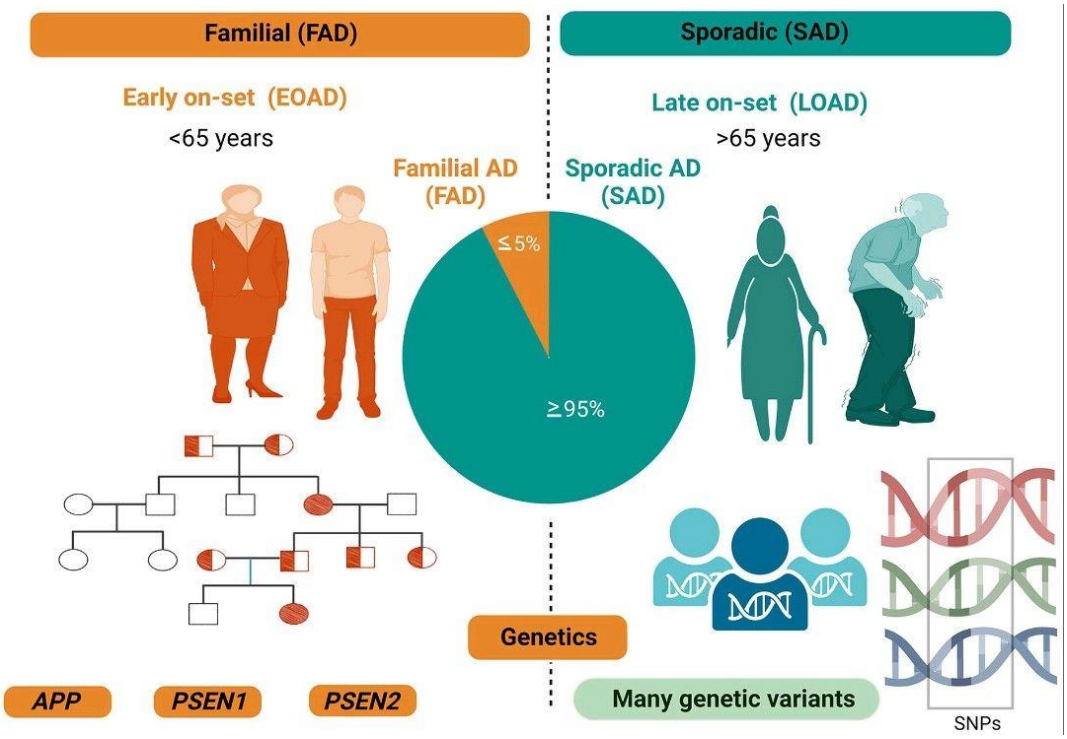

Figure 3: AD classification (Adapted from Pradeepkiran et al., 2023 with permission)

1.6 Progression of AD

The AD continuum refers to the progression of the disease from brain changes that are not noticeable to those that causes memory impairment and subsequently physical disability (Alzheimer's Dement, 2023). The three broad phases in the progression of AD are: preclinical AD, mild cognitive impairment (MCI) due to AD and dementia due to AD, also called Alzheimer's dementia (Sperling et al., 2011; Albert et

al., 2011; McKhann et al., 2011; Jack et al., 2011). The Alzheimer's dementia phase is further broken down into mild, moderate and severe dementia (Figure 4). While it has been reported that the progression of AD starts with the pre-clinical phase with no obvious symptoms and ends with severe Alzheimer's related dementia with severe symptoms, how long it takes an individual to progress from one phase to another differs and is influenced by factors such as age, genetics, biological sex and other life style related factors (Vermunt et al., 2019).

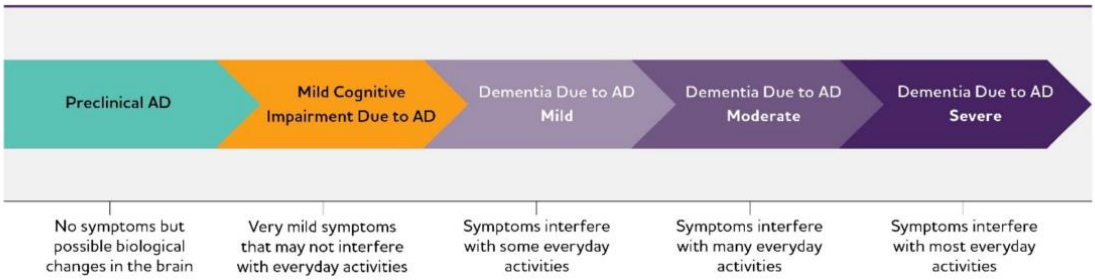

Figure 4: AD continuum. Although these arrows are of equal size, the components of the AD continuum are not equal in duration (Adapted with permission from Alzheimer's Dement, 2023).

1.7 Epidemiology of AD and related Dementia

AD is a multi-factorial degenerative disease of the brain with an estimated prevalence of 1 in 9 age 65 and older and a global population burden projected to triple by 2050 (Rajan et al., 2021; Alzheimer's Dement, 2022; GBD 2019 Dementia Forecasting Collaborators, 2022). AD is the most common cause of dementia, and it accounts for an estimated 60% to 80% of all dementia cases (Alzheimer's Dement, 2021). As at 2023, An estimated 6.7 million Americans age 65 and older are thought to be living with Alzheimer's dementia (Figure 5) with this number is projected to grow to 13.8 million by 2060 if there are no medical breakthroughs to prevent, slow or cure AD.

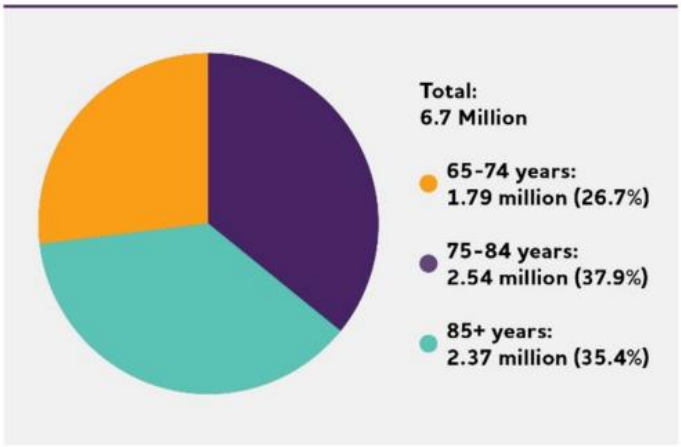

Figure 5: Number and ages of people 65 or older with Alzheimer's dementia, 2023. Percentages do not total 100 due to rounding. Created from data from (Rajan et al., 2021).

In 2020 and 2021, AD was the seventh-leading cause of death. It was reported that between 2000 and 2019, death from stroke and other chronic diseases was on the decline whereas death from AD increased more than 145% (Figure 6). In the US, the percentage of people with Alzheimer's dementia increases with age: 5.0% of people age 65 to 74, 13.1% of people age 75 to 84, and 33.3% of people age 85 and older have Alzheimer's dementia (Rajan et al., 2021). Estimates show that about 110 of 100,000 people ages 30-64 years, or about 200,000 Americans in total, have younger-onset dementia (Hendriks et al., 2021).

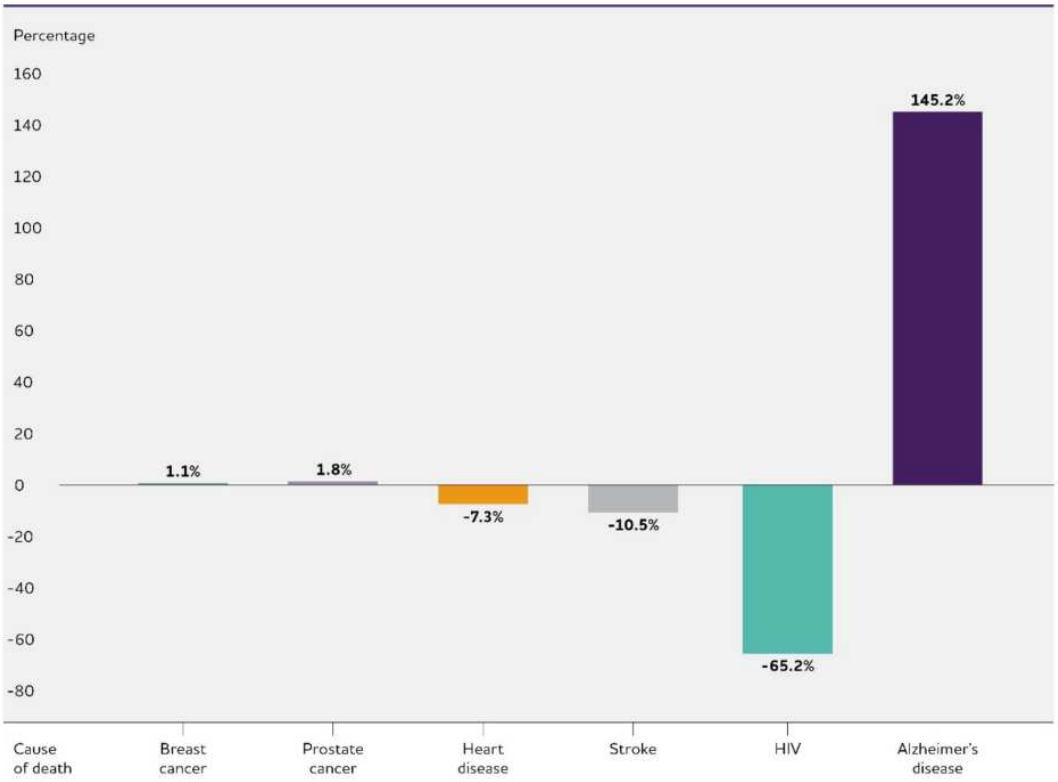

Figure 6: Percentage changes in selected causes of death (all ages) between 2000 and 2019. (Adapted with permission from Alzheimer's Dement, 2023).

In 2023, roughly 4.7 million Americans age 65 and older are classified as having dementia due to AD (Manly et al., 2022). Using the best data available, 5 to 7 million Americans age 65 and older are estimated to have MCI due to AD. Combined with the roughly 4.7 million Americans age 65 and older with dementia due to AD based on Alzheimer's brain changes, approximately 10-12 million older Americans will likely be living with AD.

1.8 Sex and Gender Differences in AD

Higher prevalence of AD in women is well reported. In fact, almost two-thirds of patients with AD are reported to be women (Burke et al., 2019; Dumitrescu et al., 2019; Ferretti et al., 2018; Gur et al., 2019; Koran et al., 2017; Laws et al., 2018; Mosconi et al., 2017; Tensil et al., 2018; Toro et al., 2019; Liesinger et al., 2018; Barnes et al., 2019; Tremblay et al., 2023). The Framingham Heart Study reported that the estimated lifetime risk for AD at age 45 was about one in five (20%) for women and one in 10 (10%) for men, and the risks for both sexes were slightly higher at age 65 (Alzheimer's Dement, 2021; Chene et al., 2020). In addition, the Cache

County Memory study also reported a higher incidence among women, suggesting longevity as a reason for this prevalence (Matyi et al., 2017; Miech et al., 2002; Zandi et al., 2002). Many factors such as lower education in women than men (Fitzpatrick et al., 2004; Kukull et al., 2002; Stern, 2012; Sando et al., 2008), survival bias (Chene et al., 2015; Plassman et al., 2007; Hebert et al., 2001), lower income and being primarily the care giver in their families (Ferretti et al., 2018) could be responsible for the reported high prevalence in women.

In addition to these factors, it is also likely that biological mechanisms might be involved. Some of the proposed biological mechanisms thought to be responsible for this sex differences include; sexual dimorphism in Central Nervous System (CNS) structures, changes in sex hormone signaling, risk genes and sex interactions, immune responses, and vascular diseases (Zhu et al., 2021). Sexual dimorphism is reported to be due to 1) deviations in brain structure, 2) depression, sleep disorders, and psychosocial stress responses, 3) pregnancy, menopause, and sex hormones, 4) genetic background (e.g., APOE), 5) inflammation, gliosis, and immune module (e.g., TREM2), 6) vascular risk factors, and 7) sex differences at single cell level (Ferretti et al., 2018; Toro et al., 2019; Fisher et al., 2018; Mathys et al., 2019). Men have been reported to usually have a larger brain volume which makes them less sensitive to pathological agents for AD and suffer less or slower structural loss as compared to women (Mielke et al., 2014). Data from quantitative proteomics revealed significant changes in the white matter and mitochondrial proteomes, redox proteins, ATP synthase and cytochrome oxidase in women, suggesting that women are more susceptible to more rapid neurodegeneration than men once the process starts (Gallart-Palau et al., 2016). Supporting this study is a report that women had higher CSF total tau and Aβ42 levels, more rapid cognitive decline and hippocampal atrophy, indicative of worse pathologic changes than men (Koran et al., 2017).
Women are found to have more sleep disturbance especially during menopause (Toro et al., 2019). In addition, studies have reported the vulnerability of women to stress-related disorders showing elevated levels of cortisol in women with mild-to-moderate AD. They were also found to be associated and increased AD pathologies including elevated amyloidosis and tauopathy (Behan et al., 1995; DeSouza, 1995).

At single cell level, a comprehensive study on single-cell transcriptomics of AD reported robust sex differences in the association of AD pathology. In this study, AD

pathology-associated cell subpopulations were found to be enriched with female cells and in females, marker genes showed higher expression (Mathys et al., 2019). In the same study, transcriptional responses between sexes were qualitatively distinct, particularly in oligodendrocytes and neurons (Mathys et al., 2019). In males, increased AD pathology was found to correlate with a global transcriptional activation in oligodendrocytes while in females, increased pathology correlated with a global gene downregulation in both excitatory neurons and inhibitory neurons (Mathys et al., 2019). Additional studies suggest that that developmental effects of sex hormones responsible for sexual differentiation of the brain may lead to a female brain that is more vulnerable to AD pathogenesis (Rosario et al., 2011; Poling and Kauffman, 2013; Li and Singh, 2014; Pike, 2017).

Immune responses to stimulations involving different pathways and immune cells are reported to be stronger in women than men, correlating with higher degree of susceptibility to infections in male but higher prevalence of autoimmune disorders in females (Tronson and Collette, 2017). Sex differences in dysregulated glia-cell mediated immune responses have also been reported in AD (Dzamba et al., 2016).

There is growing evidence linking vascular dysfunction with AD. Coronary artery disease (CAD) linked to cognitive decline with brain microvascular lesions are more prevalent in men than women in all ages (Kivipelto et al., 2001). Vascular risk factors such as hypertensive pregnancy disorders, including preeclampsia, eclampsia, and chronic gestational hypertension unique to women have been linked to brain lesions and cognitive impairment (Mielke et al., 2016; Postma et al., 2014). In a study of 668 individuals aged 60–90 years, small vessel disease (SVD) was associated with marked progression of subcortical white matter lesions and incident lacunar infarcts in women and females were linked with SVD progression (van Dijk et al., 2008). In another study involving 817 neurologically healthy men and women over 50 years of age, HDL-C and apoA-1 were reported to be inversely associated with the severity of white matter lesions in women but not in men (Yin et al., 2018).

1.9 Inflammation and AD

Inflammation is part of the clinical manifestations of AD and a possible role in the pathogenesis of AD is well documented (McGeer and McGeer, 2001; 2002a; 2002b;

McGeer and Rogers, 1992). Griffin and others reported the importance of IL-1 signaling in AD (McGeer et al., 1987; Griffin et al., 1989; Rogers et al., 1996). The presence of toxic Aß and tau proteins activates the microglia, the brain's resident macrophage and main immune cells. Microglia attempt to clear toxic proteins as well as debris from dead or dying cells (Wang and Xie, 2022). The inflammatory response is one of the important pathways involved in the cellular response to stress. It has been reported that inflammation can play either beneficial or detrimental roles in response to endogenous or exogenous stressors (Qian et al., 2017). Recent reports point to neuroinflammation as an active participant in the pathophysiology of AD rather than a mere bystander activated by emerging senile plaques and neurofibrillar tangles (Zhang et al., 2013). Furthermore, inflammatory response in AD brains is reported to be sustained over time (Akiyama et al., 2000; Azizi et al., 2015; Chen and Mobley, 2019) extending beyond a mere reaction to neuronal loss (Heneka et al., 2015). In addition, microglia, astrocytes, oligodendrocytes, mast cells, cytokines and chemokines, as well as complement (Meraz-Ríos et al., 2013) are involved, all playing an integral role in the onset and progression of the disease (Heneka et al., 2015; Businaro et al., 2018; Skaper et al., 2018). Proinflammatory cytokines are increased in the serum and brain of postmortem AD patients (Wang et al., 2015; Stamouli and Politis; 2016). Proinflammatory cytokines such as IL-6, TNF- and IL-1 secreted by the M1 microglia phenotype induce inflammation (Zhang et al., 2016), while the M2 microglia phenotype IL-4, Arg1, IL- 10 and neurotrophic substances release factors that have an anti-inflammatory effect (Turtzo et al., 2014).

Microglia activation in the CNS could be classical (M1) or alternative (M2). Classical (M1) activation is widely known to be induced by interferon- γ (IFN- γ) and lipopolysaccharide (LPS) resulting in the production of inflammatory cytokines and chemokines, like tumor necrosis factor alpha (TNF-a), interleukin (IL)-6, IL-1b, IL-12, and CC chemokine ligand (CCL) 2 (Colonna and Butovsky, 2017). Alternative (M2) activation is widely reported to be induced by anti-inflammatory cytokines such as IL-4 and IL-13, resulting in the production of microglia produce anti-inflammatory cytokines [IL-10, transforming growth factor (TGF)-β)], growth factors [insulin-like growth factor-1 (IGF-1), fibroblast growth factor (FGF), colony stimulating factor (CSF)-1] and neurotrophic growth factors [nerve derived growth factor (NGF), BDNF, neurotrophins and glial cell-derived neurotrophic factor (GDNF)]. Furthermore, M1 microglia They also release pro-survival factor progranulin and induces mannose

receptor (CD206), found in inflammatory zone 1 (FIZZ1), chitinase-3-like-3 (Chil3, Ym1 in rodents), arginase 1 (Arg1) (Colonna and Butovsky, 2017). M1 microglia induce inflammation and neurotoxicity, while M2 microglia induce anti-inflammatory and healing (Colonna and Butovsky, 2017).

Beyond the M1 and M2 microglia classification, Keren-Shaul and colleagues (2017) reported a novel sub-population of microglia associated with neurodegenerative diseases which they termed disease-associated microglia (DAM). Karen-shaul et al. (2017) suggested that microglia could transit from homeostatic microglia to DAM, usually found to localized around Aβ plaques as AD progresses. Expressions of genes found in human genome-wide association studies (GWASs) previously linked to Alzheimer's disease (AD) and other neurodegenerative diseases Like TREM2 are associated with DAM (Keren-Shaul et al., 2017; Lambert et al., 2013; Yeh et al., 2017). Detection of DAM was reported primarily in CNS regions vulnerable to AD. More specifically, in 5XFAD and APP/PS1 models of AD, co-localization of DAM with Aβ plaques was observed in cortex and not cerebellum, a brain region not associated with Aβ plaques (Keren-Shaul et al., 2017; Mrdjen et al., 2018). Furthermore, markers of a DAM signature were also observed in human AD postmortem brains (Friedman et al., 2018; Keren-Shaul et al., 2017).

1.10 AD Hypothesis

Although the exact pathogenesis of AD is still unknown, three main hypotheses, namely the cholinergic hypothesis, the Aβ cascade hypothesis and the tau protein hypothesis, have been proposed. The cholinergic hypothesis states that a possible cause of AD is a loss of central cholinergic neurons, ensuing deficiency of acetylcholine, a neurotransmitter involved in memory and learning (Francis et al., 1999). The tau hypothesis proposes that AD may result from abnormal aggregation (excessive amount or abnormal phosphorylation) of tau proteins, leading to the formation of tangles within nerve cells in the brain (Mudher and Lovestone, 2002; Iqbal and Grundke-Iqbal, 2008). The amyloid cascade hypothesis proposes that AD may be caused by accumulation of abnormally folded β-amyloid proteins generated by the proteolytic cleavage of APP (Hardy and Selkoe, 2002). Apart from these three hypotheses, the alternative two-hit vascular hypothesis proposes that cardiovascular risk factors such as hypertension, atherosclerosis, diabetes, obesity and other microvascular pathologies lead to

reduced cerebral blood flow, BBB dysfunction, hypoxia, impaired Aβ clearance, increased oxidative stress/inflammation and, ultimately, neurodegeneration and dementia (Zhu et al., 2021). This hypothesis suggest that Aβ accumulation is as a result of insult caused by vascular damage (Zlokovic 2005, 2010; de la Torre, 2010; Marchesi, 2011; Rius-Pérez et al., 2018). Supporting the two-hit vascular hypothesis is a study that showed that the dysfunctional BBB is an early event in aging brains of people with mild cognitive impairment and early clinical stages of AD (Montagne et al., 2015). Vascular abnormality is proposed to act in synergy with brain Aβ levels through a positive feedback loop where vascular risk factors promote Aβ accumulation in the brain, and Aβ accumulation in turn aggravates vascular dysfunction. Emerging data suggest a link between vascular impairment, neuronal insults and inflammation in AD in which cerebral vasculature-involved inflammation occurs before Aβ deposition and in turn promotes the inflammatory responses (Zhu et al., 2021).

1.11 Aβ Cascade Hypothesis and APP processing

The Aβ, a 4 kDa fragment of the amyloid precursor protein (APP), is a larger precursor molecule produced by brain neurons, vascular and blood cells (including platelets), and, to a lesser extent, astrocytes. According to the Aβ cascade hypothesis, Aβ is formed by two subsequent amyloidogenic proteolytic cleavages of *amyloid precursor protein* (APP) by β-secretase (β-APP-cleaving enzyme-1 (BACE1)) at the ectodomain and γ-secretase at intra-membranous sites generate Aβ (Blennow et al., 2006; Rajendran et al., 2006). Aβ generation is initiated by proteolysis of amyloid precursor protein (APP) by the γ-secretase enzyme BACE1 (Cole and Vassar, 2008). Formation of Aβ could be intracellular through the proteolytic cleavage of amyloid precursor protein (APP) localized in the plasma membrane, in endoplasmic reticulum (ER), trans-golgi network, endosomal, lysosomal and mitochondrial membranes (Glenner and Wong, 1984). APP expression has been shown to reflect the level of Aβ production (Xue et al., 2022). Factors such as APP expression (Aβ production) and oligomerization, Aβ clearance and transport across BBB, and Aβ degradation determines the concentration of Aβ in the brain. These factors are responsible for 90% of sporadic AD cases and the remaining 10% are attributed to genetic mutation in the APP or presenilin genes (Sherrington et al., 1996).

$A\beta_{40}$ peptides make up about 90% of the Aβ fragments generated, and a minor fraction of $A\beta_{42}$ that are more fibrillogenic and prone to oligomerization, while $A\beta_{43}$ peptides are found in amyloid plaques (Sisodia et al., 2002). Under physiological condition, $A\beta_{40}$ peptides are the predominant Aβ species and $A\beta_{42}$ peptides are toxic and have been reported to have faster rate of aggregation.

Experimental patho-mechanistic and proof-of-concept studies suggest that an imbalance between Aβ neuronal production and extracellular clearance of Aβ is associated with protein misfolding, aggregation, and incipient extracellular accumulation in plaques (Hardy and Selkoe, 2002; Jack et al., 2018; Selkoe and Hardy, 2016). This imbalance has been found to be due to genetic-driven dysregulation of the amyloidogenic pathway showing downstream overproduction of Aβ in early-onset AD (EOAD). In late-onset AD (LOAD), the imbalance is as a result of impaired proteostasis quality control mechanisms, from the synthesis of Aβ to its degradation, leading to insufficient Aβ clearance (Mawuenyega et al., 2010; Hampel et al., 2021).

Most pathogenic mutations in the APP gene cluster around the proteolytic sites of the β- and γ-secretases resulting in an increase of the substrate affinity with an accompanying increase in pool of total Aβ or a shift in Aβ peptides ratios. The latter favors a relative increase of $A\beta_{42}$ levels over the levels of $A\beta_{1\text{-}40}$ and shorter species (Wisniewski et al., 1985.; St George-Hyslop et al., 1987; Cruts et al., 2012; Hooli et al., 2012) and this imbalance has been implicated in protein self- aggregation (Hartley et al., 2015; Cai et al., 1993)

APP is processed through two major pathways; the amyloidogenic and non-amyloidogenic vis-a-vis the activities of three main proteases- α-, β- and γ-secretases (Figure 7). The amyloidogenic pathway promotes the production of Aβ through sequential cleavage by β- and γ-secretases while in the non- amyloidogenic pathway, Aβ is cleaved in the middle generating either soluble APPα directly by α-secretase or shorter Aβ species such as $A\beta_{15}$ and $A\beta_{16}$ by the sequential cleavage by β-secretase and α-secretase (Hampel et al., 2021). By-products generated from these two pathways have differing intrinsic functional properties, putative physiological roles, and pathophysiological implications (Hardy and Selkoe, 2002; Jack et al., 2018; Selkoe and Hardy, 2016). In addition to the activities of these secretases (α-, β- and γ-secretases), trafficking of APP due to secretory pathway is also one of the

important factors in APP metabolism. Mature APP in the endoplasmic reticulum and Golgi apparatus are translocated to the cell surface or may enter the lysosomal pathway and undergo proteolytic degradation (Nixon, 2017). The amyloidogenic peptides are either rerouted to lysosomal compartments for degradation, or secreted into the extracellular space for removal (Gali et al., 2019).

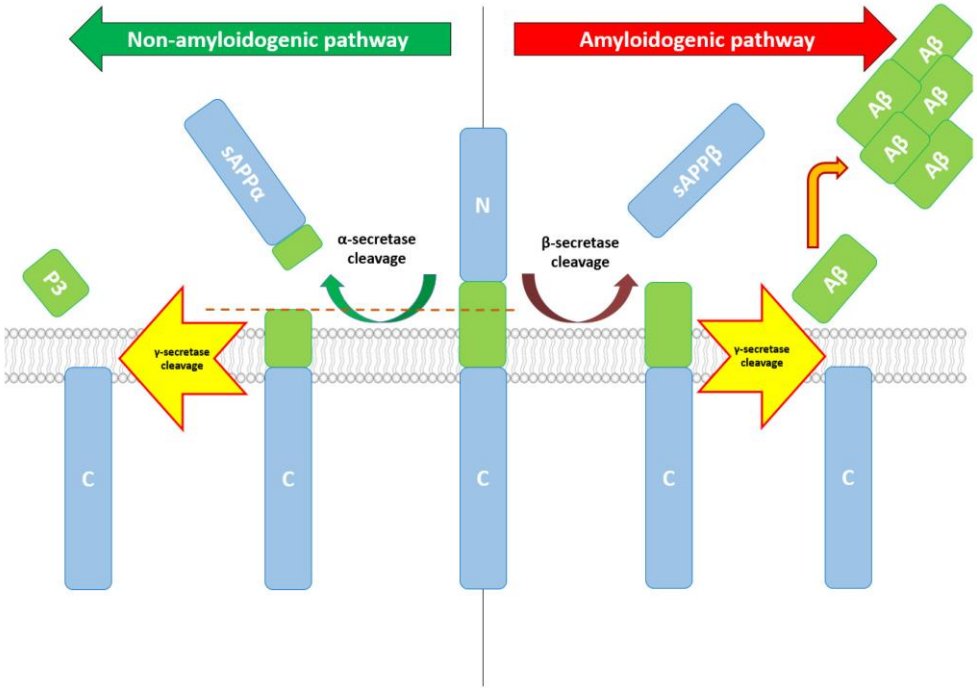

Figure 7: APP Processing Pathway. (Adapted from Schreiner et al., 2021 with permission)

1.12 Type 2 Diabetes in AD: more than just a risk factor

Type 2 Diabetes (T2D) is a complex metabolic disorder characterized by chronic hyperglycemia, insulin resistance, defective insulin secretion, loss of β cell function and mass, and accumulation of amyloid in the islets of Langerhans (Stumvoll et al., 2005, Mukherjee et al., 2017). Although the disease is thought to be due to insufficient insulin production by β cells resulting in insulin resistance, not all people with insulin resistance develop T2D (Polonsky, 2000) as impairment of insulin secretion due to pancreatic β cell dysfunction is required (Kahn, 2003). T2D is a global epidemic with the diabetic population projected to reach 552 million in 2030 (International Diabetic Federation, 2011). By 2050, about 1.2 billion of the world's population are predicted to suffer from diabetes (GBD 2021 Diabetes Collaborators, 2023). About 11.3% of the US population, 37.3 million people, have diabetes. An

estimated 96 million American adults are pre-diabetic (CDC Report, 2022). T2D is reportedly the most common form of diabetes, accounting for 90-95% of all diabetic cases (O'Brien et al., 2003; Goyal et al., 2023).

The risk of developing AD has been found to be 65% higher among diabetic patients than non-diabetic controls (Barbagallo and Dominguez, 2014). In AD patients, the rate of diabetes was found to be around 35% in a study from one large community. About 46 % of people with a diagnosis of AD were glucose intolerant, a well-known precursor for diabetes (Barbagallo and Dominguez, 2014). In fact, diabetic patients have a twice higher risk of developing AD (Ott et al., 1999; Leibson et al., 1997; Grodstein et al., 2001; Peila et al., 2002; Arvanitakis et al., 2004; Xu et al., 2004). In addition, the percentage of T2D patients among people living with AD was significantly higher compared to age-matched non-AD controls (Ott et al., 1999; Kuusisto et al., 1997). From epidemiological evidence, T2D has been reported to nearly double the risk of AD development (Biessels et al., 2006; Kopf and Frolich, 2009).

Amyloidosis, a group of conditions of diverse etiologies characterized by the accumulation of insoluble fibrillar proteins in various organs has been shown to be a key pathological feature of both AD and T2D (Milklossy and McGeer, 2016). Deposition of local amyloid mainly composed of amylin are present in over 95% T2D patients (Lopes et al., 2004; Cooper et al., 1987a, 1987b; Westermark et al, 1987). Along with Insulin, amylin is produced by β-cells in the Langerhans islets of the pancreas (Miklossy et al., 2010). The extent of amylin depositions has been reported to correlate with clinical severity of diabetes, with the impairment in insulin secretion and glucose metabolism, and with the severity of beta-cell loss (Cooper et al., 1987a; Westermark et al, 1987; Hull et al., 2004).

In addition, insulin and Aβ have a common sequence recognition motif (Miragliotta et al., 1994) and Aβ directly inhibits the binding and action of insulin, thereby impairing the autophosphorylation of the insulin receptor (Miragliotta et al., 1994). In addition, Aβ and insulin are substrates for the insulin degrading enzyme (IDE). Moreover, high-affinity interaction between Aβ and pro-amylin have been reported to result in cross-suppression of cytotoxic self-assembly of both peptides, further alluding to a molecular association between AD and T2D (Klegeris and McGeer, 2007). Furthermore, Aβ oligomers are reported to induce phosphorylation of tau and

inactivation of insulin receptor substrate via c- Jun N-terminal kinase signaling (Ma et al., 2009) and insulin dysfunction *in vivo* can lead to tau phosphorylation (Brauner et al., 1994).

Anti-inflammatory effect of insulin at low dose have been reported and conversely high level of insulin during chronic state of hyperinsulinemia is known to exacerbate inflammatory responses and increase oxidative stress (Fishel et al., 2005). A state of hyperinsulinemia leads to increased expressions of pro-inflammatory cytokines like TNF-α, IL-1β and IL-6 (Craft and Watson, 2004). Chronic imbalance between pro and anti-inflammatory action of insulin could potentially be the link between T2D and AD (Plata-Salamán and ffrench-Mullen, 1994).

Previous studies have implicated oxidative stress in many neurogenerative diseases including AD and has been suggested as one of the potential links between T2D and AD (Di Domenico et al., 2010; Butterfield et al., 2001). Onset of diabetic complications like dysregulated insulin signaling and neuropathy has close link with increased oxidative stress arising from inability to remove reactive oxygen species (ROS) implicating oxidative stress in impaired insulin signaling in AD brains (Rain and Jain, 2011).

Cognitive deficiencies including impaired verbal memory, diminished mental speed and mental flexibility are some of the manifestations in T2D patients (Brands et al., 2005; Cukierman et al., 2005). Chronic hyperglycemia, a key pathology of T2D, has been reported to be inversely correlated with cognitive function (Perlmuter et al., 1984; Jagusch et al., 1992). In addition, AD is associated with hyperglycemia (Janson et al., 2004; Carantoni et al., 2000; Razay, 2007), indicating that hyperglycemia may play a role in AD pathogenesis. Formation of neuritic plaques and neurofibrillary tangles, core features of AD, were found to be increased in diabetic mice induced by streptozocin injection (Jolivalt et al., 2010; Ke et al., 2009). Similarly, Aβ deposition was reported in not only in brain but also in kidney and pancreas of transgenic mice expressing the carboxyl-terminus of the beta APP gene (Fukuchi et al., 2004). Formation of Aβ plaques was detected in pancreas of transgenic NORBA mice over-expressing human APP (Nicolau et al., 2002). Surprisingly, aggregated Aβ and hyperphosphorylated tau were reported in brains of rat models of spontaneous diabetes, particularly of type 2 diabetes (Li et al., 2007). Reduced expression of insulin, insulin-like growth factor 1 and insulin receptor and

increased expression of tau protein and glycogen-synthase kinase-3β have been reported in post-mortem brain of patients with AD compared to controls implicating a defective metabolism in the AD patient's brain (Siino et al., 2021). Together, these data strongly suggest a molecular link between T2D and AD, further explained in Figure 8.

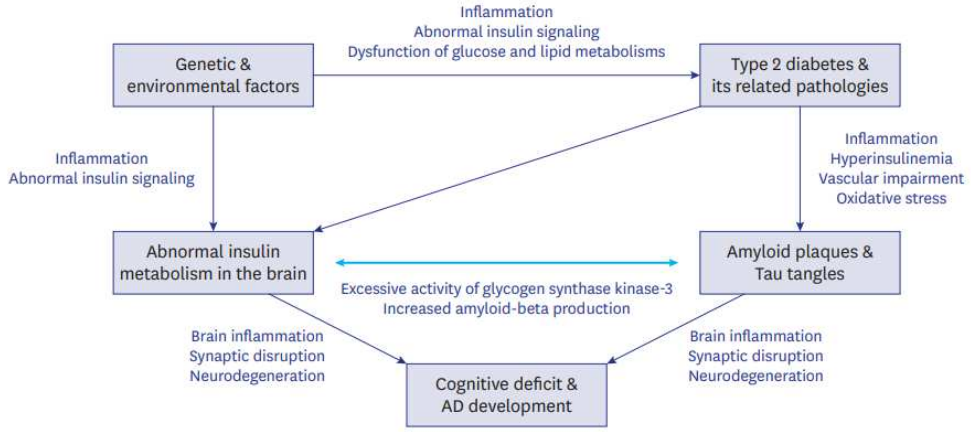

Figure 8: Potential links between diabetes mellitus and AD (Adapted from Ahn et al., 2019).

1.13 Insulin Resistance and AD

The insulin pathway is one of the evolutionary conserved aging controlling pathways (Lopez-Otin et al., 2013). In addition, insulin resistance, a component of nutrient sensing pathways, is dysregulated in aging and considered to be one of the hallmarks of aging (Lopez-Otin et al., 2013). Insulin in the CNS is associated with many physiological functions including; CNS specific molecular signaling functions such as neuronal glucose transporter translocation (Grillo et al., 2009), brain calcium signaling (Thibault et al., 2013), ATP-sensitive potassium channels (Spanswick et al., 2003), tau phosphorylation (Gratuze et al., 2017), Aβ clearance (Vandal et al., 2005). In addition, CNS insulin can affect peripheral processes including blood flow (Cabou et al., 2007), reproduction (Bruning et al., 2000), and peripheral gluconeogenesis (Ruud et al., 2017), affecting blood glucose levels, thereby regulating metabolism and cognitive functions (Banks et al., 2012). In addition, brain processes such as reward (Figlewicz, 2003), learning, and memory (Zhao and Alkon, 2001) are also reported to be regulated by CNS insulin. Hippocampus and frontal cortex, brain

regions associated with memory and cognition, are known to have high levels of insulin receptors (Ghasemi et al., 2013; Porte et al., 1998)

Insulin resistance is a state of impaired or insufficient response to insulin. In insulin sensitive tissues like skeletal muscle, liver and adipose tissue glucose metabolism regulated by insulin is required to maintain a state of euglycemia. This requires higher insulin levels to maintain the euglycemia state (Rhea et al., 2022). Resistance to insulin can be found in conditions where the blood glucose is normal (hyperinsulinemic euglycemia) as wells as those with increased glucose levels (hyperinsulinemic hyperglycemia) (Rhea et al., 2022). Insulin resistance is associated with many chronic diseases like T2D, obesity and AD (Rhea et al., 2022).

Peripheral insulin resistance is linked with hyperglycemia, hyperinsulinemia, and increased lipolysis leading to an increase in serum free fatty acids (FFAs). These alterations in serum factors affect the transport and, ultimately, CNS signaling of critical metabolic hormones (Banks, 2019). In addition, inflammation (caused by elevated cytokine levels) and increased oxidative stress are known to play role in initiating insulin resistance that impacts BBB function whose impairment is an early event in the pathogenesis of AD (Banks and Rhea, 2021; Erickson and Banks, 2018).

Insulin resistance in the CNS is entirely different from peripheral insulin resistance. The receptors of the CNS have been found not to participate in classic negative feedback between glucose and insulin levels. Hence, a deficient insulin activity in the CNS may likely have no effect on blood insulin levels. Cerebral insulin resistance has been reported in individuals with peripheral insulin resistance, in aged individuals, in those with AD (Talbot et al., 2012) and in people that are insulin resistant both in the periphery and CNS. A state of being insulin resistant in both periphery and CNS constitute about 35% of people diagnosed with AD (Janson et al., 2004).

In 2012, Talbot and others showed that insulin resistance in the periphery does not automatically confer CNS insulin resistance. They reported that insulin receptor resistance was present in majority of patients diagnosed of AD even in the absence of a diabetic state. In addition, they showed an impaired response to insulin in *post-mortem* brain regions including the cerebellar cortex and hippocampal formation compared to controls who did not have evidence of insulin resistance at peripheral tissues. Talbot and colleagues proposed that insulin resistance in the CNS occurs before cognitive decline and that the degree of resistance is in proportional to the extent of cognitive decline. This landmark study suggested that insulin resistance in

the CNS is independent of peripheral insulin resistance (Talbot et al., 2012). Both peripheral and cerebral insulin resistance can impair cognitive functions and contribute to dementia, however, likely, via different pathways.

There is a close association between insulin resistance, aging and AD irrespective of whether in the CNS, in the periphery or in both. Impaired insulin action in the CNS has been reported and a chronic state of hyperinsulinemia in the periphery was found to reduce transport of insulin into the brain (Freiherr et al., 2013; Banks et al., 1997). Studies involving human participants and experimental animals have shown a link between peripheral insulin resistance and cognitive impairment and increased risk for development of AD (Cholerton et al., 2011; de la Monte, 2014; Blazquez et al., 2014). Post-mortem evaluations of diseased brains also showed decreased expressions of key insulin signaling proteins in the brains of AD patients (Rivera et al., 2005; Liu et al., 2011; Steen et al., 2005; Rickle et al., 2004).

1.14 Protein Post-Translational Modifications in AD and T2D

Folded or nascent proteins are known to be stable under physiological conditions. The series of enzyme specific catalytic modification of the side chain or backbone of a protein is termed Post Translational Modification (PTM) (Walsh et al., 2005). These modifications include glycosylation, acetylation, acylation, ADP ribosylation, methylation, nitration, truncation, amidation, γ-carboxylation, β-hydroxylation, disulfide bond formation, phosphorylation, sumoylation, ubiquitination, proteolytic processing, and sulfation and do exert great influence on normal cell physiology and pathogenic processes (Kuriakose et al., 2016). PTMs are prevalent in most proteins involved in T2D and AD (Chatterjee and Thakur, 2018).

Altered methylation of genes like peroxisome proliferator-activated receptor-gamma gene (PPARG), potassium voltage-gated channel subfamily Q member 1 (KCNQ1), transcription factor 7-like 2 (TCF7L2) and insulin receptor substrate-1 (IRS1), are crucial for the activities of insulin in the liver, skeletal muscle and adipose tissues (Barres et al., 2009; Nilsson et al., 2014; 2015; Nitert et al., 2012; Ribel-Madsen et al., 2012; Kirchner et al., 2016; Abderrahmani et al., 2018; Baumeie et al., 2017; You et al., 2017). Under hyperglycemic conditions, hormones have been shown to be affected by protein glycation as protein glycation levels are increased in the diabetic state (Hunter et al., 2003). A continuous state of hyperglycemia and elevated advanced glycation end-products (AGEs) has been associated with oxidative stress,

resulting in increased reactive oxygen species (ROS) (Miranda-Diaz et al., 2016). This heightened oxidative state in turn accelerates the generation of AGEs and the reaction between AGES and the receptor for AGEs (RAGE) reported to be elevated in AD (Coughlan et al., 2009; Vitek et al., 1994; Fang et al., 2018; Chen et al., 2021).

In addition, glycosylation and phosphorylation of serum proteins in diabetic patients have been reported to be altered by enzymes regulating PTM (McMillan, 1972; Loukovaara et al., 2005; Itoh et al., 2007). Phosphorylation is known to play an important role in glucose stimulated insulin secretion in islets of Langerhans and serves as important mediator in insulin stimulated signaling networks (Chatterjee and Thakur, 2018). Evaluation of pancreatic islets of diabetic patients showed downregulation of genes like PPARGC1A, INS and PDX1 necessary for insulin secretion resulting from elevated methylation (Yang et al., 2011; 2012; Ling et al., 2008;). Nakae and colleagues reported that the acetylation of FOXO1, a gene that controls PDX1, significantly impacts beta cell development and glucose homeostasis (Nakae et al., 2002). In addition, deacetylation of histone 3 lysine 9 (H3K9) was implicated in the downregulation of the IRS2 protein leading to the development of insulin resistance (Dalfra et al., 2020).

1.15 Pyroglutamate modified Aβ

The proteolytic processing of the Aβ protein precursor (APP) by β- and γ-secretases results in the generation of Aβ peptides (Haass, 2004). Aβ associated plaques in brains of human AD patients have been reported to contain a diverse mixture of Aβ peptides (Walker et al., 2008). In addition to $A\beta_{40}$ and $A\beta_{42,}$ which are the main Aβ species, other variants produced by PTM such as truncation, racemization, isomerization, phosphorylation, metal induced oxidation and pyroglutamination have been demonstrated (Ku et al., 2001; Saido et al., 1996; Tekirian et al., 1998; Miravalle et al., 2005; Hartig et al., 2010; Mori et al., 1994; Tomiyama et al., 1994; Murakami et al., 2008; Shimizu et al., 2000; Saido et al., 2005; Kuo et al., 1997; Dong et al., 2003; Kumar et al., 2011; Milton, 2005; 2001). These PTM processes have the potential to promote oligomer and aggregate formation, enhance cytotoxicity and the modified Aβ variants could serve as seeding species for Aβ aggregate formation *in vivo* (Kumar et al., 2011; Millucci et al., 2010; Schilling et al., 2008; Schlenzig et al., 2009; Fabian et al., 1994; Saito et al., 2003; Schilling et al., 2006). Moreover, modified Aβ variants are reported to be present at the early stages

of AD (Hartig et al., 2010; Kumar et al., 2011; Sergeant et al., 2003; Schilling et al., 2008). N-terminal truncation and subsequent cyclization of N-terminal glutamate (Glu) to pyroglutamate (pGlu) in Aβ peptides leads to the formation of pGlu-Aβ peptides (Saido et al., 1995; 1996; Russo et al., 2000; Sevalle et al., 2009) which constitute the bulk of Aβ deposits in sporadic and familial AD (Saido et al., 1995, Miravalle et al., 2005; Piccini et al., 2005; Portelius et al., 2010), are present in senile plaques and vascular amyloid deposits (Tekirian et al., 1998; Miravalle et al., 2005; Guntert et al., 2006; Miller et al., 1993; Sergeant et al., 2003) and have been reported to be involved in the pathogenesis of the disease.

Pyroglutamination of Aβ peptides enhances Aβ aggregation, confers resistance to degradation by most aminopeptidases as well as Aβ-degrading endopeptidases (Figure 9). Strong neurotoxic effects of the pGlu modification on primary neurons, neuronal cell lines, and neurons of APP transgenic animals *in vivo* have been reported (He and Barrow, 1999; Russo et al., 2002; Schilling et al., 2006; Schlenzig et al., 2009; D'Arrigo et al., 2009; McColl et al., 2009; Saido, 1998; Acero et al., 2009; Wirths et al., 2009).

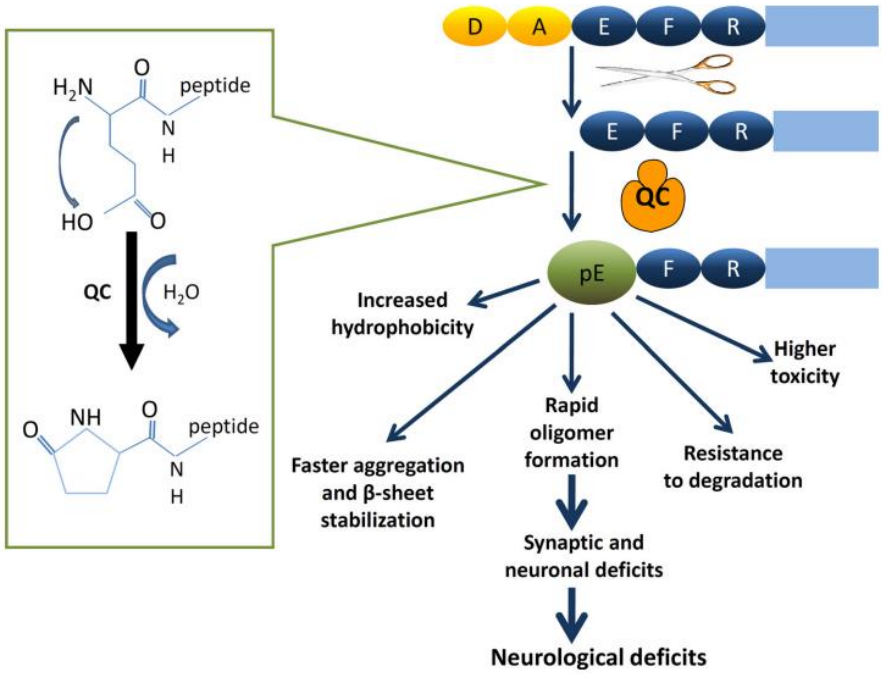

Figure 9: Properties of pyroglutamate Aβ.

The first N-terminal two amino acids, aspartate and alanine, are cleaved off by aminopeptidase A (APA), meprin-β or dipeptidyl peptidase 4 (DPP4)., exposing

glutamate at position 3 of the N terminus of Aβ. Subsequently, glutamate is post-translationally modified to N-terminal pyroglutamate (pE) by dehydration catalyzed by QC activity. The novel peptide has altered biochemical properties with severe pathological consequences. The enhanced toxicity is likely due to the higher aggregation propensity and the longer bioavailability of the Aβ-pE3 oligomers (Adapted from Jawhar et al., 2011; Bayer, 2022 with permission).

Pyroglutamination of Aβ peptides is known to be catalyzed by glutaminyl cyclase (QC) *in vitro* (Schilling et al., 2004) and *in vivo* (Cynis H et al., 2006; 2008; Schilling et al., 2008a, 2008b) (Figure 9). In transgenic mouse models, presence of pGlu-Aβ peptides led to protein aggregation and deposition, neurodegeneration, gliosis, and impairment of learning and memory. Genetic ablation or pharmacological inhibition of QC in mouse and fruit fly models of AD resulted in reduced pGlu Aβ peptide generation and improved performance in cognitive tasks (Schilling et al., 2008a; Alexandru et al., 2011; Jawhar et al., 2011).

1.16 Aβ Clearance and Degradation Mechanisms

Aβ clearance from the brain is achieved through various mechanisms including blood-brain clearance, interstitial fluid bulk-flow clearance, the perivascular and paravascular system, autophagic lysosomal degradation, and many more (Marchi et al. 2016). Inadequate clearance of protein aggregates that deposit in the brain of proteinopathies, including AD, as well as defects in clearance systems for aggregated and misfolded protein are associated with disease pathogenesis (Dakkak et al., 2022).

1.16.1 Blood brain barrier (BBB)

The blood-brain barrier (BBB) is a dynamic semi-permeable physiological membrane that restricts entrance of foreign substances from the blood into the CNS (Jackson et al., 2022). Basically, the BBB is composed of endothelial cells, astrocytes, pericyctes and junctional complexes including the tight and adherens junctions (Knopp et al., 2022; Csaszar et al., 2022; Dorrier et al., 2022; Halder et al., 2022). The BBB is in constant communication with the astrocytes (Heithoff et al., 2021; Siddharthan et al., 2007), pericytes (Daneman et al., 2010; Armulik et al., 2010), neurons (Schiera et al., 2003; Maoz et al., 2018), perivascular macrophages (Yang et al., 2019), microglia

(Haruwaka et al., 2019) and immune cells (Engelhardt et al., 2017) (Figure 10). The BBB protects the brain in order to maintain normal neuronal function (Patabendige and Janigro, 2023). The BBB helps to protect the brain from damage by keeping a constant “chemical” composition of brain interstitial fluid necessary for optimal brain function (Zlokovic, 2008; Barisano et al., 2022; Liu et al., 2022). Disruption of the BBB makes the brain vulnerable to damage. The BBB displays a net negative surface change thereby restricting the entrance of negatively charged compounds, leukocyte adhesion molecules and even some immune cells into the brain (Rossler et al., 1992; Santa-Maria et al., 2021; Zhao et al., 2023). In addition, the BBB has designated transporters, receptors and enzymes that regulate the influx of nutrients, efflux of waste products, potentially neurotoxic and vasculotoxic macromolecules from the brain (Zlokovic, 2008; Chu et al., 2008; Patabendige and Janigro, 2023). The BBB has high trans-endothelial electrical resistance that selectively restricts the number of transcellular vesicles that can pass through the vessel wall (Tietz and Engelhardt, 2015; Wilhelm et al., 2011)

Endothelial cells are the core anatomical structure of the BBB and they line the cerebral blood vessels and at the same time interact with different cells in the CNS (Daneman et al., 2015; Zhang et al., 2016). The intracellular tight junctions are an essential part of the BBB and are made up of transmembrane proteins like claudin-5, occludin and cytoplasmic plaque proteins like zonula occludens (Keep et al., 2023). Both the tight junctions and adherens junctions hold the endothelial cells together, forming luminal and abluminal compartments (Betz et al., 1980). The junctions control the movement of molecules through paracellular pathway via size and charge selectivity (Patabendige and Janigro, 2023), and allow the passive diffusion of lipid soluble drugs and substrates with molecular weight between 400-600 Da (Wu et al., 2023).

A functional BBB is crucial for the regulation of CNS homeostasis, protection of brain from changes in the levels of plasma neurotransmitters and for the delivery of energy metabolites and essential nutrients needed for normal neuronal and synaptic functions (Zlokovic, 2008; Patabendige and Janigro, 2023). Defective transport across the BBB is an important mediator of Aβ accumulation in the brain and a contributing factor in the pathogenesis of AD (Shackleton et al., 2016).

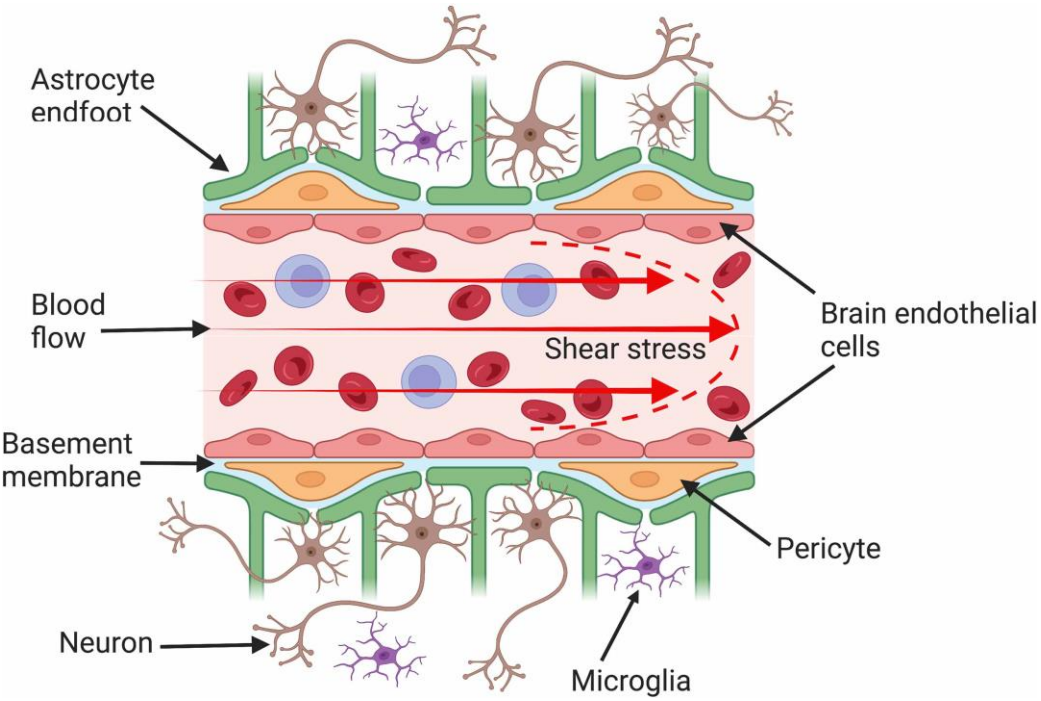

Figure 10: Structure of the blood–brain barrier (BBB) (Adapted with permission from Patabendige and Janigro, 2023)

1.16.2 Transport and Cellular Uptake of Aβ at the BBB

In the brain endothelium, the LRP1 and the Receptor for Advanced Glycation End products (RAGE) facilitate efflux and influx of Aβ from the brain to the periphery and vice versa. Once Aβ is produced and secreted into the extracellular space in the brain, LRP1 is involved in cellular uptake of Aβ in neurons, microglia, astrocytes, vascular smooth muscle cells, pericytes, endothelial cells, and the choroid plexus. Internalized Aβ might be degraded in lysosomes or accumulate in the cells causing cellular toxicity depending on the context (Shinohara et al., 2017). A portion of Aβ may be transported through LRP1 at the BBB or pulled out by sink activity of soluble LRP1 into the blood. LRP1 in the liver might also help to clear Aβ from the blood, possibly leading to the elimination of Aβ from the brain. ApoE, which is mainly produced and secreted from astrocytes in the brain, is lipidated by ABCA1 to supply cholesterol/lipids to neurons and other cells through LRP1. ApoE isoforms likely affect LRP1-mediated Aβ metabolism by directly interacting with Aβ or competing with Aβ for receptor binding (Shinohara et al., 2017). Playing opposing roles, the LRP1 mediates the outflow of Aβ from the brain to the periphery, whereas RAGE promotes Aβ influx back into the CNS (Deane et al., 2004; Pflanzner et al., 2010;

Sagare et al., 2012; Zenaro et al., 2017). Several clinical studies reported a correlation between reduced LRP1 and elevated RAGE levels in AD pathology, promoting the accumulation of Aβ peptides in the brain parenchyma (Donahue et al., 2006; Zlokovic, 2008; Deane et al., 2012; Zenaro et al., 2017). In addition, 5xFAD mice that lack LRP1 receptor showed down-regulated plasma levels of $A\beta_{1\text{-}42}$ and increased levels of brain soluble Aβ (Storck et al., 2016). Data from rodents, non-human primates models of AD and people suffering from AD showed that endothelial expression of LRP1 reduces with aging (Kang et al., 2000; Shibata et al., 2000; Bading et al., 2002; Deane et al., 2004; Donahue et al., 2006; Bell and Zlokovic, 2009). Reduced expression of LRP1 at the BBB has been associated with cerebrovascular and focal parenchymal Aβ accumulations (Zlokovic et al., 2010). LRP1 can also undergo proteolysis and soluble LRP1 is released into the extracellular space under inflammatory conditions. This proteolysis is mediated by a disintegrin and metalloproteinase (ADAM) 10 and 17 activation (García-Fernández et al., 2021). When LRP1 is shed, its circulating form (i.e., soluble LRP1, sLRP1) is released into the blood providing a key endogenous peripheral “sink” activity for Aβ, as shown in a mouse model of AD (Sagare et al., 2012). In healthy humans and mice, sLRP1 binds 70% of circulating Aβ, thereby restricting Aβ’s free access to the brain (Sagare et al. 2007, 2012). In addition, the clearance function of LRP1 in different cells of the brain seems crucial as multiple cell-specific knockout mouse models have shown that LRP1 ablation leads to an accumulation of Aβ in the brain (Van et al., 2019). In the brain endothelium, LRP1 and RAGE facilitate efflux and influx of Aβ from the brain to the periphery and vice versa. Inhibition of LRP1 expression has been shown to cause vascular endothelial damage, significantly reducing Aβ clearance, and increasing the Aβ burden in brain tissue (Jaeger et al., 2009). Gali et al. reported a reduction in cerebral and cerebrovascular LRP1 levels in brains of 9-month-old 3XTg-AD mice (Gali et al., 2019).

1.17 ABC Transporter Proteins

ATP-binding cassette (ABC) transporters are a superfamily of transporters, which constitutes an extensive range of proteins capable of transporting molecular entities across biological membranes. The involvement of transporters like ABCB1 (P-glycoprotein), ABCG2 (BCRP), ABCC1 (MRP1), ABCA1, ABCA7, ABCG1, and ABCG4 in the transport of an extensive variety of biological substrates have been

described (De Boer et al.,2003; Loscher and Potschka, 2005). This transport is usually against a concentration gradient by adenosine triphosphate (ATP) hydrolysis limiting substrate retention and influx within the cells (De Boer et al.,2003; Loscher and Potschka, 2005). In humans, ABC transporters are expressed in BBB, parenchymal cells in brain, and blood-CSF barrier (Pereira et al., 2018). In addition to the physiological role of protecting the BBB, ABC transporters are also involved in the regulation of neuronal Aβ peptides levels. Changes in their expression could increase the risk of AD (Rapposelli et al., 2009; Nicolazzo and Mehta, 2010; Abuznait et al., 2011). Altered expression of ABC transporters at the BBB can impair its ability to effectively clear neuronal Aβ peptides. This leads to aggregation of Aβ peptides on the blood vessels of the brain, known as cerebral amyloid angiopathy (CAA), the primary cause of vascular dementia in older population (Abuznait and Kaddoum, 2012).

The ABC transporters are involved in detoxifying activities in the brain as they have been shown to facilitate the extraction of interstitial fluid (ISF) and cerebrospinal fluid (CSF) metabolites into the peripheral blood and complement the selective inhibition of toxic substrates into the CNS by the tight junctions of the BBB (Zlokovic, 2008; Qosa et al., 2015; Saunders et al., 2016). In addition, the expression of ABC transporters in glial and neuronal cells enhances waste regulation and restricted passage of xenobiotics in the CNS (ElAli and Hermann, 2011).

Impaired functions of ABCA and ABCG families of transporters have been implicated in degenerative diseases of the brain as balanced concentration of cholesterol is importance for the maintenance of the CNS (Pereira et al., 2018). Changes in the expression of ABC transporters significantly impact the production and deposition of Aβ plaques thereby enhancing the development of toxic Aβ aggregates and oligomers (Bell and Zlokovic, 2009). These transporters can exhibit either protective or predisposing functions, related to the trafficking of cholesterol within the cells thereby impacting the pathology of AD (Abuznait and Kaddoumi, 2012; Wolf et al., 2012). Targeting the activities of these transporters could be a therapeutic concept for AD. Using a mouse model of AD, Fitz et al. reported that treatment with LXR agonists increased ApoE and ABCA1 levels, which correlated with cognitive improvements and reduced Aβ deposition (Fitz et al., 2010).

1.18 Autophagy and protein Clearance in AD

Amyloidogenic Aβ peptides are known to aggregate and oligomerize, leading to misfolded protein-induced stress in the endoplasmic reticulum (Fonseca et al., 2013). The two key processes of autophagy and proteasomal degradation are essential for regulating the degradation of cellular proteins and maintaining proteostasis (Boland et al., 2018; Evrard et al., 2018). Both processes can degrade fully folded as well as misfolded and aggregated proteins to reduce protein stress. Autophagy is the transport of cytoplasmic constituents into lysosomes (Mizushima, 2007). Autophagy is a well-known surveillance system that contributes to proteostasis and lysosomal degradation (Bourdenx et al., 2021). Loss of proteostasis increases with age as well as in neurodegenerative diseases such as AD (Ashkavand et al., 2020). Furthermore, defective autophagy has been proposed to be actively involved in the accumulation of protein aggregates in the elderly as well as in brain degenerative processes (Metaxakis et al., 2018). Autophagy is sub-divided into 3 groups namely: macro-autophagy (MA), micro-autophagy (MI), and chaperone-mediated autophagy (CMA) (Li et al., 2011).

Macro-autophagy is characterized by membrane elongation, which results in the formation of a double-membraned structure called an autophagosome that contains sequestered cytoplasmic material and eventually fuses with lysosomes to have its contents degraded (Nakatogawa, 2020). Macro-autophagy is further classified into selective and non-selective types, with the former specifically recognizing cargo proteins via various macro-autophagy adaptors/receptors. Macro-autophagy is strongly induced by starvation or stress (Yamamoto and Matsui, 2023).

Micro-autophagy involves inward membrane deformation of the lysosomal membranes (or endosomal membranes in endosomal micro-autophagy (Mejlvang et al., 2018)) to generate intraluminal vesicles containing cytosolic materials that are eventually broken down in the lysosomes (Schuck, 2020; Wang et al., 2023). In endosomal micro-autophagy, a portion of endosomal intra-luminal vesicles is thought to be released to the extracellular space as exosomes.

Macro-autophagy involves membrane elongation and micro-autophagy involves membrane internalization, and both pathways undergo selective or non-selective processes that transport cytoplasmic components into lysosomes to be degraded

(Figure 11). CMA, however, involves selective incorporation of cytosolic materials into lysosomes without membrane deformation (Yamamoto and Matsui, 2023). During macro-autophagy, autophagosomes deliver cytoplasmic constituents to endosomes or lysosomes, whereas during micro-autophagy lytic organelles take up cytoplasm directly (Schuck, 2020). Cargo recognition mechanisms are at least partially shared between macro-autophagy and micro-autophagy (Yamamoto and Matsui, 2023).

In chaperone-mediated autophagy (CMA), membrane deformation is not involved (Kaushik and Cuervo, 2018) but substrate targeting requires recognition of a pentapeptide motif (KFERQ- like) in the substrate protein by the cytosolic chaperone HSPA8/HSC70 (Bourdenx et al., 2021). When the substrate/chaperone complex binds at the lysosome surface to LAMP2A (lysosomal-associated membrane protein 2A), this triggers the LAMP2A multimerization into a translocation complex after substrate unfolding, mediating its lysosomal internalization for degradation (Bourdenx et al., 2021; Hosaka et al., 2021). CMA activity is at least partly regulated by the amount of LAMP2A. It has been reported that CMA activity is also correlated with macro-autophagy activity, which reflects crosstalk between CMA and macro-autophagy (Yamamoto and Matsui, 2023).

Several genetic risk variants for LOAD have been linked with autophagy (Acker et al., 2019). Reduced expression of autophagy genes for autophagosome formation, such as Beclin 1 was shown in the susceptible brain regions of LOAD with worsened cognitive functions and increased amyloid plaque load as resultant effects of the suppression of these genes in AD experimental models (Pickfold et al., 2008, Lachance et al., 2019). Expression level of Beclin 1, a key protein necessary to initiate autophagy is significantly downregulated in early stage of AD suggesting that reduced Beclin 1 level promotes neurodegeneration and accelerates the accumulation of Aβ (Pickford et al., 2008; Lee and Gao, 2015). de la Cueva et al. (2022) APP/PS1 mice using suggested that Aβ overload may increase autophagy in addition to increasing mitophagy by increasing the autophagy from early stages of the amyloidogenic process.

Reports from both *in vitro* and *in vitro* suggested that large amount of BACE1 is recruited into autophagy vesicles and transported to the soma, thereby augmenting transport to the lysosomes for degradation (Feng et al., 2017). However, in diseased

condition like AD, dysfunctional autophagy mechanism causes an impaired retrograde transport, resulting in accumulation of BACE1 and as a consequence enhances the processing of APP by BACE1 in axons (Cacace et al., 2016). Function of intracellular organelles like lysosomes are interfered with as a result of large amount of Aβ deposition, thereby increasing the accumulation of Aβ and promoting the progression of AD (Sasahara et al., 2013).

Furthermore, several studies reporting the accumulation of immature autophagosomes in dystrophic neurites in AD brains demonstrates dysfunctional autophagosome clearance in neurons (Nixon et al., 2005; Tammineni et al., 2017; Lee et al., 2022). Recently, Choi and colleagues (2023) demonstrated the protective role of microglial autophagy in regulating the homeostasis of amyloid plaques and preventing senescence; suggesting it as a potential therapeutic strategy in AD.

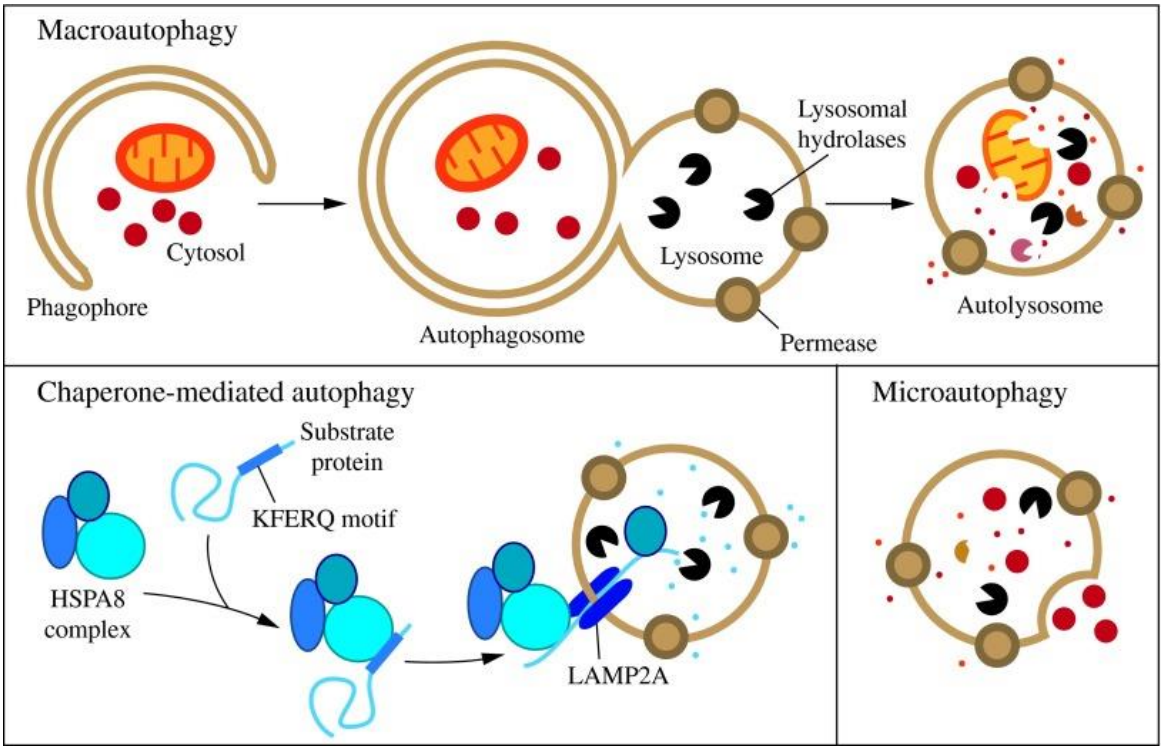

Figure 11: An overview of Autophagy (Adapted with permission from Parzych and Klionsky, 2014)

1.19 mTORC Signaling in AD

The mammalian target of rapamycin (mTOR) is a conserved protein kinase that plays a key role in controlling a balance between protein synthesis and degradation (Oddo,

2012). Its interaction with other proteins results in the formation of two major complexes namely, the mTOR complex 1 (mTORC1), that controls protein homeostasis and its activities are inhibited when treated with rapamycin as well as the mTORC2, which controls cellular shape by modulating actin function and is insensitive to rapamycin (Loewith et al., 2002, Wullschleger et al., 2006). Several studies have shown an increase of mTOR signaling following Aβ administration (Vander Haar et al., 2007; Ito et al., 2006; 2007; Zhang et al., 2009). The link between Aβ accumulation and the upregulation of mTOR signaling is supported by a study showing exposed primary neurons to different concentrations of synthetic Aβ monomers and Aβ oligomers for 24 hours results in increased phosphorylation of mTOR proteins (Bhaskar et al.,2009). mTOR is activated by upstream components such as phosphoinositide 3-kinase (PI3-K)/protein kinase B (Akt), glycogen synthase kinase 3 (GSK3), AMP-activated protein kinase (AMPK), and insulin/insulin-like growth factor 1 (IGF-1). GSK3 isoforms (GSK3α/β) are crucial factors in numerous metabolic processes including cell cycle regulation, glycogen metabolism, transcription, translation (Buller et al., 2008). Compelling evidence indicates that Aβ deposits hyperactivate mTOR which in turn hyper-phosphorylates tau, forming PHF's (Paired helical filaments), and NFT's (Neurofibrillary tangles). In addition, GSK3 hyper-phosphorylates tau at serine and threonine residues (Cai et al., 2015) and GSK3 hyperactivation is considered a link between amyloid pathology and tau hyperphosphorylation. GSK3β but not GSK3α has been reported to co-localize with neurofibrillary tangles (NFTs). GSK3β was reported in neurons in the early stages of tangle formation, implicating kinase active GSK3β in the pathogenesis of NFTs (Yamaguchi et al. 1996; Pei et al., 1999). Phosphorylation of GSK3α/β at Ser21/Ser9 residues within the N-terminal domain has been reported to inactivate this kinase.

1.20 ASX as a therapeutic candidate for T2D and AD

Current treatment strategies for AD such as acetylcholinesterase inhibitors (AChEI) (tacrine, galantamine, rivastigmine and donepezil) (Summers et al., 1981; 1986, Birks, 2006) and memantine, a low affinity NMDA receptor antagonist (McShare et al., 2006; Schmidt et al., 2015) focus on increasing cholinergic activity in the brain of AD patients to address the cholinergic deficit which, however, only brings about symptomatic relief without addressing the probable main and underlying causes of AD involving tau proteins and β-amyloid proteins. Furthermore, anti-tau antibodies

have failed in clinical trials (Mullard et al., 2021; Dam et al., 2021; Höglinger et al., 2021; Shulman et al., 2021; Monteiro et al., 2021; Slomski, 2022), and two recently approved anti-amyloid monoclonal antibodies, Aducanumab and Lecanemab, are expensive and have considerable side effects (Mintun et al., 2021; Swanson et al., 2021; Lacorte et al., 2022; Cummings, 2023). It is, therefore, important to look for other possible interventions to develop new experimental drugs and/or repurpose approved drugs that target tau proteins and amyloid proteins and that are relatively inexpensive and easily accessible.

ASX is a lipid-soluble keto carotenoid synthesized by a number of microorganisms and various types of marine organisms (Choi, 2019). ASX is one of the most potent antioxidants found in nature (Ambati et al., 2014). ASX, a xanthophyll carotenoid can be obtained from Algae species like *Chlorella zofingiensis*, *Chlorococcum*, and *Phaffia rhodozym, Hematococcus pluvialis* (Ambatti et al., 2004). ASX can also be obtained in natural or supplemented form from aquatic foods like salmon, trout, krill, shrimp, crayfish, and crustaceans. Studies from our group and others have also reported the ability of ASX to cross the BBB thereby ameliorating BBB dysfunction (Zhang et al., 2014; Danesh-Fanaee et al., 2019).

PPARα is a member of the nuclear receptor PPAR family (Yoo et al., 2021). Natural ligands like fatty acid and synthetic ligands such as hypolipidemic fibrates activate PPARα, resulting in a stimulation of tart gene transcription via formation of heterodimer complexes with retinoid x receptor (RXR) (Fruchart et al., 1999). ASX activates PPARα and antagonizes PPARγ, another member of the PPAR family (Jia et al., 2012; Choi et al., 2019). ASX was reported to increase the expression of peroxisome proliferator-activated receptor-alpha (PPARα), downregulate peroxisome proliferator-activated receptor-gamma (PPARγ), to stimulate the bile acid synthesis pathway and inhibit cholesterol biosynthesis (Jia et al., 2012). In addition, ASX exhibits potential pharmacological activities, like immunomodulation, antioxidant, anti-apoptotic, anti-inflammatory, anti-cancerous and antidiabetic properties (Ambati et al., 2014; Zhang et al., 2014a; 2014b; Zhou et al., 2015). The neuroprotective effects of ASX have been corroborated previously *in vitro* (Lobos et al., 2016), *in vivo* (Che et al., 2018; Rahman et al., 2019; Danesh-Fanaee et al., 2019) and in clinical studies (Ito et al., 2018). Due to ASX's high antioxidant and anti-inflammatory properties,

several studies suggest its potentials in ameliorating wide range of brain disorders like AD, Parkinson, depression, brain stroke and autism (Cunha et al., 2023).

In a randomized double-blind placebo-controlled study by Katagiri et al., ASX supplementation was reported to improve cognition in healthy middle-aged and elderly subjects who complained of age-related forgetfulness (Katagiri et al., 2015). Furthermore, Yook et al., reported that ASX supplementation improved adult hippocampal neurogenesis (ADH), plasticity and spatial memory in male C57BL/6J mice fed diet supplemented with ASX (Yook et al., 2015). ASX was also reported to protect against deleterious effects caused by high glucose exposure (Kim et al., 2009). In addition, Xu and colleagues showed that ASX was able to enhance cognitive function and reduce cerebral inflammation in a diabetic rat model (Zu et al., 2015).

Recently, we reported the Aβ clearance ability of ASX in primary porcince brain capillary endothelial cells (pBCECs) and its anti-inflammatory potentials in LPS stimulated Organotypic hippocampal slice culture (OHSC) (Babalola et al., 2023).

2 STUDY RATIONALE AND HYPOTHESIS

Aggregation and misfolding of Aβ and tau proteins are believed to arise from post-translational modification processes like phosphorylation, truncation, racemization, isomerization and pyroglutamylation. Defective degradation and clearance of misfolded amyloid-β as well as inflammation *per se* are crucial players in the pathology of AD. A defective transport across the blood-brain barrier is causative for amyloid-β (Aβ) accumulation in the brain and has been reported to be an early event in the pathophysiology AD. Numerous studies link metabolic dysfunctions such as obesity, T2D, and dyslipidemia with the pathophysiology of AD. However, to date, no disease modifying therapeutic agents with clear clinical benefits exist. Tau targeting antibodies have failed in clinical trials and there are controversies regarding the already FDA approved anti-amyloid antibodies. Hence, there is an urgent need to look into other potential strategies to devise new experimental drugs and/or repurposing approved drugs targeting tau proteins and β-amyloid proteins that are relatively cheap and easily accessible.

To this end, we hypothesized that adding another risk factor (T2D) beside pyroglutamylation (hQC) could lead to a more severe AD pathology and that ASX supplementation could ameliorate pathophysiological manifestations associated with AD. To test our hypothesis *in vitro*, we used a BBB model composed of primary porcine brain capillary endothelial cells (pBCEC) and Organotypic hippocampal slice culture (OHSC) containing neurons, astrocytes and microglia cells. For *in vivo* studies we worked with APPxhQC mice, a model for pGlu-Aβ and their non-transgenic (NTG) littermates.

Hence, the dissertation is divided into two parts.

Part One: *In vitro* studies

Aim: To interrogate the Aβ clearance and anti-inflammation activities of ASX *in vitro*

We evaluated:

- the ability of ASX to lower APP levels and clear Aβ at the BBB even in the presence of exogenous Aβ in pBCEC via endothelial receptor mediated efflux (ABC Transporters and LRP1).

- the anti-inflammatory activity of ASX in LPS stimulated OHSC.

Part 2: *In vivo* studies

Aim 1: To understand the impact of T2D on AD pathology in APPxhQC mice expressing higher levels of pGlu-Aβ peptides and their non-transgenic littermates.

We examined:

- Impact of the presence or absence of hQC (pyroglutamylation)/APP and T2D mimicking diet on glycemic and lipid parameters.
- Impact of the presence or absence of hQC (pyroglutamylation)/APP and T2D mimicking diet on Aβ metabolism.
- Impact of the presence or absence of hQC (pyroglutamylation)/APP and T2D mimicking diet on cognitive function.
- Impact of the presence or absence of hQC (pyroglutamylation)/APP and T2D mimicking diet on peripheral (liver) and cerebral (brain) nutrient sensing pathways.

Aim 2: To investigate if ASX supplementation could ameliorate accompanying pathophysiological manifestations due to combined effects of the presence or absence of hQC (pyroglutamylation)/APP and T2D mimicking diet and the mechanism(s) involved.

We evaluated:

- Effect of ASX supplementation on glycemic and lipid parameters.
- Effect of ASX supplementation on Aβ burden.
- Effect of ASX supplementation on cognition.
- Effect of ASX supplementation on nutrient sensing pathways.

3.0 MATERIALS AND METHODS

3.1 Chemicals and reagents used for *in vitro* studies

Chemicals bought are listed in Table 2

Table 2: Cell culture reagents and chemicals

Product	Company
75 cm^2 cell culture flasks	Greiner Bio-One
6-,12-well and 96-well plates	Greiner Bio-One
Fisherbrand™ Superfrost™ Plus	Fischer Scientific
Medium 199 (1x)	Life technologies
Minimum essential medium (MEM, 10x)	Life technologies
Dispase	Life technologies
Collagen G from bovine calf skin	M&B Stricker
Penicillin/streptomycin/gentamycin	PAA Laboratories
Trypsin-ethylene diamine tetra acetic	PAA Laboratories
Horse serum	PAA Laboratories
L-glutamine	PAA Laboratories
Collagenase/dispase	Roche
Percoll® pH 8.5- 9.5	Sigma- Aldrich
Dextran	VWR
ASX	Sigma- Aldrich

3.1.1 Phosphate buffer saline (PBS)

40 g NaCl, 1.5 g KCl, 0.1 g KH2PO4, 0.457 g Na2HPO4 (2 H2O) and 10 g glucose were weighed and dissolved in five liters of double distilled water (d2 H20), filter sterilized and autoclaved.

3.1.2 Collagenase/dispase solution

100 mg collagenase/dispase was dissolved in 10 mL plating medium A, sterile filtered through a 0.2 µm pore size nylon wool filter, 350 µl aliquots were made and stored at – 20°C.

3.1.3 Dextran solution

200 g dextran, 2.4 g NaHCO3 and 109.1 ml MEM (10x) were dissolved in 1.2 L of d2H2O, stirred overnight at 4°C to dissolve, d2H2O was added to adjust density to 1.0612. The solution was autoclaved and stored in 500 ml glass bottles at 4°C.

3.1.4 Percoll® biphase solution

- 1.03 g/ml density solution: 40 ml 1 X PBS, 9 ml Percoll® pH 8.5- 9.5 and 1 ml DMEM (1x) were mixed and stored in 50 ml falcon tubes at 4°C.
- 1.07 g/ml density solution: 20 ml 1 X PBS, 27 ml Percoll® pH 8.5- 9.5 and 3 ml DMEM (1x) were mixed and were stored as 50 ml aliquots at 4°C.

3.1.5 Collagen G solution for coating flasks and cell culture plates

Mix 450 µl (for 60 µg/ml) or 900 µl (for 120 µg/ml) of Collagen G stock solution (4 mg/ml) with 30 ml PBS (1x) freshly for every coating experiment.

3.1.6 Preparation medium

M199 (1x) medium with 1% penicillin/ streptomycin, 1% gentamycin and 1 mM L-glutamine.

3.1.7 Plating medium A

M199 (1x) medium with 10% horse serum, 1% penicillin/ streptomycin, 1% gentamycin and 1 mM L-glutamine.

3.1.8 Plating medium B

Same as medium A without 1% gentamycin.

3.1.9 Serum free (SF) medium

To 500 ml Medium M199 (1x), 1 % penicillin/ streptomycin and 1 mM L-glutamine were added and the resulting medium was stored at 4°C.

3.1.10 Preparation of slicing solution for organotypic hippocampal slice cultures (OHSC)

One µl of Glucose (20 µM) was added to 50 ml Opti-MEM, solution was equilibrated at 4°C.

3.1.11 Preparation of HBSS medium for organotypic hippocampal slice cultures (OHSC)

Two hundred and fifty µl of Glucose (10 mM) was added to 25 ml CMF-HBSS, solution was equilibrated at 4°C.

3.1.12 Preparation of culture medium for organotypic hippocampal slice cultures (OHSC)

1250 µl of Glucose (25 mM), 0.5 % penicillin/ streptomycin, 25 % Horse serum, 25 % CMF-HBSS were added to 25 ml MEM/EBSS medium.

3.1.13 Dexamethasone stock preparation

0.4 mg of Dexamethasone purchased from Sigma Aldrich was dissolved in 0.102 ml DMSO (10 mM) as a stock solution and freshly.

3.1.14 Lipopolysaccharide (LPS) stock preparation

LPS purchased from Sigma Aldrich was prepared as 1000 µg/ml stock solution and stored at 4°C

3.1.15 Amyloid-β peptide stock solution

One mg recombinant human amyloid-beta peptide (Aβ1-40) vials were purchased from Rpeptide, USA, as hexafluoroisopropanol (HFIP) dissolved films. Each 1 mg vial was dissolved in 1 ml of 1% NH_4OH, vortexed for 30 sec until the film was invisible. Twenty µl aliquots of 1 µg/µl $A\beta_{40}$ stocks were made, stored at - 20°C and were used within 1 month.

3.1.16 ASX stock solution

2.7 mg of ASX purchased from Sigma Aldrich was dissolved in 4.54 ml DMSO (1 mM) as a stock solution and stored in aliquots at -20^{o}C.

3.1.17 Fenofibrate stock solution

2.4 mg of Fenofibrate bought from Sigma Aldrich was dissolved in 6.65 ml DMSO (1 mM) as a stock solution and stored in aliquots at -20^{o}C.

3.1.18 GW6417 stock solution

1 mg of GW6417 purchased from Cayman chemicals was dissolved in 1 ml DMSO (6.1 mM) as a stock solution and stored in aliquots at -20^{o}C.

3.1.19 Bafilomycin A1 stock solution

Bafilomycin A1 purchased from Sigma Aldrich was dissolved in DMSO as 10 µM stock solution and stored in aliquots at -20^{o}C.

3.2 Chemicals and solutions used for RNA isolation, cDNA synthesis and quantitative Real time PCR (RT-qPCR)

All products and reagents used for RNA isolation and RT-qPCR are listed in Table 3. Pre-validated primers for RT-qPCR were purchased from Invitrogen by Thermo Fisher Scientific (Table 3)

Table 3: Materials used for RNA isolation, cDNA synthesis, and RT-qPCR

Product	Company
SsoAdvanced™ Universal SYBR®	Biorad
Hard-Shell® Low-profile thin-wall 96-	Biorad
High-Capacity cDNA Reverse	Thermo Fisher Scientific
Microseal ‘B’ Adhesive seals for PCR	Biorad
0.2 ml PCR tubes	Biorad
Icycler iQ™, Real-time PCR detection	Biorad
OneTouch filter-tips, 10 µl	Biozym
Nuclease-free water	Carl Roth
TriReagent RT	Molecular Research Center, Inc
PCR thermal cycler XT 96	VWR

3.3 Isolation and culture of primary porcine brain capillary endothelial cells

Primary porcine brain capillary endothelial cells (pBCEC) were isolated from 3 pooled hemispheres of freshly slaughtered pigs (~6 months old, male and female) according to the protocol previously described by Franke and colleagues with minor modifications (Chirackal et al., 2014; Franke et al., 2000). Porcine brains were obtained from the local slaughterhouse and meninges and blood vessels were removed. The gray and white matter of the brain cortex were then chopped using a cutter with rolling plates. To isolate the capillaries, dispase, a protease (70 mg/brain) was dissolved in 40 ml of Preparation Medium (Earle's medium M199 1X, 1% P/S, 1% gentamycin and 1 mM L-glutamine), chopped brains added and incubated for 1 h in the water bath at 37 °C with gentle stirring. After incubation, 150 ml dextran solution (200 g dextran, 2.4 g $NaHCO_3$ and 109.1 ml MEM (10x) were dissolved in 1.2 L of d2H_2O, stirred overnight at 4°C to dissolve, density was adjusted to 1.0612 g/l) was added, mixed, and the suspension was centrifuged (8,000 *g*, 10 min, 4°C). The pellet was resuspended in Medium A (Earle's medium M199 1X, 1% P/S, 1% gentamycin, 1 mM L-glutamine and 10% porcine serum) and the capillaries were isolated by filtering the suspension through a nylon mesh. Then, capillaries were disrupted enzymatically by adding 350 µl collagenase/dispase (10 mg/ml). The suspension was carefully pipetted onto a percoll bi-phase gradient (15 ml of 1.07 g/ml percoll solution on the bottom, 20 ml of 1.03 g/ml percoll solution on top) and centrifuged (1,300 *g*, 10 min, RT) in a swinging bucket rotor. Endothelial cells were aspirated from the interphase and washed once with Medium A. Cells were plated onto collagen-coated 75 cm² cell culture flasks in Medium A and incubated at 37°C in humified air containing 5% CO2. After 24 h, pBCEC were washed twice with 1x PBS and cultured in Medium B (Earle's medium M199 1X, 1% P/S, 1 mM L-glutamine and 10% porcine serum) until reaching confluency. After 3 days, confluent pBCEC were trypsinized using 0.5% trypsin solution and split onto collagen-coated 6-well (60 µg/ml collagen) or chamber slides (120 µg/ml collagen) and incubated for 3 days in Medium B. Media were changed to serum-free on the day of treatment and pBCEC were incubated with ASX (10 µM), GW6417 (1 µM) and fenofibrate (1 µM) for 16 hour prior to $A\beta_{40}$ (240 nM) for another 6 hour (Gali et al., 2019) or bafilomycin A1 (100 nM) for 4 hour. Media were removed, cells were washed twice with cold 1x PBS

and lysed in either protein lysis buffer (50 µl/well) or Tri Reagent (500 µl/well) for protein and RNA isolation, respectively.

3.4 Culture and treatment of organotypic hippocampal slice cultures (OHSC)

Organotypic hippocampal slice cultures were performed according to the protocol previously described by Croft and others (Croft et al., 2019). P9/P10 mouse pups were decapitated, skin and skull gently removed, and brains immersed in slicing medium. Brains were hemisected and the hippocampus was isolated. The hippocampus was placed on the cutting disc of a McIlwain Tissue Chopper (Cavey Laboratory Engineering Co, Surrey, UK). Hippocampal slices of 300 µm thickness were chopped transversely. Nine slices per hippocampus were placed onto porous (0.4 µm), transparent membrane inserts (30 mm in diameter) and incubated for 1 h on ice in HBSS medium containing 10 mM glucose. Afterwards inserts were transferred to fresh 6-well plates containing 1.2 ml culture medium (50% MEM/EBSS, 25% horse serum, 25%CMF-HBSS, 25 mM glucose, 0.5% pen/strep). Slices were maintained at 37°C and 5% CO_2. The full medium was changed between days in vitro (DIV) 3 and 5. On DIV8, culture medium was replaced with serum-reduced treatment medium (MEM/EBSS, 5% horse serum, 25 mM glucose) and slices were maintained in this medium for the remaining treatment period. After changing to serum-reduced medium, ASX (50 µM) and the control compound dexamethasone (10 µM) were added 2 hours before LPS stimulation (10 ng/ml in medium). Cells treated with vehicle and cells treated with LPS alone served as controls. Twenty-four hours after LPS stimulation, cell supernatants were collected for cytokine measurements. Slices were lysed with 500 µl of TRIzol for RNA and protein isolation.

3.5 RNA isolation from mouse tissue or endothelial cells

Cell culture plates were transferred on ice to a fume hood, 500 µl Tri reagent was added to each well, and contents were scraped and transferred into 1.5 ml Eppendorf tubes. For liver sample, 1 ml tri reagent was added to liver tissues in each tube. Tissue samples with 1 ml of tri reagent were homogenized with Ultra-Turrax homogenizer prior to incubation. Tubes were incubated at room temperature (RT) for 5 min to allow complete dissociation of nucleoprotein complexes. Fifty µl 4-bromoanisole (BAN) phase separation reagent was added, tubes were vortexed for 10 seconds and, were incubated for 20 min at RT. After incubation, tubes were centrifuged at 12,000 g at 4°C for 15 min. Following centrifugation, phase separation

is achieved, indicated by residual DNA, proteins and polysaccharide precipitate in the organic phase at the bottom of tube, while RNA residues stay as soluble supernatant. 400 µl of supernatant was carefully pipetted in to a new tube without collecting the residuals at the interface. Equal amounts of isopropanol were added to each tube and RNA was precipitated for 10 min at RT. Next, tubes were centrifuged 12,000 g for 10 min to pellet the RNA precipitate. Washing was performed by adding 500 µl of 75% ethanol (v/v) to each tube and centrifugation at 8,000 g for 5 min, washing step with 75% ethanol (v/v) was repeated once more to remove residual isopropanol contamination from RNA pellet. The RNA pellet was dissolved in 60 µl of RNAse-free water and incubated for 10 min at 55°C on a heat block with shaking to dissolve the pellet in water.

RNA concentrations were measured at 260 nm using NanoDrop (Thermo scientific, Wilmington, USA). Two µl RNA solution was used to determine the concentration. Using the following equation RNA concentration was determined:

c(ngRNA/µl) = λ 260nm x 40

3.5.1 cDNA preparation

Complementary DNA was prepared from RNA by reverse transcription. One µg RNA in 10 µl (adjusted with NF d2H2O) was reversely transcribed by using a High-capacity cDNA Reverse Transcription kit (Applied Biosystems, Foster City, CA).

Table 4: High-Capacity cDNA Reverse Transcription (master mix composition)

Component	Volume (µl) /reaction
10 x RT buffer	2.0
25x dNTP-Mix (100mM)	0.80
10x Random Primer	2.0
Multiscribe reverse transcriptase	1
NF H_2O	4.20
1 µg RNA/10 µl NF H_2O	10
Total volume per reaction	20

Table 5: Reverse transcription thermal cycling conditions

Steps	S1	S2	S3	S4
Temperature	25°C	37°C	85°C	4°C
Time	10 min	120 min	5 sec	∞

3.5.2 RT-qPCR

For RT-qPCR analyses, cDNA (1000 ng/20 µl) was diluted 1:10 in NF d2H_2O to achieve 5 ng/µl cDNA. Two µl of 5 ng/µl cDNA, 0.2 µl of forward and reverse primers (stock solution of 100 µM, diluted 1:10 with NF H_2O), 2.6 µl of NF H_2O and 5 µl SsoAdvanced™ Universal SYBR® Green Supermix were pipetted into a Hard-Shell 96 well PCR plate.

Table 6: Primers used for RT-qPCR

Gene	Specie	Forward sequence	Reverse sequence
gapdh	*Mus musculus*	GACTTCAACAGC	TCCACCACCCTGT
neprilysin	*Mus musculus*	TCCTGACTATCA	GACGTTGCGTTTC
lrp1	*Mus musculus*	CCGCATCTTCTT	ACAGAGCCCACA
abca1	*Mus musculus*	ATTGCCAGACGG	TGCCAAAGGGTG
abcg1	*Mus musculus*	CAAGACCCTTTT	GCCAGAATATTCA
fgf21	*Mus musculus*	TCCAAATCCTGG	CAGCAGCAGTTC
pparα	*Mus musculus*	AGAGCCCCATCT	ACTGGTAGTCTG
pparγ2	*Mus musculus*	GATGCACTGCCT	GAATGGCATCTCT
pgc1α	*Mus musculus*	AGCCGTGACCA	GCTCATGGTTCTG
pgc1β	*Mus musculus*	GGACGCCAGTG	TTCATCCAGTTCT
srebf1	*Mus Musculus*	GGAGCCATGGA	GGCCCGGGAAGT
srebf2	*Mus musculus*	CCAAAGAAGGA	CGCCAGACTTGT
lxrα	*Mus musculus*	CTCAATGCCTGA	TCCAACCCTATCC
cd 31	*Sus scrofa*	CGAGGTCTGGG	AGCCTTCCGTTCT
zo-1	*Sus scrofa*	ACCCACCAAACC	CCATCTCTTGCTG
pdgfr-β	*Sus scrofa*	TGGACACCGGA	ACTCGGCATGGA
gfap	*Sus scrofa*	ACATCGAGATCG	ACATCACATCCTT

map2	*Sus scrofa*	TGCCGGAAGAG	CTGATCAAACTCC
abca1	*Sus scrofa*	GCCATTCTCCGG	GGCTTCACGCCG
abcg1	*Sus scrofa*	GTTCTCCACGTC	TCAGGGTTCTTG
lrp1	*Sus scrofa*	GCAGATGTATCA	GGGTGCTAGAGC
tubulin	*Sus scrofa*	CCCTCAGCCTTC	GGTTACCCAGAA
hprt	*Sus scrofa*	AGGACCTCTCGA	CAGATGGCCACA
arginase 1	*Mus musculus*	TGCTCACACTGA	TCTACGTCTCGCA

Gene	Specie	Assay Name	Cat No	Lot
il-10	*Mus musculus*	Mm_Il10_1_SG	QT00106169	231424760
il-6	*Mus musculus*	Mm_Il6_1_SG	QT00098875	231424816
itgam	*Mus musculus*	Mm_Itgam_1_SG	QT00156471	341211764
hprt	*Mus musculus*	Mm_Hprt_1_SG	QT00166768	231424759

Table 7: Real-time PCR mix

Constituent	Volume
SsoAdvanced™ Universal SYBR®	5 µl
cDNA	2 µl
Forward primer (0.2 µM)	0.2 µl
Reverse primer (0.2 µM)	0.2 µl
Nuclease free water	2.6 µl
Total volume	10 µl

The 96-well plate was centrifuged for 1 min at 400 rpm to collect the mixture at bottom of the well and was loaded onto an Icycler iQ™, RT-qPCR Detection System (Biorad).

Table 8: RT-qPCR program conditions

Steps	Temperature	Time	Cycles

Denaturation	95°C	5 min	1
Amplification	95°C	10 sec	40
Melting Curve	95°C	10 sec	1
Cool down	40°C	20 sec	1

Tubulin, hypoxanthine guanine phosphoribosyl transferase (HPRT) and Glyceraldehyde 3-phosphate dehydrogenase (GAPDH) were used as housekeeping gene for relative gene expressions. The 2-ΔΔCT method was used to calculate relative gene expression of desired gene, later normalized to the house-keeping genes

3.6 Protein isolation from cell and tissues

Proteins from pBCEC were isolated by lysing the samples in Protein lysis buffer (PLB) by sonicating the lysates in water bath with ice (3 min X 2 times), vortexing the tubes for 30 sec and by centrifuging (Microcentrifuge, Qualitron DW- 41) the lysates at 12,000 g for 10 min at 4°C. Supernatants containing proteins were collected in fresh tubes and pellets were discarded. For isolation of secreted proteins, pBCEC medium was collected and stored at -80°C. Proteins were precipitated by adding 30% (v/v) trichloroacetic acid. After 1 hour incubation on ice, the suspension was centrifuged at 10,000 g for 10 min at 4°C. The pellet was washed twice with ice-cooled acetone, centrifuged at 10,000 g for 10 min at 4°C, and dissolved in 1x sample buffer (Biorad) containing 1x reducing agent (Kober et al., 2017). Brain and liver tissues were weighted and lysed in 10 volumes of tissue homogenizing buffer (TBH) containing protease and phosphatase inhibitor using Ultra-Turrax T8 Tissue homogenizer (IKA Labor Technik).

3.6.1 Determining protein concentration of cell or tissue lysates

To identify the protein concentration of tissue samples or cell lysates, Bicinchoninic acid assay (BCA) was performed. Bovine serum albumin (BSA) standards were prepared in PLB buffer from a BSA stock solution (2 mg/ml). A serial dilution of BSA standard was made to achieve concentrations from 2 mg/ ml to 0.125 mg/ml to attain a standard curve. Four µl of standard and protein samples were pipetted in replicates into a microplate well. BCA reagent A and B were mixed in a ratio 1:50, vortexed and

100 µl of the mixture was dispensed in the wells containing standards, samples and PLB blank. Plates were incubated for 30 min at 37°C in a water bath. After incubation, absorbance was determined at 562 nm using a plate reader. Protein concentration of each sample was determined using the linear regression of the BSA standard curve.

3.7 Western blotting (WB)

Table 9: Buffers and reagents used for WB

Product	Company
XT sample buffer (4x)	Biorad
XT sample reducing agent (20x)	Biorad
Blotting-grade blocker, non-fat dry milk	Carl Roth
Clarity Western ECL-Substrate	Biorad
IKA® Model MS1 minishaker	Carl Roth
Microcentrifuge, Qualitron DW- 41	Carl Roth
PhosSTOP™	Sigma Aldrich
Trans-Blot Turbo RTA midi 0.2 µM	Biorad
4–12% Criterion™ XT Bis-Tris Protein	Biorad
XT MES Running Buffer	Biorad
Pierce® BCA Protein Assay Kit	Thermo Scientific
BSA, 2 mg/ml	Thermo Scientific
ChemiDoc™ Imaging Systems	Biorad
Centrifuge Sigma 3K15 with angle	Sigma
Protease Inhibitor Cocktail tablets	Sigma Aldrich
Magnetic stirrer with heating, MR	VWR
Ultra-Turrax T8 Tissue homogenizer	IKA Labor Technik
Cell Proliferation Reagent WST-1	Roche
Spectro Star Nano	BMG LABTECH

Table 10: Wash buffer (TBS-T) (pH 8.5)

Compound	Volume
Tris, (1 M; pH 7.5)	20 ml
NaCl (5 M)	100 ml
Tween 20	1 ml
d2H2O	Up to 1 L

3.7.1 Tissue Homogenizing Buffer (THB)

Forty-two-point eight g of Sucrose, 10 ml Tris (1 M, pH 7.4), 5 ml EDTA (100 mM), 12.5 ml EGTA (40 mM) 1 tablet of protease inhibitor cocktail, 1 tablet of phosphatase inhibitor were dissolved in 300 ml d2H2O, the final volume was adjusted to 500 ml with d2H2O.

3.7.2 Protein lysis buffer (PLB)

Fifty mM Tris, pH 7.5, 10 mM EDTA, 1% Triton-X-100, 1 tablet of protease inhibitor cocktail, 1 tablet of phosphatase inhibitor were dissolved in 5 ml of d2H2O, the final volume was adjusted to 10 ml with d2H2O and 1 ml aliquots were stored at -20°C until use.

3.7.3 Blocking buffer

Blotting-grade blocker (non-fat dry milk) was dissolved in TBS-T to achieve 5% milk protein, herein referred to as blocking buffer.

3.7.4 Sample preparation and SDS-polyacrylamide gel electrophoresis (PAGE)

Equal concentrations of protein lysates were mixed with XT loading dye and reducing agent to achieve a 1X final concentration, samples were heated on a heat block at 95°C for 5 min to denature the proteins. Sample tubes were spun-down on a tabletop centrifuge to collect the mixture. Samples (10 or 20 µg of protein) were loaded onto 4–12% Criterion™ XT Bis-Tris Protein gels and electrophoresis were performed using MES running buffer, for 140V for 80 min to achieve separation of proteins.

3.7.5 Protein transfer from gel to membrane

Semi dry electrophoretic transfer of proteins to nitrocellulose membranes was done in a Trans-blot turbo transfer system (Biorad). Prior to building the sandwich in the cassette, membrane and transfer stacks were soaked in transfer buffer for 5 min to remove any trapped air bubbles. The transfer sandwich was prepared starting with the wetted transfer stack, membrane, gel and finally wetted transfer stack. Semi dry transfer was performed at 2.5V, 1.0A for 30 min or 2.5V, 2.5A for 7 min.

3.7.6 Ponceau S staining of proteins

Half a g of Ponceau S was dissolved in 25 ml acetic acid and the volume adjusted with d2H2O to 1 L. To stain proteins immediately after the transfer, blots were incubated with 50 ml of fresh Ponceau S solution for 10 min at RT with gentle shaking. After 10 min incubation, blots were washed with tap water 3 times until the background was clear. Ponceau S images were taken using a ChemiDoc™ imaging system. Immediately, blots were washed with tap water 3 X 5 min with shaking at RT to destain Ponceau S. After destaining, blots were processed for blocking.

3.7.7 Membrane blocking

Membranes were blocked using blocking buffer (pH 8.5) for 1 hour with constant gentle shaking at RT.

3.7.8 Primary antibody incubation

Primary antibodies were prepared in 5% non-fat dry milk protein or BSA (for phosphorylated proteins) dissolved in TBS-T (pH 8.5) according to the manufacturers' suggestions. Blots were incubated overnight at 4°C in a cold room with constant shaking.

3.7.9 Washing the blots

Washing was done using washing buffer (1x) (Table 10), 3 X 5 min at RT with constant shaking after every primary and secondary antibody incubations.

3.7.10 Secondary antibody incubation

Rabbit, mouse, and goat HRP labeled secondary antibodies were used. Antibody incubations were performed in 5% non-fat dry milk protein in TBS-T (pH 8.5) for 60 min at RT with constant shaking.

3.7.11 Signal detection on Western blots and semi-quantitative analysis

Signal detection was performed using Clarity Western ECL substrate (Bio-Rad, Germany). In brief, 8.5 X 13.5 cm blots were incubated with 1 ml ECL substrate mixture for 5 min at RT. Chemiluminescence was detected using a ChemiDoc™ imaging system. Signal quantification was performed by densitometry using ImageLab™ software, band intensities were normalized to corresponding band intensities of the housekeeping proteins GAPDH or Tubulin.

Table 11: List of antibodies used for western blotting

Antibody	Dilution	Company	Protein
Mouse anti-ABCA1	1:1000	Abcam	ABCA1
Rabbit-anti-LC3B	1:1000	Cell Signaling	LC3B I/II
Rabbit-anti-p62	1:1000	Cell Signaling	p62
Rabbit-anti-S6rp (5G10)	1:1000	Cell Signaling	S6rp
Rabbit-anti-p-S6rp	1:1000	Cell Signaling	p-S6rp
Rabbit-anti-p-mTOR	1:1000	Cell Signaling	p-mTOR
Mouse-anti-mTOR	1:1000	Cell Signaling	mTOR
Mouse-anti-Tubulin	1:1000	Cell Signaling	Tubulin
Goat anti-rabbit IgG-	1:10000	Cell Signaling	
Goat anti-mouse IgG-	1:5000	Cell Signaling	
Rabbit -anti-AKT (pan)	1:2000	Cell Signaling	Total AKT
Rabbit-anti-p-AKT	1:2000	Cell Signaling	p-AKT
Rabbit-anti- p44/42	1:2000	Cell Signaling	ERK
Rabbit-anti-p- 44/42	1:2000	Cell Signaling	p-ERK
Rabbit-anti-p-65NFκB	1:2000	Cell Signaling	p-65 NFκB
Rabbit-anti-p38-MAPK	1:2000	Cell Signaling	p-38

Rabbit-anti-p-p38 MAPK	1:2000	Cell Signaling	p-p38
Rabbit-anti-LRP1	1:1000	Abcam	LRP1
Rabbit-anti-IR-β (4B8)	1:1000	Cell Signaling	IR-β
Rabbit-anti-LAMP2A	1:1000	Abcam	LAMP2A
Rabbit-anti-Beclin1	1:1000	Cell Signaling	Beclin1
Rabbit-anti-ATG5	1:1000	Cell Signaling	ATG5

3.8 Immune-fluorescent staining (IF) for pBCECs

For immunocytochemistry (Zandl-Lang et al., 2018), pBCEC were cultured on Lab-Tek chamber slides (Thermo Fisher Scientific, NY, USA). Cells were fixed with 4% PFA and air dried. Cells were rinsed and blocked with donkey serum prior to primary antibodies incubation for 1 hour. Negative controls were incubated with the appropriate IgG fractions as isotope controls. After washing with TBST, secondary antibodies were applied. DAPI was used to visualize nuclei. Slides were rinsed with TBST before mounting with Vectashield mounting medium (Vector Lab, Inc., Burlingame, CA, USA). To acquire computerized images of sections and cells, a Leica DM4000 B microscope (Leica Cambridge Ltd.) equipped with Leica DFC 320 Video camera (Leica Cambridge Ltd.) was used. All primary and secondary antibodies used are listed in Table 12.

Table 12: List of Antibodies used for Immuno-fluorescent staining (IF)

Antibody	Concentration	Company
Mouse anti-human CD31	2.0 µg/ml	Thermo Fisher, IL, USA
Rabbit anti-human ZO-1	0.625 µg/ml	Thermo Fisher, IL, USA
Rabbit anti-human LRP1	2.0 µg/ml	Santa Cruz Biotechnology
LC3B (D11) Clone 2775S	0.4 µg/ml	Cell Signaling Technology
Mouse-anti-beta-amyloid	2.0 µg/ml	BioLegend, San Diego,
Donkey anti-rabbit IgG	3.50 µg/ml	Jackson Immuno Lab, Inc.
Alexa Fluor 488 Donkey	3.75µg/ml	Jackson Immuno Lab, Inc.
DAPI (Nuclear stain)	5.0 µg/ml	Thermo Fisher Scientific

3.9 Animals & housing

All mice used in this study were bred in the animal facility of QPS Austria. Animal breeding and experiments were approved by the Austrian Federal Ministry of Science and Research, Vienna, Austria (approval number: ABT13-78Jo365-2022). Animals were housed in individual ventilated cages on standardized rodent bedding supplied by Rettenmaier & Söhne GmbH + Co KG (Vienna, Austria). The temperature was maintained between 20 to 24°C and the relative humidity was maintained between 45 to 65 %. Animals were housed under a constant light-cycle (12-hour light/dark). Male and female APPxhQC and NTG mice from the same breeding were used in this study. APPxhQC mice, crossbreds of APP_{SL} and hQC mice, were used. APP_{SL} mice express human APP751 with the Swedish and the London mutation on a C57Bl/6RccHsd background. hQC mice on B6CBAF1/J background express human glutaminyl cyclase (hQC) enzyme. The crossbreeding results in an increased generation of N-terminal modified pGlu Aβ peptides (APPSL x hQC Transgenic Mouse Model - QPS Austria (qpsneuro.com, accessed on 27th June, 2023).

3.9.1 Feeding and Experimental Timeline

Mice in the control groups were fed Control diet (CD) containing 10% kJ fat, 7% sucrose. T2D model groups were fed High Fat Diet (HFD) containing 95% (60KJ% Fat) + 5 % maltodextrin placebo diet with 3 injections of 40mg/kg streptozocin while the intervention groups were given HFD containing 95% (60KJ% Fat) + 5% NOVASTA alongside 3 injections of 40mg/kg streptozocin for 13 weeks starting from 11-12 months of age. HFD was used because it is a reliable mouse diet for induce visceral obesity, hyperglycemia and hyperinsulinemia. Body weights were recorded, and food was changed weekly. Twenty-two APPxhQC and 22 non transgenic mice aged 11 months raised in-house, were allocated to groups with n=6-8 animals each (see Table 15) and used for the study. After 3 weeks of feeding, the type 2 diabetes model and treatment groups were intraperitoneally treated with 40mg/kg Streptozocin once daily for 3 days while the control groups were injected with 50nM Sodium Citrate buffer (see Figure 11 – Experimental timeline). Intraperitoneal glucose tolerance test (ipGTT)/ Intraperitoneal insulin tolerance tests (ipITT) were conducted prior to feeding start and in treatment weeks 7, 9 and 12. Behavioral testings were carried out on mice at treatment week 13 of feeding. Plasma and tissue harvesting were done after treatment week 13.

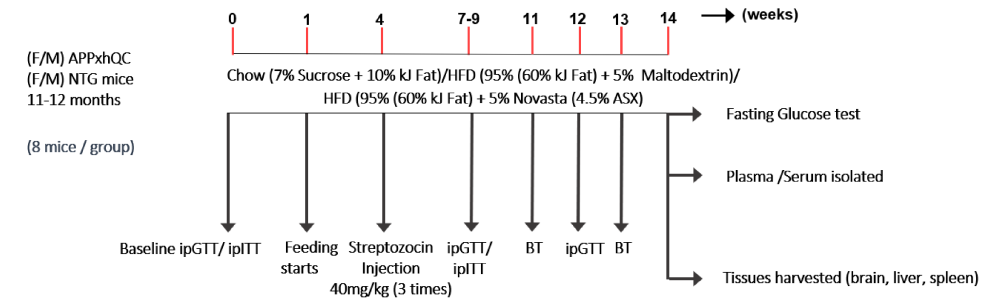

HFD: High fat diet
ipGTT: intraperitoneal glucose tolerance test (Glucose: 2g/kg)
ipITT: intraperitoneal insulin tolerance test (0.75UI/kg)
BT: Behavioural testing (Morris Water Maze)
F: Female
M: Male
NTG: Non-Transgenic
APP: Amyloid Precursor Protein
hQC: human glutaminyl cyclase

Figure 12: Experimental timeline

3.9.1.1 Diets

Twenty- two (22) male and female APPxhQC and twenty-four (22) non-transgenic mice were allocated to one of the following groups in two cohorts (males and females).

Table 13: Experimental Groups

Group	Number of mice (f/m)
NTG chow diet	(4 males, 3 females)
NTG T2D mimicking diet	(4 males, 4 females)
NTG T2D mimicking diet + ASX	(4 males, 3 females)
APPxhQC chow	(3 males, 3 females)
APPxhQC T2D mimicking diet	(3 males, 5 females)
APPxhQC T2D mimicking diet + ASX	(4 males, 4 females)

Table 14: Composition of Control diet -10% kJ fat, 7% sucrose (Lard/Soy bean oil) (EF D12450J, Ssniff® diets

Crude Nutrient	**%**
Crude Protein	18.2
Crude Fat	4.1
Crude Fibre	5.0
Crude Ash	5.3
Starch	43.5
Sugar	6.8
Additives	**Quantity**
Vitamin A	15000 (IE/IU)
Vitamin D3	1500 (IE/IU)
Vitamin E	150 mg
Vitamin C	30 mg
Copper	12 mg

Table 15: Composition of T2D mimicking diet – EF D12492 (95 %) + 5% Maltodextrin Placebo (EF D12492, Ssniff® diets)

Crude Nutrient	**%**
Crude Protein	23.2
Crude Fat	33.1
Crude Fibre	5.7
Crude Ash	5.2
Starch	0.1
Sugar	9.0
Additives	**Quantity**
Vitamin A	14250 (IE/IU)
Vitamin D3	1425 (IE/IU)
Vitamin E	144 mg
Vitamin C	29 mg
Copper	13 mg

Table 16: Composition of T2D mimicking + ASX diet- EF D12492 (95 %) + 5% Novasta (4.5% ASX (EF D12492, Ssniff® diets)

Crude Nutrient	**%**
Crude Protein	23.2
Crude Fat	33.1
Crude Fibre	5.7
Crude Ash	5.2
Starch	0.1
Sugar	9.0
Additives	**Quantity**
Vitamin A	14250 (IE/IU)
Vitamin D3	1425 (IE/IU)
Vitamin E	144 mg
Vitamin C	29 mg
Copper	13 mg

3.9.2 Streptozocin Preparation

4 mg of Streptozocin (Sigma Aldrich, Germany) was dissolved in 1ml 50mM Sodium citrate buffer (pH 4.5) to a final concentration of 4 mg/ml.

3.9.3 Glucose solution preparation

2 g of Glucose (Saccharose) was dissolved in 10 ml of distilled water to make a 20% glucose solution

3.9.4 Insulin stock preparation

Insulin obtained from Actrapid (Novo Nordisk, Denmark) was diluted 1:400 in 0.9% NaCl (Stock: 100 U/ml insulin) to prepare a working concentration of 0.75U insulin /ml

3.9.5 Intraperitoneal glucose tolerance test (ipGTT)

Mice were fasted 5 hours before tail veins of all animals were punctured and basal blood glucose concentrations were measured. Subsequently, a single dose of a 20% glucose solution was applied intraperitoneally (2 g/kg bodyweight) before additional blood glucose concentration measurements after 15-, 30-, 60- and 120-min post injection using the glucose analyzer (e.g., Nova StatStrip Xpress®-i) (Method adapted from Rotermund et al. 2014).

3.9.6 Intraperitoneal insulin tolerance test (ipITT)

Mice were fasted for 5 hours before fasting blood glucose levels (“0”) were measured from tail vein blood. A single dose of dose of 0.75 U human insulin peptide per kilogram (kg) of body weight was injected intraperitoneally before additional blood glucose concentration measurements were taken after 15-, 30-min post injection using the glucose analyzer (Nova StatStrip Xpress®-i) (Method adapted from Rotermund et al. 2014). Mice were closely observed for 30 minutes and in case blood glucose dropped below 20 mg/dl, or animal appeared hypoglycemic (tremor, heightened anxiety or apathy, paresthesia, loss of consciousness and rarely convulsions), 300 µl of 20% glucose solution was administered.

3. 9. 7 Behavioral testing

3.9.7.1 Morris Water Maze

Spatial learning capacities of all animals was tested in the Morris Water Maze (MWM). The MWM was performed using the following pattern: four trials on each of four consecutive days was performed. In all trials, the platform was in the northeast (NE) quadrant of the pool. Mice started from predefined positions (southeast (SE), southwest (SW), northwest (NW)). A single trial lasted for a maximum of 60 seconds. In case the mouse does not find the hidden, diaphanous platform within this time, the experimenter guided the mouse to the target. Mice were allowed to rest on the platform for 10-15 sec to orientate in the surrounding.

On day five mice were tested in the probe trial (PT). During the PT, the platform was removed from the pool and the number of crossings over the former target position as well as the abidance in the target quadrant was recorded.

For the quantification of escape latency (the time [sec] to find the hidden platform), of pathway (the length of the trajectory [meters] to reach the target), of target zone crossings and of the abidance in the target quadrant in the PT, a computerized video tracking system (Noldus Ethovision XT 14) was used.

The start positions in the different trials was, as follow:

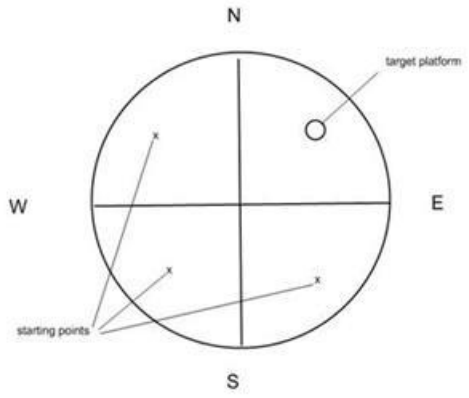

Figure 13: Diagram showing MWM trial quadrants

Table 17: Table showing the trial quadrants

	Trial 1	Trial 2	Trial 3	Trial 4	PT	Plattform
Day 1	SE	SW	NW	SW	-	NE
Day 2	NW	SE	SW	NW	-	NE
Day 3	SW	NW	SE	NW	-	NE
Day 4	SE	SW	NW	SE	-	NE
Day 5	-	-	-	-	SW	(NE)

3.10. Tissue Sampling

After 13 weeks of feeding with HFD or CD and a week after MWM, animals were fasted for 5 hour and sacrificed. From each animal blood (whole blood, plasma,

serum), brain, liver and spleen were sampled and further investigated. All mice were anesthetized by Pentobarbital injection (600 mg/kg).

3.10.1 Blood sampling and serum/plasma preparation

The thorax was opened, and blood was collected by heart puncture, 50 µl of whole blood was transferred into K2-EDTA tubes and the rest divided into two halves, and transferred into two vials using K2-EDTA for plasma and serum gel clotting activator micro tube (from SARSTEDT) for serum.

1 vial - Serum: after incubation for at least 20-60 min at RT, serum was prepared from the blood samples by centrifugation for 5 min at 10000 x g and collecting the supernatant. Serum was transferred to Eppendorf LoBind tubes [1 aliquot → 50µl + 1 aliquots of rest]. Serum was frozen at -80°C until biochemical analysis.

1 vial - Plasma: was sampled into K2-EDTA (Potassium ethylenediaminetetraacetic acid) tubes. The tube inverted thoroughly to facilitate homogeneous distribution of the EDTA and prevent clotting. The blood samples were centrifuged (3000 x g, 10 min, room temperature). Plasma was transferred to pre-labeled Eppendorf LoBind tubes [1 aliquot of 50µl + 1 aliquots of rest]. Plasma samples were stored frozen at -80°C until biochemical analysis.

Mice were transcardially perfused with 0.9% saline. For this purpose, a 23G needle connected to a bottle containing 0.9% saline was inserted into the left ventricle The right ventricle was opened with scissors. A constant pressure of 100 to 120 mm Hg was maintained on the perfusion solution by connecting the solution bottle to a manometer-controlled air compressor. Perfusion continued until all tissue (e.g., liver) has turned pale and no visible blood passes out of the right ventricle.

Thereafter, the skulls were opened, and the brains were removed and hemisected. The left-brain hemispheres and Cerebella used biochemical evaluation were weighed and immediately frozen on dry ice and stored at -80°C.The right brain hemispheres were fixed by immersion in freshly prepared 4% PFA for two hours at room temperature. Thereafter, right hemispheres were transferred to 15% sucrose in PBS solution until sunk (at 4°C) to ensure cryoprotection. Afterwards fixed hemispheres were frozen in OCT medium in cryo molds in dry-ice cooled isopentane and stored at -80°C until used for histological analysis.

The whole liver was weighed, and the left liver lobes were fixed in freshly prepared 4% PFA for two hours at room temperature. Thereafter, the left liver lobes were transferred to 15% sucrose in PBS solution until sunk (at 4°C) to ensure cryoprotection. Afterwards the left liver lobes were frozen in OCT medium in cryo molds in dry-ice cooled isopentane and stored at -80°C until used for histological analysis. The remains of the livers were frozen immediately on dry ice and stored at -80°C.The spleens in cryo vials were weighed before being frozen immediately on dry ice and stored at -80°C.

3.11 Measurement of Plasma Lipid and Serum liver function enzymes

Determination of Cholesterol, Triglyceride, Aspartate Aminotransferase (AST) and Alanine Aminotransferase (ALT) concentrations were be performed using the CHOL2 (item # 03039773190), TRIGL (item # 20767107322), ASTLP (item # 04467493190) and ALTLP (item # 04467388190) reagents (Roche, Germany). Absorbance was read at 700/505 nm for plasma cholesterol, triglycerides and 700/340 nm for serum AST and ALT using Roche Cobas 6000 Chemistry Analyzer (Roche Diagnostics Corporation, Indianapolis, IN 46250).

3.12 Measurement of Blood HbA1c

Determination of average blood glucose level over the past 8-12 weeks (HbA1c) was performed using the mouse HbA1c ELISA kit 80310 (Crystal Chem, Inc. Netherlands). Briefly, 5 µl of whole blood, calibrator and control were added to 62.5 µl of lysis buffer. Hemolysate was mixed by vortexing and incubated at room temperature for 10 min to completely lyse the red blood cells. One hundred and twelve µl of reagent 1 and 48 µl of reagent 2 were added into each well of a microplate and mixed well by repeated pipetting. In each well containing reagents 1 and 2, 25 µl of hemolysed sample, calibrator and control were added and mixed well by repeated pipetting. Microplates were placed in an incubator and allowed to equilibrate at 37°C for 5 min. Plates were read at 700 nm on the µQuant reader (Biotek, Vermont, USA). Seventy µl of Reagent CC2 was added and mixed well by repeated pipetting. Increase in absorbance was read at 700 nm on the µQuant reader (Biotek, Vermont, USA) after 3 min incubation at 37°C.

To determine the HbA1c concentration;

Calculate the change in absorbance ΔA (5 min ~ 8 min)

$\Delta A = (OD_{700nm,\ 8min}) - (OD_{700nm,\ 5\ min})$ X (185/255)). Using linear graph paper, HbA1c calibration curve was constructed by plotting the mean change in the absorbance value for each calibrator on the Y axis versus the corresponding HbA1c concentration on the X-axis.

3.13 Quantification of Plasma insulin levels

Ultra-Sensitive Mouse Insulin ELISA Kit 90080 (Crystal Chem, Inc. Netherlands) was used for analysis of insulin levels in serum samples. Samples were diluted 1:19 in sample diluent and analyzed according to the manufacturer's protocol. In brief, after dilution, 100 µl of the sample was added to the pre-coated well and incubated for 2 hr at RT with gentle agitation on a vibratory plate (800 rpm). Wells were washed three times with assay wash buffer and 100 µl of the conjugate solution was added. After 30 min incubation (RT, 800 rpm) wells were again washed three times. Thereafter, 100 µl of substrate solution was added and incubated for 40 min (RT, 800 rpm). 100 µl stop reagent was added and plates were read at 450 nm (reference wavelength 620-650 nm) on the µQuant reader (Biotek, Vermont, USA). The insulin concentration (ng/ml) in each sample was determined using a standard curve method.

3.14 Extraction of soluble and insoluble Aβ from mouse brain

3.14.1 Preparation of DEA extraction solution

DEA- solution (0.4 % DEA, 100 mM NaCl) was prepared by adding 200 µl diethylamine, 1 ml (5 M) NaCl, the final volume was adjusted to 50 ml with d2H2O.

3.14.2 Preparation of FA neutralizing solution

FA neutralizing solution (1 M Tris, 0.5 M Na_2HPO_4, 0.05% NaN_3) was prepared by dissolving 60.57 g Tris and 44.5 g $Na_2HPO_4.2H_2O$ and 2.5 ml Sodium Azide (10 %) in 400 ml d2H2O, the final volume was adjusted to 50 ml with d2H2O.

3.14.3 Extraction of DEA soluble and FA-insoluble Aβ fractions

Left brain samples were homogenized in tissue homogenization buffer. For extraction of non-plaque associated proteins, THB homogenates were mixed with 1-part

diethylamine (DEA) solution (0.4% DEA, 100 mM NaCl). The mixture was centrifuged for 106 minutes at 20,817 g at 4°C. The supernatants were neutralized with 1/10 of the volume 0.5 M Tris-HCl, pH 6.8, vortexed briefly and stored at -20°C. For extraction of plaque associated proteins, THB homogenates were mixed with 2.2 parts cold formic acid (FA), sonicated for 30 sec on ice and centrifuged for 106 min at 20,817 x g at 4°C. The supernatant was diluted with 19 parts FA Neutralization Solution, vortexed briefly and stored at -20°C.

3.15 $A\beta_{38}$, $A\beta_{40}$ and $A\beta_{42}$ MSD

3.15.1 Preparation of Washing buffer (1x PBS, 0.05% Tween)

To prepare 1X washing buffer, 0.5 ml Tween20 was added to 1000 ml PBS

3.15.2 Preparation of Read T Buffer

To prepare 1X Read T buffer, 4 ml of 4X Read T stock (proprietary composition) was added to 4 ml of d2H2O.

3.15.3 Preparation of Detection Antibody

25 µl of 50X 6E10 antibody was diluted in 1225 µl of Diluent 100.

3.15.4 $A\beta_{38}$, $A\beta_{40}$ and $A\beta_{42}$ MSD evaluation

$A\beta_{38}$, $A\beta_{40}$ and $A\beta_{42}$ were measured in the DEA and FA fractions from left-brain homogenates using an immunosorbent assay (Aβ Peptide Panel 1 (6E10); K15200E-2; Meso Scale Discovery) according to the instructions of the manufacturer. In brief 150 µl of diluent 35 were added to each well. The plate was sealed and incubated at RT with shaking for 1 hour. Then the plate was washed 3 times with 150 µl/well wash buffer. After that 25 µl of detection solution and 25 µl of prepared samples, calibrators or controls was added to each well. The plate was sealed and incubated at RT with shaking for 2 hours. The plate was washed again 3 times (150 µl/well of wash buffer), 150 µl 2x Read Buffer T was added to each well and then the plate was read on a Meso Quick Plex SQ 120 instrument (MSD, USA). Aβ levels were evaluated in comparison to standards provided in the kit and were stated as pg per mg brain wet weight.

3.16. pGlu3-Aβ$_{42}$ ELISA

3.16.1 Preparation of pGlu3-Aβ$_{42}$ ELISA washing solution

To prepare 162 ml 1X washing solution, 4.05 ml 40X stock (proprietary composition) washing solution was added to 157.95 ml d2H2O.

3.16.2 Preparation of labelled antibody

To prepare 6 ml 1X labelled antibody, 200 µl 30X antibody was added to 5,800 µl EIA solution.

3.16.3 Preparation of pGlu3-Aβ$_{42}$ ELISA diluted standard

Standard stock (992 pg/ml) was diluted in 0.5 ml d2H2O. Seventy µl of standard stock was pipetted into a tube containing 70 µl of EIA solution and further serially diluted seven times.

3.16.4 pGlu3-Aβ$_{42}$ ELISA measurement

Assessment of pGlu3-Aβ$_{42}$ was done using ELISA kit from IBL (JP27716) according to the instructions of the manufacture. Briefly, 50 µl of EIA buffer was pipetted in wells marked as blank, 50 µl of standard and diluted samples were pipetted into wells. Precoated plate was incubated at 4°C overnight. The plate was washed with 350 µl of washing buffer 4 times, 100 µl of labelled antibody was pipetted into each well except the well for Reagent blank and incubated at 4°C for 60 min with a plate lid. The plate was washed 5 times with 350 µl of washing buffer, 100 µl of Chromogen- TMB solution was added into each well and incubated for 30 min at room temperature shielded from light. The reaction was stopped by adding 100 µl of stop solution and plate was read at 450 nM within 30 min of adding stop solution.

3.17 Histological Evaluations

3.17. 1 Sectioning

Five consecutive cryosections were sagittally cut at 10 µm thickness on a Leica CM1950 or Thermo Scientific NX70 cryotome. The next 25 sections were discarded. This collection scheme was repeated for 5 levels (Levels 2,4,6,8 and 10). In total 5 x 5 = 25 sections were collected. Sectioning levels were chosen according to the brain atlas of Paxinos and Franklin (“The Mouse Brain in Stereotaxic Coordinates”, 2nd

edition, 2001). Collection of sections started at a level ~0.2 mm lateral from midline and extend through the hemisphere, in order to ensure systematic random sampling through the target regions (Figure 13). Sections were stored at -20°C. Almost the entire brain was sectioned, the residual tissue block was disposed when all sections were collected.

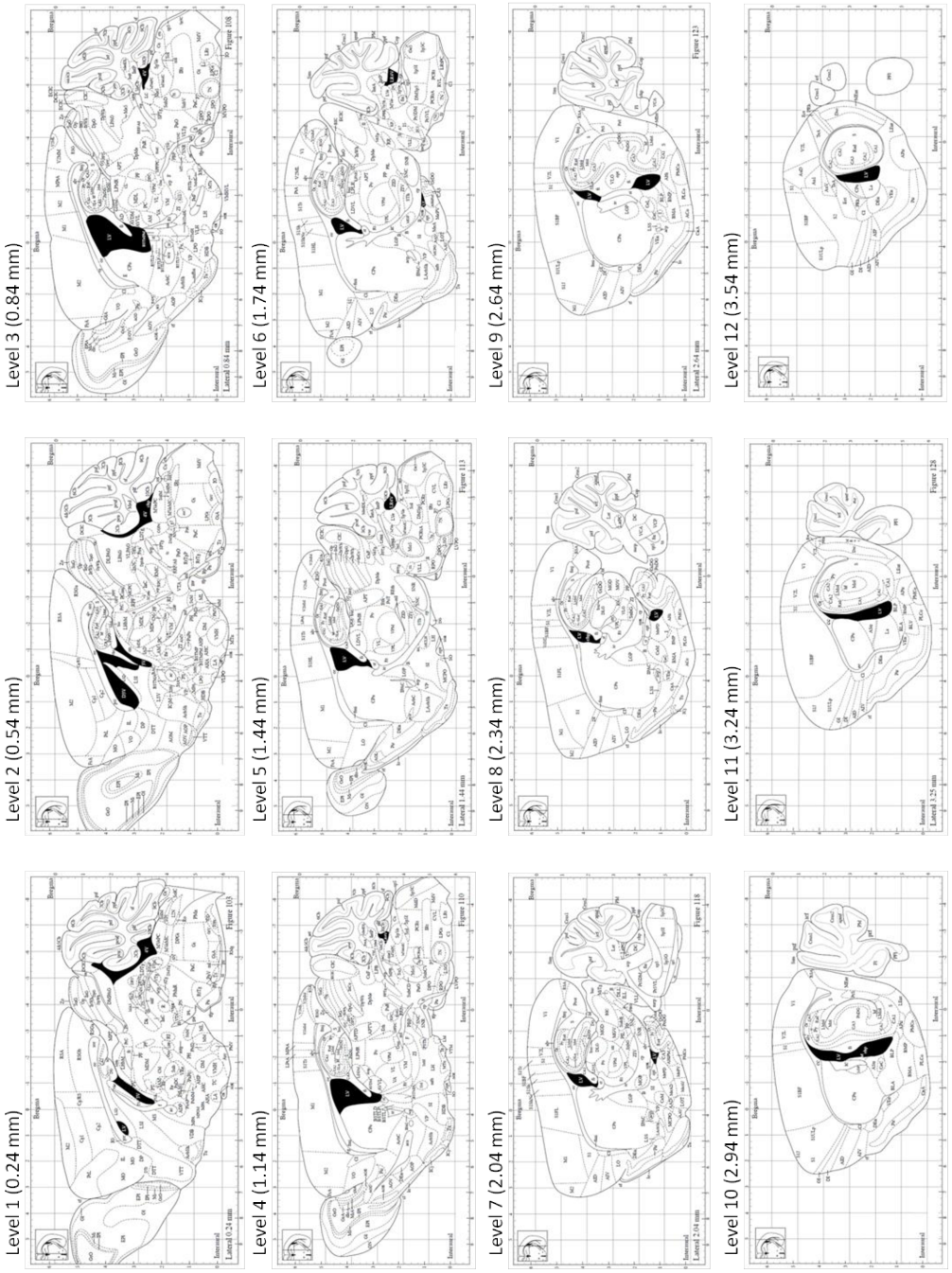

Figure 14: Sectioning levels. Approximate medio-sagittal levels obtained following the sectioning protocol. Drawings are taken from Paxinos & Franklin "The Mouse Brain Atlas, 2nd edition", showing the stereotactic coordinates.

3.17. 2 Immunofluorescence

For each incubation a uniform systematic random set of five sections per mouse were selected (one section each from levels 2, 4, 6, 8, 10). The following histological labelling experiments were carried out on these sets of sections:

3.17.3 Basic investigations

The following three channel incubations were used.

Combination:

DAPI

rabbit anti pE3-Amyloid

mouse anti Abeta (6E10)

guinea pig anti Iba1

goat anti GFAP

This combination was used to quantify plaque-associated deposited Aβ and inflammation. All sections were counterstained with the nuclear dye DAPI. Binding of primary antibodies were visualized using highly cross-absorbed secondary antibodies.

Table 18: List of Antibodies used for Histological evaluation

Antibody	Dilution	Company
Mouse monoclonal [6E10] anti-amyloid beta conjugated Alexa Fluor 488 B803013 # B350019	1:2000	BioLegend
Rabbit Abeta-pE3 antibody (218003) #218003_8 (2)	1:2000	Synaptic Systems G
Iba1/AIF-1 (234308) Clone Gp311H9 #1-3	1:3000	Synaptic Systems GmbH
GFAP (ab53554) # GR3414930-3	1:2000	Abcam
Alexa Fluor 750 (ab175745) #GR3441783-2	1:500	Abcam
Cy3 (706-165-148) #159084	1:500	Jackson Immuno Research

Donkey Anti-Rabbit IgG DyLight 650 (ab96922) # GR3378799-7	1:500	Abcam
DAPI (A1001.0025)		Appli Chem

3.17.4 Imaging

Whole slide scans of the stained sections were recorded on a Zeiss automatic microscope AxioScan Z1 with high aperture lenses, equipped with a Zeiss Axiocam 506 mono and a Hitachi 3CCD HV-F202SCL camera and Zeiss ZEN 3.3 software.

3.17.5 Quantification

Image analysis was done with Image Pro 10 (Media Cybernetics). At the beginning the target areas (hippocampus and cortex) were identified by drawing regions of interest (ROI) on the images. Additional ROIs excluded wrinkles, air bubbles, or any other artifacts interfering with the measurement. Signals of respective markers was quantitatively evaluated within the identified areas.

For quantification, background correction was employed where necessary. Adequate thresholding and morphological filtering (size, shape) were used to detect immunoreactive objects. Different object features were quantified, among them the percentage of cumulative object area based on ROI size (immunoreactive area; this is the most comprehensive parameter indicating whether there are differences in immunoreactivity), the number of objects normalized to ROI size (object density), the mean signal intensity of objects identified (mean intensity; this indicates if there are differences in the cellular expression level of target proteins), and the size of above-threshold objects. Once the parameters of the targeted objects had been defined in a test run, the quantitative image analysis runs automatically assuring that the results are operator-independent and fully reproducible.

Raw data were organized and sorted in Excel, and then transferred to GraphPad Prism for statistical analysis and preparation of graphs.

3.18 Statistics

Basic statistical analyses were performed using GraphPad 10.1.0 (316) (GraphPad Software Inc, USA) Data are presented as mean ± standard error of mean (SEM) and group differences are evaluated by two tailed unpaired student’s t-test, one or two-

way ANOVA followed by Turkey's or Dunnett's multiple comparisons tests. Group differences were considered statistically significant for $p < 0.05$ (*), $p < 0.01$ (**), and $p < 0.001$ (***).

4.0 RESULTS

4.1 Part One: *In vitro* studies

4.1.1 Purity of isolated pBCECs

Isolation of highly pure brain capillary endothelial cells is key to study the mechanisms of endothelial function. qPCR was performed to validate the purity of the isolated pBCEC. mRNA expression of marker genes such as platelet endothelial cell adhesion molecule (PECAM1=CD31) for endothelial cells, platelet-derived growth factor receptor (PDGFR) for pericytes, glial fibrillary acidic protein (GFAP) for astrocytes, microtubule-associated protein 2 (MAP2) for neurons as well as zonula occludens-1 (ZO-1) for tight junctions were performed (Figure 15A, 15B). These results confirmed that the isolated pBCEC fraction was highly enriched in CD31-positive endothelial cells.

A

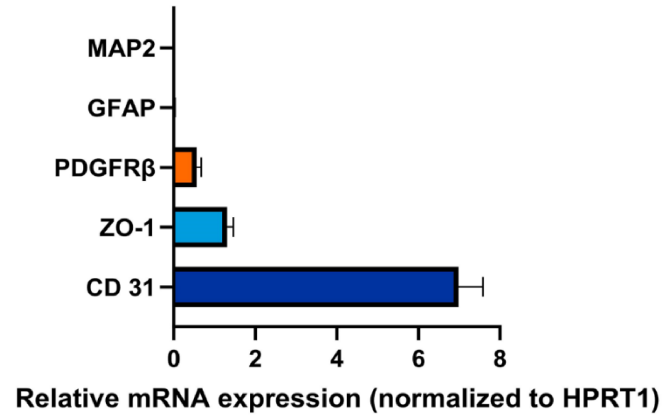

B

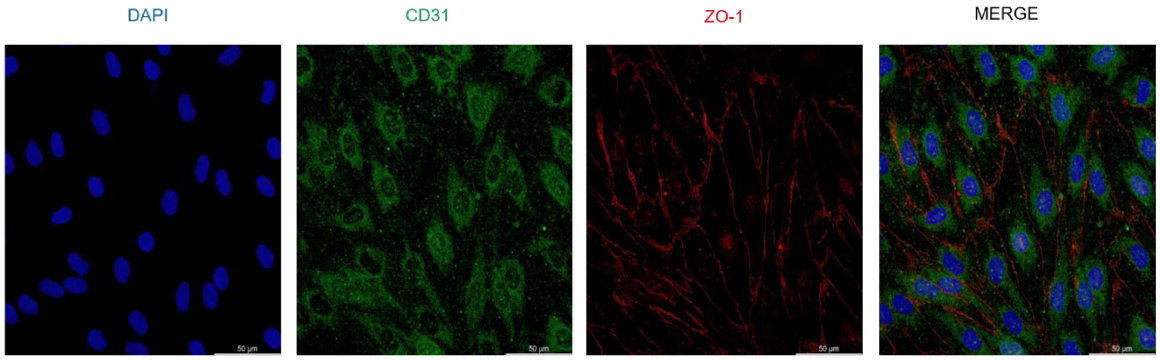

Figure 15: Expression of marker genes in isolated pBCEC preparations.

Isolated pBCECs were highly enriched in CD31-positive endothelial cells. Relative mRNA expressions of *cd 31, zo-1*, *pdgfrβ*, *map2* and *gfap* normalized to *hprt1* (A). Endothelial cell and tight junction markers staining in purified pBCEC (B) *cd31* (green) and *zo-1* (red). N=6 (Reproduced from Babalola et al., 2023 with permission from Brain Res).

4.1.2 ASX might lead to changes within autophagy pathway in Aβ$_{40}$-treated pBCECs

It has been suggested that defective autophagy is one of the dysregulated processes that lead to the accumulation of protein aggregates in the brain of the elderly and/or the diseased (Metaxakis et al., 2018). To evaluate the effect of ASX on Aβ-induced autophagy, pBCECs were incubated with ASX for 22 h and/or Aβ$_{40}$ for 6 h under serum-free conditions. Treatment of pBCECs with ASX alone ($P<0.001$) or together with Aβ$_{40}$ ($P=0.006$) increased the protein levels of LC3B compared to vehicle control (VC) (Figure 16A, 16B). Similarly, ASX alone ($P=0.003$) or together with Aβ$_{40}$ resulted in a significant increase of LC3B-II compared to VC ($P=0.01$; Figure 16A, 16C). Elevated LC3B-II protein levels are considered to be a marker for the induction of autophagy (Kabeya et al., 2000, Tanida et al., 2005). Interestingly, treatment of pBCECs with Aβ$_{40}$ resulted in increased mTOR phosphorylation ($P=0.08$), which was significantly reduced upon ASX treatment ($P=0.05$; Figure 16A, 16D). In addition, activated mTORC1 is known to phosphorylate ribosomal S6 kinase (S6K) on Thr389, followed by activation of S6K to phosphorylate ribosomal protein S6 (S6RP), a

component of the 40S ribosomal subunit often referred to as ad mTORC1/S6K activity (Biever et al., 2015). Accordingly, a significant increase in phosphorylation of S6RP protein was observed in $A\beta_{40}$-treated pBCECs compared to VC (P=0.02). Phosphorylation of S6RP protein was significantly reduced when pBCECs were treated with ASX alone (P=0.002; Figure 16A, 16E) and somewhat lower when simultaneously incubated with ASX and $A\beta_{40}$, although the differences were not statistically significant.

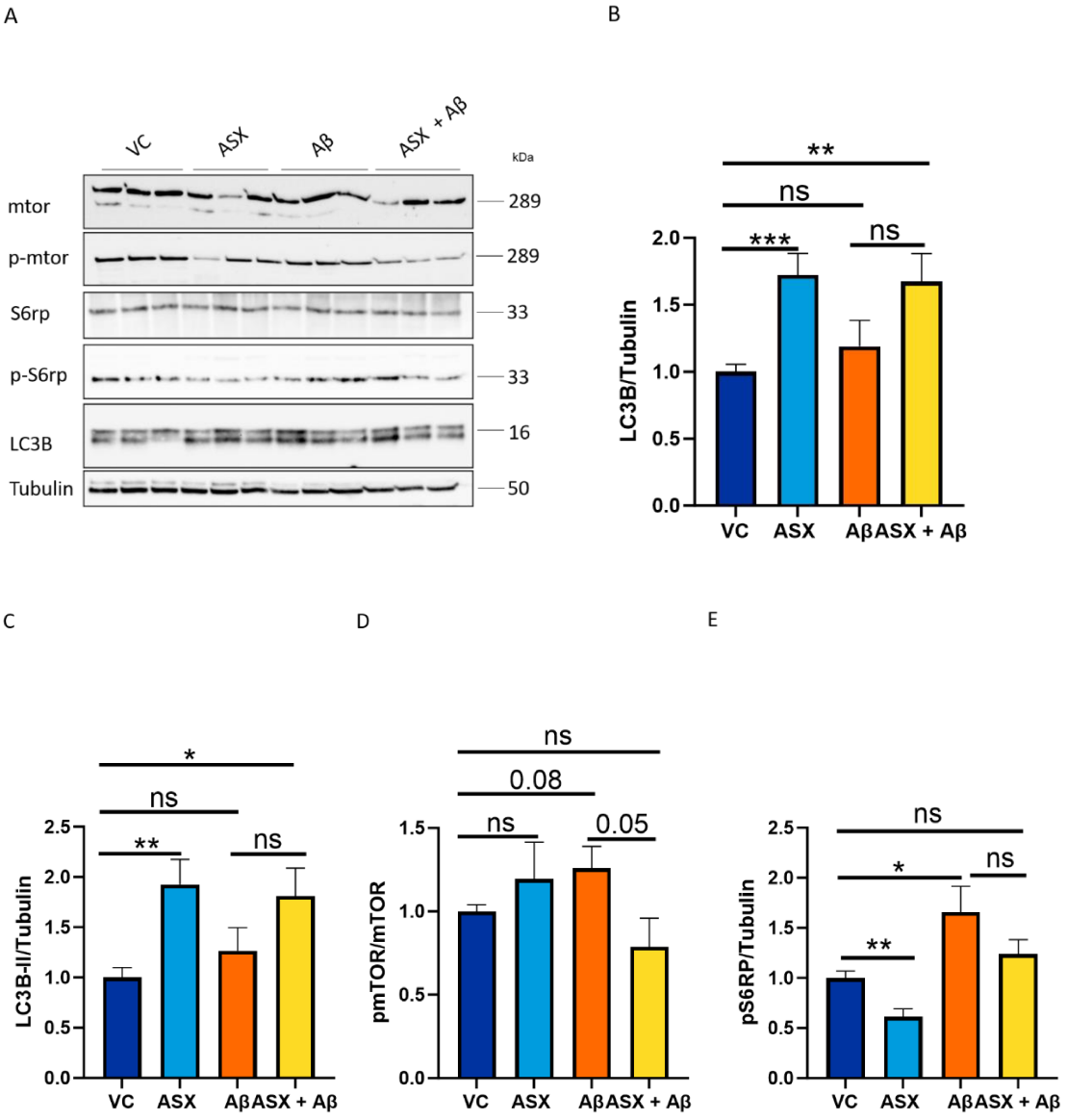

Figure 16: Autophagy and mTORC1 signaling in Aβ-treated pBCEC.

Incubation of pBCEC with Aβ and ASX increased expression of total LC3B and lipidated LC3B-II while reducing the phosphorylation of mTOR protein. Serum-free

Aβ-treated pBCECs were pre-incubated with 10 µM ASX for 16 hr and further incubated with 240 nM $Aβ_{40}$ for 6 hr. Immunoblot showing LC3B, LC3B-II, p-mTOR/mTOR and p-S6RP protein expression levels (A). Densitometric analyses of LC3B (B), LC3B-II (C), p-mTOR/mTOR (D) and p-S6RP (E) protein levels in ASX and Aβ-treated pBCECs. Solvent was used as vehicle control (VC). Data are mean + SEM, n=6-10; significant differences between the groups were calculated using two-tailed, unpaired students t-test; *p < 0.05; **p < 0.01 and ***p < 0.001. (Reproduced from Babalola et al., 2023 with permission from Brain Res).

To assess autophagic flux, we incubated pBCECs with ASX, $Aβ_{40}$ and bafilomycin A1 (a widely used inhibitor of autophagosome-lysosome fusion) or treated them simultaneously with a combination of these compounds for 4 h. Significantly increased lipidation of LC3B was observed in pBCECs incubated with bafilomycin A1 alone (P = 0.005), in combination with $Aβ_{40}$ (P<0.001), or both $Aβ_{40}$ and ASX (P<0.001) compared to cells incubated with vehicle control and bafilomycin A1 in combination with $Aβ_{40}$ (P<0.001) or both $Aβ_{40}$ and ASX (P<0.001) compared to pBCECs incubated with $Aβ_{40}$ (Figure 17A, 17B). Taken together, these data suggest that treatment of pBCECs with ASX might likely result to a change within the autophagy pathway even in the presence of $Aβ_{40}$.

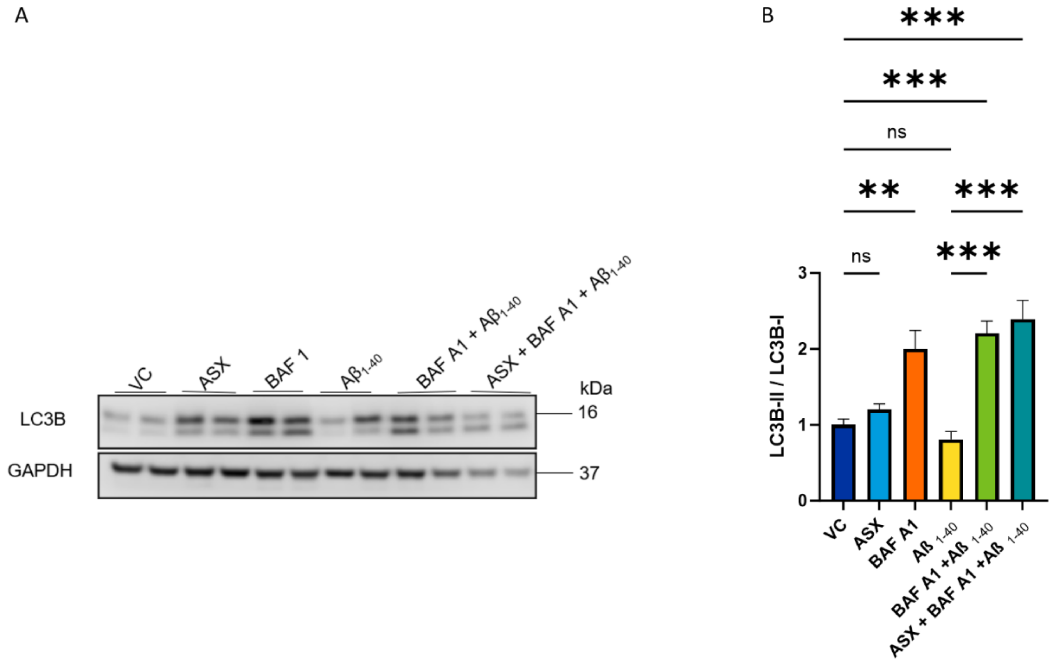

Figure 17: Autophagic flux in Aβ-treated pBCECs

ASX enhances autophagic flux in Aβ-treated pBCECs in the presence of the lysosomal inhibitor bafilomycin (BAF) A1. Serum-free Aβ-treated pBCECs were pre-incubated with 10 µM ASX for 16 hr further incubated with 240 nM $A\beta_{40}$ for 6 hr. 100 nM BAF A1 was added during the last 4 hr of the experiment. Western blot showing LC3B in pBCECs treated or co-treated with $A\beta_{40}$, ASX and BAF A1 (A). Densitometric analyses of LC3B (B) protein expression levels in pBCECs treated or co-treated with $A\beta_{40}$, ASX and bafilomycin A1. Solvent was used as vehicle control (VC). Data are mean + SEM; n=6-7. *p*-Values were calculated by one-way ANOVA followed by *Dunnett's post hoc* test; **p < 0.01 and ***p < 0.001 as compared to $A\beta_{40}$ and vehicle control. (Reproduced from Babalola et al., 2023 with permission from Brain Res).

4.1.3 ASX reduces APP levels and enhance Aβ clearance in $A\beta_{40}$-treated pBCECs

Increased production as well as impaired clearance of Aβ contribute to the development of AD (Wildsmith et al., 2013). To evaluate the effect of ASX on Aβ production and impaired Aβ clearance, pBCECs were incubated with ASX for 22 h and $A\beta_{40}$ for 6 h under serum-free conditions. Interestingly, co-incubation of pBCECs with $A\beta_{40}$ and ASX reduced the expression of amyloid precursor protein (APP)/Aβ compared to VC (P=0.003) and $A\beta_{40}$ (P<0.001, Figure 18A, 18B). This was confirmed by lower protein levels of APP/Aβ in the incubation media of $A\beta_{40}$ and ASX-co-treated cells compared to those of $A\beta_{40}$-treated cells (Figure 18C, Figure 18D). Incubation of pBCECs with ASX or simultaneous incubation with $A\beta_{40}$ and ASX significantly increased mRNA expression of ABCA1 compared to VC (P=0.04 and P=0.01, respectively, Figure 18E). ASX-treated pBCECs significantly increased the expression of ABCG1 mRNA compared to VC (P=0.009, Figure 18F). Low density lipoprotein receptor-related protein 1 (LRP1) in brain endothelial cells is known to be a critical regulator of BBB integrity and function (Storck et al., 2021). Furthermore, LRP1 has been reported to be important for the rapid removal of Aβ from the brain (Storck et al., 2018). In pBCECs, we observed a significant reduction of LRP1 mRNA upon treatment with $A\beta_{40}$ compared to the VC (P=0.04). Co-incubation of pBCECs with $A\beta_{40}$ and ASX increased LRP1 mRNA expression compared to $A\beta_{40}$ control

(P=0.04, Figure 18G). Taken together, increased expression of ABC transporters as well as LRP1 suggest that ASX increases Aβ clearance in pBCECs.

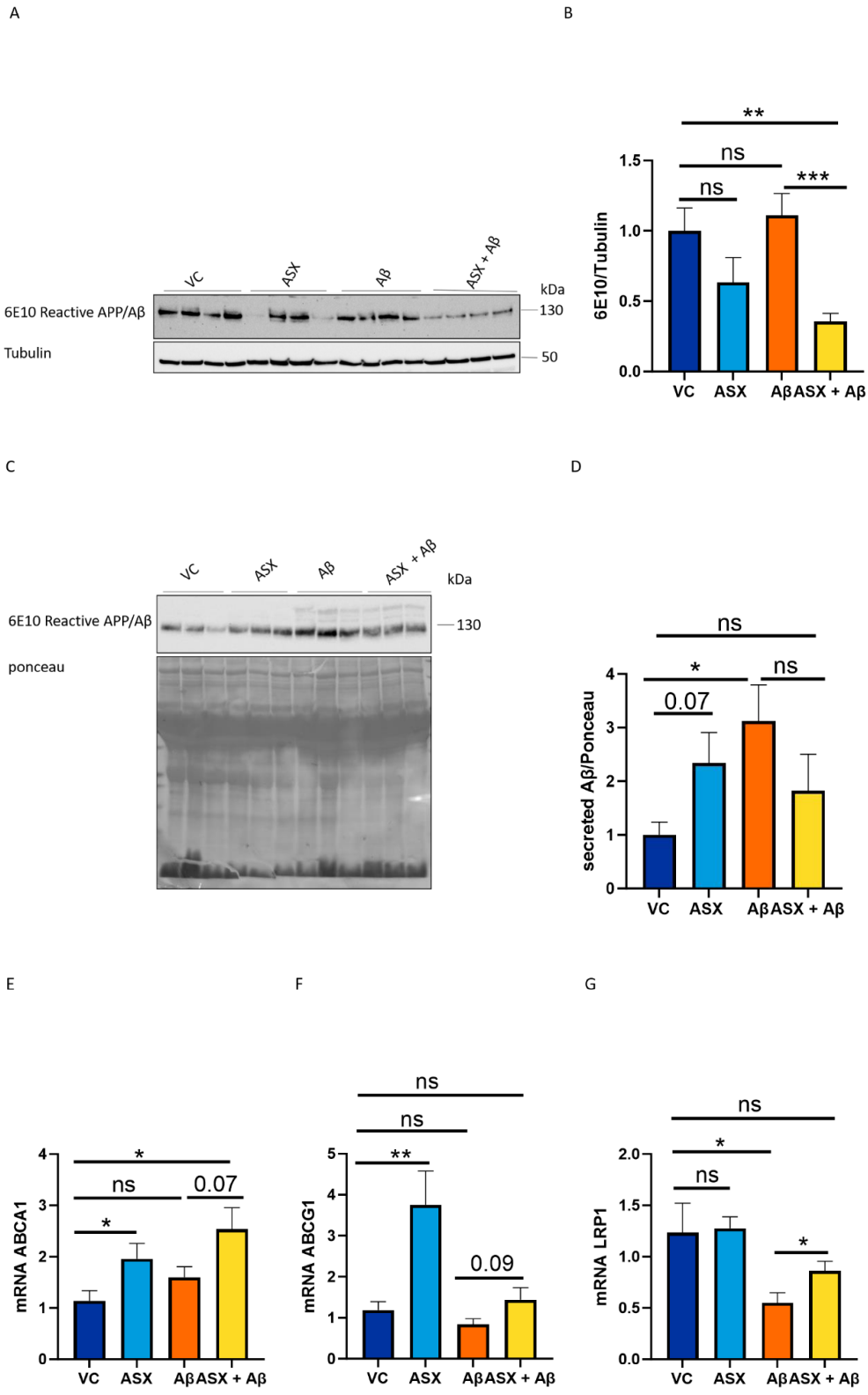

Figure 18: ASX reduces protein expression of APP/Aβ as well as increases expression of genes involved in Aβ clearance in Aβ-treated pBCECs.

ASX alters Aβ processing while enhancing its clearance in $Aβ_{40}$-treated pBCEC**.** Proteins were extracted from cells and TCA-precipitated from supernatants. Protein levels of Aβ species (normalized to tubulin levels) were detected by immunoblot using 6E10 as primary antibody. Western blot showing intracellular 6E10 reactive APP/Aβ (A). Densitometric analyses of intracellular 6E10 reactive APP/Aβ (B). Western blot showing secreted 6E10 reactive APP/Aβ in the culture media (C). Densitometric analyses of secreted 6E10 reactive APP/Aβ in the culture media normalized to ponceau (D). Quantitative analyses of ABCA1 (E), ABCG1 (F) and LRP1 (G) mRNA expression levels by qPCR of Aβ-treated pBCECs. Data are mean + SEM, n=4-8; significant differences between the groups were calculated using two-tailed, unpaired students t-test; *$p < 0.05$; **$p < 0.01$ and ***$p < 0.001$. (Reproduced from Babalola et al., 2023 with permission from Brain Res).

4.1.4 ASX enhances Aβ clearance, with PPARα activation being a likely mechanism.

ASX has been reported to act as a PPAR agonist (Choi, 2019). To investigate the mechanism of ASX function, pBCECs were incubated with ASX, fenofibrate (PPAR activator), GW6417 (PPAR antagonist), and solvent as vehicle control (VC) for 22 h and $Aβ_{40}$ for 6 h under serum-free conditions. Simultaneous incubation of pBCECs with $Aβ_{40}$ and either ASX (P=0.01) or fenofibrate (P=0.03, Figure 19A) significantly increased mRNA expression of ABCA1 compared to VC. Double immunofluorescence labelling of pBCECs co-incubated with $Aβ_{40}$ and ASX, fenofibrate, or GW6417 showed reduced LRP1 in $Aβ_{40}$-treated cells and cells co-incubated with $Aβ_{40}$ and GW6417 (Figure 19B). Furthermore, reduced LC3B staining was observed in pBCECs co-incubated with Aβ and ASX, fenofibrate, or GW6417 (Figure 19C). Taken together, these results suggest that ASX increases Aβ clearance in $Aβ_{40}$-treated pBCECs, likely via PPAR activation.

A

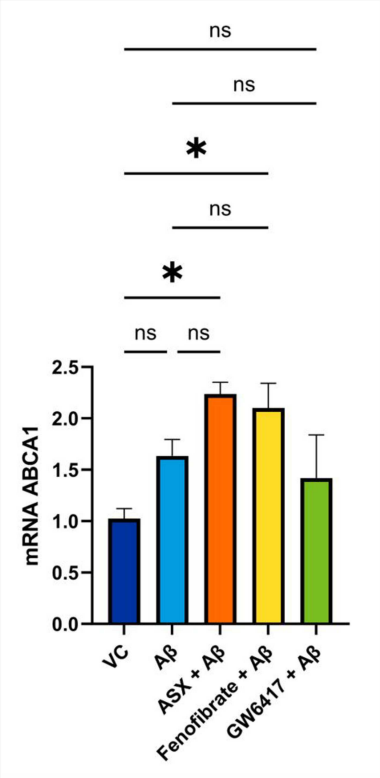
ns
ns
*
ns
*
ns ns
mRNA ABCA1
2.5
2.0
1.5
1.0
0.5
0.0
VC
Aß
ASX + Aß
Fenofibrate + Aß
GW6417 + Aß

B

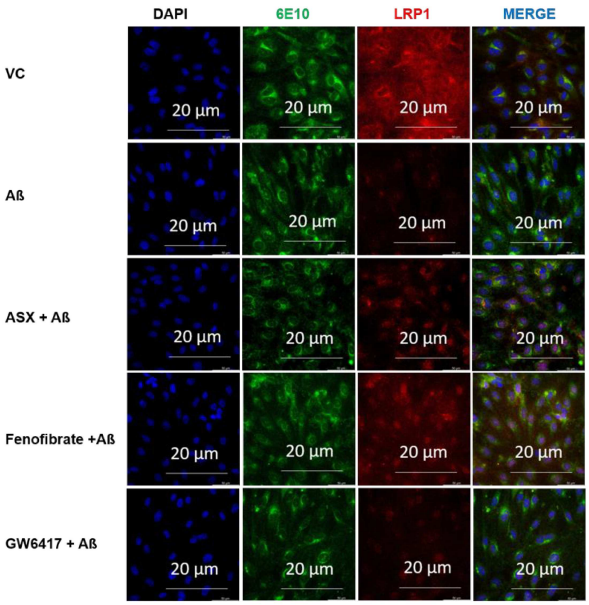
DAPI
6E10
LRP1
MERGE
VC
Aß
ASX + Aß
Fenofibrate +Aß
GW6417 + Aß
20 µm

C

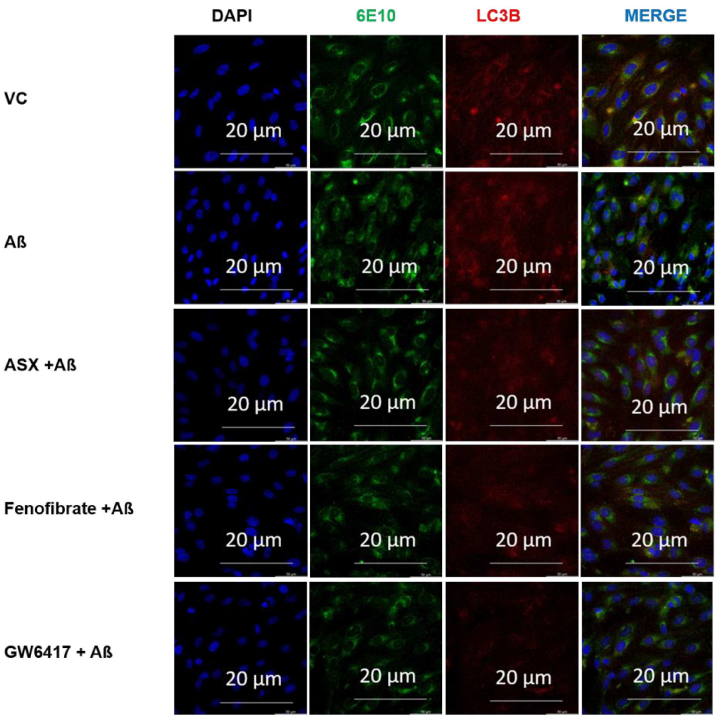
DAPI
6E10
LC3B
MERGE
VC
Aß
ASX +Aß
Fenofibrate +Aß
GW6417 + Aß
20 µm

Figure 19: ASX enhances Aβ clearance, likely via PPARα activation.

ASX ameliorates impaired Aβ clearance in Aβ-treated pBCEC via PPARα signaling**.** Serum-starved Aβ-treated pBCECs were pre-incubated with 10 µM ASX, 1 µM fenofibrate and 1 µM GW6417 for 16 hr further incubated with 240 nM $A\beta_{40}$ for 6 hr. Quantitative analyses of ABCA1 (A) mRNA expression level by qPCR in Aβ-treated pBCECs. pBCECs were pre-incubated with 10 µM ASX, 1 µM Fenofibrate and 1 µM GW6417 for 16 hr and further incubated in the absence of serum with 240 nM $A\beta_{40}$ for 6 hr, fixed with 4% PFA, probed with antibodies against 6E10 (green) and LRP1 (red) to visualize Aβ-LRP1interaction (Blue) (B) or against 6E10 (green) and LC3B (red) to visualize Aβ-LC3B interaction (blue) (C). Solvent was used as vehicle control (VC). Data are mean + SEM, n=5-6. *p*-Values were calculated by one-way ANOVA followed by *Turkey's post hoc* test; *p < 0.05 as compared to vehicle control and $A\beta_{1-40}$. (Reproduced from Babalola et al., 2023 with permission from Brain Res).

4.1.5 ASX reduces the secretion of inflammatory cytokines in LPS-stimulated organotypic hippocampal brain slices

The dysregulation of the neuronal immune system plays a central role in the pathology of AD. To examine the anti-inflammatory function of ASX, hippocampal organotypic brain slices were preincubated with ASX and then treated with LPS for 24 hours. LPS stimulation of brain slices resulted in significant increases in almost all cytokines analyzed, including TNF-α, IL-6, IL-10, IL-1β and KC/GRO, but not IL-4 (Figure 20). Treatment of hippocampal brain slices with LPS in combination with ASX resulted in significant reductions of inflammatory cytokines TNF-α (P<0.001), IL-6 (P<0.001), IL-10 (P=0.03), and KC/ GRO (P=0.02; Figures 20A C and E), but not of IL-1β and IL-4 (Figures 20D and F). As expected, concomitant treatment with LPS and dexamethasone further reduced almost all cytokine levels except IL-4 (Figures 20A–F). In addition, we determined mRNA of the pro- and anti-inflammatory cytokines IL-6 and IL-10 and observed that treatment of LPS-stimulated brain slices with ASX resulted in decreased mRNA expression of IL- 6 (P=0.03) but not of IL-10 (P=0.61) (Figures 20G, H), while dexamethasone treatment nearly attenuated IL-6 and IL-10 mRNA levels (Figures 20G, H).

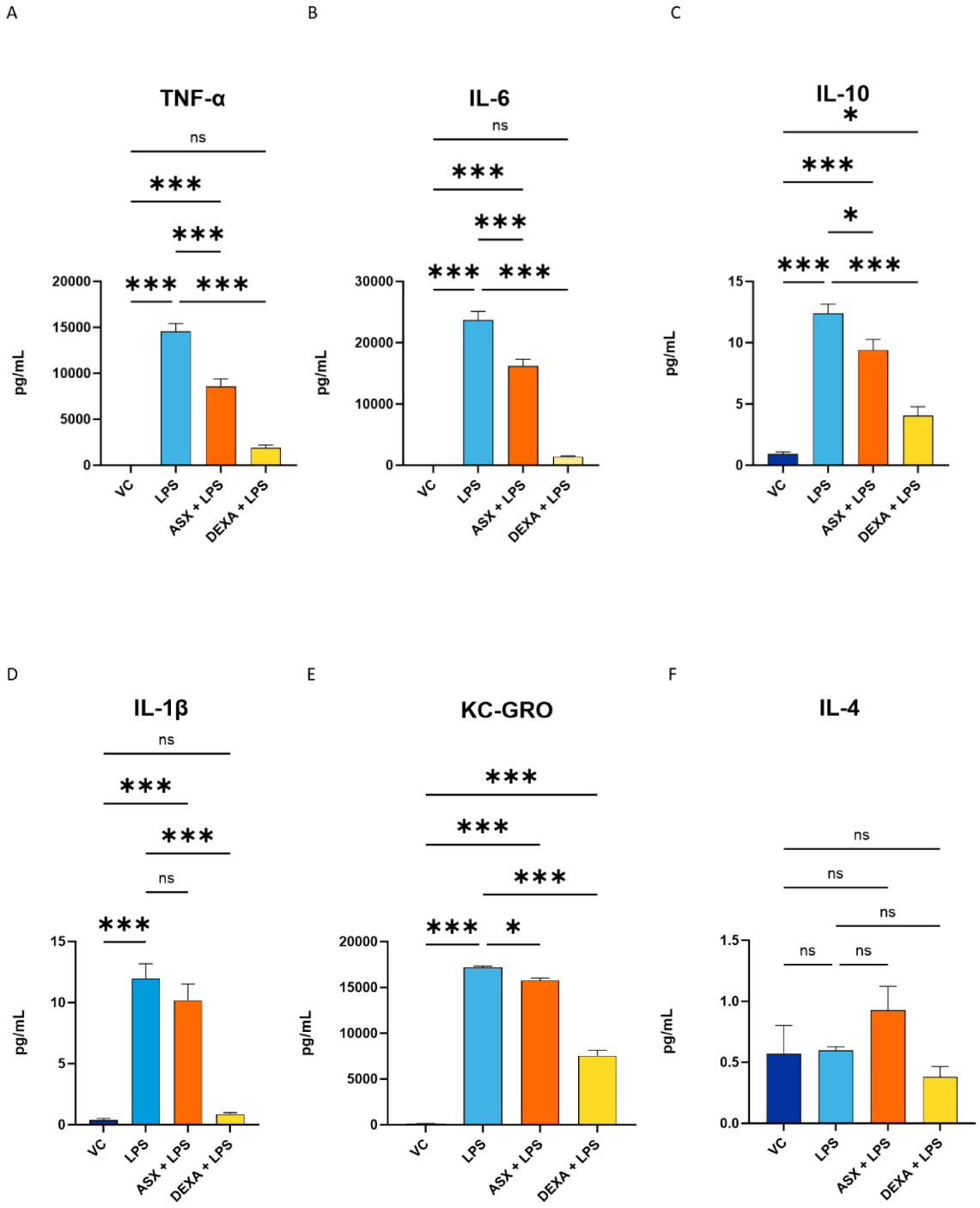
A
TNF-α
pg/mL
ns
***
***
***
***
20000
15000
10000
5000
0
VC
LPS
ASX + LPS
DEXA + LPS
B
IL-6
pg/mL
ns
***
***
***
***
30000
20000
10000
0
VC
LPS
ASX + LPS
DEXA + LPS
C
IL-10
pg/mL
*
***
*
***
***
15
10
5
0
VC
LPS
ASX + LPS
DEXA + LPS
D
IL-1β
pg/mL
ns
***
***
ns
***
15
10
5
0
VC
LPS
ASX + LPS
DEXA + LPS
E
KC-GRO
pg/mL
***
***
***
***
*
20000
15000
10000
5000
0
VC
LPS
ASX + LPS
DEXA + LPS
F
IL-4
pg/mL
ns
ns
ns
ns
ns
1.5
1.0
0.5
0.0
VC
LPS
ASX + LPS
DEXA + LPS

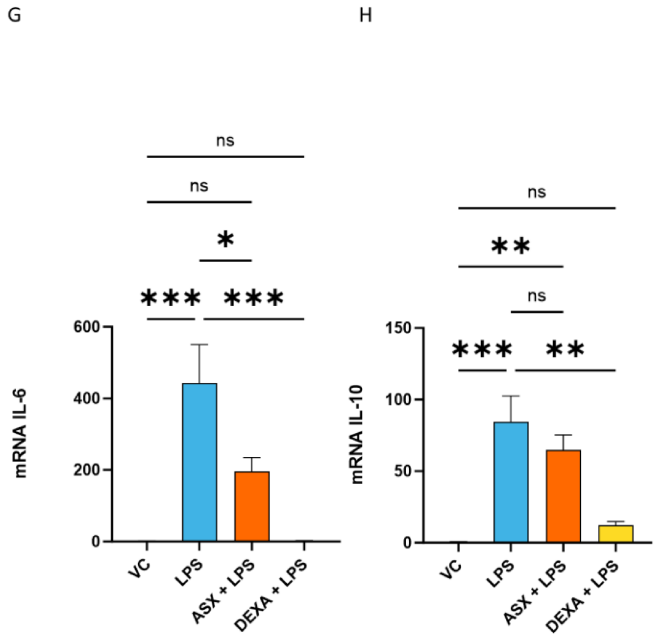

Figure 20: Cytokine release in LPS-stimulated brain slices.

Organotypic hippocampal brain slices were incubated with 10 ng/mL LPS as well as with 10 ng/mL LPS in combination with 50 µM ASX and 10 µM dexamethasone (Dexa) for 24 hr, followed by detection of cytokine release in the supernatant and mRNA expression levels in brain slices by qRT-PCR. Solvent was used as vehicle control (VC). *p*-Values were calculated by one-way ANOVA with *Turkey's post hoc* test; *p < 0.05; **p < 0.01 and ***p < 0.001. Data are mean + SEM, n=5-10 for Figure A-F and 4-6 for Figure G and H. (Reproduced from Babalola et al., 2023 with permission from Brain Res).

4.1.6 ASX decreases M1 while increasing M2 polarization in LPS-stimulated organotypic hippocampal brain slices

Microglia polarize in two directions and produce two distinct phenotypes. These can be either the pro-inflammatory M1 or the anti-inflammatory M2 phenotype (Zhang et al., 2019). Since an organotypic hippocampal slice culture (OHSC) includes various CNS cell types including glial cells, we examined the effects of LPS stimulation on glial cell activation. As expected, treatment of brain slices with LPS and simultaneous treatment with LPS and ASX resulted in an increase in mRNA expression of ITGAM, a marker of activated microglia, compared to brain slices treated with vehicle control (P=0.08 and P<0.001, respectively) (Figure 21A). Co-treatment with ASX resulted in an even further increase in ITGAM mRNA expression compared to LPS-stimulated

brain slices (P=0.03, Figure 21A), while dexamethasone downregulated LPS-induced ITGAM expression.

ASX-induced ITGAM (microglial marker) expression was accompanied by the decreased secretion of inflammatory cytokines described above (Figures 21A, 21B, and 21D). Taken together, this could indicate a shift from the M1 to the M2 microglial phenotype. To investigate whether microglial activation resulted in an M1 or M2 microglial phenotype, we assessed the expression levels of arginase 1, (ARG1) a marker for the M2 microglial phenotype, at both mRNA and protein levels. LPS treatment or co-treatment with LPS and ASX induced ARG1 mRNA expression (P=0.0013 and P=0.0001, respectively) (Figure 21B), while dexamethasone reduced ARG1 mRNA expression, which were comparable to those of VC (P= 0.0081), Figure 21B). Also at the protein level, LPS and even more co-treatment with ASX induced Arg1 protein expression (P=0.002, Figure 21C, 21D) compared to vehicle control, while dexamethasone reduced ARG1 expression (Figure 21D). Our results suggest that ASX shifts the microglial phenotype from the deleterious M1 type to the protective M2 type in LPS-stimulated brain slices.

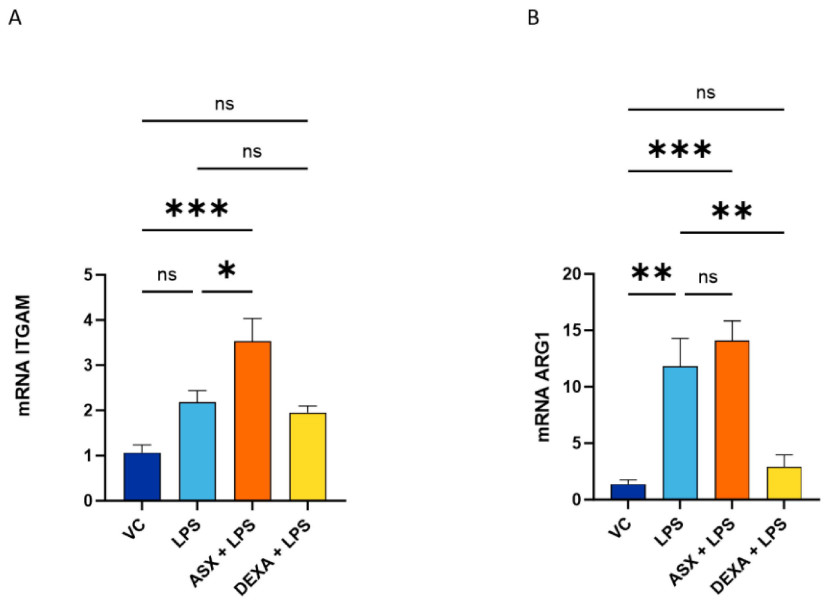

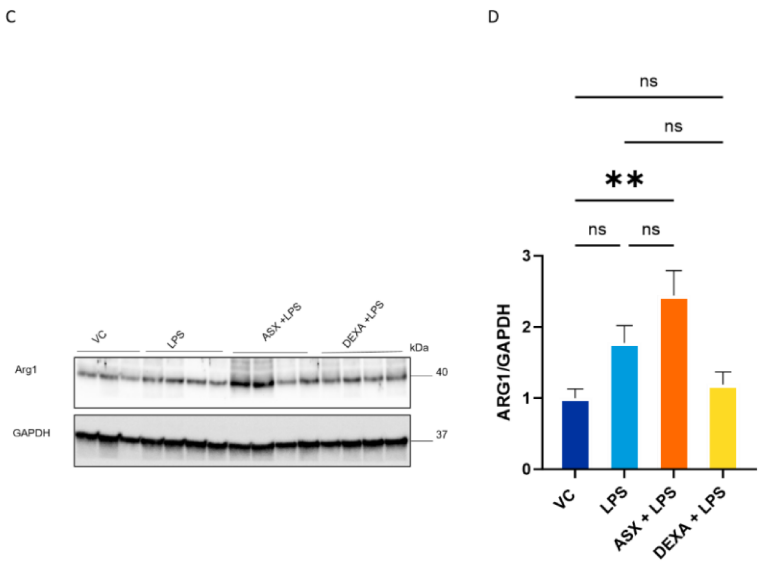

Figure 21: Microglial marker expression in lipopolysaccharide-stimulated brain slices.

Organotypic hippocampal brain slices were incubated with 10 ng/mL LPS as well as with 10 ng/mL LPS in combination with 50 µM ASX and 10 µM dexamethasone (Dexa) for 24hr followed by qRT-PCR mRNA quantification of ITGAM (A) and arginase 1 (B) and immunoblotting for arginase 1 protein relative to GAPDH (C and D). Solvent was used as vehicle control (VC). *p*-Values were calculated by one-way ANOVA with *Turkey's post hoc* test; *p < 0.05; **p < 0.01 and ***p < 0.001. Data are shown as mean + SEM, n=5-8. (Reproduced from Babalola et al., 2023 with permission from Brain Res).

5.0 DISCUSSION

BCECs are integral components of both the BBB and the neurovascular unit (Graves and Baker, 2020). Defective transport across the BBB is an important mediator of Aβ accumulation in the brain and a factor contributing to the pathogenesis of AD (Shackleton et al., 2016). OHSCs represent a physiologically relevant 3D model of the brain. It includes various cell types of the central nervous such as neurons, astrocytes, microglia and oligodendrocytes system almost in their original architecture and allows to study neuroinflammatory and pathological processes (Croft et al., 2019). We investigated the protective effects of ASX on Aβ clearance and brain inflammation, common features in proteinopathies such as AD, using induced pBCEC and OSHC as AD models. Clearance from the brain is achieved through various mechanisms, including blood-brain clearance and interstitial fluid bulk flow clearance, the perivascular and paravascular systems, autophagic lysosomal degradation, and more (Marchi et al. 2016). Our study showed that ASX alone or when co-treated with Aβ might lead to changes within the autophagy pathway, as evidenced by increased expression of LC3B and LC3B-II in pBCECs, thereby increasing the clearance of Aβ. This is consistent with other studies by Wani et al. (2000) and Li et al. (2019), in which they show that induction of autophagy increased Aβ clearance.

Numerous studies have shown increased mTOR signaling following Aβ administration (Vander Haar et al., 2007; Ito et al., 2006; 2007; Zhang et al., 2009). Further evidence for the connection between Aβ accumulation and upregulation of mTOR signaling comes from a study showing that primary neurons exposed to different concentrations of synthetic Aβ oligomers result in increased phosphorylation of mTOR proteins (Bhaskar et al., 2009). Consistent with previous reports by others (Vander Haar et al., 2007; Ito et al., 2006; 2007; Zhang et al., 2009), accumulation in pBCECs upregulated the phosphorylation of S6RP and mTOR proteins, indicating increased mTORC1 activation. Notably, co-treatment of pBCECs with Aβ and ASX reduced the phosphorylation of both proteins, likely by inhibiting the mTORC1 signaling pathway. Aβ is produced from APP via the amyloidogenic pathway by β- and γ-secretase (Chun et al., 2020), and APP expression has been shown to reflect the level of Aβ production (Xue et al., 2022). In this study, ASX significantly reduced the expression of intracellular and secreted APP/ Aβ species, suggesting reduced Aβ

production. Impaired functions of the ABCA and ABCG transporter families have been linked to brain degenerative diseases due to the importance of balanced cholesterol concentration in maintaining CNS functions (Pereira et al., 2018).

Using a mouse model of AD, Fitz et al. reported that treatment with LXR agonists increased ApoE and ABCA1 levels, which correlated with cognitive improvements and reduced Aβ deposition (Fitz et al., 2010). Furthermore, the clearance function of LRP1 appears to be crucial in various cells of the brain, as several cell-specific knockout mouse models have shown that ablation of LRP1 leads to accumulation of Aβ in the brain (Van Gool et al., 2019). In the brain endothelium, LRP1 and receptor for advanced glycation end products (RAGE) facilitate the efflux and influx of Aβ from the brain to the periphery and vice versa. Inhibition of LRP1 expression has been shown to result in vascular endothelium damage, to significantly reduce Aβ clearance, and to increase Aβ load in brain tissue (Jaeger et al., 2009). Gali et al. (2019) reported a reduction in cerebral and cerebrovascular LRP1 levels in the brains of 9-month-old 3XTg-AD mice. We observed reduction of ABCG1 and LRP1 mRNA in Aβ-treated pBCECs, suggesting increased Aβ production. ASX reversed Aβ-mediated mRNA downregulation of ABCG1 and LRP1 and simultaneously increased ABCA1 mRNA expression, indicating improved Aβ clearance. This is consistent with similar studies (Fanaee-Danesh et al., 2019; Sano et al., 2016; Matsuo et al., 2011; Vance et al., 2010) showing that increased ABCA1, ABCG1 and LRP1 expression decreases secretase activity, suppresses Aβ production, and increases clearance of Aβ from cerebrovascular endothelial cells.

PPARα is a member of the nuclear receptor PPAR family (Ghost and Pahan, 2016). Natural ligands such as fatty acids and synthetic ligands such as hypolipidemic fibrates activate PPARα, resulting in stimulation of transcription of the target gene via the formation of heterodimer complexes with the retinoid x receptor (RXR) (Fruchart et al., 1999). ASX activates PPARα and antagonizes PPARγ, another member of the PPAR family (Jia et al., 2012; Choi et al., 2019), while fenofibrate is a known activator of PPARα (Deplanque et al., 2003; Harano et la. ,2006; Villavicencio-Tejo et al., 2021). When pBCECs were co-incubated with Aβ and either ASX or fenofibrate, ABCA mRNA expression was significantly increased, while a decrease was observed in pBCECs co-incubated with Aβ and GW6417, a known antagonist of PPAR. Indeed, incubation of pBCECs with Aβ resulted in reduced protein expression of

ABCA1, which was ameliorated by co-treatment with ASX (Supplementary Figure 1). Conversely, treatment of pBCECs with Aβ increased the expression of ABCA1 at the mRNA level. This is consistent with other reports showing that the relative distribution of ABCA1 mRNA in tissues can differ significantly from protein expression patterns (Albrecht et al., 2004; Wellington et al., 2002; Schmitz & Orso, 2001). Treatment of pBCECs with Aβ alone or in combination with GW6417 reduced the expression of LRP1. Simultaneous incubation of pBCECs with Aβ and ASX or fenofibrate resulted in increased expression of LRP1, another receptor critical for Aβ efflux from the brain to the blood.

Concentrations of proinflammatory cytokines are reported to be increased in the serum and postmortem brain samples of AD patients (Wang et al., 2015; Stamouli and Politis, 2016). Proinflammatory cytokines such as IL-6, TNF- and IL-1 secreted by the M1 microglia phenotype induce inflammation (Zhang et al., 2016), while the M2 microglia phenotype IL-4, Arg1, IL- 10 and neurotrophic substances release factors that have an anti-inflammatory effect (Turtzo et al., 2014). We demonstrate that ASX influences inflammation in hippocampal brain slices. Consistent with previously published reports (Papageorgiou et al., 2016; Delbridge et al., 2020), our data show that stimulation of hippocampal brain slices with LPS IL-1, TNF-, IL-6, IL-10, KC induced /GRO, IL-2, and IL-12p70 secretion in the supernatant. Furthermore, we confirmed the anti-inflammatory effect of ASX in LPS-stimulated hippocampal brain slices. This anti-inflammatory effect was mediated by reduced expression of proinflammatory cytokines. Co-treatment of LPS-stimulated brain slices with ASX resulted in a reduction in the secretion of most of these cytokines into the supernatant (TNF-, IL-6, IL-10 and KC/GRO) and in a reduced mRNA expression of IL-6.

It has been reported that the pro-inflammatory functions of M1 type (killer cells) microglia and the anti-inflammatory functions of M2 type (repair cells) are regulated by cytokines and microbially derived products, including LPS (Orihuela et al., 2016). To determine whether the anti-inflammatory activities of ASX are due to the polarization of M2 microglia, we examined the expression of ITGAM and ARG1. We demonstrated increased mRNA expression of ITGAM, a marker of activated macrophages, and increased mRNA and protein expression of ARG1, a marker of M2 microglial polarization, after concurrent treatment of LPS-stimulated brain slices

with ASX. These results suggest that ASX shifts microglial polarization from M1 to M2, consistent with a similar report by Wen and colleagues (Wen et al., 2017).

Our study shows that co-incubation of ASX with Aβ induces autophagy, reduces Aβ production and increases Aβ clearance in pBCECs. Our results could have important implications for Aβ production and clearance at the BBB. Furthermore, the anti-inflammatory potentials of ASX impact inflammation by reducing the secretion of pro-inflammatory cytokines and activating anti-inflammatory proteins. Thus, ASX is an interesting potential therapeutic candidate that may be relevant based on its ability to ameliorate impaired Aβ clearance, inflammation, and possibly other pathophysiological processes associated with AD. A major limitation of our study is the use of *in vitro* model systems. Further studies are needed to validate our findings using preclinical *in vivo* models and to investigate potential interventions to address tau protein involvement in AD pathology.

6.0 RESULTS

6.1 *In vivo* studies

6.1.1 Presence or absence of hQC/APP and T2D mimicking diet impacts APPxhQC mice and their NTG littermates' response to glucose inversely and in a sex dependent manner.

Prior to inducing T2D in the experimental groups, mice were subjected to basal ipGTT and ipITT. Analysis of the Area under the curve (AUC) for ipGTT showed an unanticipated genotype difference, in which NTG male and female mice were intolerant to glucose (p=0.002, p=0.02 respectively, Figures 22A, 22B, 22C and 22D). However, no statistical significance was found for ipITT in males (p=0.43; Figures 23A, 23C) and females (p=0.83; Figures 23B, 23D). After 6 weeks of HFD feeding and 3 weeks of low dose streptozocin injection, mice were subjected to another round of ipGTT. Two-way Anova analysis of the AUC showed a significant effect of the diet ($F_{2, 17}$ = 10.30, P=0.001, genotype $F_{1, 17}$ = 4.376e-005, P>0.99, interaction $F_{2, 17}$ = 5.064, P=0.02, Figures 24A) in male mice but significant effects of both diet and genotype in female mice (Diet $F_{2, 18}$ = 10.38, P=0.001; genotype $F_{1, 18}$ = 29.19, P<0.001, interaction $F_{2, 18}$ = 6.638, P=0.007, Figures 24B). In addition, T2D model APPxhQC male mice were intolerant to glucose compared to their age-matched chow fed control (P=0.001, Figure 24A). However, in female mice, T2D model NTG mice were intolerant to glucose compared to their age-matched chow fed control (P<0.001, Figure 24B). After 8 weeks of initiating T2D mimicking diet, mice were fasted for 5 hours and ipITT was performed. As observed during ipGTT at week 7, diet significantly impacted the tolerance of male mice in response to glucose after 0.75IU of insulin injection (Diet $F_{2, 16}$ = 6.358, P=0.009, Genotype $F_{1, 16}$ = 1.689, P=0.21, Interaction $F_{2, 16}$ = 0.2012, P=0.82, Figures 25A) whereas in female mice, a significant effect of genotype and a trend towards significance for diet was noticed (Diet $F_{2, 16}$ = 3.414, P=0.06, Genotype $F_{1, 16}$ = 6.480, P=0.02, Interaction $F_{2, 16}$ = 5.079, P=0.02, Figures 25B). In addition, T2D model NTG male mice tend to be intolerant to glucose when given insulin compared to their age-matched chow fed control (P=0.08, Figure 25A) whereas T2D model NTG female mice were indeed insensitive to glucose (P=0.006, Figure 25B) but ASX supplementation reversed the

insensitivity to glucose (P=0.03, Figure 25B). At the end of the study, we repeated ipGTT. The effect of T2D mimicking diet was observed to be significant for male mice (Diet $F_{2,\ 16}$ = 3.976, P=0.04, Genotype $F_{1,\ 16}$ = 1.487, P=0.24, Interaction $F_{2,\ 16}$ = 0.2301, P=0.8, Figures 26A) while both diet and genotype greatly influence glucose sensitivity in female mice (Diet $F_{2,\ 16}$ = 9.795, P=0.002, Genotype $F_{1,\ 16}$ = 8.280, P=0.01, Interaction $F_{2,\ 16}$ = 5.576, P=0.01, Figures 26B). Moreover, female T2D model NTG mice were glucose insensitive when compared to their chow diet fed age matched control littermates (P<0.001, Figure 8D), while ASX supplementation showed a trend towards reversing this observed glucose intolerance (P=0.09, Figure 26B). Taken together, these results suggest that T2D mimicking diet impaired glucose metabolism in APPxhQC mice and their NTG littermates.

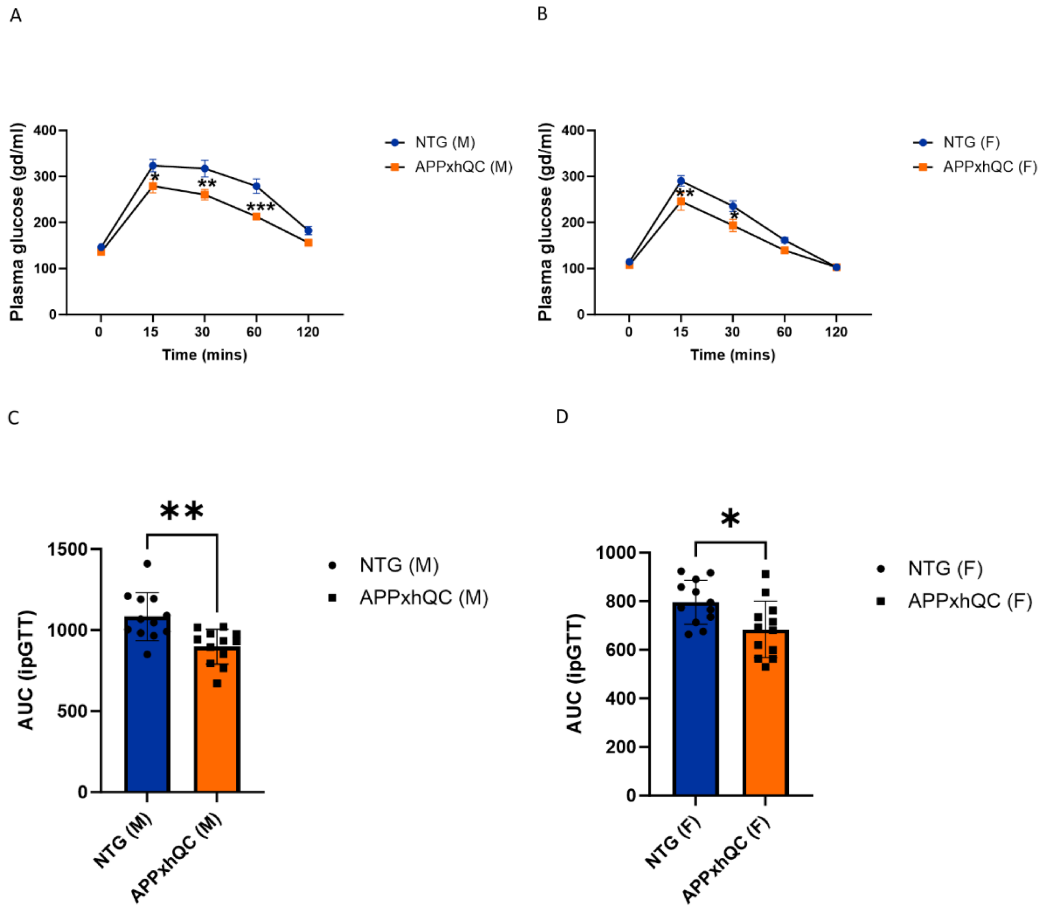

Figure 22: NTG mice are more intolerant to glucose.

Glucose tolerance test was carried out in male and female APPxhQC and NTG mice after 5 hours of fasting. Area under the curve (AUC), a measure of plasma glucose over 120 mins for the glucose tolerance test was calculated for male (A) and female

(B) APPxhQC and NTG mice. Data are mean + SEM, n=10 per sex and genotype. *p*-Values are calculated using two-tailed, unpaired students t-test, *p < 0.05; **p < 0.01.

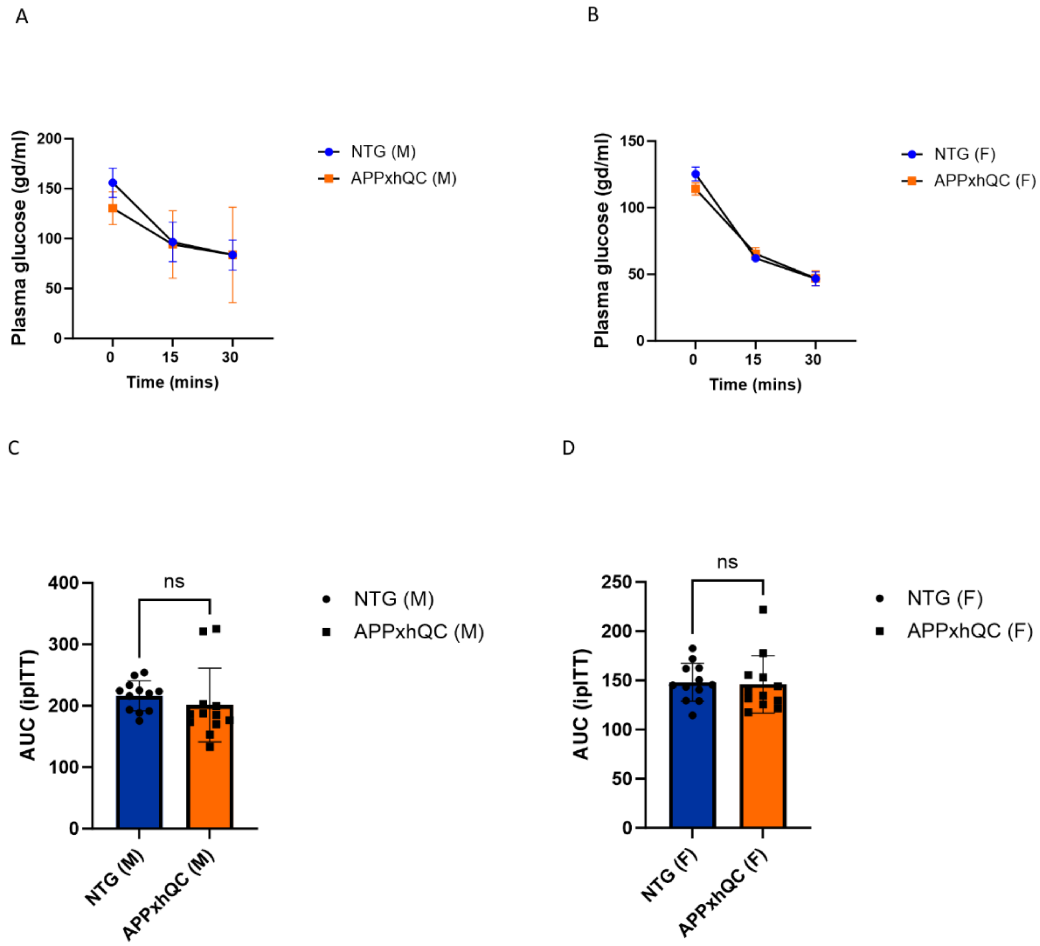

Figure 23: APPxhQC and NTG mice do not differ significantly in their response to glucose after insulin bolus.

Glucose tolerance testing in response to insulin was carried out in male and female APPxhQC and NTG mice after 5 hours of fasting. Area under the curve (AUC), a measure of plasma glucose over 120 mins for the glucose tolerance test was calculated for male (A) and female (B) APPxhQC and NTG mice. Data are mean + SEM, n=10 per sex and genotype. *p*-Values are calculated using two-tailed, unpaired students t-test, *p < 0.05; **p < 0.01.

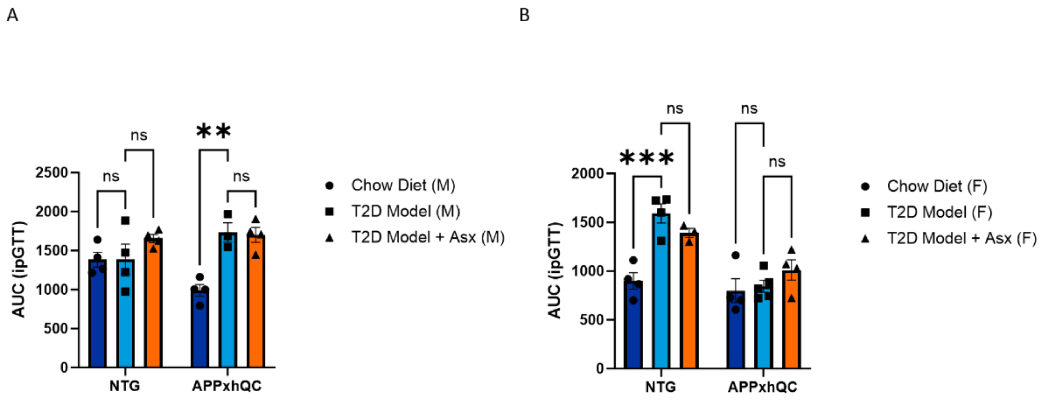

Figure 24: Impaired glucose response in APPxhQC male and NTG female mice after 6 weeks of HFD feeding and 3 weeks of streptozocin injection.

Sensitivity to glucose was assessed in male and female APPxhQC and NTG mice after 5 hours of fasting. Area under the curve (AUC), a measure of plasma glucose over 120 mins for the glucose tolerance test was calculated for male (A) and female (B) APPxhQC and NTG mice. Data are mean + SEM, n=3-5 per sex and genotype. *p*-Values are calculated using Two-way ANOVA followed by *Turkey's* Multiple Comparison test, **p < 0.01 and ***p < 0.001.

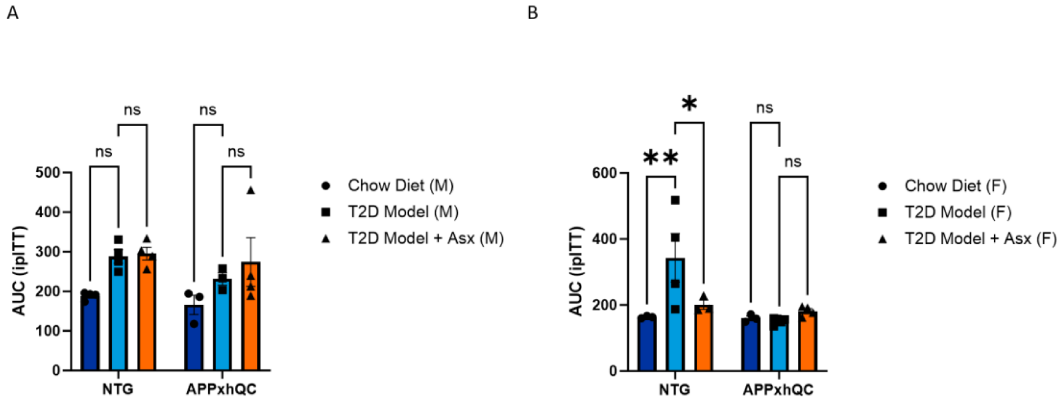

Figure 25: Impaired sensitive to glucose in response to insulin in NTG male and female mice after 8 weeks of HFD feeding and 5 weeks of streptozocin injection.

Glucose tolerance in response to insulin was carried out in male and female APPxhQC and NTG mice after 5 hours of fasting. Area under the curve (AUC), a measure of plasma glucose over 120 mins for the glucose tolerance test was calculated for male (A) and female (B) APPxhQC and NTG mice. Data are mean + SEM, n=3-5 per sex and genotype. *p*-Values are calculated using Two-way ANOVA followed by *Turkey's* Multiple Comparison test, *p < 0.05; **p < 0.01.

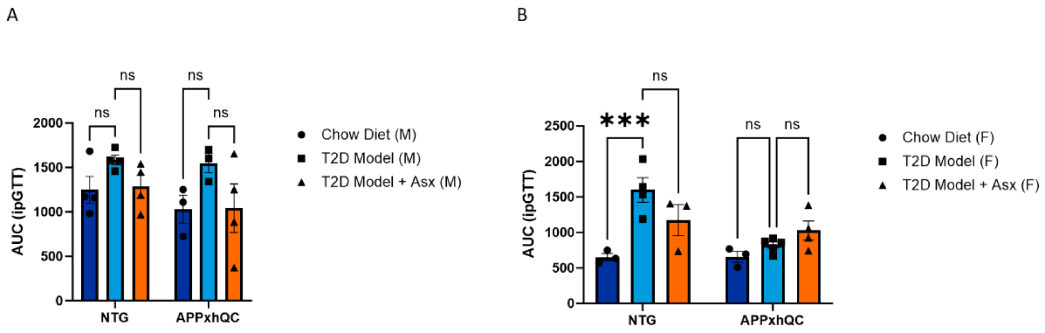

Figure 26: Severe glucose insensitivity in T2D model **NTG female mice.**
Tolerance to glucose was evaluated in male and female APPxhQC and NTG mice after 5 hours of fasting. Area under the curve (AUC), a measure of plasma glucose over 120 mins for the glucose tolerance test was calculated for male (A) and female (B) APPxhQC and NTG mice. Data are mean + SEM, n=3-5 per sex and genotype. *p*-Values are calculated using Two-way ANOVA for A, B followed by *Dunnett's* Multiple Comparison test, ***p < 0.001.

6.1.2 T2D mimicking diet impacts food consumption, tissue weight and body weight of APPxhQC mice and their NTG littermates.

We evaluated weight gain, liver weight and amount of food consumed during the 13 weeks of feeding. As expected, diet greatly influenced the amount of food consumed by the mice irrespective of their genotype; for male mice ($F_{2, 16}$ = 39.58, P<0.001, Figure 27A) and female mice ($F_{2, 16}$ = 8.631, P=0.003, Figure 27B). We observed a drop in quantity of food consumed in the T2D model group regardless of sex or genotype. Both T2D model NTG (P <0.001) and T2D model APPxhQC (P=0.01, Figure 27A) consumed less food when compared to their age-matched chow fed control group. In female mice, significantly decreased food intake was observed in T2D model APPxhQC mice (P=0.02, Figure 27B) and a trend towards significance in T2D model NTG (P=0.08, Figure 27B).

We observed a significant effect of diet on weight gain and a trend towards significance for the genotype in male mice (Diet $F_{2, 16}$ = 12.98, P<0.001, Genotype $F_{1, 16}$ = 3.302, P=0.09, Figure 27C). In female mice, the effect of genotype was significant (Genotype $F_{1, 16}$ = 7.976, P=0.01, Diet $F_{2, 16}$ = 3.086, P=0.07, Figure 27D). T2D model NTG male mice showed significant weight gain compared to their chow fed age matched littermates (P=0.002, Figure 27C). Since the liver is the main organ of metabolism and T2D is known to influence the liver differentially, we evaluated

liver weights in the 3 dietary groups. We observed a strong effect of genotype (for male mice, $F_{1, 16}$ = 19.38, P<0.001 and $F_{1, 16}$ = 6.552, P=0.02 for female mice, Figures 28A, 28B). In addition, we evaluated the liver to body weight ratio in the dietary group and observed a strong effect of genotype for male mice ($F_{1, 16}$ = 10.31, P=0.005, Figure 28C) and a trend towards significance for female mice ($F_{2, 16}$ = 3.556, P=0.05, Figure 28D), albeit groups did not statistically differ from one another. Taken together, these data suggest that T2D mimicking diet influenced food consumption irrespective of sex or genotype and weight gain in the absence of hQC in male mice.

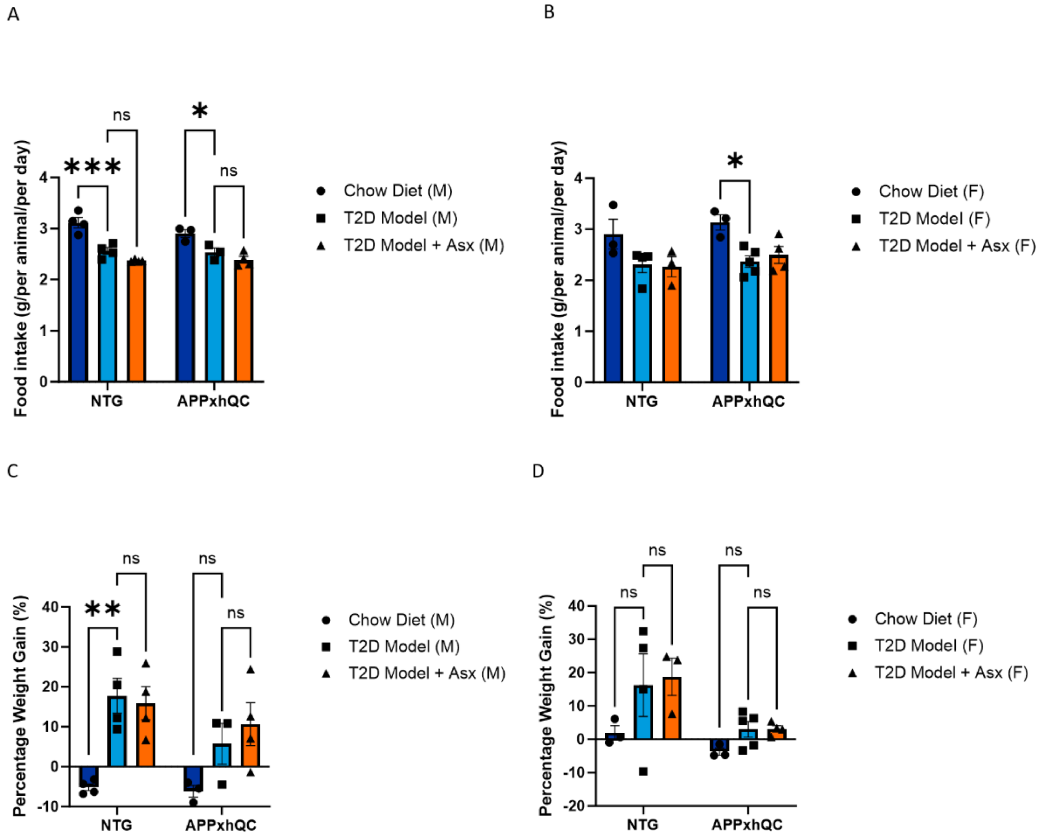

Figure 27: Food Consumption and weight gain in T2D model APPxhQC and NTG mice.

Food intake of each animal and weight gain were measured weekly. Food intake in male (A) and female (B), percentage gain in weight in male (C) and female mice (D) were evaluated over the course of 13 weeks of the study. Data are mean + SEM, n=3-5 per sex and genotype. *P*-Values are calculated using Two-way ANOVA followed by *Turkey's* Multiple Comparison test; *p < 0.05; **p < 0.01 and ***p < 0.001.

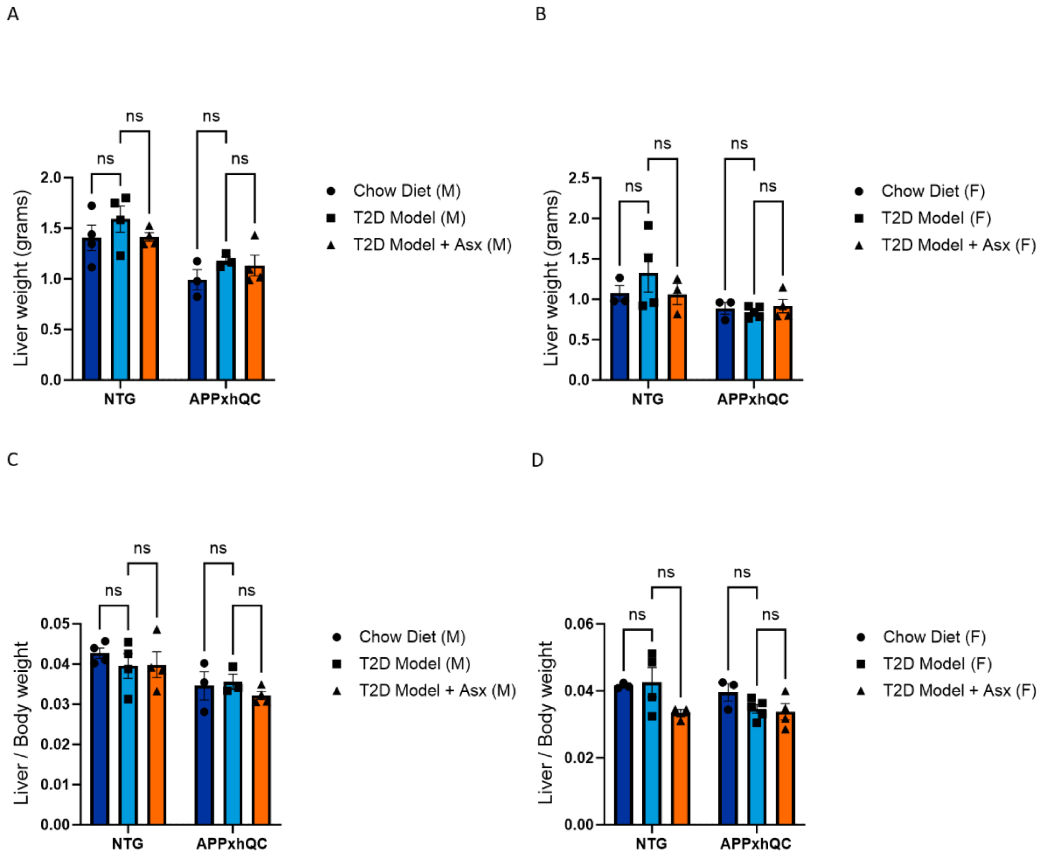

Figure 28: Tissue and organ weight /body ratio.

Liver weight in male (A) and female mice (B). Liver to body weight ratio in male (C) and female mice (D). Data are mean + SEM, n=3-5 per sex and genotype. *p*-Values are calculated using Two-way ANOVA followed by *Turkey's* Multiple Comparison test.

6.1.3 T2D mimicking diet impacts glycemic parameters in a sex and genotype dependent manner with a more pronounced effect in T2D model NTG female mice.

We evaluated the effect of T2D on fasting plasma insulin (FPI), fasting plasma glucose (FPG), Homeostatic Model Assessment for Insulin Resistance (HOMA-IR), Homeostasis Model Assessment of Beta-cell function (HOMA-β) and hemoglobin A1c (HbA1c).

In male mice, we observed increased FPG in T2D model relative to age matched chow fed controls, irrespective of genotype (APPxhQC/T2D-7.20 ±0.18 vs APPxhQC/chow fed-6.31 ± 0.70; NTG/T2D-8.53 ± 0.56 vs NTG/chow fed-7.70 ± 0.24, Table 3). Conversely, in female mice, T2D elevated fasting glucose only in NTG

mice (APPxhQC/T2D- 5.68 ± 0.35 vs APPxhQC/chow fed-6.44 ± 0.27; NTG/T2D-8.09 ± 1.60 vs NTG/chow fed-5.83 ± 0.47, Table 3). Surprisingly, age matched chow fed NTG male mice had increased FPI (25.03 ± 4.71) when compared to mice on T2D mimicking diet (22.2 ± 1.69) whereas, we noticed increased fasting insulin in APPxhQC male mice on T2D mimicking diet (23.88 ± 5.94) compared to their age matched chow fed control littermates (13.1 ± 0.63). In female mice, we observed an increase in FPI in mice on T2D mimicking diet compared to the age matched chow fed control littermate, irrespective of genotype (APPxhQC/T2D-11.51 ± 2.11 vs APPxhQC/chow fed-7.49 ± 0.80; NTG/T2D-15.24 ± 2.35 vs NTG/chow fed-14.24 ± 2.15, Table 3). Furthermore, we noted that age matched chow fed NTG mice (Male-25.03 ± 4.71; Female- 14.24 ± 2.15, Table 19) had elevated FPI when compared to chow fed APPxhQC mice (Male- 13.1 ± 0.63; Female- 7.49 ± 0.80, Table 19) irrespective of the sex.

We also evaluated the effect of T2D mimicking on insulin resistance (HOMA-IR) and insulin secretion (HOMA-β). Age matched chow fed NTG male mice were more insulin resistant as seen in their HOMA-IR compared to those in the T2D model group (NTG /chow fed 12.17 ± 3.19 vs NTG/T2D - 8.52 ± 1.20, Table 19). Conversely, T2D mimicking diet led to increased insulin resistance in both NTG (T2D- 5.10 ± 0.66 vs chow fed- 3.78 ± 0.86) and APPxhQC female mice (T2D- 2.80 ± 0.40 vs chow fed- 2.16 ± 0.32). Both male (T2D- 89.70 ± 6.01 vs chow fed- 116.51 ± 16.62) and female (T2D-106.60 ± 39.15 vs chow fed-125.14 ± 6.83) NTG mice on T2D mimicking diet had impaired insulin secretion (HOMA-β), whereas T2D mimicking diet increases insulin secretion in APPxhQC mice (Table 19).

Table 19: Glycemic Parameters.

Group	Sex	Fasting Insulin (mIU/L)	Fasting Glucose(mmol/L)	HOMA-IR	HOMA-β
NTG-Chow	male	25.03 ± 4.71	7.70 ± 0.24	12.17 ± 3.19	116.51 ± 16.62
NTG-T2D Model	male	22.2 ± 1.69	8.53 ± 0.56	8.52 ± 1.20	89.70 ± 6.01
NTG-T2D Model + Asx	male	24.41 ± 3.17	7.65 ± 0.16	8.22 ± 0.95	119.95 ± 18.65
APPxhQC-Chow	male	13.1 ± 0.63	6.31 ± 0.70	3.69 ± 0.46	121.49 ± 37.87
APPxhQC-T2D Model	male	23.88 ± 5.94	7.20 ± 0.18	7.78 ± 2.06	125.42 ± 26.97
APPxhQC-T2D Model + Asx	male	19.90 ± 0.61	8.44 ± 0.95	7.22 ± 0.78	93.86 ± 17.68

Group	Sex	Fasting Insulin	Fasting Glucose	HOMA-IR	HOMA-β
NTG-Chow	female	14.24 ± 2.15	5.83 ± 0.47	3.78 ± 0.86	125.14 ± 6.83
NTG-T2D Model	female	15.24 ± 2.35	8.09 ± 1.60	5.10 ± 0.66	106.60 ± 39.15
NTG-T2D Model + Asx	female	16.22 ± 1.83	6.12 ± 0.33	4.36 ± 0.41	134.78 ± 31.66
APPxhQC-Chow	female	7.49 ± 0.80	6.44 ± 0.27	2.16 ± 0.32	50.85 ± 0.67
APPxhQC-T2D Model	female	11.51 ± 2.11	5.68 ± 0.35	2.80 ± 0.40	136.09 ± 48.35
APPxhQC-T2D Model + Asx	female	15.30 ± 3.09	6.67 ± 0.43	4.48 ± 0.80	108.03 ± 34.06

Fasting plasma insulin, fasting plasma glucose, HOMA-IR and HOMA-β were evaluated after 5 hours of fasting. Groups did not statistically differ from one another. Data are mean + SEM, n=3-5 per sex and genotype except for APPxhQC and NTG chow fed control group where n=2 for Fasting Insulin, HOMA-IR and HOMA-β.

The HbA1c assay is a simple test that measures the average blood sugar level over the past 2-3 months. We investigated HbA1c in whole blood. Both diet and genotype had significant effects on HbA1c levels in female mice (Diet $F_{2,\ 15}$ = 8.026, P=0.004, Genotype $F_{1,\ 15}$ = 6.582, P=0.02, Interaction $F_{2,\ 15}$ = 5.853, P=0.01, Figure 29B). Furthermore, we observed a significant increase in the HbA1c levels of T2D model APPxhQC female mice (P=0.009, Figure 29B) compared to their age matched chow fed control littermates suggesting impaired glycemic control in APPxhQC female mice. However, ASX supplementation had no effect on HbA1c (P=0.32, Figure 29B). Taken together, these results suggest a more severe T2D model phenotype in T2D model NTG female mice.

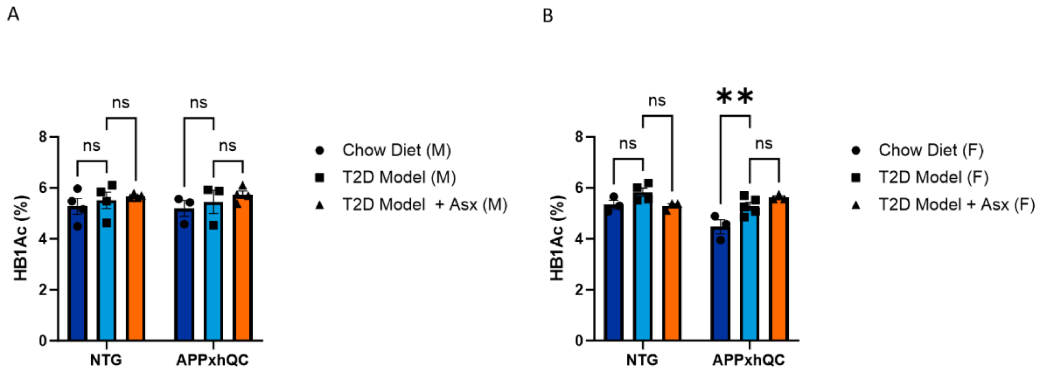

Figure 29: HbA1c evaluation in in T2D model APPxhQC and NTG mice.

Blood HbA1c level was determined using a commercially available ELISA kit in Male (A) and female (B) mice. Data are mean + SEM, n=3-5 per sex and genotype. *p*-Values are calculated using Two-way ANOVA followed by *Turkey's* Multiple Comparison test; **p < 0.01.

6.1.4 Impaired lipid and cholesterol metabolism and liver damage in T2D model **APPxhQC and NTG mice.**

Dyslipidemia and impaired cholesterol metabolism are associated with both AD and T2D. We investigated the influence of T2D mimicking diet and pyroglutamylation on cholesterol and lipid metabolism in APPxhQC mice and their NTG littermate. Diet and genotype significantly influenced cholesterol metabolism irrespective of sex (Male - Diet $F_{2, 16} = 12.96$, P<0.001), Genotype $F_{1, 16} = 15.22$, P=0.001; Female – Diet $F_{2, 15} = 14.97$, P<0.001, Genotype $F_{1, 15} = 11.07$, P=0.005, Interaction $F_{2, 15} = 2.775$, P=0.09, Figures 30A, 30B). Both T2D model APPxhQC (P=0.03) male mice and their NTG littermates (P=0.009) showed increased plasma cholesterol levels compared to their chow fed age-matched control group (Figure 30A). On the other hand, only T2D model NTG female mice had elevated plasma cholesterol when compared to their age matched chow fed controls (P<0.001, Figure 30B). ASX supplementation did not lower the elevated total plasma cholesterol irrespective of sex or genotype. Genotype had a significant impact on plasma triglyceride levels only in female mice ($F_{1, 15} = 6.413$, P=0.02, Figure 30D) but did not differ significantly between the groups.

Liver function is reported to be impaired in T2D model patients. Therefore, we investigated the effects of diet and genotype on two common liver function enzymes in APPxhQC mice and their NTG littermates. Both AST ($F_{2, 16} = 4.552$, P=0.03,

Figure 31B) and ALT ($F_{1, 16}$ = 6.180, P=0.02, Figure 31D) were significantly affected by diet in female mice. In addition, T2D model NTG female mice showed increased levels of serum AST (P=0.010, Figure 31B) and ALT (P=0.02, Figure 31D) when compared to their age matched chow fed group. ASX supplementation could not lower the elevated serum liver function enzymes irrespective of sex or genotype. Taken together, this suggests that T2D mimicking diet dysregulated cholesterol and lipid metabolism and impaired the liver function in NTG mice, especially in females.

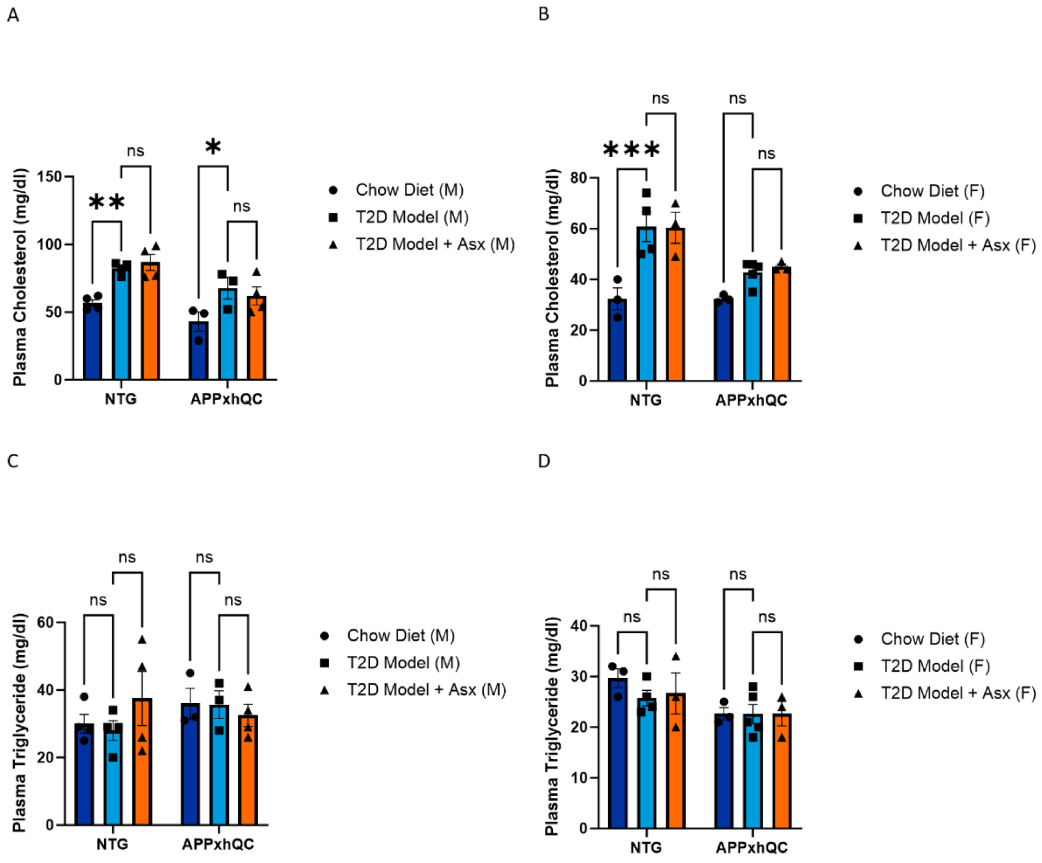

Figure 30: Total Plasma Cholesterol and Triglycerides in T2D model APPxhQC and NTG mice.

Total plasma cholesterol levels were elevated in T2D model mice irrespective of sex or genotype. Plasma cholesterol level in male (A) and female mice (B); Triglyceride levels in male (C) and female mice (D). Data are mean + SEM, n=3-5 per sex and genotype. *p*-Values are calculated using Two-way ANOVA followed by *Turkey's* Multiple Comparison test; *p < 0.05; **p < 0.01 and ***p < 0.001.

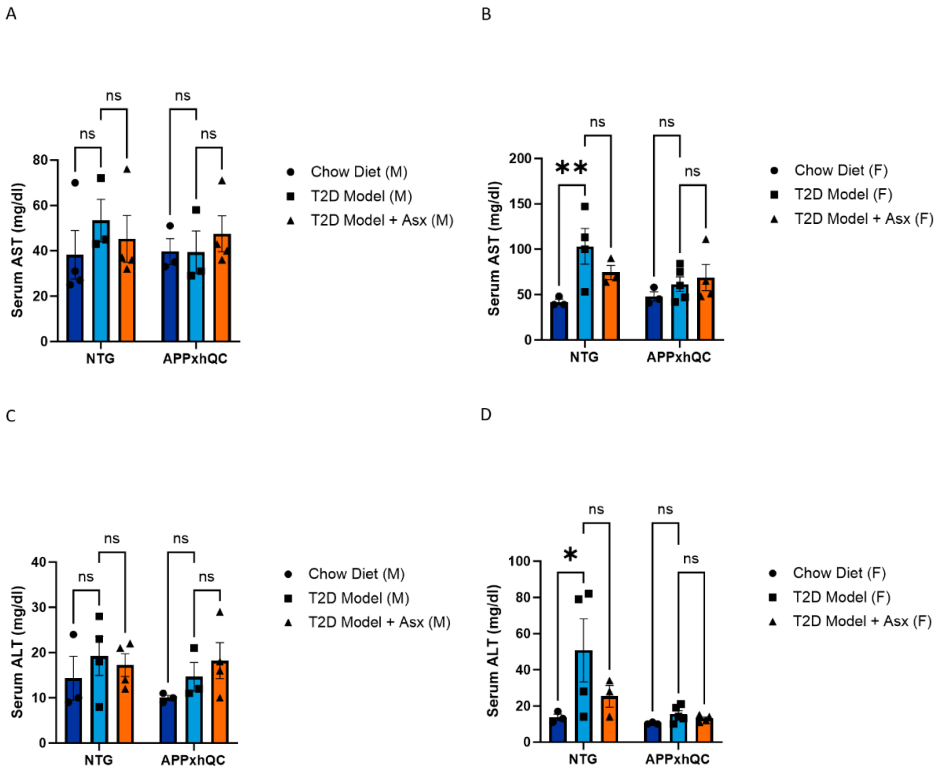

Figure 31: AST and ALT are elevated in serum of T2D model **APPxhQC and NTG mice.**

Liver damage in T2D model NTG female mice. Serum AST levels were assessed in male (A) and female mice (B), ALT levels in male (C) and female mice (D). Data are mean + SEM, n=3-5 per sex and genotype. *p*-Values are calculated using Two-way ANOVA followed by *Turkey's* Multiple Comparison test; *p < 0.05; **p < 0.01.

6.1.5 T2D mimicking diet downregulates hepatic mRNA expression levels of genes involved in cholesterol efflux, lipid metabolism and Aβ transport in a sex dependent manner.

Sterol regulatory element-binding factor 1 gene (SREBF1), Peroxisome proliferator-activated receptor gamma coactivator-1 alpha / beta (PGC1 α/β), Peroxisome proliferator-activated receptor-α (PPARα), Peroxisome proliferator-activated receptor-γ (PPARγ) and Fibroblast Growth Factor-21 (FGF21) are some of the transcription genes involved in insulin sensitivity, gluconeogenesis, cholesterol synthesis and lipid homeostasis.

To investigate how T2D mimicking diet dysregulates cholesterol and lipid metabolism in our study model, we evaluated the effects of T2D mimicking diet and genotype on the regulation of genes associated with insulin sensitivity, gluconeogenesis, cholesterol synthesis and lipid metabolism in APPxhQC mice and their NTG littermates. In female mice, T2D mimicking diet significantly influenced the expression of SREBF1 ($F_{2, 16}$ = 4.991, P=0.02, Figure 32B), diet ($F_{2, 16}$ = 5.103, P=0.02, Figure 32D), influenced PGC1β expression. However, in male mice, T2D mimicking diet significantly influenced PGC1α expression ($F_{2, 16}$ = 3.891, P=0.04, Figure 32F). The expression of SREBF1 and PGC1β were significantly down-regulated in T2D model NTG female mice compared to their age matched chow fed group (P=0.04 and P=0.03, Figures 32B, 32D).

Neprilysin (NEP) - a rate-limiting endopeptidase**,** Low density lipoprotein receptor related protein 1 (LRP1) and Adenosine Binding Cassette Transporter Proteins 1 (ABCA1) are genes involved in cholesterol efflux and amyloid transport from brain to the blood. We analyzed the effects of T2D mimicking diet and genotype on the hepatic mRNA expressions of these genes. In female mice, we observed a significant effect of genotype on the expression of Neprilysin ($F_{1, 16}$ = 8.978, P=0.009, Figure 32H). T2D mimicking diet ($F_{2, 16}$ = 6.932, P=0.007, Figure 32J) accompanied by a genotype effect ($F_{1, 16}$ = 5.066, P=0.04, Figure 32J) influenced LRP1 expression. In female mice, T2D mimicking diet had significant influence on ABCA1 expression ($F_{2, 16}$ = 4.236, P=0.03, Figure 32L). In addition, mRNA expressions of LRP1 and ABCA1 were significantly down-regulated in T2D model NTG female mice compared to their age matched chow fed group and a trend towards significance for NEP (P=0.008; P= 0.04 and P=0.06 respectively, Figures 32H, 32J and 32L).

T2D mimicking diet had a significant effect on PPARα expression ($F_{2, 16}$ = 5.591, P=0.01, Figure 32F) while genotype showed a trend towards significance ($F_{1, 16}$ = 3.221, P=0.09, Figure 32N). In addition, T2D mimicking diet had a significant effect on PPARγ2 expression in male mice ($F_{2, 16}$ = 4.980, P=0.02, Figure 32O). Moreover, mRNA expressions of PPARα and PPARγ2 were significantly downregulated in T2D model NTG female and male mice, respectively, compared to their age matched chow fed control group (P=0.02, P=0.02, Figures 32N, Figure 32O).

T2D mimicking diet had a significant effect on ABCG1 expression ($F_{2, 16}$ = 5.388, P= 0.02, Figure 32S) and genotype showed a trend towards significant effect on FGF21 expression ($F_{1, 16}$ = 3.412, P= 0.08, Figure 32U) in female mice but the differences

within groups were not statistically significant. Taken together, T2D mimicking diet and absence of hQC downregulated hepatic genes crucial for insulin sensitivity, gluconeogenesis, cholesterol efflux and lipid metabolism especially in NTG female mice.

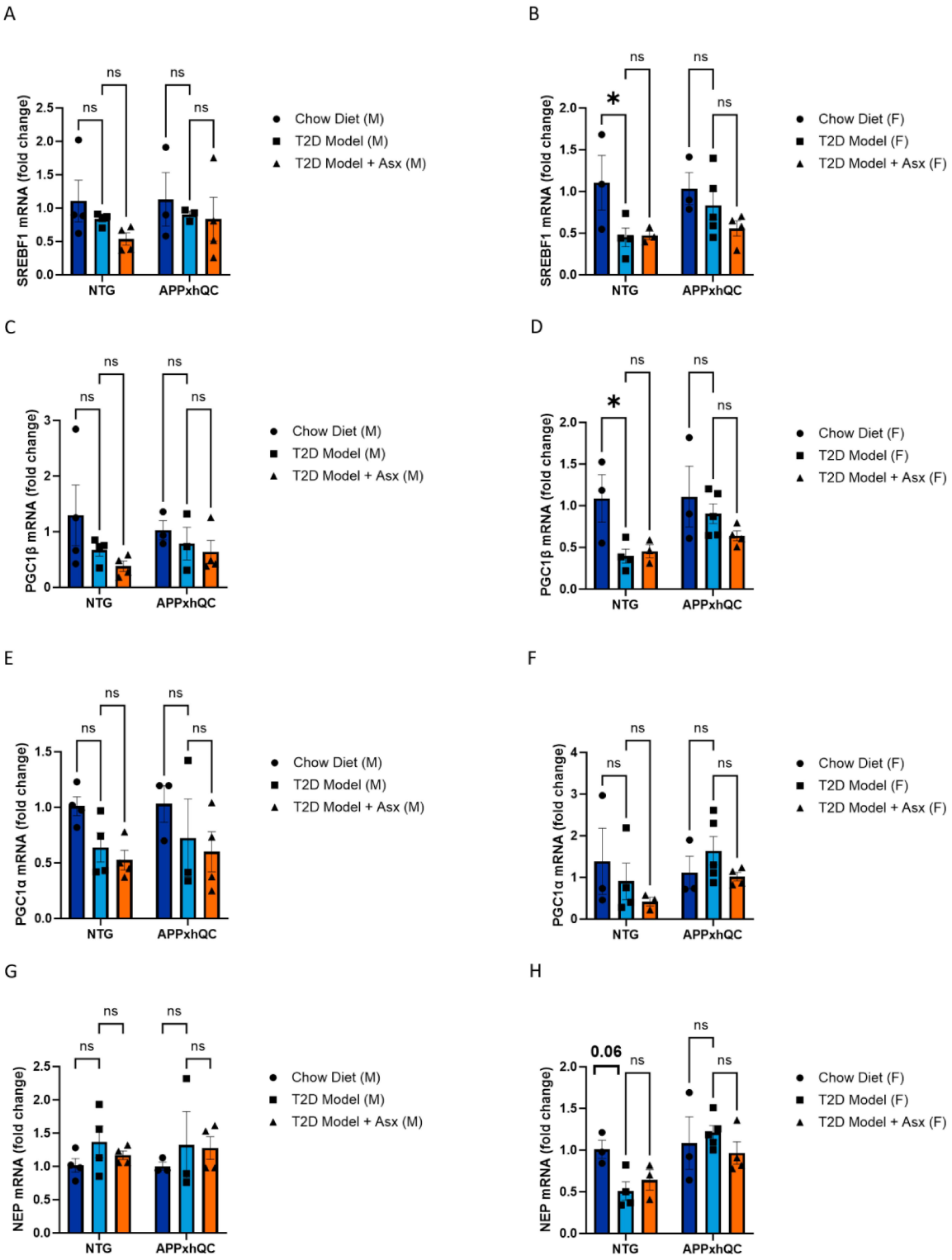

I

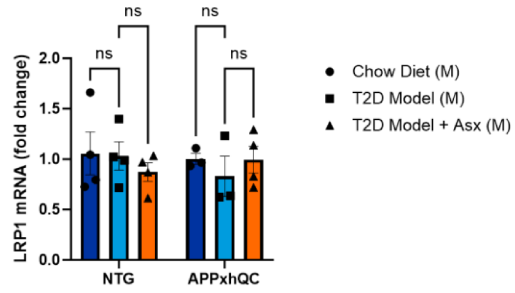
LRP1 mRNA (fold change)
2.0
1.5
1.0
0.5
0.0
ns
ns
ns
ns
NTG
APPxhQC
Chow Diet (M)
T2D Model (M)
T2D Model + Asx (M)

J

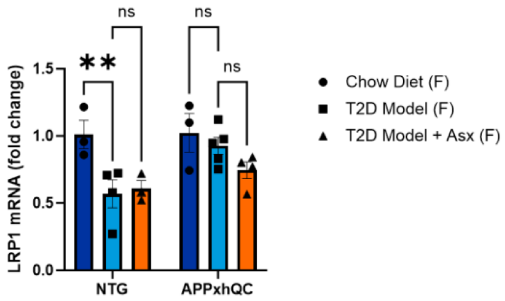
LRP1 mRNA (fold change)
1.5
1.0
0.5
0.0
**
ns
ns
ns
NTG
APPxhQC
Chow Diet (F)
T2D Model (F)
T2D Model + Asx (F)

K

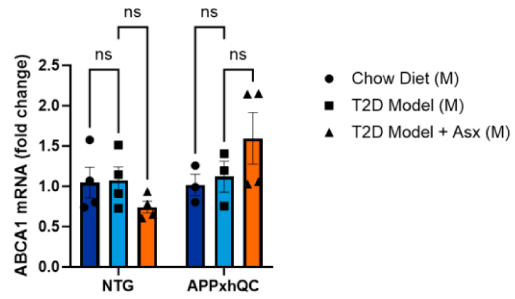
ABCA1 mRNA (fold change)
2.5
2.0
1.5
1.0
0.5
0.0
ns
ns
ns
ns
NTG
APPxhQC
Chow Diet (M)
T2D Model (M)
T2D Model + Asx (M)

L

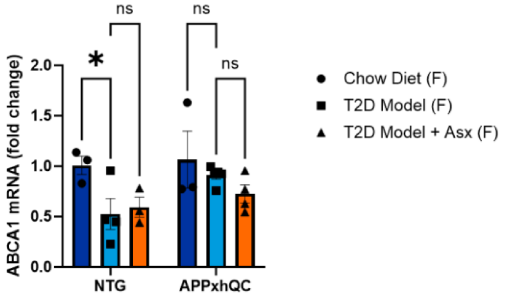
ABCA1 mRNA (fold change)
2.0
1.5
1.0
0.5
0.0
*
ns
ns
ns
NTG
APPxhQC
Chow Diet (F)
T2D Model (F)
T2D Model + Asx (F)

M

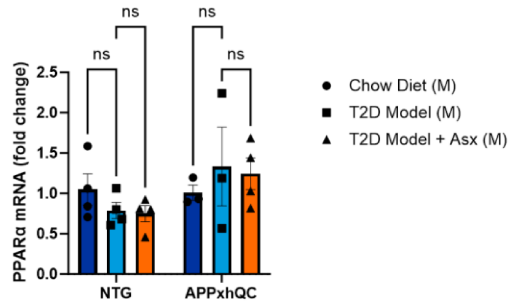
PPARα mRNA (fold change)
2.5
2.0
1.5
1.0
0.5
0.0
ns
ns
ns
ns
NTG
APPxhQC
Chow Diet (M)
T2D Model (M)
T2D Model + Asx (M)

N

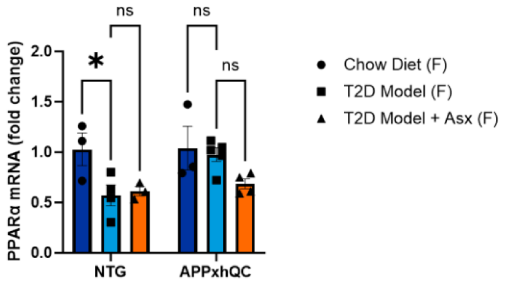
PPARα mRNA (fold change)
2.0
1.5
1.0
0.5
0.0
*
ns
ns
ns
NTG
APPxhQC
Chow Diet (F)
T2D Model (F)
T2D Model + Asx (F)

O

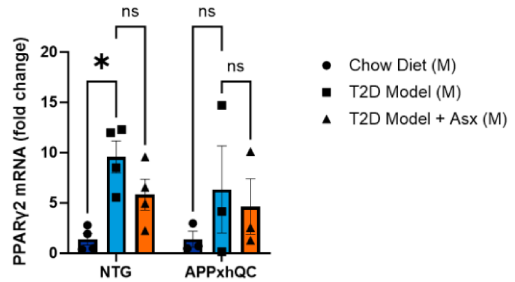
PPARγ2 mRNA (fold change)
20
15
10
5
0
*
ns
ns
ns
NTG
APPxhQC
Chow Diet (M)
T2D Model (M)
T2D Model + Asx (M)

P

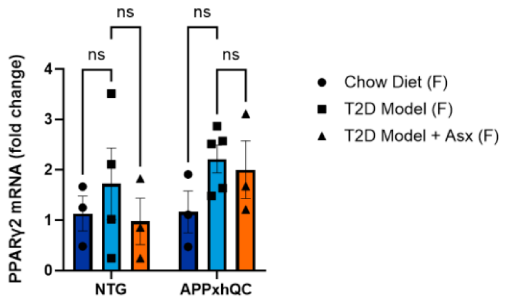
PPARγ2 mRNA (fold change)
4
3
2
1
0
ns
ns
ns
ns
NTG
APPxhQC
Chow Diet (F)
T2D Model (F)
T2D Model + Asx (F)

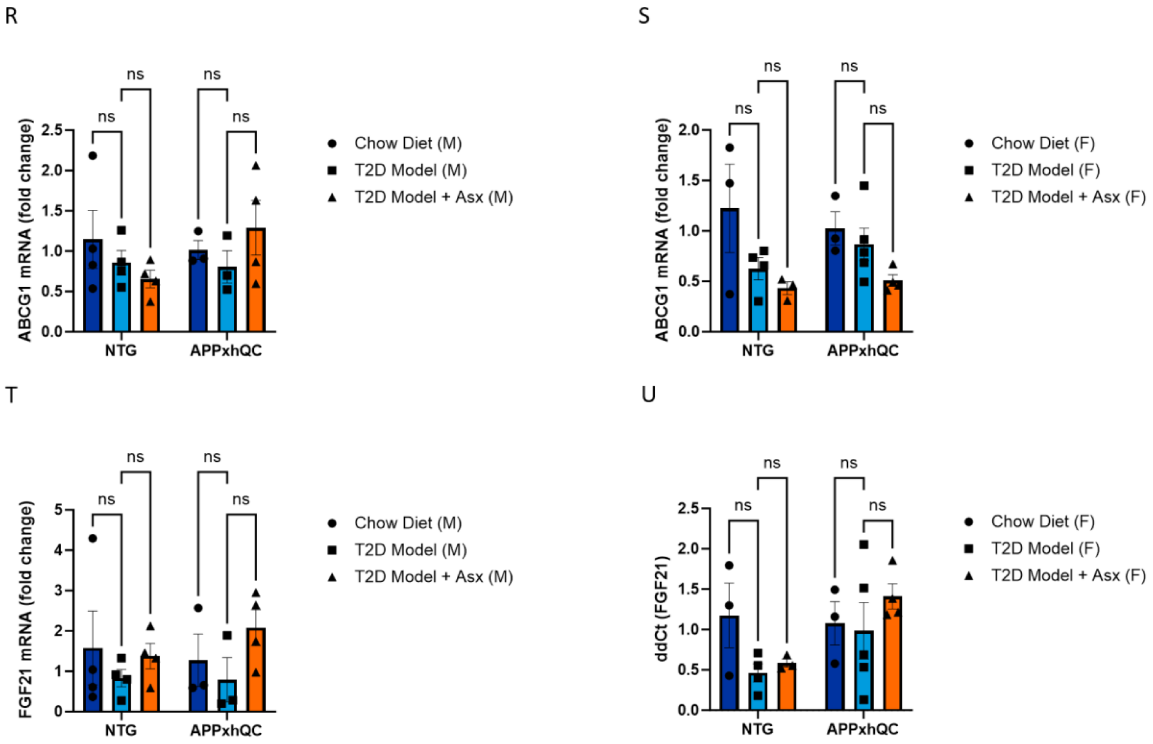

Figure 32: Transcription genes implicated in lipid biogenesis and cholesterol efflux are altered in T2D model NTG female mice.

Genes involved in glucose and lipid metabolism are significantly down-regulated in T2D model NTG female mice. Quantitative qPCR assessment of SREBF1 in male (A) and female mice (B); PGC1β in male (C) and female mice (D); PGC1α in male (E) and female mice (F); NEP in male (G) and female mice (H); LRP1 in male (I) and female mice (J); ABCA1 in male (K) and female mice (L); PPARα in male (M) and female mice (N); PPARγ2 in male (O) and female mice (P). Data are mean + SEM, n=3-5 per sex and genotype. *p*-Values are calculated using Two-way ANOVA followed by *Turkey's* Multiple Comparison test; *p < 0.05.

6.1.6 T2D mimicking diet is associated with a shift from soluble to large insoluble Aβ isoforms in the brains of APPxhQC mice in a sex dependent manner.

Misfolding / aggregation of the Aβ protein is thought to play a central role in the pathophysiology of AD. Abnormal Aβ production was proposed as the mechanistic link that underlies pathology of insulin resistance and diabetes in AD. We

investigated the effect of T2D on the aggregation of Aβ in APPxhQC mice. Therefore, we measured the amount of soluble (DEA fractions) and plaque-associated insoluble (FA fractions) Aβ isoforms in whole brain lysates of T2D model APPxhQC mice, their chow fed age matched control and ASX supplemented T2D group.

Diet had significant effect on the amount of soluble Aβ fractions deposited in the brain of the mice, especially the males ($F_{2, 21}$ = 18.86, P<0.001, Figure 33A). For the plaque associated conventional Aβ isoforms ($Aβ_{38}$, $Aβ_{40}$ and $Aβ_{42}$), diet had a significant impact on their deposition irrespective of the sex (Male - $F_{2, 21}$ = 7.180, P=0.004; Female - $F_{2, 18}$ = 4.020, P=0.04, Figures 33C, 33D). In male mice, T2D mimicking diet resulted in a reduced amount of soluble $Aβ_{40}$ deposited in the brain when compared to chow fed age matched control albeit not to a level of statistical significance (P=0.18, Figure 33A). ASX supplementation led to a significant reduction in the deposited soluble Aβ especially for $Aβ_{40,}$ when compared to the T2D model group (P=0.03, Figure 33A), but only a trend towards reduction for $Aβ_{38}$ (P=0.07, Figure 33A) was noted. In female mice, T2D mimicking diet had no effect on the deposition of conventional soluble brain Aβ isoforms. In addition, T2D mimicking diet led to a significant increase in the amount of plaque associated $Aβ_{40}$ deposits in brains of the male mice in comparison to their chow fed age matched control group (P=0.01, Figure 33C) which was significantly reduced by ASX supplementation (P=0.007, Figure 33C).

A

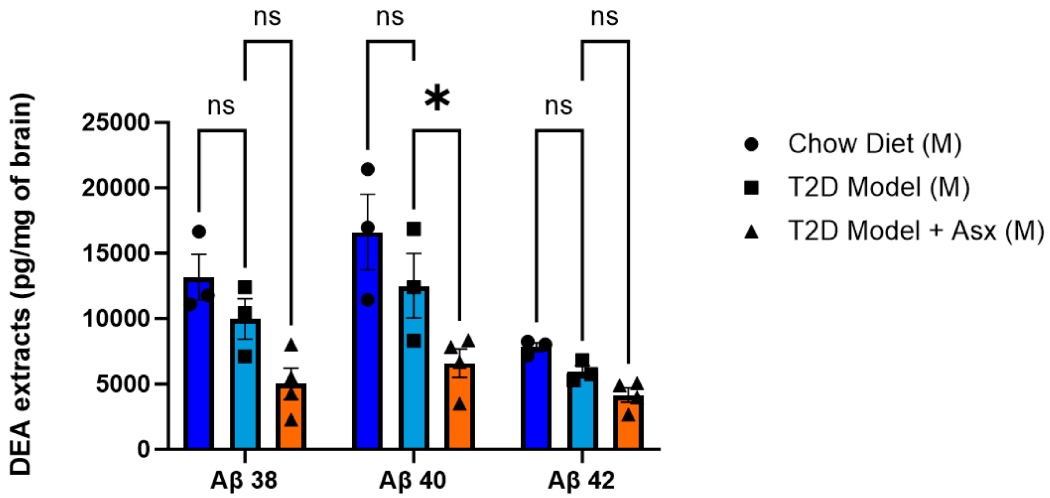
DEA extracts (pg/mg of brain)
25000
20000
15000
10000
5000
0
ns
ns
ns
ns
*
ns
Aβ 38
Aβ 40
Aβ 42
Chow Diet (M)
T2D Model (M)
T2D Model + Asx (M)

B

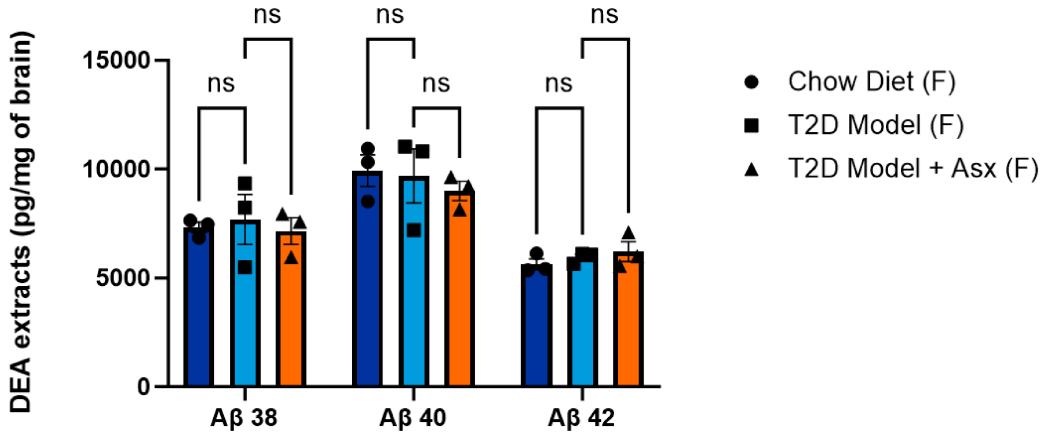
DEA extracts (pg/mg of brain)
15000
10000
5000
0
ns
ns
ns
ns
ns
ns
Aβ 38
Aβ 40
Aβ 42
Chow Diet (F)
T2D Model (F)
T2D Model + Asx (F)

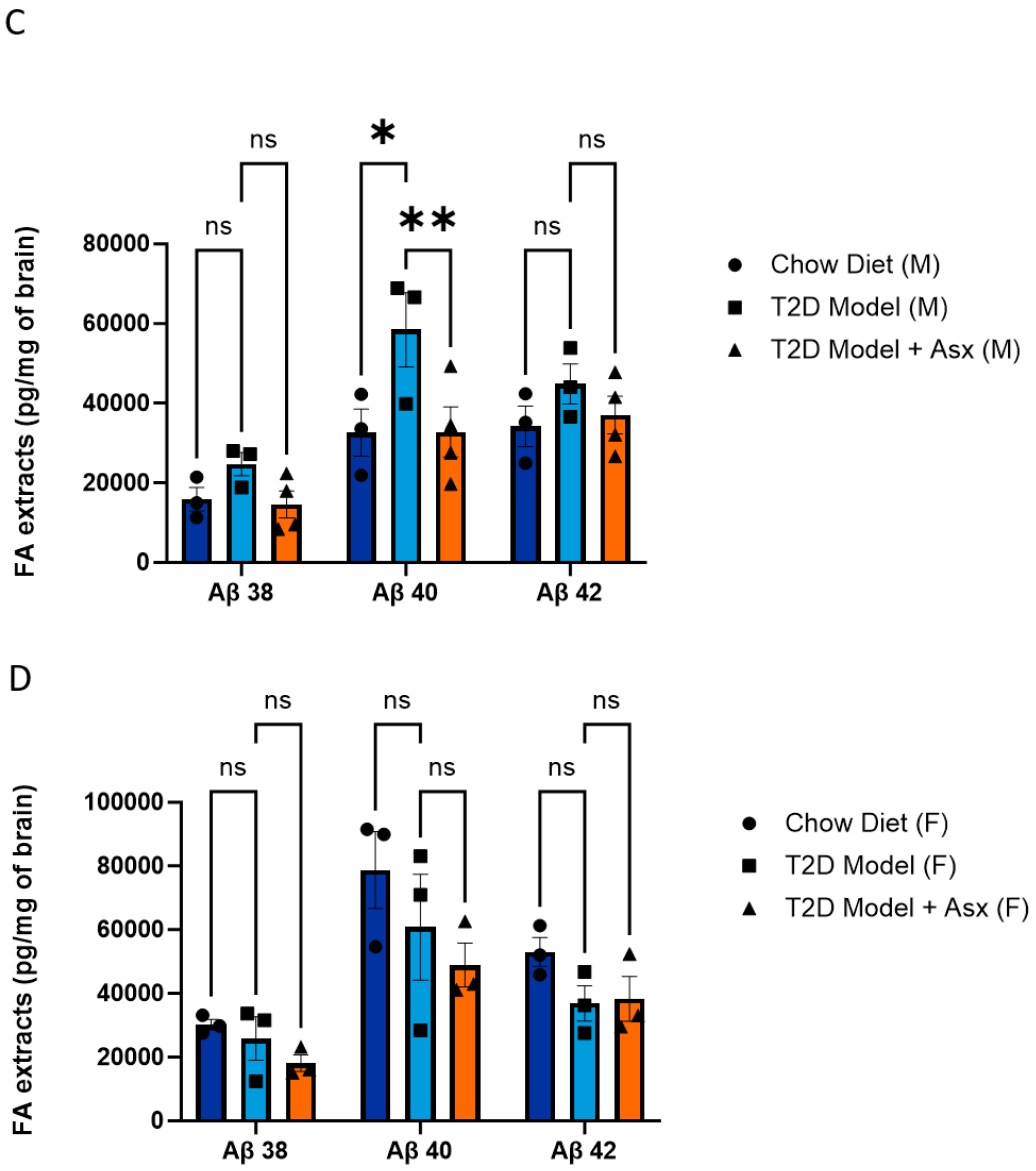

Figure 33: T2D mimicking diet causes a shift from soluble to insoluble Aβ pool in T2D model APPxhQC male mice.

Reduced expression of soluble Aβ and elevated plaque associated insoluble Aβ isoforms in T2D model APPxhQC male mice. Levels of deposited soluble and insoluble Aβ isoforms in brains of APPxhQC mice were evaluated by the MSD assay. DEA extracted soluble $A\beta_{38}$, $A\beta_{40}$ and $A\beta_{42}$ levels in male (A) and female mice (B). FA extracted plaque associated insoluble $A\beta_{38}$, $A\beta_{40}$ and $A\beta_{42}$ levels in male (C) and female mice (D). Data are mean + SEM, n=3-4 per sex and genotype. *p*-Values are calculated using Two-way ANOVA followed by *Turkey's* Multiple Comparison test; *p < 0.05; **p < 0.01.

In addition, we evaluated the impact of T2D mimicking diet on pyroglutamylation. The amount of soluble and insoluble pGlu-3 $A\beta_{42}$ deposits were assessed by ELISA. T2D mimicking diet significantly influenced the deposition of soluble pGlu-3 $A\beta_{42}$ in female mice ($F_{2, 9} = 25.15$, $P<0.001$, Figure 34B). In APPxhQC female mice, T2D mimicking diet was associated with a significant increase in the amount of soluble pGlu-3 $A\beta_{42}$ deposits in the brain when compared with their chow fed age matched control group ($P=0.002$) and this was significantly reduced by ASX supplementation ($P<0.001$, Figure 34B). Taken together our data show that T2D mimicking diet is associated with a shift from soluble to large insoluble polymers of Aβ in the brain of APPxhQC mice and ASX supplementation reduced the expression of both conventional and modified Aβ isoforms in a sex dependent manner.

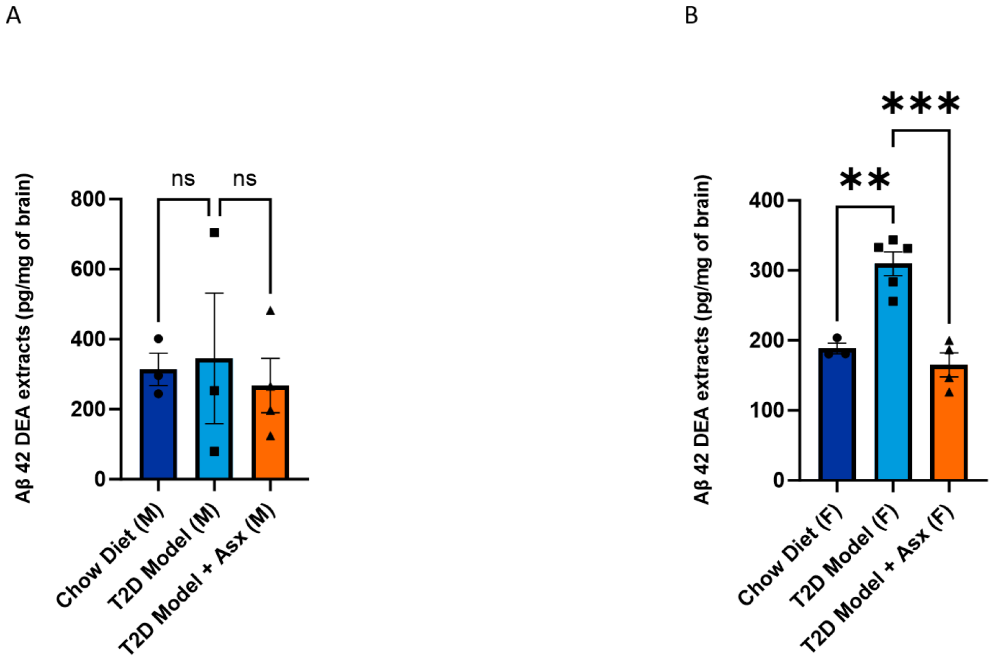

C

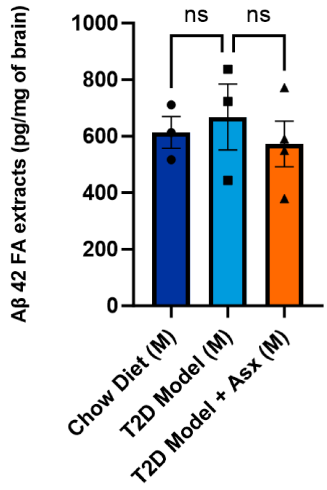

D

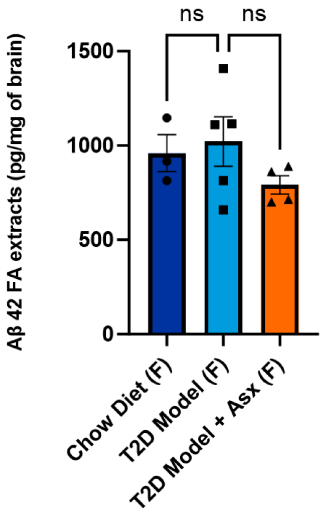

Figure 34: Soluble and insoluble pGlu-3 Aβ$_{42}$ deposits are elevated in T2D model APPxhQC female mice.

DEA extracted soluble pGlu-3 Aβ$_{42}$ deposits are elevated in T2D model T2D APPxhQC female mice. Levels of soluble pGlu-3 Aβ$_{42}$ in male (A) and female mice (B). FA extracted plaque associated insoluble pGlu-3 Aβ$_{42}$ in male (C) and female mice (D). Data are mean + SEM, n=3-5 per sex and genotype. *p*-Values are calculated using One-way ANOVA followed by *Turkey's* Multiple Comparison test; **p < 0.01 and ***p < 0.001.

6.1.7 T2D mimicking diet impairs the cognitive ability in male NTG and female APPxhQC mice.

The Morris water maze (MWM) is used to evaluate the spatial learning and memory performance. In MWM, mice learn to swim in a pool to find an escape platform hidden under the water. Learning is measured by shorter latencies to escape and a decrease length of the path to find the platform (Morris, 1984). T2D have been reported to impair memory in rat and mice diabetic models (Wang et al., 2020; Lawal et al., 2021; Zhang et al., 2021; Zhu et al., 2022).

In the training phase of the MWM test, ASX supplemented T2D model NTG male mice spent shorter time to find the hidden platforms in terms of escape latency

(P<0.001, Figure 35A) and decreased length of path to find the hidden platform (P<0.001, Figure 35C) on the fourth day compared to the first day. Decreased length of path to find the hidden platform at the fourth day compared to the first day was also observed for ASX supplemented T2D model APPxhQC male mice (P=0.02, Figure 35C) and ASX supplemented T2D model NTG female mice (P=0.06, Figure 35D). Surprisingly, T2D mimicking diet seems to be beneficial in APPxhQC male mice (P=0.04, Figure 35C) and NTG female mice (P=0.03, Figure 35D) as we observed a decreased length of path to find the hidden platform and velocity to find the hidden platform (P=0.02, Figure 35F) on the fourth day compared to the first day. We also observed a significant decrease in velocity to find the hidden platform in ASX supplemented T2D model NTG female mice (P=0.04, Figure 35F) and trend towards significance in ASX supplemented T2D model NTG male (P=0.09, Figure 35E) at the fourth day compared to the first day.

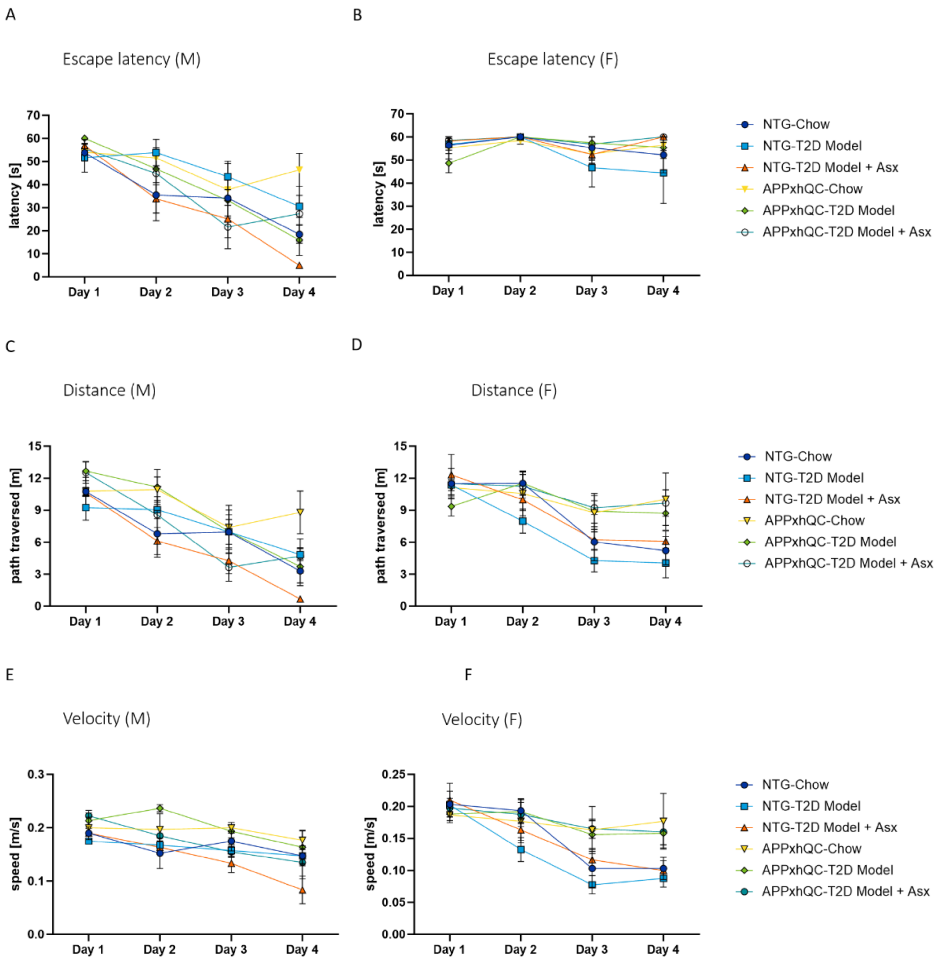

Figure 35: Hippocampal dependent memory function is impaired in T2D model **NTG male and APPxhQC female mice.**

Escape latency, distance and velocity during four days training phase of MWM significantly improved in ASX supplemented T2D model NTG mice. Time spent to find hidden platform in male (A) and female mice (B); length of path to find hidden platform in male (C) and female (D); Velocity to find hidden platform in male (E) and female mice (F). Data are mean + SEM, n=3-5 per sex and genotype. *p*-Values are calculated using Two-way ANOVA followed by *Dunnett's* Multiple Comparison test; *p < 0.05; **p < 0.01 and ***p < 0.001.

For the probe trial, the hidden platform was removed, and the number of target zone crosses made, and time spent in target quadrant (SW) were evaluated. Reduced number of target zone crosses in T2D model NTG male (P=0.04, Figure 36A) and female APPxhQC mice (P=0.09, Figure 36B) compared to the chow fed age matched control groups reflected the extent of spatial memory deficits. ASX supplementation reversed this memory deficits as ASX supplemented T2D model NTG male mice made more target quadrant crosses compared to their T2D model counterpart (P=0.04, Figure 36A). ASX supplemented T2D model APPxhQC male mice tend to spend more time in the target quadrant compared to their chow fed age matched control group (Figure 36C). ASX supplementation did not improve spatial learning in T2D model APPxhQC mice irrespective of the sex (Figures 36A, 36B). Taken together, our results demonstrated that ASX supplementation reversed T2D mimicking diet associated spatial memory deficits in NTG male mice.

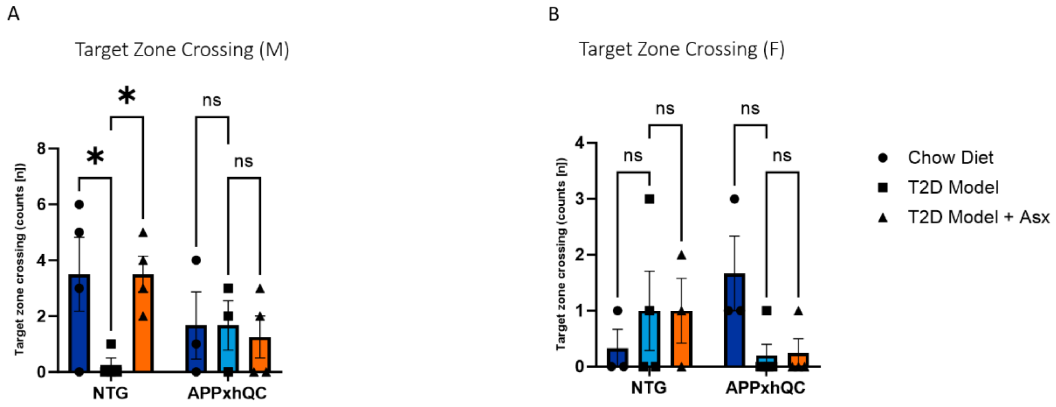

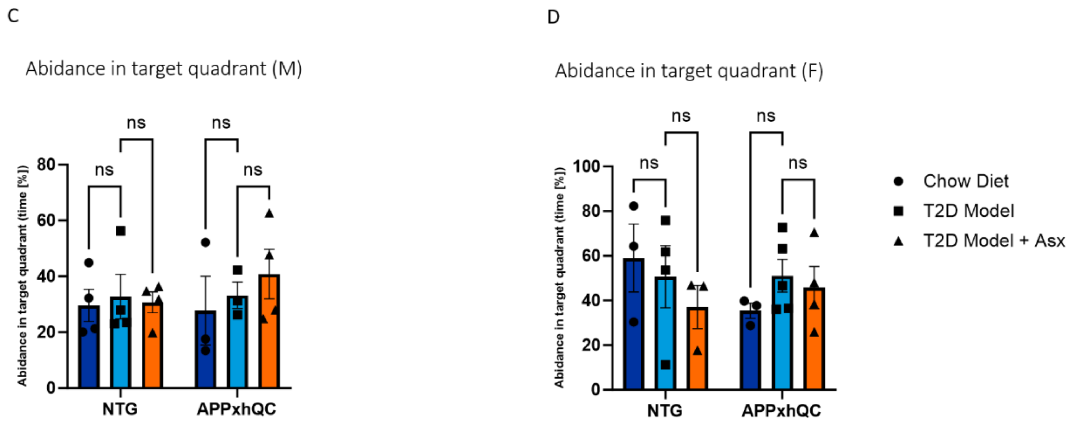

Figure 36: T2D model **NTG male and APPxhQC female mice had reduced number of target zone crosses.**

Hippocampal dependent memory function was severely impaired in T2D model NTG male and APPxhQC female mice. Number of target zone crosses made by male (A) and female mice (B) on Day 5 of MWM during the probe trial. Abidance of male (C) and female mice (D) in target quadrant (South-west) during probe trial. Data are mean + SEM, n=3-5 per sex and genotype. *p*-Values are calculated using Two-way ANOVA followed by *Dunnett's* Multiple Comparison test; *p < 0.05.

6.1.8 Presence or absence of hQC/APP impacts cerebral autophagy signaling in APPxhQC mice compared to their NTG littermates in a sex dependent manner.

Multiple studies have reported the role of autophagy in T2D, AD and resulting complications. Autophagy clears protein aggregates and damaged organelles and confers protection of neurons from demyelination and bioenergetic crisis (Gonçalves et al., 2017; Renna et al., 2010; Towns et al., 2005).

We investigated cerebral autophagy pathway signaling by western blotting. Genotype had a significant effect irrespective of sex on protein expressions of the macro-autophagy signaling marker-LC3B (Male - $F_{1, 12}$ = 12.87, P=0.004; Female - $F_{1, 12}$ = 15.13, P=0.002) and the chaperone mediated autophagy marker-LAMP2A (Male - $F_{1, 12}$ = 9.989, P=0.008; Female - $F_{1, 12}$ = 12.20, P=0.004). In male mice, a trend towards significance for ATG5 ($F_{1, 12}$ = 3.425, P=0.09). In addition, we observed decreased expression of Beclin 1 in ASX supplemented T2D model APPxhQC male mice when compared with the T2D model APPxhQC group (P=0.02, Figures 37A, 37C) but a

trend towards an increase of Beclin 1 in the NTG group (P=0.07, Figures 37A, 37C). Surprisingly, significantly decreased expression of LAMP2A was observed for ASX supplemented T2D model APPxhQC male mice when compared with T2D model APPxhQC group (P=0.03, Figures 37A, 37E). ASX supplementation significantly reduced LC3B-II/ LC3B-I ratio in NTG female mice compared to their T2D model counterparts (P=0.003, Figures 37B, 37H).

A

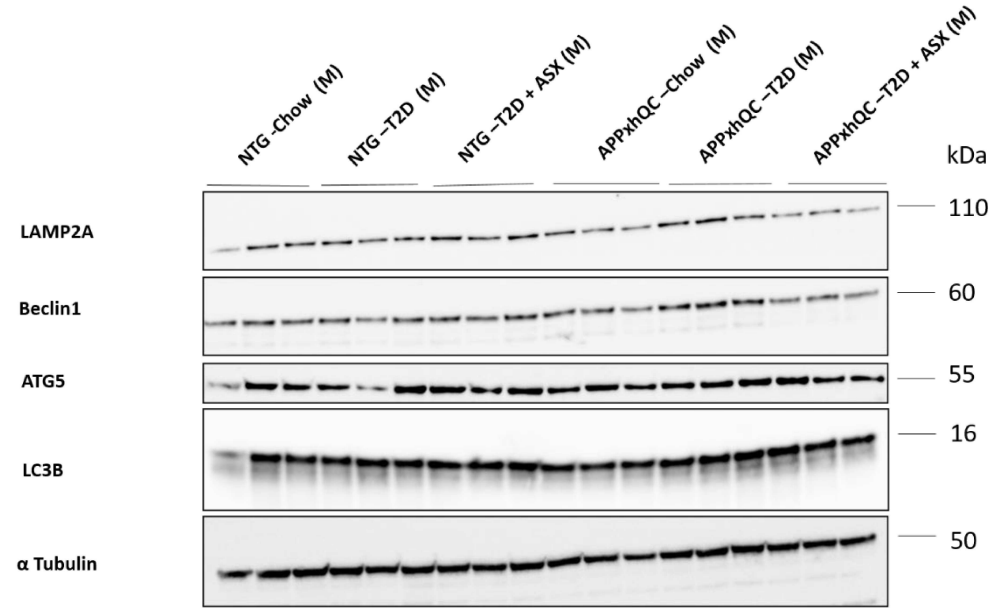

B

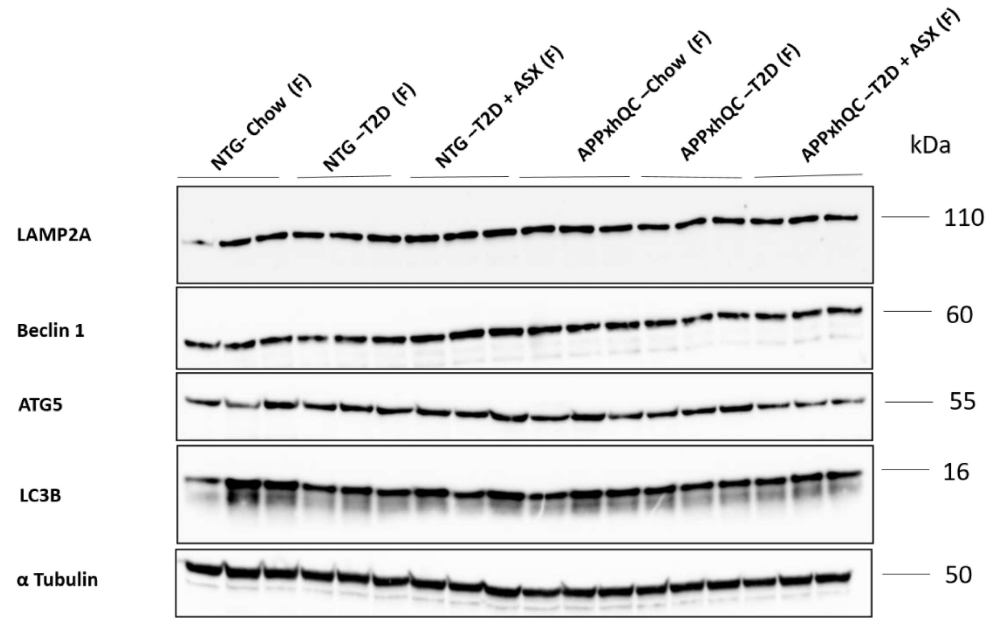

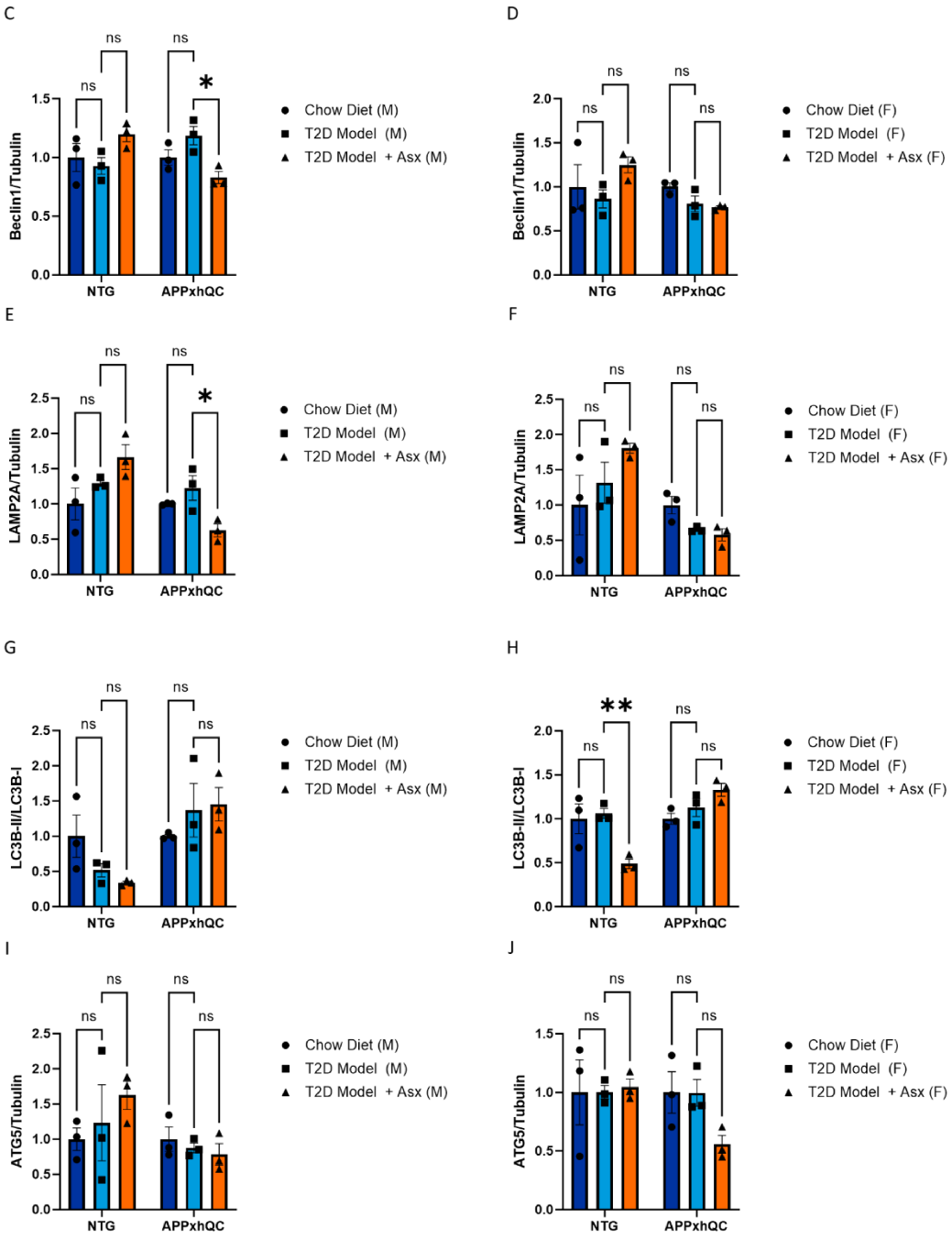

Figure 37: Cerebral autophagy signaling is impaired in APPxhQC and NTG mice.

Western blots analysis of autophagy proteins in brains of APPxhQC and NTG mice. Representative immunoblots from male (A) and female mice (B); Beclin1 expression in male (C) and female mice (D); LAMP2A expression in male (E) and female mice (F); LC3B expression in male (G) and female mice (H); ATG5 expression in male (I) and female mice (J) normalized to Tubulin. Data are mean + SEM, n=3 per sex and genotype. *p*-Values are calculated using Two-way ANOVA followed by *Turkey's* Multiple Comparison test; *p < 0.05; **p < 0.01.

6.1.9 T2D mimicking diet impacts insulin signaling differently in APPxhQC mice and their NTG littermates in a sex dependent manner.

Central response to insulin is suspected to be defective in AD (Leclerc et al., 2023). In addition to amyloid-β (Aβ) and tau pathologies, another hallmark of AD is defective brain uptake of glucose and impaired response to insulin (Arnold et al., 2018; Kellar and Craft, 2020; De Felice, 2013; Baglietto- Vargas et al., 2016; de La Monte, 2019; Stanley et al., 2016). To determine the effect of diet and genotype on insulin signaling, brain homogenates from APPxhQC mice and their NTG littermates were subjected to immunoblotting. Expression of Insulin signaling associated protein markers like ABCA1, AKT, LRP1 and IR-β were evaluated. Diet had a strong influence on LRP1 expression in male mice compared to female mice (Male – $F_{2, 12}$ = 6.225, P=0.01; Female – $F_{2, 12}$ = 1584, P=0.25) while only a trend was observed for genotype in both sexes (Male – $F_{1, 12}$ = 3.610, P=0.08; Female – $F_{1, 12}$ = 4.469, P=0.06). Surprisingly, we observed increased expression of LRP1 in T2D model NTG mice when compared to their age matched chow fed control group (P=0.03, Figures 38A, 38C). Both diet (Male – $F_{2, 12}$ = 5.612, P=0.02; Female – $F_{2, 12}$ = 0.7310, P=0.5) and genotype (Male – $F_{1, 12}$ = 6.709, P=0.02; Female – $F_{1, 12}$ = 0.3801, P=0.55) had a significant effect on IR-β expression in male mice. T2D mimicking diet increased phosphorylation of AKT at Serine 473 only in male mice (Male – $F_{2, 12}$ = 4.016, P=0.05; Female – $F_{2, 12}$ = 0.5620, P=0.58). T2D model APPxhQC male mice had significantly increased phosphorylated AKT when compared to their age matched chow fed control group (P=0.02, Figures 38A, 38G). Effects of diet and genotype were not significant on ABCA1 expression in both sexes, but we observed a trend in ABCA1 expression in T2D model APPxhQC male when compared to their age matched chow fed control group (P=0.06, Figures 38A, 38I). ASX supplementation did not significantly impact cerebral insulin signaling irrespective of sex or genotype. Taken together, these results suggests that T2D mimicking diet seems to positively impact cerebral insulin signaling in APPxhQC mice in a sex dependent manner.

A

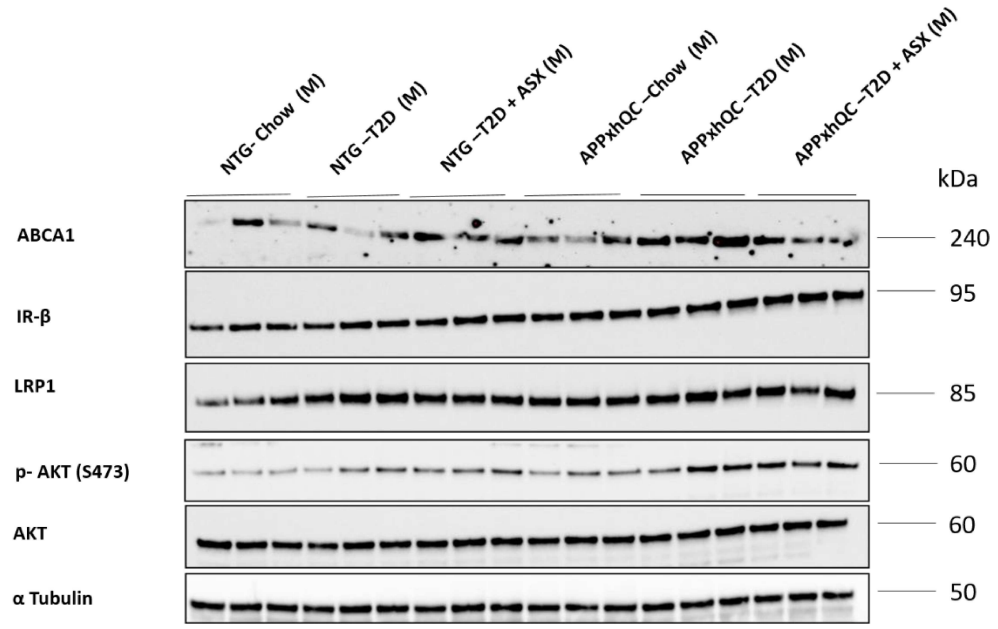
NTG- Chow (M)
NTG –T2D (M)
NTG –T2D + ASX (M)
APPxhQC –Chow (M)
APPxhQC –T2D (M)
APPxhQC –T2D + ASX (M)
kDa
ABCA1
IR-β
LRP1
p- AKT (S473)
AKT
α Tubulin
240
95
85
60
60
50

B

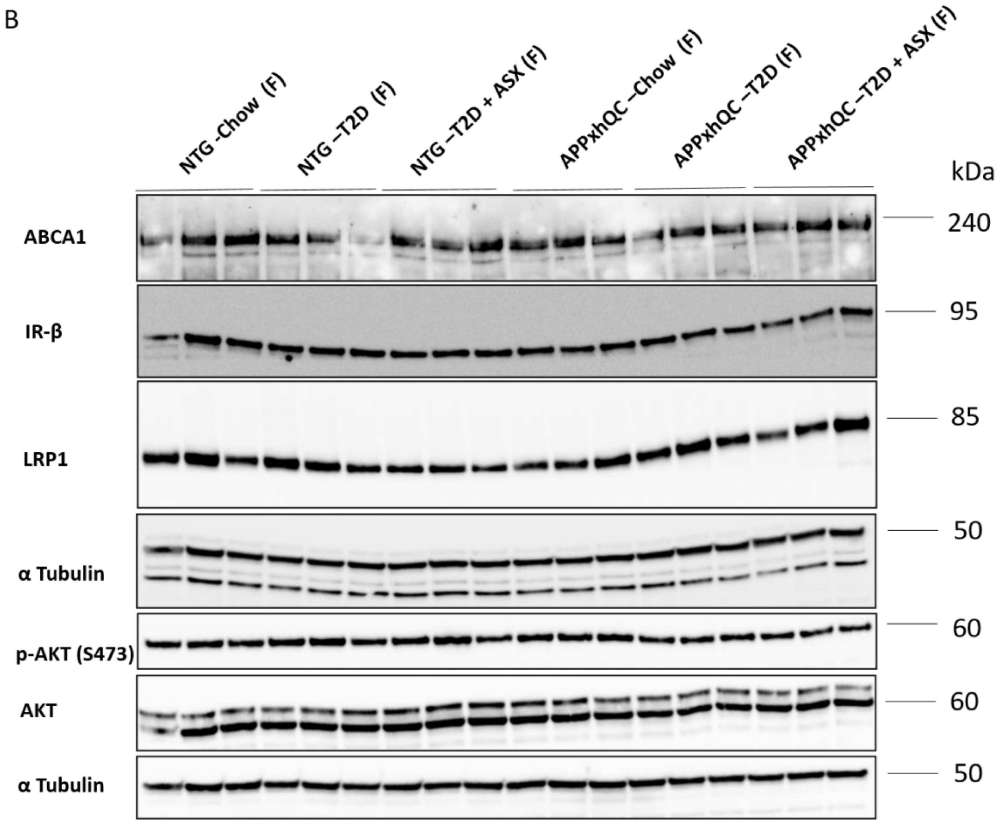
NTG -Chow (F)
NTG –T2D (F)
NTG –T2D + ASX (F)
APPxhQC –Chow (F)
APPxhQC –T2D (F)
APPxhQC –T2D + ASX (F)
kDa
ABCA1
IR-β
LRP1
α Tubulin
p-AKT (S473)
AKT
α Tubulin
240
95
85
50
60
60
50

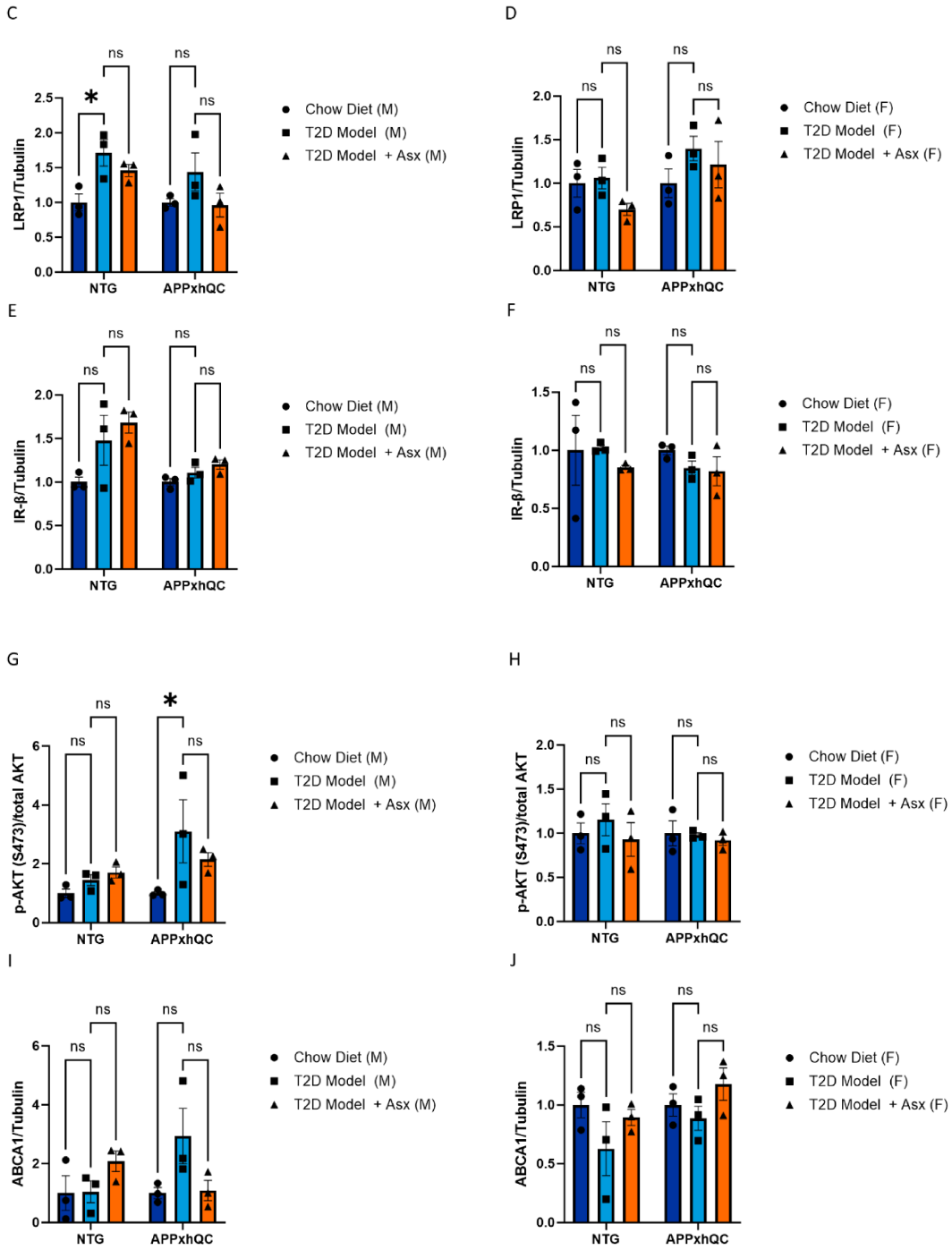

Figure 38: Cerebral insulin signaling is altered in T2D model APPxhQC and NTG mice.

Western blots and quantitative analysis of insulin signaling proteins in brains of APPxhQC and NTG mice. Representative immunoblots from male (A) and female mice (B); LRP1 expression in male (C) and female mice (D); IR-β expression in male (E) and female mice (F); AKT expression in male (G) and female mice (H); ABCA1 expression in male (I) and female mice (J) normalized to Tubulin. Data are mean +

SEM, n=3 per sex and genotype. *p*-Values are calculated using Two-way ANOVA followed by *Turkey's* Multiple Comparison test; *p < 0.05.

6.1.10 Presence or absence of hQC/APP and T2D mimicking diet influences cerebral MAP kinase signaling in APPxhQC mice and their NTG littermates in a sex and genotype dependent manner.

Various studies have reported the activation of *mitogen-activated protein kinase* (*MAPK*) pathways in vulnerable neurons in AD patients. We investigated the impact of T2D mimicking diet and presence or absence of hQC/APP on expressions of some of the best characterized MAPK pathway genes, ERK, p38 and p65 NF-κB.

We observed a significant impact of genotype on the phosphorylation of the ERK protein in male mice (Male – $F_{1, 12}$ = 6.595, P=0.02; Female – $F_{1, 12}$ = 0.6076, P=0.45) and a trend towards an effect for diet (Male – $F_{2, 12}$ = 3.243, P=0.07; Female – $F_{2, 12}$ = 1.285, P=0.31). T2D model APPxhQC male mice had significantly increased level of phosphorylated ERK when compared to their age matched chow fed control group (P=0.02, Figures 39A, 39C). p65 NF-κB, another member of the MAPK pathway, has been reported to be involved in neuritogenesis. Surprisingly, diet (Male – $F_{2, 12}$ = 4.878, P=0.03; Female – $F_{2, 12}$ = 0.5384, P=0.6) had a significant impact on p65 expressions in male mice while genotype (Male – $F_{1, 12}$ = 0.8716, P=0.37; Female – $F_{1, 12}$ = 28.43, P<0.001) greatly influenced its expressions in female mice. ASX supplemented T2D model NTG male mice had increased expression of p65 when compared to their T2D model counterparts (P=0.02, Figures 39A, 39E). In ASX supplemented T2D model APPxhQC female mice, we observed a reduced expression of p65 relative to their T2D model group (P=0.01, Figures 39B, 39F). Neither diet nor genotype had a significant effect on p38 MAPK signaling (Figures 39A, 39B, 39G, 39H). These results suggest that both T2D mimicking diet and presence or absence of hQC/APP impact cerebral MAPK signaling in APPxhQC mice in a sex and genotype dependent way.

A

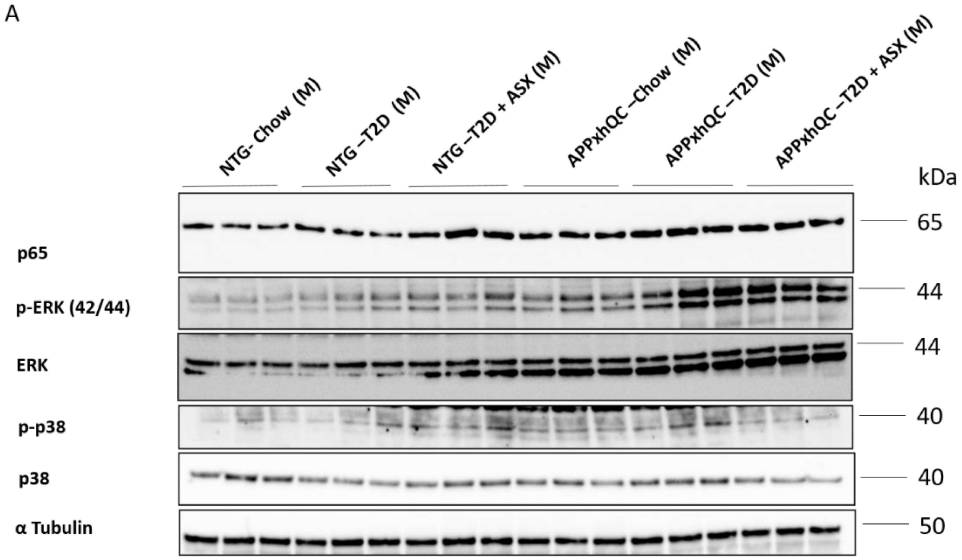
NTG- Chow (M)
NTG –T2D (M)
NTG –T2D + ASX (M)
APPxhQC –Chow (M)
APPxhQC –T2D (M)
APPxhQC –T2D + ASX (M)
kDa
p65
p-ERK (42/44)
ERK
p-p38
p38
α Tubulin
65
44
44
40
40
50

B

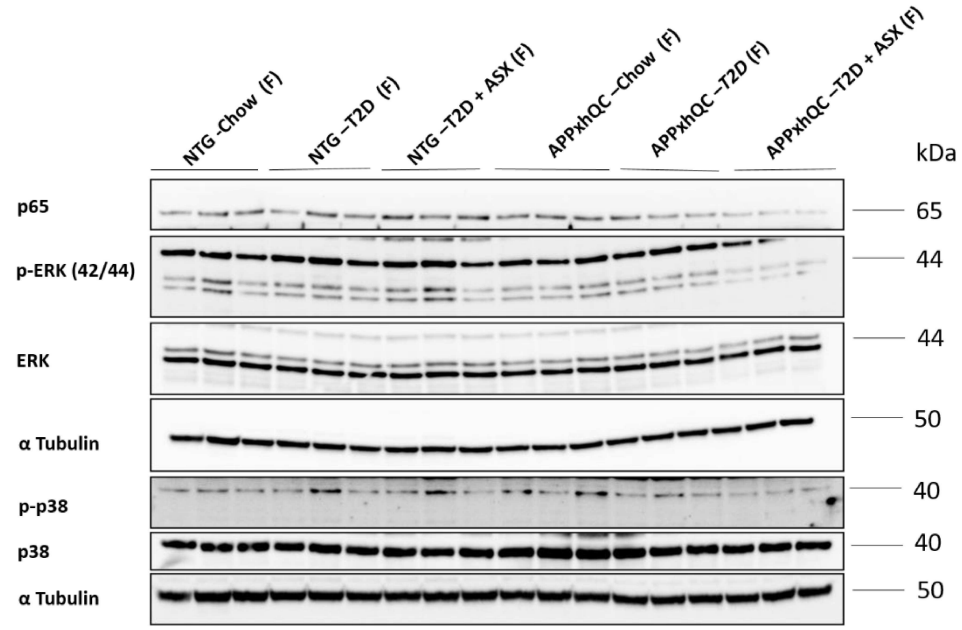
NTG -Chow (F)
NTG –T2D (F)
NTG –T2D + ASX (F)
APPxhQC –Chow (F)
APPxhQC –T2D (F)
APPxhQC –T2D + ASX (F)
kDa
p65
p-ERK (42/44)
ERK
α Tubulin
p-p38
p38
α Tubulin
65
44
44
50
40
40
50

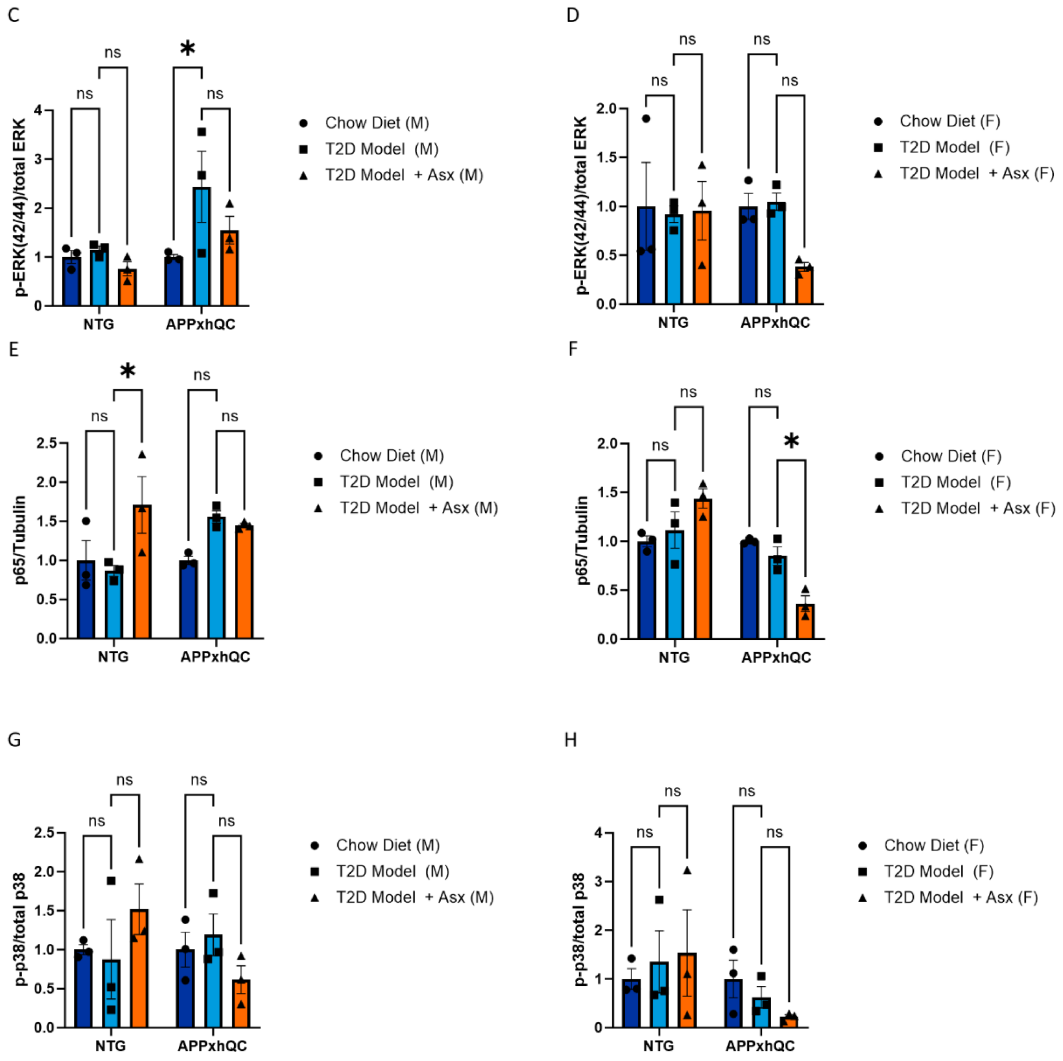

Figure 39: Cerebral MAPKinase signaling in T2D model APPxhQC and NTG mice

Western blots and quantitative analysis of MAPKinase proteins in brains of APPxhQC and NTG mice. Representative immunoblots from male (A) and female mice (B); ERK expression in male (C) and female mice (D); p65 expression in male (E) and female mice (F); p38 expression in male (G) and female mice (H) normalized to GAPDH. Data are mean + SEM, n=3 per sex and genotype. *p*-Values are calculated using Two-way ANOVA followed by *Turkey's* Multiple Comparison test; *p < 0.05.

6.1.11 T2D mimicking diet dysregulates cerebral mTORC1 signaling differentially in APPxhQC mice and their NTG littermates.

Dysregulation of the mTOR pathway has been implicated in the pathophysiology of many chronic diseases including T2D and AD (Ma et al., 2010). We evaluated combinational effects of diet and genotype on the phosphorylation of S6 ribosomal protein (S6rp). Diet (Male – $F_{2, 12}$ = 6.957, P=0.01; Female – $F_{2, 12}$ = 5.791, P=0.02) and genotype (Male – $F_{1, 12}$ = 9.180, P=0.01; Female – $F_{1, 12}$ = 19.97, P=0.001) significantly influenced phosphorylation of S6rp irrespective of sex. There was strong interaction between diet and genotype for both sexes (Male – $F_{2, 12}$ = 13.07, P<0.001; Female – $F_{2, 12}$ = 9.557, P=0.003). ASX supplemented T2D model NTG male mice showed increased phosphorylation of S6rp when compared to the T2D model group (P=0.005, Figures 40A, 40C). Similar increases in phosphorylation of S6rp was observed for ASX supplemented T2D model NTG female mice when compared to their T2D model counterparts (P=0.008, Figures 40B, 40D). ASX supplementation tends to reduce phosphorylation of S6rp in T2D model APPxhQC male mice when compared to their T2D model group (P=0.06, Figure 40A, 40C). Furthermore, we evaluated the effect of diet and genotype on the phosphorylation of mammalian target of rapamycin (mTOR) protein. Diet had a significant influence on its expression in female mice while only a trend was observed in male mice (Male – $F_{2, 12}$ = 3.743, P=0.05; Female – $F_{2, 12}$ = 5.934, P=0.02, Figure 22A, 22B). Both diet (Male – $F_{2, 12}$ = 1.019, P=0.39; Female – $F_{2, 12}$ = 4.429, P=0.04) and genotype (Male – $F_{1, 12}$ = 0.06886, P=0.8; Female – $F_{2, 12}$ = 5.627, P=0.04) significantly influenced the expression of mTOR protein in female mice. There was strong interaction between diet and genotype for both sexes (Male – $F_{2, 12}$ = 7.778, P=0.007; Female – $F_{2, 12}$ = 5.170, P=0.02). Cerebral expression of mTOR was reduced in ASX supplemented T2D model APPxhQC male mice compared to the T2D model group (P=0.07, Figures 40A, 40G). mTOR expression level was significantly increased in T2D model NTG female mice relative to their chow fed counterparts (P=0.01, Figures 40B, 40H).

A

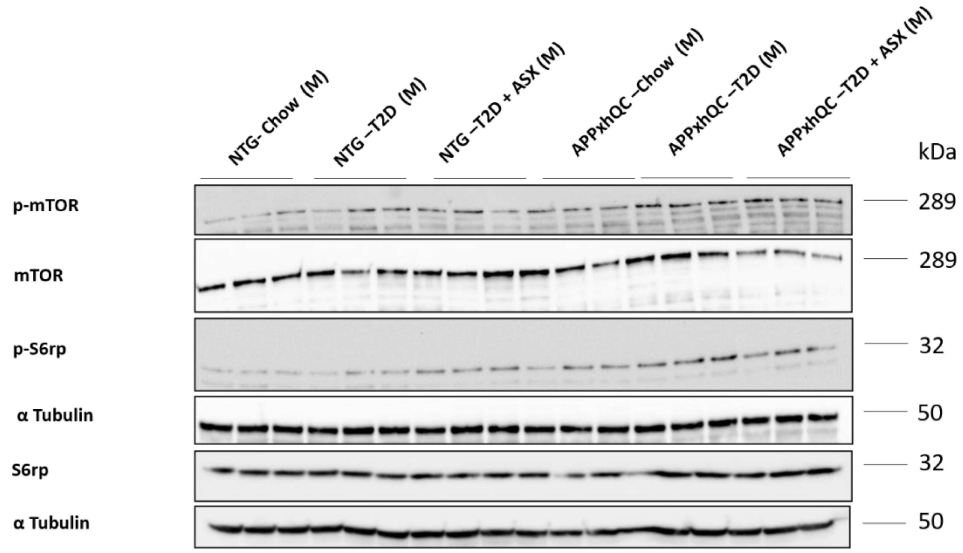
NTG- Chow (M)
NTG –T2D (M)
NTG –T2D + ASX (M)
APPxhQC –Chow (M)
APPxhQC –T2D (M)
APPxhQC –T2D + ASX (M)
kDa
p-mTOR
289
mTOR
289
p-S6rp
32
α Tubulin
50
S6rp
32
α Tubulin
50

B

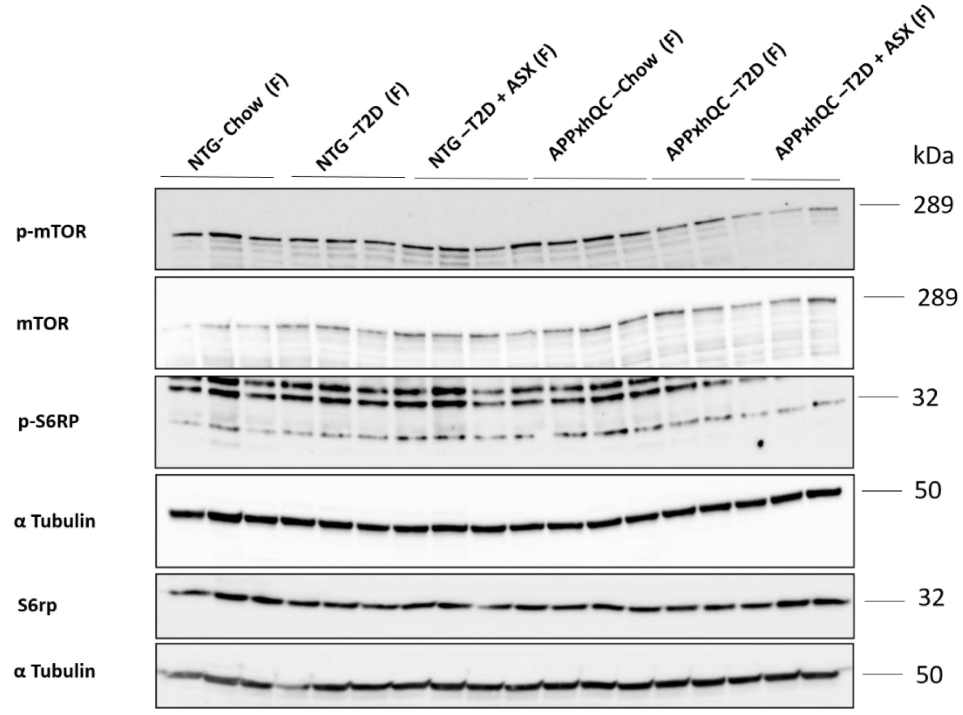
NTG- Chow (F)
NTG –T2D (F)
NTG –T2D + ASX (F)
APPxhQC –Chow (F)
APPxhQC –T2D (F)
APPxhQC –T2D + ASX (F)
kDa
p-mTOR
289
mTOR
289
p-S6RP
32
α Tubulin
50
S6rp
32
α Tubulin
50

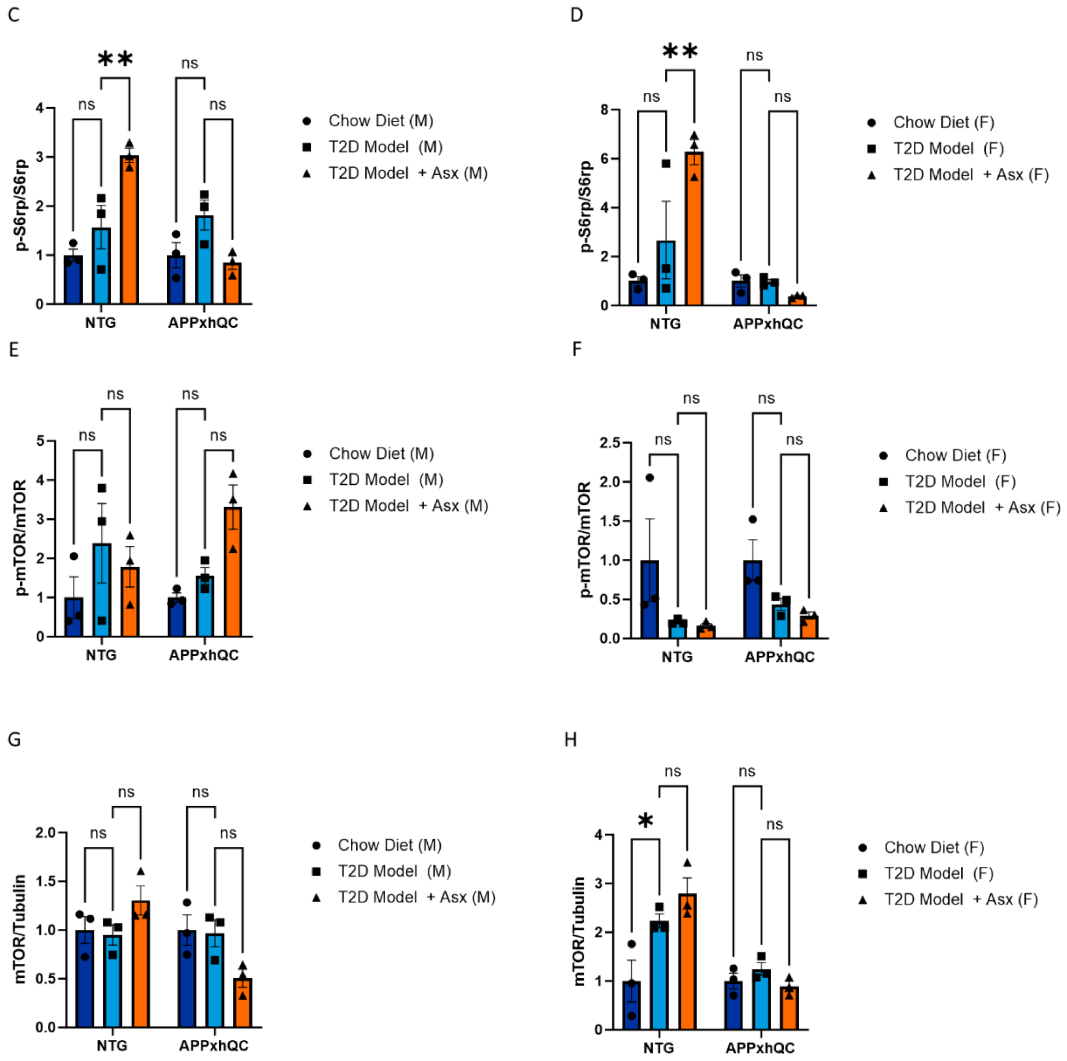

Figure 40: Cerebral mTORC1 signaling is dysregulated in T2D model APPxhQC and NTG mice.

Western blots and quantitative analysis of mTORC1 signaling proteins from brains of APPxhQC and NTG mice. Representative immunoblots from male (A) and female mice (B); S6rp expression in male (C) and female mice (D); p-mTOR/mTOR expression in male (E) and female mice (F); mTOR expression in male (G) and female mice (H) normalized to Tubulin. Data are mean + SEM, n=3 per sex and genotype. *p*-Values are calculated using Two-way ANOVA followed by *Turkey's* Multiple Comparison test; *p < 0.05; **p < 0.01.

6.1.12 ASX supplementation enhances hepatic autophagy signaling in T2D model NTG male mice.

Brain-liver organ cross talk in the pathophysiology of many metabolic syndromes including T2D and AD has been reported. Therefore, we evaluated the influence of diet and genotype on hepatic autophagy signaling in this AD model. A significant effect of diet on autophagic protein marker Beclin1 protein expression in male mice was noted (Male – $F_{2, 12}$ = 5.664, P=0.02; Female – $F_{2, 12}$ = 0.6608, P=0.53, Figure 33A-D). ASX supplementation tends to increase the expression of Beclin1 in ASX supplemented T2D model NTG female mice when compared to T2D model group (P=0.09, Figures 33B, 33D). Diet significantly influenced the expression of the chaperone mediated autophagy marker- LAMP2A in male mice (Male – $F_{2, 12}$ = 11.66, P=0.002; Female – $F_{2, 12}$ = 2.381, P=0.13). ASX supplementation tends to increase the expression of LAMP2A in T2D model NTG male mice compared to T2D model group (P=0.09, Figures 33A, 33E). Increased expression of LAMP2A was also observed in ASX supplemented T2D model APPxhQC male mice when compared to their T2D model counterparts (P=0.010, Figures 33A, 33E). Moreover, diet and genotype influenced lipidation of hepatic LC3B differentially in a sex dependent manner. Diet (Male – $F_{2, 12}$ = 4.305, P=0.04; Female – $F_{2, 12}$ = 2.048, P=0.17) had a significant influence on LC3B-II/ LC3B-1 expression in male mice while its expression was impacted by genotype in female mice (Male – $F_{1, 12}$ = 3.939, P=0.07; Female – $F_{1, 12}$ = 13.02, P=0.004). We observed a significant increase in LC3B-II/ LC3B-1 expression in T2D model NTG male mice compared to their age matched chow fed control group (P=0.03, Figures 33A, 33G) while observing the same in T2D model APPxhQC female mice relative to their age matched chow fed control group (P=0.02, Figures 33B, 33H). Taken together, these results showed the ASX supplementation might enhance hepatic autophagy signaling in T2D model NTG male mice.

A

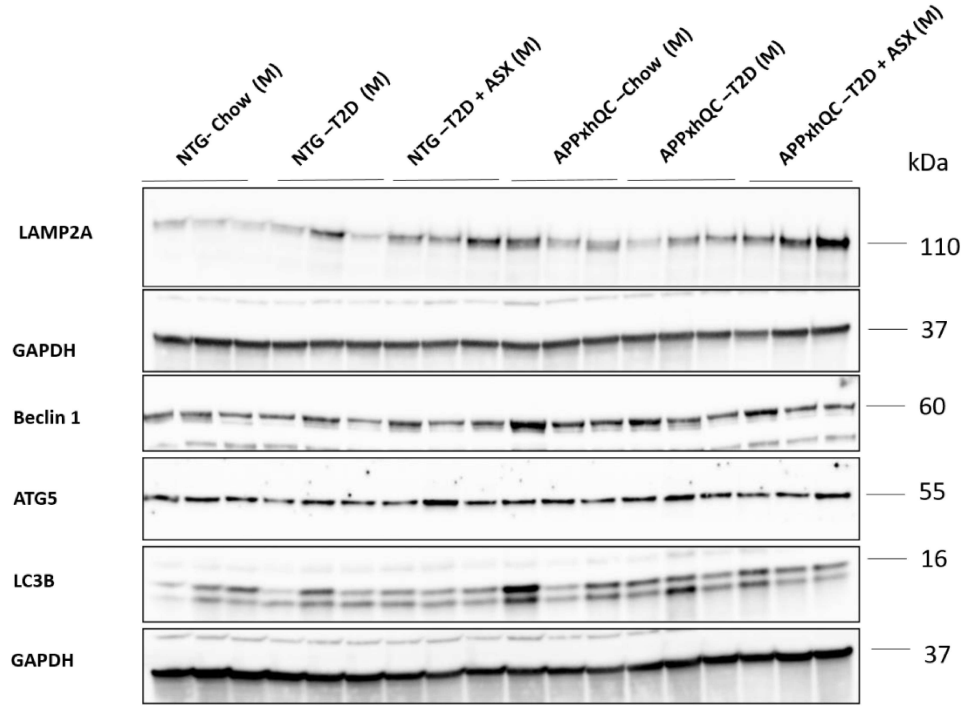
NTG- Chow (M)
NTG –T2D (M)
NTG –T2D + ASX (M)
APPxhQC –Chow (M)
APPxhQC –T2D (M)
APPxhQC –T2D + ASX (M)
kDa
LAMP2A
110
GAPDH
37
Beclin 1
60
ATG5
55
LC3B
16
GAPDH
37

B

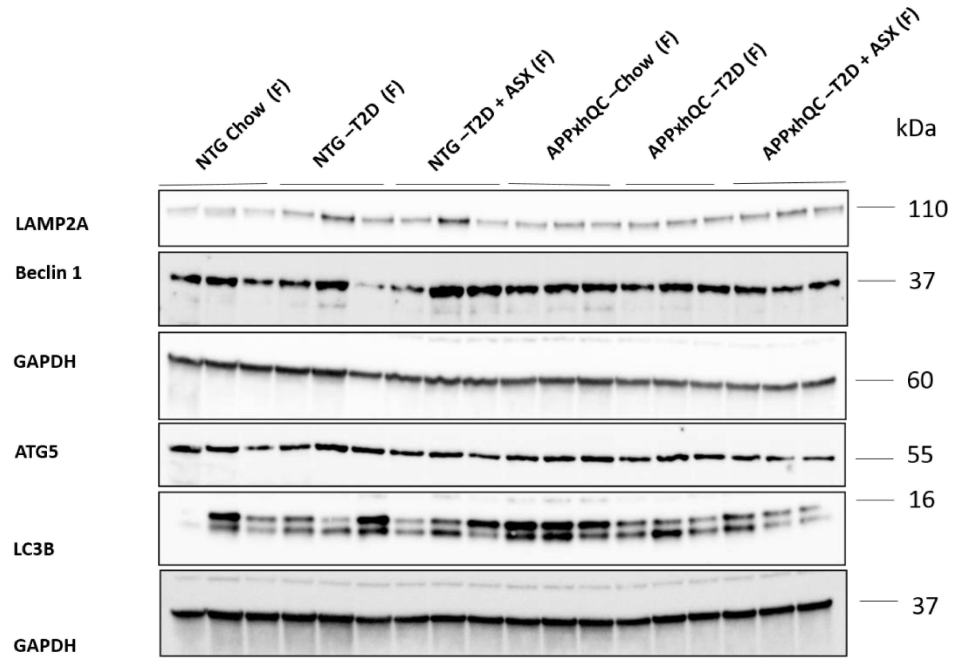
NTG Chow (F)
NTG –T2D (F)
NTG –T2D + ASX (F)
APPxhQC –Chow (F)
APPxhQC –T2D (F)
APPxhQC –T2D + ASX (F)
kDa
LAMP2A
110
Beclin 1
37
GAPDH
60
ATG5
55
16
LC3B
GAPDH
37

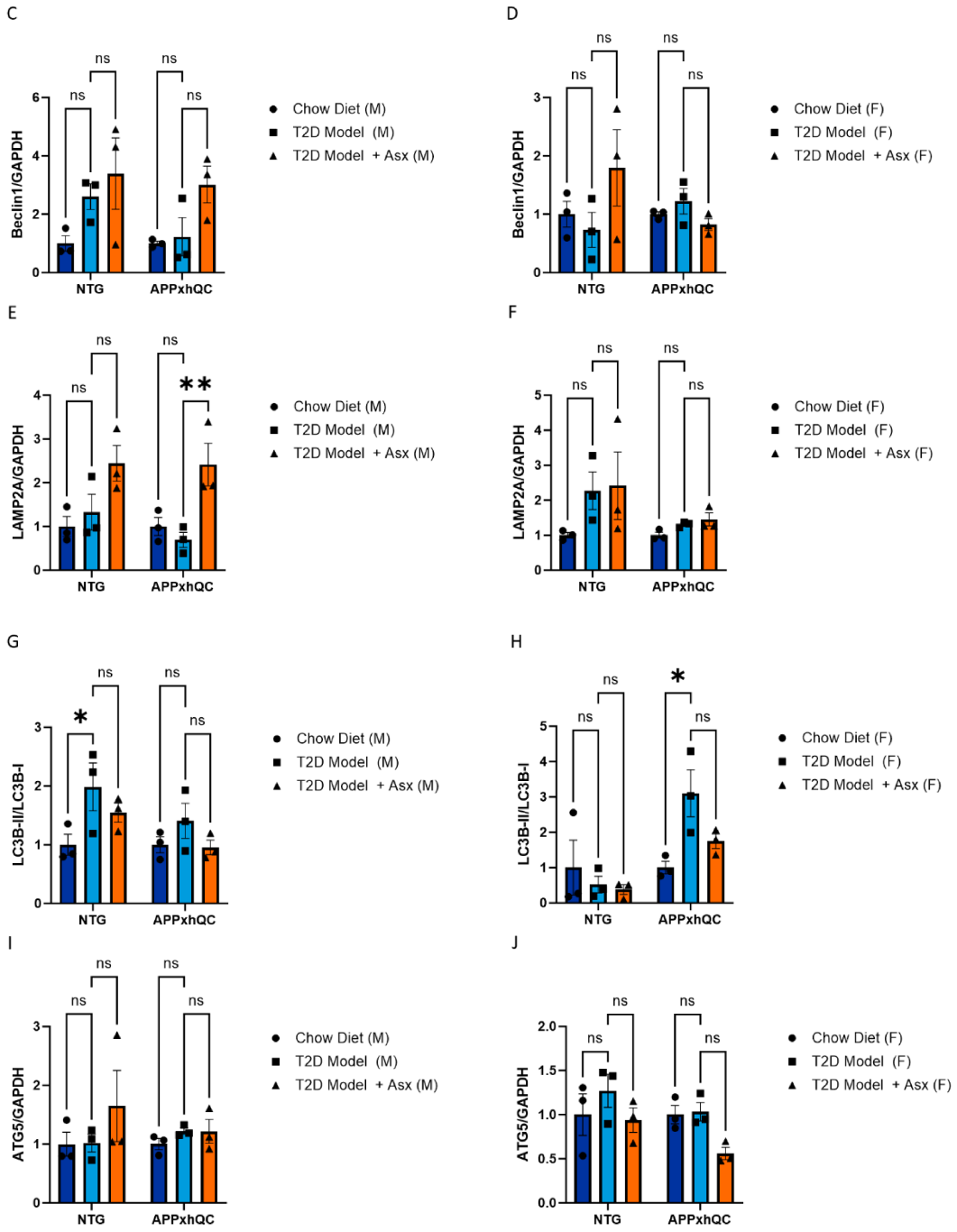

Figure 41: Hepatic autophagy signaling in APPxhQC and NTG mice.

Hepatic autophagy signaling is elevated in livers of ASX supplemented T2D model NTG male mice. Western blots and quantitative analysis of autophagy proteins in livers of APPxhQC and NTG mice. Representative immunoblots from male (A) and female mice (B); Beclin1 expression in male (C) and female mice (D); LAMP2A expression in male (E) and female mice (F); LC3B expression in male (G) and female mice (H); ATG5 expression in male (I) and female mice (J) normalized to GAPDH.

Data are mean + SEM, n=3 per sex and genotype. *p*-Values are calculated using Two-way ANOVA followed by *Turkey's* Multiple Comparison test; *p < 0.05; **p < 0.01.

6.1.13 ASX supplementation improves hepatic insulin signaling in T2D NTG male mice.

The liver is the key metabolic organ which governs body energy metabolism (Rui, 2014). To investigate hepatic insulin signaling, we evaluated the effects of both diet and genotype on protein expressions of ABCA1, AKT and IR-β. Genotype had a significant effect on IR-β protein expression in male mice (Male – $F_{1, 12}$ = 6.702, P=0.02; Female – $F_{1, 12}$ = 0.09569, P=0.76). Moreover, T2D model NTG male mice tend to increase IR-β protein expression relative to their age matched chow fed control group (P=0.08, Figures 42A, 42C).

Genotype significantly influenced phosphorylation of AKT in male mice (Male – $F_{2, 12}$ = 8.615, P=0.01; Female – $F_{2, 12}$ = 0.3979, P=0.54). In ASX supplemented T2D model NTG male mice, we observed increased expression of phosphorylated AKT relative to their T2D model control (P=0.01, Figures 42A, 42E). Both diet (Male – $F_{2, 12}$ = 5.259, P=0.02; Female – $F_{2, 12}$ = 0.1444, P=0.87) and genotype (Male – $F_{1, 12}$ = 18.93, P=<0.001; Female – $F_{1, 12}$ = 4.591e-005, P>0.99) significantly influenced ABCA1 expression. Surprisingly, ABCA1 protein expression was upregulated in T2D model NTG male mice when compared to their age matched chow fed control group (P=0.001, Figures 42A, 42G) but downregulated in the ASX supplemented group relative to their T2D model counterpart (P=0.11, Figures 42A, 42G). Taken together, the results suggests that ASX supplementation improves hepatic insulin signaling in T2D model NTG male mice.

A

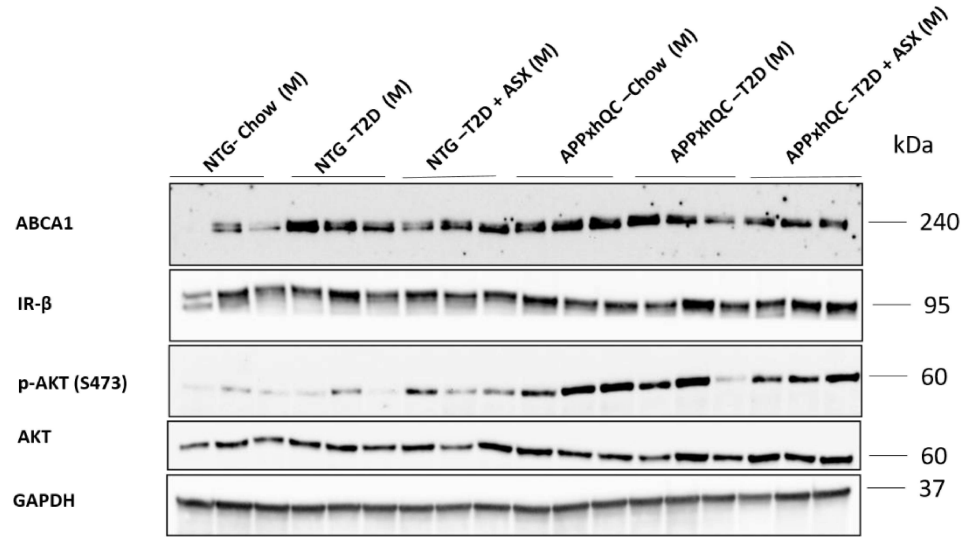
NTG- Chow (M)
NTG –T2D (M)
NTG –T2D + ASX (M)
APPxhQC –Chow (M)
APPxhQC –T2D (M)
APPxhQC –T2D + ASX (M)
kDa
ABCA1
240
IR-β
95
p-AKT (S473)
60
AKT
60
GAPDH
37

B

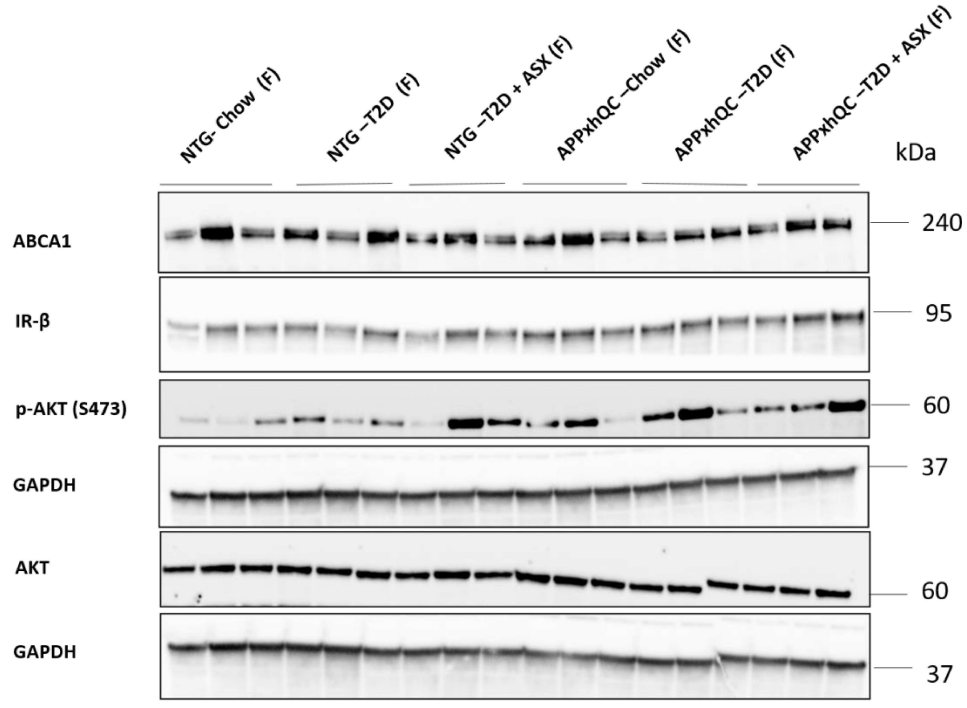
NTG- Chow (F)
NTG –T2D (F)
NTG –T2D + ASX (F)
APPxhQC –Chow (F)
APPxhQC –T2D (F)
APPxhQC –T2D + ASX (F)
kDa
ABCA1
240
IR-β
95
p-AKT (S473)
60
GAPDH
37
AKT
60
GAPDH
37

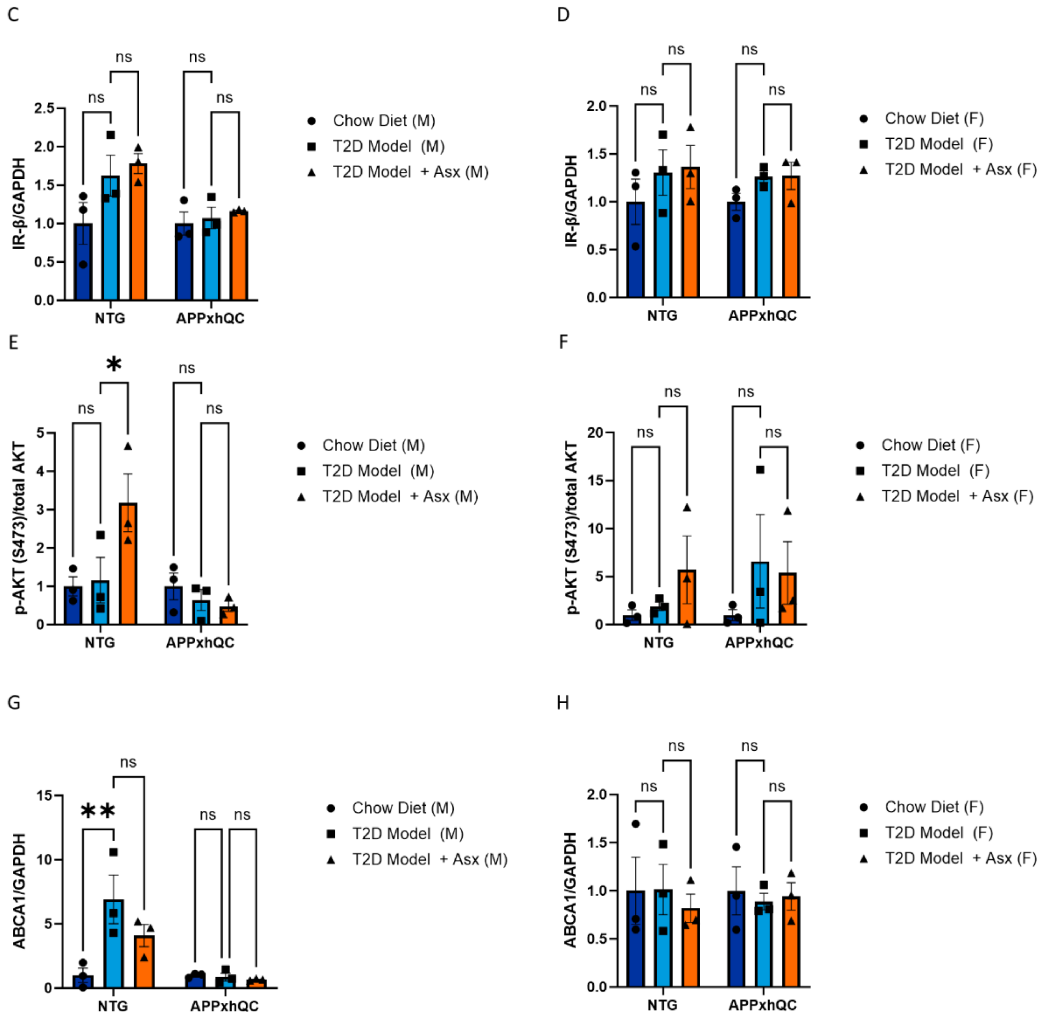

Figure 42: Hepatic insulin signaling in APPxhQC and NTG mice.

Hepatic insulin signaling is increased in ASX supplemented T2D model NTG male mice. Western blots and quantitative analysis of insulin signaling proteins in livers of APPxhQC and NTG mice. Representative immunoblots from male (A) and female mice (B); IR-β expression in male (C) and female mice (D); ABCA1 expression in male (E) and female mice (F); AKT expression in male (G) and female mice (H) normalized to GAPDH. Data are mean + SEM, n=3 per sex and genotype. *p*-Values are calculated using Two-way ANOVA followed by *Turkey's* Multiple Comparison test; *p < 0.05; **p < 0.01.

6.1.14 ASX supplementation reduces hepatic inflammation in T2D model NTG male mice.

Furthermore, we checked the effects of both diet and genotype on protein expressions of hepatic p65 and ERK. We observed a significant effect of diet on the

expression of p65 in male mice (Male – $F_{2, 12}$ = 4.956, P=0.03; Female – $F_{2, 12}$ = 1.573, P=0.25) and a strong interaction between diet and genotype (Male – $F_{2, 12}$ = 7.662, P=0.007; Female – $F_{2, 12}$ = 2.923, P=0.09). Only a trend was observed for the effect of diet on ERK expression (Male – $F_{2, 12}$ = 2.956, P=0.09; Female – $F_{2, 12}$ = 0.4602, P=0.64). In addition, we noted increased hepatic protein expression of p65 in T2D model male mice relative to their age matched chow fed control group (P=0.010, Figures 43A, 43C) which was reduced following ASX supplementation (P=0.05, Figures 43A, 43C). Hepatic expression of ERK was significantly increased in T2D model NTG female mice relative to the age-matched chow fed group (P=0.001, Figures 43B, 43F). Taken together, these data suggest that ASX supplementation ameliorates hepatic inflammation in T2D model NTG male mice.

A

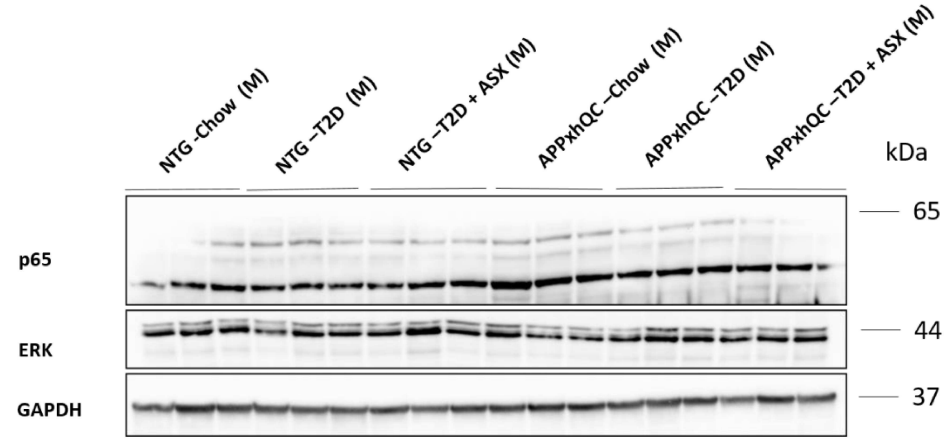

B

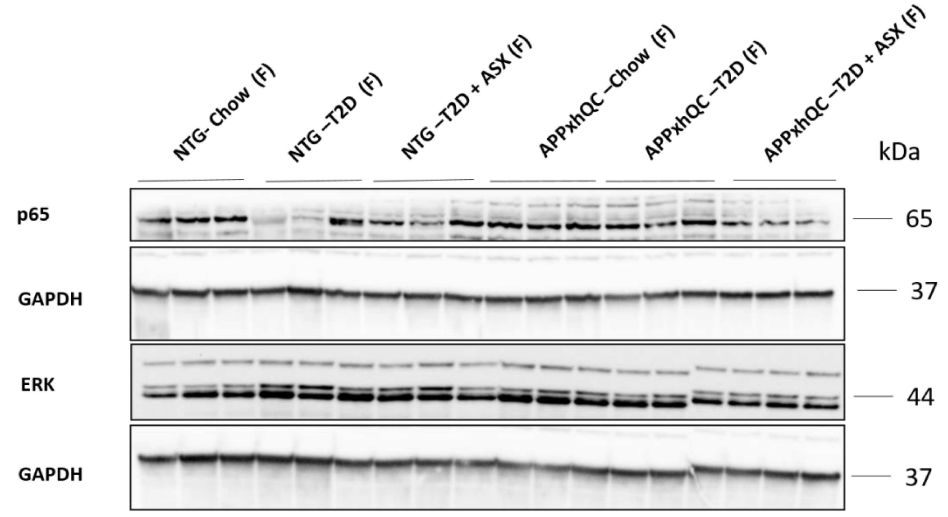

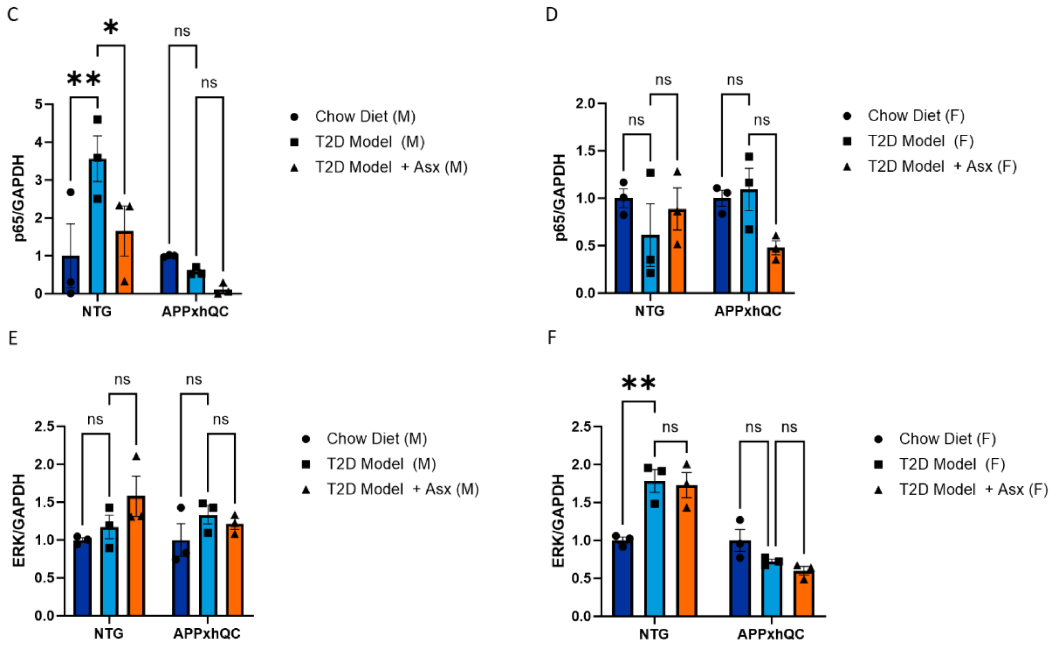

Figure 43: ASX supplementation reduces hepatic inflammation in ASX supplemented T2D model NTG male mice.

Western blots and quantitative analysis of inflammatory proteins in livers of APPxhQC and NTG mice. Representative immunoblots in male (A) and female mice (B); p65 expression in male (C) and female mice (D); ERK expression in male (E) and female mice (F) normalized to GAPDH. Data are mean + SEM, n=3 per sex and genotype. *p*-Values are calculated using Two-way ANOVA followed by *Turkey's* Multiple Comparison test; *p < 0.05; **p < 0.01.

6.1.15 Histological stainings of markers for Aβ deposition and inflammation in T2D model APPxhQC male mice brains.

Immunofluorescence double staining was performed on brain cryosections from male APPxhQC mice. Immunostaining for 6E10 and pyroglutamated modified Aβ in both hippocampal and cortical sections of the brain were performed. T2D mimicking diet increased the deposition of 6E10 and pGlu-3 Aβ reactive plaques in the hippocampal and cerebral brain regions relative to the chow-fed age matched control and this was reduced by ASX supplementation (Figure 44). In addition, cortical and hippocampal brain sections were stained for glial and microglial activations, markers for inflammation using GFAP and Iba1 antibodies. We observed a reduced cortical

GFAP activation and increased Iba1 activation in ASX supplemented T2D model APPxhQC mice albeit not to a level of statistical significance (Figure 44).

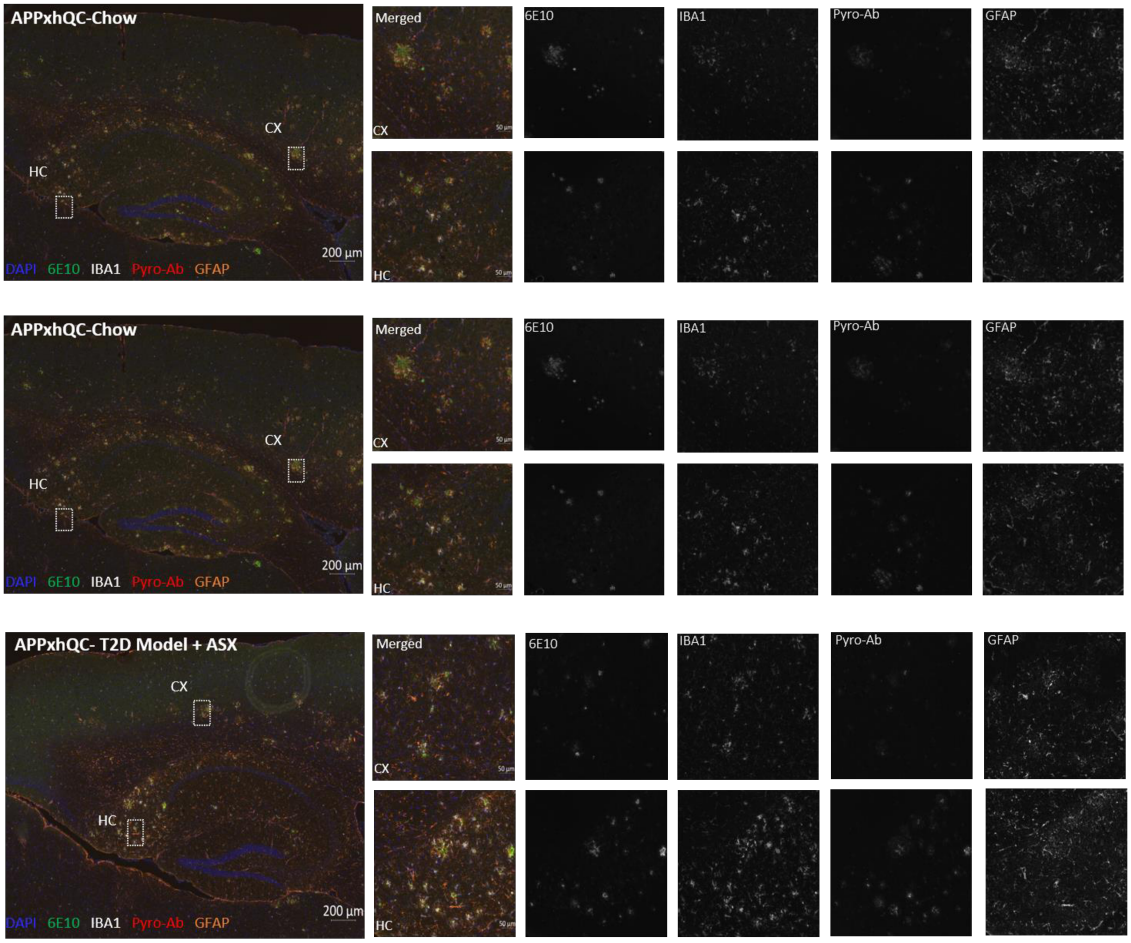

Figure 44: **Histological staining for Aβ, astrocytes and microglia in T2D model APPxhQC male mice.**

Histological stainings for conventional Aβ (6E10); pyro-glutamate modified Aβ (Abeta-pE3); astrocyte activation (GFAP); microglia activation (IBA1) in cortex and hippocampus of APPxhQC male mice.

7.0 DISCUSSION

Post-translational modifications of the Aβ protein (amyloid cascade hypothesis) have been regarded as the classic hypothesis for the cause of AD. Even though successful AD clinical trials with antibodies targeting various Aβ species seem to a certain degree support this hypothesis, genetic, clinical, imaging and biochemical data are suggesting a more complex disease etiology (Kepp et al., 2023). Recently, evidence is emerging that links metabolic syndromes such as obesity, T2D, and dyslipidemia with the pathophysiology of AD. Nonetheless, little is known about the combined effects of human glutaminyl cyclase activity (pyroglutamination) and type 2 diabetes (metabolic impairment) in the pathophysiology and progression of AD in transgenic mice. This study investigated APPxhQC mice, a model for experimental AD and their non-transgenic littermates under diabetic or control conditions with and without ASX treatment to understand the combined consequences of metabolic impairment, pyroglutamylation and the effect of ASX supplementation in AD pathophysiology, with special focuses on nutrient sensing signaling pathways, Aβ metabolism and spatial cognitive impairment.

In summary, our results suggest a sex and genotype specific effect of the interaction of diet, glutaminyl cyclase activity and ASX supplementation in this model on nutrient sensing signaling pathways, Aβ metabolism and cognitive impairment with implications for human AD pathophysiology. Absence of both APP and hQC influenced insulin secretion as NTG chow fed mice have higher FPI, a measure of insulin resistance, compared to APPxhQC mice irrespective of sex. Insulin secretion remained unchanged in T2D model APPxhQC male mice but improved in female mice whereas insulin secretion was impaired in both male and female T2D model NTG mice. T2D mimicking diet influenced food consumption irrespective of sex or genotype and weight gain in the absence of hQC in male mice. In addition, T2D mimicking diet elevated total plasma cholesterol level irrespective of genotype except in APPxhQC female mice. Diabetes caused significant liver damage in NTG female mice. In addition, T2D mimicking diet downregulated hepatic genes involved in cholesterol efflux, lipid metabolism in the absence of hQC, especially in female mice. We observed sex differences in how T2D mimicking diet affects metabolism of Aβ (conventional and modified). ASX supplementation impacts Aβ deposition and might be an hQC inhibitor. T2D mimicking diet impaired cognitive function in T2D model

NTG male and APPxhQC female mice. ASX supplementation was only able to rescue memory impairment in NTG male mice. Diet, genotype and sex tends to influence nutrient sensing pathways differentially while ASX supplementation might likely enhance nutrient signaling in T2D model NTG male mice.

We investigated the glycemic status of the mice before introducing the dietary intervention. At basal level, glucose sensitivity was impaired in NTG mice irrespective of the sex. T2D mimicking diet led to severe glucose intolerance in NTG mice, especially in the female mice. Damage of pancreatic cells resulting from Streptozocin injection leads to hyperinsulinemia and hyperglycemia (Ali and Ali, 2022).

T2D mimicking diet led to reduced food consumption in male mice irrespective of the genotype and female APPxhQC mice. Our results agree with reports from a similar study by Mazzei et al., (2021). Surprisingly, despite the reduced rate of food consumed, T2D model NTG male mice had significant weight gain similar to a report of Sankar and colleagues (Sankar et al., 2020) using APP/PS1xdb/db as a model for T2D-AD.

The T2D mimicking phenotype was most severe in the T2D model NTG female mice. These mice had elevated glycemic parameters (FPG, FPI, HOMA-IR, HOMA-β and HbA1c above 5.7%). HbA1c less than 5.7% is considered normal (Qinna and Badwan, 2015). Diabetic complications are established when HbA1c exceeds 5.7% as this indicates the prolonged presence of excessive sugar in circulation (Miedema, 2005). In patients diagnosed of T2D, hyperinsulinemia, insulin resistance, and β cell failure are commonly associated with Diabetic dyslipidemia (Athyros et al., 2018). In agreement, T2D model NTG female mice showed impaired β cell insulin secretion, were insulin resistant and had a high amount of glucose attached to their haemoglobin.

Hyperinsulinemia is an early event in the progression of T2D (Vandal et al., 2015). In this study, T2D model APPxhQC mice had increased FPI relative to their age matched chow fed control irrespective of sex. In addition, both male and female NTG mice on chow diet had high level of FPI compared to their APPxhQC counterpart. The high level of fasting insulin found in the plasma of chow fed NTG mice could be due to an impaired hepatic clearance of insulin (Brandt et al., 1977; Johnston et al., 1977) as the liver is known to rapidly degrade insulin (Faber et al., 1978; Ferrannini et al., 1983).

Hyperlipidemia refers to an increase of one or more plasma or serum lipids, usually cholesterol and triglycerides, and the term dyslipidemia is used to describe either an increase or decrease in the concentration of one or more plasma or serum lipids. We observed that T2D model diet led to increased plasma cholesterol irrespective of sex or genotype. Plasma cholesterol was significantly elevated in T2D model NTG (male and female) mice and APPxhQC male mice, supporting a similar study by Skrzypski and colleagues (Skrzypski et al., 2022). Conversely, T2D mimicking diet has no impact on plasma triglycerides as they do not differ irrespective of sex or genotype. Increased plasma cholesterol in T2D model NTG (male and female) mice and APPxhQC male mice further validates the increased intolerance to glucose and the elevated glycemic parameters (FPG, FPI, HOMA-IR, HOMA-β and HbA1c above 5.7%) in these mice, especially in T2D model NTG female mice. *In vitro* and *in vivo* studies have shown that elevated extracellular and intracellular cholesterol levels lead to functional disturbances in pancreatic beta cells (Hao et al., 2007; Brunham et al., 2007; Kruit et al., 2011). Moreover, Simonen and co-workers (Simonen et al., 2002) reported that T2D was associated with high cholesterol synthesis as well as with mildly elevated serum and lipoprotein triglyceride levels. Furthermore, clinical studies reported that increased cholesterol levels lead to reduced glucose tolerance, and that a high total cholesterol (TC) to high-density lipoprotein cholesterol (HDL-C) ratio can predict T2D (Seo et al., 2011; Wada et al., 2016). In addition, evidence suggests that hypercholesterolemia itself could reduce glucose-stimulated insulin secretion and insulin sensitivity (Hao et al., 2007; Dirkx and Solimena, 2012).

Alanine aminotransferase and AST, markers for liver dysfunction, have been reported to be good indicator of liver injury (Giannini et al., 2005; Sookoian and Pirola, 2012; Sookoian et al., 2016; Wang et al., 2016), hepatic insulin resistance (Hanley et al., 2004) and odds of T2D (Ballestri et al., 2016) and even cognitive impairments (Fillit et al., 2008; Santos et al., 2017; Nho et al., 2019). Concomitant with increased expression of plasma cholesterol, we also found increased expression of serum liver function enzymes AST and ALT in T2D model NTG mice, especially females, suggesting impaired liver function. These results are in accordance with similar reports for mice (Skrzypski et al., 2022) and humans (Wang et al., 2016; Ismal et al., 2020; Alam et al., 2021) that showed increased liver enzymes and a higher prevalence in diabetic females compared to diabetic males (Noroozi et al., 2022).

The liver is a vital metabolic organ involved in insulin sensitivity, gluconeogenesis, cholesterol synthesis and lipid metabolism. Genes such as SREBF1, PGC1α, PGC1β, PPARα, NEP, LRP1, ABCA1, ABCG1 and PPARγ and many others are crucial players in glucose and lipid metabolism.

Concomitant with impaired lipid metabolism, increased expression of liver function enzymes AST and ALT, we also observed associated with reduced transcription of genes involved in insulin sensitivity, gluconeogenesis, cholesterol synthesis and lipid metabolism. Gene products of SREBF1, PGC1α, PGC1β, PPARα, NEP, LRP1, ABCA1, ABCG1 and PPARγ involved in cholesterol efflux, amyloid transport, *de novo*-lipogenesis showed altered expression in livers of T2D model APPxhQC and NTG mice.

Sterol regulatory element-binding protein-1 (SREBF1) is a key transcription factor known to regulate genes involved in *de novo* lipogenesis and glycolysis pathways (Horton et al., 2002). Its expression has been reported to be significantly upregulated in obese patients and in animal models of obesity and type 2 diabetes (Ruiz et al., 2014; Shimomura et al., 1999). Contrary to previous reports, hepatic SREBF1 expression was downregulated in our T2D model NTG female mice. The reason for this result needs to be further investigated.

In addition to SREBF1, PPAR family members like PPARα, PPARβ, and PPARγ are transcriptional regulators known to play key roles in lipid metabolism (Kawada T, 1998; Takeyama et al., 2000; Michalik et al., 2006; Barak et al., 2008). Down regulation of PPARα was reported when β cells were exposed to elevated glucose and in T2D (Roduit et al., 2000; Shao et al., 2019; Zhu et al., 2021). Moreover, PPARα is required for the expression of FGF21, a liver secreted hormone with many endocrine and hepatoprotective functions (Badman et al., 2007; Fisher et al., 2014; Iroz et al., 2017; Singhal et al., 2018). In our study, PPARα was downregulated in T2D model NTG female mice. T2D mimicking diet resulted in an increased expression of PPARγ irrespective of sex or genotype but upregulation was more pronounced in NTG male mice which agrees with reports by Bedoucha et al., Morán-Salvador and colleagues, Jia and co-workers (Bedoucha et al., 2001; Morán-Salvador et al., 2011; Jia et al., 2016). Hepatic mRNA expression of FGF21 was downregulated in T2D model male mice irrespective of genotype and T2D model NTG female mice, suggesting an impaired metabolic state. Our result differs from

previous studies that reported increased circulating FGF21 in serum and liver of obese and T2D model patients correlating with abnormal glucose metabolism (Chavez et al., 2009; Martin et al., 2009; Fisher et al., 2010; Hale et al., 2012; So et al., 2013; Wang et al., 2018). The reasons for this variation need to be further investigated.

Furthermore, the peroxisome proliferator-activated receptor g coactivators-1α and β (PGC1α and PGC1β) are additional crucial genes involved in the pathophysiology of T2D (Mootha et al., 2003; Patti et al., 2003; Finck et al., 2006; Villena, 2015). In this study, hepatic PGC1β expression was significantly downregulated in T2D model NTG female mice. We observed reduced expression of PGC1α in T2D model male mice regardless of genotype and female NTG mice. This agrees with previous studies that reported decreased expression of PGC1α in liver and muscle, organs associated with glucose intolerance and insulin resistance (Mootha et al., 2003; Westerbacka et al., 2007; Handschin et al., 2007; Estall et al., 2009; Liu et al., 2011; Kleiner et al., 2012; Sczelecki et al., 2014). In addition, down regulation of PGC1α has been reported in islets of patients with T2D, correlating with decreased insulin secretion (Ling et al., 2008).

In addition, low-density lipoprotein receptor-related protein 1 (LRP1), a member of the low-density lipoprotein receptor (LDL-R) family (Gonias and Campana, 2014) has been implicated in insulin signaling pathways and cerebral glucose homeostasis (Nakajima et al., 2014). LRP1 is known to be a major receptor for Aβ in the liver and responsible for clearance of plasma Aβ (Hone et al., 2003; Ghiso et al., 2004; Tamaki et al., 2006). In our study, hepatic expression of LRP1 was significantly downregulated in T2D model NTG female mice. This is not surprising as these mice were hyperglycemic and hyperglycemia is known to suppress LRP1 expression while accelerating Aβ accumulation (Liu et al., 2015) and modulate the compensatory responses of β-cells to glucotoxicity and lipotoxicity (Ye at al., 2018).

Moreover, hepatic mRNA expression of NEP was increased in T2D model male mice irrespective of the genotype, although not statistically significant, whereas, it was downregulated in T2D model NTG female mice. This agrees partially with other studies that reported increased NEP in plasma and metabolic tissues of mice with diet-induced obesity and its expression level correlated with decreased insulin sensitivity and reduced beta cell function (Standeven et al., 2011; Willard et al.,

2017). In addition, NEP inhibitors are known to increase the level of substrates like angiotensin II (Campbell et al., 1998), thereby impairing insulin sensitivity and secretion and subsequently promoting insulin resistance and beta cell dysfunction. Moreover, increasing NEP activity is associated with a compensatory increase in pancreatic β cell mass to overcome glucose dyshomeostasis (Jurgens et al., 2011).

Some studies have linked mutation and defects in ABC transporter genes to T2D (Waller et al., 2013; Norton et al., 2017). Both ABCA1 and ABCG1 play important roles in transporting excess cholesterol out of the cell (Waller et al., 2013) and down regulation of ABCG1 has been reported in T2D patients (Solini et al., 2017). In our study, hepatic mRNA expressions of ABCA1 and ABCG1 were also reduced in T2D model NTG female mice. ASX supplementation slightly increased the expressions of ABCA1 and ABCG1 in T2D model APPxhQC male mice, albeit not to a statistically significant level. Significant alterations of transcription genes SREBF1, PPARα, LRP1, ABCA1, NEP and PGC1β implicated in glucose and lipid homeostasis, in agreement with other parameters used to access diabetic state in our model affirms the severity of T2D mimicking diet in our T2D model NTG female mice.

Effects of T2D mimicking diet on Aβ metabolism and cognitive impairment in animal models appears to be dependent on factors depending on which mouse strain is used and how T2D was induced. We evaluated the effect of T2D mimicking diet on Aβ metabolism in APPxhQC mice and observed a sex specific difference in the deposition of conventional and pGlu-3 Aβ isoforms. In male APPxhQC mice, T2D mimicking diet led to decreased deposition of soluble Aβ isoforms ($Aβ_{38}$, $Aβ_{40}$, $Aβ_{42}$) levels, with its effect more pronounced for $Aβ_{40}$. T2D mimicking diet resulted in increased FA insoluble Aβ isoforms especially $Aβ_{40}$. T2D mimicking diet had no noticeable influence on conventional Aβ metabolism in female mice. ASX supplementation significantly reduced the amount of deposited soluble and insoluble $Aβ_{40}$ in male mice. This agrees with a recent publication from our group where we reported that co-treatment of ASX with $Aβ_{40}$ enhances Aβ clearance in pBCECs by reducing intracellular and secreted APP/Aβ (Babalola et al., 2023). Slightly different from what we observed for conventional Aβ isoforms, T2D mimicking diet caused an increase in the deposition of soluble and plaque associated pGlu-3 $Aβ_{42}$. Increased deposition of soluble pGlu-3 $Aβ_{42}$ was more pronounced in female mice and was significantly reduced by ASX supplementation. Similar to results obtained from our

experimental T2D-AD model, Wang et al., also reported an increased pool of insoluble $A\beta_{40}$ and $A\beta_{42}$ in post-mortem brains of AD patients and a significant decrease in the solubility of Aβ peptides in pathologic aging compared to normal aging and in AD compared to pathologic aging and normal aging (Wang et al., 1999). In contrast, in studies using APP/PS1xdb/db mice, increased deposition of soluble $A\beta_{40}$ and $A\beta_{42}$ and reduced deposition of insoluble $A\beta_{40}$ and $A\beta_{42}$ both in the cortex and hippocampus were reported after T2D diet, connoting a shift in Aβ levels towards more toxic soluble species (Ramos-Rodriguez et al., 2015; Infante-Garcia et al., 2016; Sankar et al., 2020). Conversely, Carus-Cadavieco and co-workers (Carus-Cadavieco et al., 2023) reported a reduction in both soluble and insoluble Aβ in streptozocin-HFD fed hAPP NL/F mice. Using hAPP NL/F mice fed HFD containing 40% kcal from fat for 12 months, Mazzie and others (Mazzie et al., 2021) reported an increased deposition of insoluble Aβ while soluble Aβ remained unchanged. Furthermore, they suggested that the T2D phenotype induced in their model promoted Aβ aggregation and deposition by suppressing its clearance. Using HFD fed 3xTg-AD mice, Vandal and others, reported an increased soluble $A\beta_{40}$ and $A\beta_{42}$ in the cerebral cortex of 15-month-old animals (Vandal et al., 2014; Julien et al., 2010). Ho and colleagues (Ho et al., 2004) reported an increase in soluble $A\beta_{40}$ and $A\beta_{42}$ in cortex of female HFD fed Tg 2576 mice. In AppNL/NL HFD- fed mice carrying the Swedish “NL” mutation, Salas and co-workers (Salas et al., 2018) reported no change in soluble $A\beta_{40}$ and $A\beta_{42}$ at 4 months and 16 months. In our study, an observed shift from soluble to insoluble Aβ isoforms in the brains of T2D model APPxhQC male mice, similar to that reported in post-mortem brains of AD patients, suggests that peripheral metabolic dysfunctions might affect Aβ metabolism (deposition, clearance and degradation). The reduced deposition of soluble pGlu-3 $A\beta_{42}$ in our T2D model APPxhQC female mice suggests that ASX might be an hQC inhibitor. This potential of ASX as hQC inhibitor needs to be further investigated.

Sex and genotype specific differences were observed with respect to the impact of T2D mimicking diet on hippocampal dependent spatial memory dysfunction.T2D mimicking diet severely impaired cognitive function in T2D model NTG male and APPxhQC female mice. Spatial memory deficits were more pronounced in mice from these groups as they showed reduced number of target zone crosses. T2D has been reported to cause memory impairment both in rats (Wang et al., 2020; Lawal et al., 2021) and mice (Zhu et al., 2022, Zhang et al., 2021). In 2017, Kang and colleague

showed that streptozotocin-induced diabetic mice accumulate cerebral Aβ and develop memory dysfunction (Kang et al., 2017). However, we could not replicate this in our T2D model APPxhQC male mice. Numbers of target zone crosses did not differ significantly in T2D model APPxhQC male mice from the chow fed control group even though T2D mimicking diet significantly elevated the amount of plaque associated insoluble Aβ isoforms deposited in their brains. This result is not outright surprising as reports on the effect of T2D on cognitive performance in experimental animal models have been varying; ranging from increased Aβ deposition due to T2D with accompanying memory impairments (Barron et al., 2013; Vandal et al., 2014; Ettcheto et al., 2016; Walker et al., 2017; Mazzei et al., 2021; Carus-Cadavieco et al., 2023) to no memory impairment or only mild memory dysfunction (Bracko et al., 2020; Yeh et al., 2015; Salas et al., 2018). There are even studies that reported impaired memory function due to T2D without increased Aβ deposition (Knight et al., 2014; Sah et al., 2017). ASX supplementation reversed impaired hippocampal dependent spatial memory function in T2D model NTG male mice. These mice spent shorter time to find the hidden platform in terms of escape latency, decreased length of path and decreased velocity during the training phase. Furthermore, we recorded more target zone crosses during the probe trial in same mice suggesting a potential of ASX supplementation to reverse spatial memory deficits due to T2D mimicking diet.

In order to unravel the mechanism(s) by which ASX supplementation ameliorate hippocampal dependent cognitive impairment, we evaluated the effects of ASX supplementation on nutrient sensing pathways. Hyperglycemia and hyperlipidemia have been reported to inhibit autophagy (Ji et al., 2019) and ASX is a well reported autophagy inducer (Kim and Kim, 2019; Lee et al., 2020). In our model, cerebral LC3B lipidation was reduced in ASX supplemented T2D model NTG mice, especially in female mice. Expressions of cerebral LAMP2A, ATG5 and Beclin 1 proteins were elevated in ASX supplemented T2D model NTG male mice but reduced in APPxhQC male mice. Despite the downregulation of LC3B, elevation of other markers of autophagy might suggest a change in autophagy pathway.

Similar to reports from Gali and colleagues (Gali et al., 2019), cerebral p-AKT and p-ERK were elevated in our T2D model APPxhQC male mice, suggesting a hyperactive downstream insulin signaling whereas in ASX supplemented T2D model NTG male

mice, insulin signaling was improved as both IR-β and ABCA1 expressions were elevated. In addition, ASX supplementation reduced p-ERK and increased p65 expression in T2D model NTG male mice. p65 expression has been linked with neurogenesis (Bhakar et al., 2002; Azoitei et al., 2005; Zhang et al., 2012; FitzPatrick et al., 2018) and enhancement of neurogenesis has been reported to support improvement in behavioral learning and memory tasks (Lazarov and Hollands, 2015).

Furthermore, ASX supplementation partially inhibits mTORC1 signaling by increasing p-S6rp while decreasing p-mTOR in T2D model NTG male mice. This partial inhibition of mTORC1 signaling might be responsible for improved cognitive function in these mice as mTOR signaling is necessary for memory formation and acute inhibition of mTORC1 may greatly impacts synaptic function and, as a consequence, impairs memory retrieval (Bekinschtein et al., 2006; Pereyra et al., 2018).

To evaluate brain-liver cross talk in the neuroprotective potential of ASX, we also examined its impact on nutrient sensing pathways in the liver. Lipidation of LC3B was upregulated in livers of T2D model NTG male mice and APPxhQC regardless of sex. Expression of hepatic LAMP2A was elevated in ASX supplemented T2D model NTG male mice while Beclin 1 expression was upregulated in ASX supplemented T2D model male and female NTG mice. Changes within autophagy pathway observed in our ASX supplemented T2D model NTG male mice agrees with reports from other studies that evaluated the effect of ASX on hepatic autophagy pathway (Shen et al., 2014; Jia et al., 2016). In addition, in agreement with reports from previous studies (Ni et al., 2015; Li et al., 2016), hepatic expressions of IR-β and p-AKT were elevated in ASX supplemented T2D model NTG male mice, suggesting enhanced insulin signaling. Comparable to a report on the effect of T2D mimicking diet on hepatic ABCA1 in $LDLR^{-/-}$ mice (Tang et al., 2010), hepatic ABCA1 was elevated in our T2D model NTG male group. Furthermore, ASX supplementation ameliorates hepatic inflammation in T2D model NTG male mice. Elevated expression of p65, a pro-inflammatory marker in liver of T2D model NTG male mice, was reduced following ASX supplementation. Increased hepatic expression of ERK was also observed in same group. Increased hepatic expression of ERK and decreased expression of p65 following ASX supplementation corroborate reports from similar studies that showed that ASX suppressing p65 NF-κB expression enhancing its anti-inflammatory function (Fakhri et al., 2018; 2019; Galasso et al., 2018).

Finally, we examined sections from brains of APPxhQC male mice fed chow diet, T2D model diet and T2D model diet supplemented with ASX histologically. We observed an increased amounts of 6E10, pGlu-3 Aβ, GFAP and iba1 in both cortex and hippocampus of T2D model APPxhQC male mice which was reduced in ASX supplemented T2D model APPxhQC male mice suggesting reduced Aβ deposition and inflammation.

This present study is limited by the lower power and number of mice tested per experimental groups. Moreso, western blotting technique used is a semi- quantitative technique with lots of technical variability. Hence, results are preliminary.

In conclusion, we demonstrated that T2D mimicking diet poses an additional risk for AD development and that metabolic dysfunction induced cognitive impairments. T2D mimicking diet influences Aβ metabolism and cognitive impairment with sex and genotype playing divergent roles. T2D mimicking diet resulted in a progressive shift from soluble to insoluble Aβ pools in APPxhQC male mice. Increased deposition of soluble and insoluble pGlu-3 $A\beta_{42}$ was more pronounced in T2D model APPxhQC female mice. T2D mimicking diet impaired memory functions in T2D model APPxhQC female and NTG male mice. The T2D mimicking phenotype was more pronounced in T2D model NTG female mice. ASX supplementation reduced Aβ deposition and may likely act as an hQC inhibitor. Our study is the first to report the potential of ASX as an hQC inhibitor. ASX supplementation ameliorated T2D mimicking diet induced memory dysfunction in T2D model NTG male mice possibly by enhancing NTG Aß clearance and degradation via autophagy and improving nutrient signalling pathways (autophagy, insulin and inflammatory signaling pathways) in both brain and liver. ASX supplementation alone may not be effective in presence of comorbidities and in late-stage AD.

8.0 REFERENCES

2020 Alzheimer's disease facts and figures. Alzheimers Dement. 2020 Mar 10. doi: 10.1002/alz.12068. Epub ahead of print. PMID: 32157811

2022 Alzheimer's disease facts and figures. Alzheimers Dement. 2022 Apr;18(4):700-789. doi: 10.1002/alz.12638. Epub 2022 Mar 14. PMID: 35289055.

2023 Alzheimer's disease facts and figures. Alzheimers Dement. 2023 Apr;19(4):1598-1695. doi: 10.1002/alz.13016. Epub 2023 Mar 14. PMID: 36918389.

Abderrahmani A, Yengo L, Caiazzo R, Canouil M, Cauchi S, Raverdy V, Plaisance V, Pawlowski V, Lobbens S, Maillet J, Rolland L, Boutry R, Queniat G, Kwapich M, Tenenbaum M, Bricambert J, Saussenthaler S, Anthony E, Jha P, Derop J, Sand O, Rabearivelo I, Leloire A, Pigeyre M, Daujat-Chavanieu M, Gerbal-Chaloin S, Dayeh T, Lassailly G, Mathurin P, Staels B, Auwerx J, Schürmann A, Postic C, Schafmayer C, Hampe J, Bonnefond A, Pattou F, Froguel P. Increased Hepatic PDGF-AA Signaling Mediates Liver Insulin Resistance in Obesity-Associated Type 2 Diabetes. Diabetes. 2018 Jul;67(7):1310-1321. doi: 10.2337/db17-1539. Epub 2018 May 4. PMID: 29728363.

Abuznait AH, Cain C, Ingram D, Burk D, Kaddoumi A. Up-regulation of P-glycoprotein reduces intracellular accumulation of beta amyloid: investigation of P-glycoprotein as a novel therapeutic target for Alzheimer's disease. J Pharm Pharmacol. 2011 Aug;63(8):1111-8. doi: 10.1111/j.2042-7158.2011.01309. x. Epub 2011 Jun 11. PMID: 21718295; PMCID: PMC3163078.

Abuznait AH, Kaddoumi A. Role of ABC transporters in the pathogenesis of Alzheimer's disease. ACS Chem Neurosci. 2012 Nov 21;3(11):820-31. doi: 10.1021/cn300077c. Epub 2012 Oct 11. PMID: 23181169; PMCID: PMC3504479.

Acero G, Manoutcharian K, Vasilevko V, Munguia ME, Govezensky T, Coronas G, Luz-Madrigal A, Cribbs DH, Gevorkian G. Immunodominant epitope and properties of pyroglutamate-modified Abeta-specific antibodies produced in rabbits. J Neuroimmunol. 2009 Aug 18;213(1-2):39-46. doi: 10.1016/j.jneuroim.2009.06.003. Epub 2009 Jul 9. PMID: 19545911; PMCID: PMC2725226.

Ahn KC, Learman CR, Baker GB, Weaver CL, Chung PS, Kim HG, Song MS. Regulation of Diabetes: A Therapeutic Strategy for Alzheimer's Disease? J Korean

Med Sci. 2019 Dec 2;34(46): e297. doi: 10.3346/jkms.2019.34. e297. PMID: 31779058; PMCID: PMC6882941.

Akiyama H, Barger S, Barnum S, Bradt B, Bauer J, Cole GM, Cooper NR, Eikelenboom P, Emmerling M, Fiebich BL, Finch CE, Frautschy S, Griffin WS, Hampel H, Hull M, Landreth G, Lue L, Mrak R, Mackenzie IR, McGeer PL, O'Banion MK, Pachter J, Pasinetti G, Plata-Salaman C, Rogers J, Rydel R, Shen Y, Streit W, Strohmeyer R, Tooyoma I, Van Muiswinkel FL, Veerhuis R, Walker D, Webster S, Wegrzyniak B, Wenk G, Wyss-Coray T. Inflammation and Alzheimer's disease. Neurobiol Aging. 2000 May-Jun;21(3):383-421. doi: 10.1016/s0197-4580(00)00124-x. PMID: 10858586; PMCID: PMC3887148.

Alam S, Raghav A, Reyaz A, Ahsan A, Ahirwar AK, Jain V, Agarwal S, Tripathi P. Prevalence of elevated liver enzymes and its relationship with type 2 diabetes mellitus in North Indian adults. Metabol Open. 2021 Sep 24; 12:100130. doi: 10.1016/j.metop.2021.100130. PMID: 34622192; PMCID: PMC8479470.

Albert MS, DeKosky ST, Dickson D, Dubois B, Feldman HH, Fox NC, Gamst A, Holtzman DM, Jagust WJ, Petersen RC, Snyder PJ, Carrillo MC, Thies B, Phelps CH. The diagnosis of mild cognitive impairment due to Alzheimer's disease: recommendations from the National Institute on Aging-Alzheimer's Association workgroups on diagnostic guidelines for Alzheimer's disease. Alzheimers Dement. 2011 May;7(3):270-9. doi: 10.1016/j.jalz.2011.03.008. Epub 2011 Apr 21. PMID: 21514249; PMCID: PMC3312027.

Albrecht C, Soumian S, Amey JS, Sardini A, Higgins CF, Davies AH, Gibbs RG. ABCA1 expression in carotid atherosclerotic plaques. Stroke. 2004 Dec;35(12):2801-6. doi: 10.1161/01.STR.0000147036.07307.93. Epub 2004 Nov 4. PMID: 15528463.

Alexandru A, Jagla W, Graubner S, Becker A, Bäuscher C, Kohlmann S, Sedlmeier R, Raber KA, Cynis H, Rönicke R, Reymann KG, Petrasch-Parwez E, Hartlage-Rübsamen M, Waniek A, Rossner S, Schilling S, Osmand AP, Demuth HU, von Hörsten S. Selective hippocampal neurodegeneration in transgenic mice expressing small amounts of truncated Aβ is induced by pyroglutamate-Aβ formation. J Neurosci. 2011 Sep 7;31(36):12790-801. doi: 10.1523/JNEUROSCI.1794-11.2011. PMID: 21900558; PMCID: PMC6623394.

Ali SK, Ali RH. Effects of antidiabetic agents on Alzheimer's disease biomarkers in experimentally induced hyperglycemic rat model by streptozocin. PLoS One. 2022 Jul 8;17(7): e0271138. doi: 10.1371/journal.pone.0271138. PMID: 35802659; PMCID: PMC9269384.

Allcock RJ, Barrow AD, Forbes S, Beck S, Trowsdale J. The human TREM gene cluster at 6p21.1 encodes both activating and inhibitory single IgV domain receptors and includes NKp44. Eur J Immunol. 2003 Feb;33(2):567-77. doi: 10.1002/immu.200310033. PMID: 12645956.

Alzgene (2010) Meta-analysis of all published AD association studies (case control only) APOE_E2/3/4. http:// www. alzge ne. org/ meta. asp? geneID= 83

Alzheimer's Association. 2013 Alzheimer's disease facts and figures. Alzheimers Dement. 2013 Mar;9(2):208-45. doi: 10.1016/j.jalz.2013.02.003. PMID: 23507120

Alzheimer's Association. 2019 Alzheimer's disease facts and figures. Alzheimer’s Dement. 2019; 15:321-387. doi.org/10.1016/j.jalz.2019.01.010

Ambati RR, Phang SM, Ravi S, Aswathanarayana RG. Astaxanthin: sources, extraction, stability, biological activities and its commercial applications--a review. Mar Drugs. 2014 Jan 7;12(1):128-52. doi: 10.3390/md12010128. PMID: 24402174; PMCID: PMC3917265.

Armulik A, Genové G, Mäe M, Nisancioglu MH, Wallgard E, Niaudet C, He L, Norlin J, Lindblom P, Strittmatter K, Johansson BR, Betsholtz C. Pericytes regulate the blood-brain barrier. Nature. 2010 Nov 25;468(7323):557-61. doi: 10.1038/nature09522. Epub 2010 Oct 13. PMID: 20944627.

Arnold SE, Arvanitakis Z, Macauley-Rambach SL, Koenig AM, Wang HY, Ahima RS, Craft S, Gandy S, Buettner C, Stoeckel LE, Holtzman DM, Nathan DM. Brain insulin resistance in type 2 diabetes and Alzheimer disease: concepts and conundrums. Nat Rev Neurol. 2018 Mar;14(3):168-181. doi: 10.1038/nrneurol.2017.185. Epub 2018 Jan 29. PMID: 29377010; PMCID: PMC6098968.

Arvanitakis Z, Wilson RS, Bienias JL, Evans DA, Bennett DA. Diabetes mellitus and risk of Alzheimer disease and decline in cognitive function. Arch Neurol. 2004 May;61(5):661-6. doi: 10.1001/archneur.61.5.661. PMID: 15148141.

Ashkavand Z, Sarasija S, Ryan KC, Laboy JT, Norman KR. Corrupted ER-mitochondrial calcium homeostasis promotes the collapse of proteostasis. Aging Cell. 2020 Jan;19(1): e13065. doi: 10.1111/acel.13065. Epub 2019 Nov 12. PMID: 31714672; PMCID: PMC6974732.

Athyros VG, Doumas M, Imprialos KP, Stavropoulos K, Georgianou E, Katsimardou A, Karagiannis A. Diabetes and lipid metabolism. Hormones (Athens). 2018 Mar;17(1):61-67. doi: 10.1007/s42000-018-0014-8. Epub 2018 Apr 16. PMID: 29858856.

Azizi G, Navabi SS, Al-Shukaili A, Seyedzadeh MH, Yazdani R, Mirshafiey A. The Role of Inflammatory Mediators in the Pathogenesis of Alzheimer's Disease. Sultan Qaboos Univ Med J. 2015 Aug;15(3): e305-16. doi: 10.18295/squmj.2015.15.03.002. Epub 2015 Aug 24. PMID: 26357550; PMCID: PMC4554263.

Azoitei N, Wirth T, Baumann B. Activation of the Ikappa B kinase complex is sufficient for neuronal differentiation of PC12 cells. J Neurochem. 2005 Jun;93(6):1487-501. doi: 10.1111/j.1471-4159.2005.03148. x. PMID: 15935065.

Babalola JA, Lang M, George M, Stracke A, Tam-Amersdorfer C, Itxaso I, Lucija D, Tadic J, Schilcher I, Loeffler T, Flunkert S, Prokesch M, Leitinger G, Lass A, Hutter-Paier B, Panzenboeck U, Hoefler G. Astaxanthin enhances autophagy, amyloid beta clearance and exerts anti-inflammatory effects in in vitro models of Alzheimer's disease-related blood brain barrier dysfunction and inflammation. Brain Res. 2023 Aug 12; 1819:148518. doi: 10.1016/j.brainres.2023.148518. Epub ahead of print. PMID: 37579986.

Bading JR, Yamada S, Mackic JB, Kirkman L, Miller C, Calero M, Ghiso J, Frangione B, Zlokovic BV. Brain clearance of Alzheimer's amyloid-beta40 in the squirrel monkey: a SPECT study in a primate model of cerebral amyloid angiopathy. J Drug Target. 2002 Jun;10(4):359-68. doi: 10.1080/10611860290031831. PMID: 12164385.

Badman MK, Pissios P, Kennedy AR, Koukos G, Flier JS, Maratos-Flier E. Hepatic fibroblast growth factor 21 is regulated by PPARalpha and is a key mediator of hepatic lipid metabolism in ketotic states. Cell Metab. 2007 Jun;5(6):426-37. doi: 10.1016/j.cmet.2007.05.002. PMID: 17550778.

Baglietto-Vargas D, Shi J, Yaeger DM, Ager R, LaFerla FM. Diabetes and Alzheimer's disease crosstalk. Neurosci Biobehav Rev. 2016 May; 64:272-87. doi: 10.1016/j.neubiorev.2016.03.005. Epub 2016 Mar 9. PMID: 26969101.

Ballatore C, Lee VM, Trojanowski JQ. Tau-mediated neurodegeneration in Alzheimer's disease and related disorders. Nat Rev Neurosci. 2007 Sep;8(9):663-72. doi: 10.1038/nrn2194. PMID: 17684513.

Ballestri S, Zona S, Targher G, Romagnoli D, Baldelli E, Nascimbeni F, Roverato A, Guaraldi G, Lonardo A. Nonalcoholic fatty liver disease is associated with an almost twofold increased risk of incident type 2 diabetes and metabolic syndrome. Evidence from a systematic review and meta-analysis. J Gastroenterol Hepatol. 2016 May;31(5):936-44. doi: 10.1111/jgh.13264. PMID: 26667191.

Banks WA, Jaspan JB, Kastin AJ. Effect of diabetes mellitus on the permeability of the blood-brain barrier to insulin. Peptides. 1997;18(10):1577-84. doi: 10.1016/s0196-9781(97)00238-6. PMID: 9437719.

Banks WA, Owen JB, Erickson MA. Insulin in the brain: there and back again. Pharmacol Ther. 2012 Oct;136(1):82-93. doi: 10.1016/j.pharmthera.2012.07.006. Epub 2012 Jul 17. PMID: 22820012; PMCID: PMC4134675.

Banks WA, Rhea EM. The Blood-Brain Barrier, Oxidative Stress, and Insulin Resistance. Antioxidants (Basel). 2021 Oct 27;10(11):1695. doi: 10.3390/antiox10111695. PMID: 34829566; PMCID: PMC8615183.

Banks WA. The blood-brain barrier as an endocrine tissue. Nat Rev Endocrinol. 2019 Aug;15(8):444-455. doi: 10.1038/s41574-019-0213-7. PMID: 31127254.

Barak Y, Sadovsky Y, Shalom-Barak T. PPAR Signaling in Placental Development and Function. PPAR Res. 2008;2008: 142082. doi: 10.1155/2008/142082. PMID: 18288278; PMCID: PMC2225458.

Barbagallo M, Dominguez LJ. Type 2 diabetes mellitus and Alzheimer's disease. World J Diabetes. 2014 Dec 15;5(6):889-93. doi: 10.4239/wjd. v5.i6.889. PMID: 25512792; PMCID: PMC4265876.

Barisano G, Kisler K, Wilkinson B, Nikolakopoulou AM, Sagare AP, Wang Y, Gilliam W, Huuskonen MT, Hung ST, Ichida JK, Gao F, Coba MP, Zlokovic BV. A "multi-omics" analysis of blood-brain barrier and synaptic dysfunction in APOE4 mice. J Exp

Med. 2022 Nov 7;219(11): e20221137. doi: 10.1084/jem.20221137. Epub 2022 Aug 30. PMID: 36040482; PMCID: PMC9435921.

Barnes LL, Lamar M, Schneider JA. Sex differences in mixed neuropathologies in community-dwelling older adults. Brain Res. 2019 Sep 15; 1719:11-16. doi: 10.1016/j.brainres.2019.05.028. Epub 2019 May 22. PMID: 31128096; PMCID: PMC6636678.

Barrès R, Osler ME, Yan J, Rune A, Fritz T, Caidahl K, Krook A, Zierath JR. Non-CpG methylation of the PGC-1alpha promoter through DNMT3B controls mitochondrial density. Cell Metab. 2009 Sep;10(3):189-98. doi: 10.1016/j.cmet.2009.07.011. PMID: 19723495.

Barron AM, Rosario ER, Elteriefi R, Pike CJ. Sex-specific effects of high fat diet on indices of metabolic syndrome in 3xTg-AD mice: implications for Alzheimer's disease. PLoS One. 2013 Oct 28;8(10): e78554. doi: 10.1371/journal.pone.0078554. PMID: 24205258; PMCID: PMC3810257.

Barthélemy NR, Li Y, Joseph-Mathurin N, Gordon BA, Hassenstab J, Benzinger TLS, Buckles V, Fagan AM, Perrin RJ, Goate AM, Morris JC, Karch CM, Xiong C, Allegri R, Mendez PC, Berman SB, Ikeuchi T, Mori H, Shimada H, Shoji M, Suzuki K, Noble J, Farlow M, Chhatwal J, Graff-Radford NR, Salloway S, Schofield PR, Masters CL, Martins RN, O'Connor A, Fox NC, Levin J, Jucker M, Gabelle A, Lehmann S, Sato C, Bateman RJ, McDade E; Dominantly Inherited Alzheimer Network. A soluble phosphorylated tau signature links tau, amyloid and the evolution of stages of dominantly inherited Alzheimer's disease. Nat Med. 2020 Mar;26(3):398-407. doi: 10.1038/s41591-020-0781-z. Epub 2020 Mar 11. PMID: 32161412; PMCID: PMC7309367.

Bateman RJ, Xiong C, Benzinger TL, Fagan AM, Goate A, Fox NC, Marcus DS, Cairns NJ, Xie X, Blazey TM, Holtzman DM, Santacruz A, Buckles V, Oliver A, Moulder K, Aisen PS, Ghetti B, Klunk WE, McDade E, Martins RN, Masters CL, Mayeux R, Ringman JM, Rossor MN, Schofield PR, Sperling RA, Salloway S, Morris JC; Dominantly Inherited Alzheimer Network. Clinical and biomarker changes in dominantly inherited Alzheimer's disease. N Engl J Med. 2012 Aug 30;367(9):795-804. doi: 10.1056/NEJMoa1202753. Epub 2012 Jul 11. Erratum in: N Engl J Med. 2012 Aug 23;367(8):780. PMID: 22784036; PMCID: PMC3474597.

Baumeier C, Saussenthaler S, Kammel A, Jähnert M, Schlüter L, Hesse D, Canouil M, Lobbens S, Caiazzo R, Raverdy V, Pattou F, Nilsson E, Pihlajamäki J, Ling C, Froguel P, Schürmann A, Schwenk RW. Hepatic DPP4 DNA Methylation Associates with Fatty Liver. Diabetes. 2017 Jan;66(1):25-35. doi: 10.2337/db15-1716. Epub 2016 Oct 10. PMID: 27999105.

Bayer TA. Pyroglutamate Aβ cascade as drug target in Alzheimer's disease. Mol Psychiatry. 2022 Apr;27(4):1880-1885. doi: 10.1038/s41380-021-01409-2. Epub 2021 Dec 8. PMID: 34880449; PMCID: PMC9126800.

BD 2019 Dementia Forecasting Collaborators. Estimation of the global prevalence of dementia in 2019 and forecasted prevalence in 2050: an analysis for the Global Burden of Disease Study 2019.Lancet Public Health. 2022 Feb;7(2): e105-e125. doi: 10.1016/S2468- 2667(21)00249-8. Epub 2022 Jan 6. PMID: 34998485; PMCID: PMC8810394.

Bedoucha M, Atzpodien E, Boelsterli UA. Diabetic KKAy mice exhibit increased hepatic PPARgamma1 gene expression and develop hepatic steatosis upon chronic treatment with antidiabetic thiazolidinediones. J Hepatol. 2001 Jul;35(1):17-23. doi: 10.1016/s0168-8278(01)00066-6. PMID: 11495036

Behan DP, Heinrichs SC, Troncoso JC, Liu XJ, Kawas CH, Ling N, De Souza EB. Displacement of corticotropin releasing factor from its binding protein as a possible treatment for Alzheimer's disease. Nature. 1995 Nov 16;378(6554):284-7. doi: 10.1038/378284a0. PMID: 7477348.

Bekinschtein P, Katche C, Slipczuk LN, Igaz LM, Cammarota M, Izquierdo I, Medina JH. mTOR signaling in the hippocampus is necessary for memory formation. Neurobiol Learn Mem. 2007 Feb;87(2):303-7. doi: 10.1016/j.nlm.2006.08.007. Epub 2006 Sep 26. PMID: 17005423.

Bekris LM, Yu CE, Bird TD, Tsuang DW. Genetics of Alzheimer disease. J Geriatr Psychiatry Neurol. 2010 Dec;23(4):213-27. doi: 10.1177/0891988710383571. PMID: 21045163; PMCID: PMC3044597.

Bell RD, Zlokovic BV. Neurovascular mechanisms and blood-brain barrier disorder in Alzheimer's disease. Acta Neuropathol. 2009 Jul;118(1):103-13. doi:

10.1007/s00401-009-0522-3. Epub 2009 Mar 25. PMID: 19319544; PMCID: PMC2853006.

Bell RD, Zlokovic BV. Neurovascular mechanisms and blood-brain barrier disorder in Alzheimer's disease. Acta Neuropathol. 2009 Jul;118(1):103-13. doi: 10.1007/s00401-009-0522-3. Epub 2009 Mar 25. PMID: 19319544; PMCID: PMC2853006.

Betz AL, Firth JA, Goldstein GW. Polarity of the blood-brain barrier: distribution of enzymes between the luminal and anti-luminal membranes of brain capillary endothelial cells. Brain Res. 1980 Jun 16;192(1):17-28. doi: 10.1016/0006-8993(80)91004-5. PMID: 6103738.

Bhakar AL, Tannis LL, Zeindler C, Russo MP, Jobin C, Park DS, MacPherson S, Barker PA. Constitutive nuclear factor-kappa B activity is required for central neuron survival. J Neurosci. 2002 Oct 1;22(19):8466-75. doi: 10.1523/JNEUROSCI.22-19-08466.2002. PMID: 12351721; PMCID: PMC6757785.

Bhaskar K, Miller M, Chludzinski A, Herrup K, Zagorski M, Lamb BT. The PI3K-Akt-mTOR pathway regulates Abeta oligomer induced neuronal cell cycle events. Mol Neurodegener. 2009 Mar 16; 4:14. doi: 10.1186/1750-1326-4-14. PMID: 19291319; PMCID: PMC2663563.

Biessels GJ, Staekenborg S, Brunner E, Brayne C, Scheltens P. Risk of dementia in diabetes mellitus: a systematic review. Lancet Neurol. 2006 Jan;5(1):64-74. doi: 10.1016/S1474-4422(05)70284-2. Erratum in: Lancet Neurol. 2006 Feb;5(2):113. PMID: 16361024.

Biessels GJ, Staekenborg S, Brunner E, Brayne C, Scheltens P. Risk of dementia in diabetes mellitus: a systematic review. Lancet Neurol. 2006 Jan;5(1):64-74. doi: 10.1016/S1474-4422(05)70284-2. Erratum in: Lancet Neurol. 2006 Feb;5(2):113. PMID: 16361024.

Biever A, Valjent E, Puighermanal E. Ribosomal Protein S6 Phosphorylation in the Nervous System: From Regulation to Function. Front Mol Neurosci. 2015 Dec 16; 8:75. doi: 10.3389/fnmol.2015.00075. PMID: 26733799; PMCID: PMC4679984.

Birks J. Cholinesterase inhibitors for Alzheimer's disease. Cochrane Database Syst Rev. 2006 Jan 25;2006(1):CD005593. doi: 10.1002/14651858.CD005593. PMID: 16437532; PMCID: PMC9006343.

Blázquez E, Velázquez E, Hurtado-Carneiro V, Ruiz-Albusac JM. Insulin in the brain: its pathophysiological implications for States related with central insulin resistance, type 2 diabetes and Alzheimer's disease. Front Endocrinol (Lausanne). 2014 Oct 9; 5:161. doi: 10.3389/fendo.2014.00161. PMID: 25346723; PMCID: PMC4191295.

Blennow K, de Leon MJ, Zetterberg H. Alzheimer's disease. Lancet. 2006 Jul 29;368(9533):387-403. doi: 10.1016/S0140-6736(06)69113-7. PMID: 16876668.

Bloomingdale P, Karelina T, Ramakrishnan V, Bakshi S, Véronneau-Veilleux F, Moye M, Sekiguchi K, Meno-Tetang G, Mohan A, Maithreye R, Thomas VA, Gibbons F, Cabal A, Bouteiller JM, Geerts H. Hallmarks of neurodegenerative disease: A systems pharmacology perspective. CPT Pharmacometrics Syst Pharmacol. 2022 Nov;11(11):1399-1429. doi: 10.1002/psp4.12852. Epub 2022 Aug 17. PMID: 35894182; PMCID: PMC9662204.

Boland B, Yu WH, Corti O, Mollereau B, Henriques A, Bezard E, Pastores GM, Rubinsztein DC, Nixon RA, Duchen MR, Mallucci GR, Kroemer G, Levine B, Eskelinen EL, Mochel F, Spedding M, Louis C, Martin OR, Millan MJ. Promoting the clearance of neurotoxic proteins in neurodegenerative disorders of ageing. Nat Rev Drug Discov. 2018 Sep;17(9):660-688. doi: 10.1038/nrd.2018.109. Epub 2018 Aug 17. PMID: 30116051; PMCID: PMC6456907

Bourdenx M, Martín-Segura A, Scrivo A, Rodriguez-Navarro JA, Kaushik S, Tasset I, Diaz A, Storm NJ, Xin Q, Juste YR, Stevenson E, Luengo E, Clement CC, Choi SJ, Krogan NJ, Mosharov EV, Santambrogio L, Grueninger F, Collin L, Swaney DL, Sulzer D, Gavathiotis E, Cuervo AM. Chaperone-mediated autophagy prevents collapse of the neuronal metastable proteome. Cell. 2021 May 13;184(10):2696-2714.e25. doi: 10.1016/j.cell.2021.03.048. Epub 2021 Apr 22. PMID: 33891876; PMCID: PMC8152331.

Braak H, Thal DR, Ghebremedhin E, Del Tredici K. Stages of the pathologic process in Alzheimer disease: age categories from 1 to 100 years. J Neuropathol Exp Neurol. 2011 Nov;70(11):960-9. doi: 10.1097/NEN.0b013e318232a379. PMID: 22002422

Bracko O, Vinarcsik LK, Cruz Hernández JC, Ruiz-Uribe NE, Haft-Javaherian M, Falkenhain K, Ramanauskaite EM, Ali M, Mohapatra A, Swallow MA, Njiru BN, Muse V, Michelucci PE, Nishimura N, Schaffer CB. High fat diet worsens Alzheimer's disease-related behavioral abnormalities and neuropathology in APP/PS1 mice, but not by synergistically decreasing cerebral blood flow. Sci Rep. 2020 Jun 18;10(1):9884. doi: 10.1038/s41598-020-65908-y. PMID: 32555372; PMCID: PMC7303150.

Brands AM, Biessels GJ, de Haan EH, Kappelle LJ, Kessels RP. The effects of type 1 diabetes on cognitive performance: a meta-analysis. Diabetes Care. 2005 Mar;28(3):726-35. doi: 10.2337/diacare.28.3.726. PMID: 15735218.

Brandt MR, Kehlet H, Faber O, Binder Chr. C-peptide and insulin during blockade of the hyperglycaemic response to surgery by epidural analgesia. Clin Endocrinol (Oxf). 1977 Feb;6(2):167-70. doi: 10.1111/j.1365-2265.1977. tb 02008.x. PMID: 844223.

Brauner A, Carlsson B, Sundkvist G, Ostenson CG. False-positive treponemal serology in patients with diabetes mellitus. J Diabetes Complications. 1994 Jan-Mar;8(1):57-62. doi: 10.1016/1056-8727(94)90013-2. PMID: 8167389.

Brodaty H, Seeher K, Gibson L. Dementia time to death: a systematic literature review on survival time and years of life lost in people with dementia. Int Psychogeriatr. 2012 Jul;24(7):1034-45. doi: 10.1017/S1041610211002924. Epub 2012 Feb 13. PMID: 22325331.

Brookmeyer R, Corrada MM, Curriero FC, Kawas C. Survival following a diagnosis of Alzheimer disease. Arch Neurol. 2002 Nov;59(11):1764-7. doi: 10.1001/archneur.59.11.1764. PMID: 12433264.

Brunham LR, Kruit JK, Pape TD, Timmins JM, Reuwer AQ, Vasanji Z, Marsh BJ, Rodrigues B, Johnson JD, Parks JS, Verchere CB, Hayden MR. Beta-cell ABCA1 influences insulin secretion, glucose homeostasis and response to thiazolidinedione treatment. Nat Med. 2007 Mar;13(3):340-7. doi: 10.1038/nm1546. Epub 2007 Feb 18. PMID: 17322896.

Brüning JC, Gautam D, Burks DJ, Gillette J, Schubert M, Orban PC, Klein R, Krone W, Müller-Wieland D, Kahn CR. Role of brain insulin receptor in control of body

weight and reproduction. Science. 2000 Sep 22;289(5487):2122-5. doi: 10.1126/science.289.5487.2122. PMID: 11000114.

Buller CL, Loberg RD, Fan MH, Zhu Q, Park JL, Vesely E, Inoki K, Guan KL, Brosius FC 3rd. A GSK-3/TSC2/mTOR pathway regulates glucose uptake and GLUT1 glucose transporter expression. Am J Physiol Cell Physiol. 2008 Sep;295(3):C836-43. doi: 10.1152/ajpcell.00554.2007. Epub 2008 Jul 23. PMID: 18650261; PMCID: PMC2544442.

Burke SL, Hu T, Fava NM, Li T, Rodriguez MJ, Schuldiner KL, Burgess A, Laird A. Sex differences in the development of mild cognitive impairment and probable Alzheimer's disease as predicted by hippocampal volume or white matter hyperintensities. J Women Aging. 2019 Mar-Apr;31(2):140-164. doi: 10.1080/08952841.2018.1419476. Epub 2018 Jan 10. PMID: 29319430; PMCID: PMC6039284.

Businaro R, Corsi M, Asprino R, Di Lorenzo C, Laskin D, Corbo RM, Ricci S, Pinto A. Modulation of Inflammation as a Way of Delaying Alzheimer's Disease Progression: The Diet's Role. Curr Alzheimer Res. 2018 Feb 22;15(4):363-380. doi: 10.2174/1567205014666170829100100. PMID: 28847284.

Butterfield DA, Drake J, Pocernich C, Castegna A. Evidence of oxidative damage in Alzheimer's disease brain: central role for amyloid beta-peptide. Trends Mol Med. 2001 Dec;7(12):548-54. doi: 10.1016/s1471-4914(01)02173-6. PMID: 11733217.

Cabou C, Cani PD, Campistron G, Knauf C, Mathieu C, Sartori C, Amar J, Scherrer U, Burcelin R. Central insulin regulates heart rate and arterial blood flow: an endothelial nitric oxide synthase-dependent mechanism altered during diabetes. Diabetes. 2007 Dec;56(12):2872-7. doi: 10.2337/db07-0115. Epub 2007 Sep 5. PMID: 17804761.

Cacace R, Sleegers K, Van Broeckhoven C. Molecular genetics of early-onset Alzheimer's disease revisited. Alzheimers Dement. 2016 Jun;12(6):733-48. doi: 10.1016/j.jalz.2016.01.012. Epub 2016 Mar 24. PMID: 27016693

Cacace R, Sleegers K, Van Broeckhoven C. Molecular genetics of early-onset Alzheimer's disease revisited. Alzheimers Dement. 2016 Jun;12(6):733-48. doi: 10.1016/j.jalz.2016.01.012. Epub 2016 Mar 24. PMID: 27016693.

Cai XD, Golde TE, Younkin SG. Release of excess amyloid beta protein from a mutant amyloid beta protein precursor. Science. 1993 Jan 22;259(5094):514-6. doi: 10.1126/science.8424174. PMID: 8424174.

Cai Z, Chen G, He W, Xiao M, Yan LJ. Activation of mTOR: a culprit of Alzheimer's disease? Neuropsychiatr Dis Treat. 2015 Apr 9; 11:1015-30. doi: 10.2147/NDT.S75717. PMID: 25914534; PMCID: PMC4399516.

Calero M, Gómez-Ramos A, Calero O, Soriano E, Avila J, Medina M. Additional mechanisms conferring genetic susceptibility to Alzheimer's disease. Front Cell Neurosci. 2015 Apr 9; 9:138. doi: 10.3389/fncel.2015.00138. PMID: 25914626; PMCID: PMC4391239.

Campbell DJ, Anastasopoulos F, Duncan AM, James GM, Kladis A, Briscoe TA. Effects of neutral endopeptidase inhibition and combined angiotensin converting enzyme and neutral endopeptidase inhibition on angiotensin and bradykinin peptides in rats. J Pharmacol Exp Ther. 1998 Nov;287(2):567-77. PMID: 9808682.

Campion D, Charbonnier C, Nicolas G. SORL1 genetic variants and Alzheimer disease risk: a literature review and meta-analysis of sequencing data. Acta Neuropathol. 2019 Aug;138(2):173-186. doi: 10.1007/s00401-019-01991-4. Epub 2019 Mar 25. PMID: 30911827.

Carantoni M, Zuliani G, Munari MR, D'Elia K, Palmieri E, Fellin R. Alzheimer disease and vascular dementia: relationships with fasting glucose and insulin levels. Dement Geriatr Cogn Disord. 2000 May-Jun;11(3):176-80. doi: 10.1159/000017232. PMID: 10765049.

Carús-Cadavieco M, Berenguer López I, Montoro Canelo A, Serrano-Lope MA, González-de la Fuente S, Aguado B, Fernández-Rodrigo A, Saido TC, Frank García A, Venero C, Esteban JA, Guix F, Dotti CG. Cognitive decline in diabetic mice predisposed to Alzheimer's disease is greater than in wild type. Life Sci Alliance. 2023 Apr 14;6(6): e202201789. doi: 10.26508/lsa.202201789. PMID: 37059474; PMCID: PMC10105330.

Center for Disease Control and Prevention. National Diabetes Statistics Report website. https://www.cdc.gov/diabetes/data/statistics-report/index.html.Accessed (August 21, 2023).

Chatterjee B, Thakur SS. Investigation of post-translational modifications in type 2 diabetes. Clin Proteomics. 2018 Sep 24; 15:32. doi: 10.1186/s12014-018-9208-y. PMID: 30258344; PMCID: PMC6154926.

Chavez AO, Molina-Carrion M, Abdul-Ghani MA, Folli F, Defronzo RA, Tripathy D. Circulating fibroblast growth factor-21 is elevated in impaired glucose tolerance and type 2 diabetes and correlates with muscle and hepatic insulin resistance. Diabetes Care. 2009 Aug;32(8):1542-6. doi: 10.2337/dc09-0684. Epub 2009 Jun 1. PMID: 19487637; PMCID: PMC2713625.

Che H, Li Q, Zhang T, Wang D, Yang L, Xu J, Yanagita T, Xue C, Chang Y, Wang Y. Effects of Astaxanthin and Docosahexaenoic-Acid-Acylated Astaxanthin on Alzheimer's Disease in APP/PS1 Double-Transgenic Mice. J Agric Food Chem. 2018 May 16;66(19):4948-4957. doi: 10.1021/acs.jafc.8b00988. Epub 2018 May 7. PMID: 29695154.

Chen J, Mooldijk SS, Licher S, Waqas K, Ikram MK, Uitterlinden AG, Zillikens MC, Ikram MA. Assessment of Advanced Glycation End Products and Receptors and the Risk of Dementia. JAMA Netw Open. 2021 Jan 4;4(1): e2033012. doi: 10.1001/jamanetworkopen.2020.33012. PMID: 33416887; PMCID: PMC7794665.

Chen XQ, Mobley WC. Alzheimer Disease Pathogenesis: Insights from Molecular and Cellular Biology Studies of Oligomeric Aβ and Tau Species. Front Neurosci. 2019 Jun 21; 13:659. doi: 10.3389/fnins.2019.00659. PMID: 31293377; PMCID: PMC6598402.

Chêne G, Beiser A, Au R, Preis SR, Wolf PA, Dufouil C, Seshadri S. Gender and incidence of dementia in the Framingham Heart Study from mid-adult life. Alzheimers Dement. 2015 Mar;11(3):310-320. doi: 10.1016/j.jalz.2013.10.005. Epub 2014 Jan 10. PMID: 24418058; PMCID: PMC4092061.

Chêne G, Beiser A, Au R, Preis SR, Wolf PA, Dufouil C, Seshadri S. Gender and incidence of dementia in the Framingham Heart Study from mid-adult life. Alzheimers Dement. 2015 Mar;11(3):310-320. doi: 10.1016/j.jalz.2013.10.005. Epub 2014 Jan 10. PMID: 24418058; PMCID: PMC4092061.

Chirackal Manavalan AP, Kober A, Metso J, Lang I, Becker T, Hasslitzer K, Zandl M, Fanaee-Danesh E, Pippal JB, Sachdev V, Kratky D, Stefulj J, Jauhiainen M,

Panzenboeck U. Phospholipid transfer protein is expressed in cerebrovascular endothelial cells and involved in high density lipoprotein biogenesis and remodeling at the blood-brain barrier. J Biol Chem. 2014 Feb 21;289(8):4683-98. doi: 10.1074/jbc.M113.499129. Epub 2013 Dec 25. PMID: 24369175; PMCID: PMC3931031.

Cho HM, Ha TK, Doan TP, Dhodary B, An JP, Lee BW, Yang JL, Oh WK. Neuroprotective Effects of Triterpenoids from *Camellia japonica* against Amyloid β-Induced Neuronal Damage. J Nat Prod. 2020 Jul 24;83(7):2076-2086. doi: 10.1021/acs.jnatprod.9b00964. Epub 2020 Jun 22. PMID: 32569471.

Choi CI. Astaxanthin as a Peroxisome Proliferator-Activated Receptor (PPAR) Modulator: Its Therapeutic Implications. Mar Drugs. 2019 Apr 23;17(4):242. doi: 10.3390/md17040242. PMID: 31018521; PMCID: PMC6521084.

Choi I, Wang M, Yoo S, Xu P, Seegobin SP, Li X, Han X, Wang Q, Peng J, Zhang B, Yue Z. Autophagy enables microglia to engage amyloid plaques and prevents microglial senescence. Nat Cell Biol. 2023 Jul;25(7):963-974. doi: 10.1038/s41556-023-01158-0. Epub 2023 May 25. PMID: 37231161.

Cholerton B, Baker LD, Craft S. Insulin resistance and pathological brain ageing. DiabMed 2011; 28:1463–75

Chu C, Li JY, Boado RJ, Pardridge WM. Blood-brain barrier genomics and cloning of a novel organic anion transporter. J Cereb Blood Flow Metab. 2008 Feb;28(2):291-301. doi: 10.1038/sj.jcbfm.9600538. Epub 2007 Aug 1. PMID: 17667996; PMCID: PMC2892270.

Chun YS, Cho YY, Kwon OH, Zhao D, Yang HO, Chung S. Substrate-Specific Activation of α-Secretase by 7-Deoxy-Trans-Dihydronarciclasine Increases Non-Amyloidogenic Processing of β-Amyloid Protein Precursor. Molecules. 2020 Feb 3;25(3):646. doi: 10.3390/molecules25030646. PMID: 32028607; PMCID: PMC7037359.

Cole SL, Vassar R. The role of amyloid precursor protein processing by BACE1, the beta-secretase, in Alzheimer disease pathophysiology. J Biol Chem. 2008 Oct 31;283(44):29621-5. doi: 10.1074/jbc. R800015200. Epub 2008 Jul 23. PMID: 18650431; PMCID: PMC2662048

Coleman PD, Flood DG. Neuron numbers and dendritic extent in normal aging and Alzheimer's disease. Neurobiol Aging. 1987 Nov-Dec;8(6):521-45. doi: 10.1016/0197-4580(87)90127-8. PMID: 3323927.

Colonna M, Butovsky O. Microglia Function in the Central Nervous System During Health and Neurodegeneration. Annu Rev Immunol. 2017 Apr 26;35:441-468. doi: 10.1146/annurev-immunol-051116-052358. Epub 2017 Feb 9. PMID: 28226226; PMCID: PMC8167938.

Cooper GJ, Willis AC, Clark A, Turner RC, Sim RB, Reid KB. Purification and characterization of a peptide from amyloid-rich pancreases of type 2 diabetic patients. Proc Natl Acad Sci U S A. 1987 Dec;84(23):8628-32. doi: 10.1073/pnas.84.23.8628. PMID: 3317417; PMCID: PMC299599.

Cooper GJ, Willis AC, Reid KB, Clark A, Baker CA, Turner RC, Lewis CE, Morris JF, Howland K, Rothbard JB. Diabetes-associated peptide. Lancet. 1987 Oct 24;2(8565):966. doi: 10.1016/s0140-6736(87)91444-9. PMID: 2889879.

Corbo RM, Scacchi R. Apolipoprotein E (APOE) allele distribution in the world. Is APOE*4 a 'thrifty' allele? Ann Hum Genet. 1999 Jul;63(Pt 4):301-10. doi: 10.1046/j.1469-1809.1999.6340301.x. PMID: 10738542

Coughlan MT, Thorburn DR, Penfold SA, Laskowski A, Harcourt BE, Sourris KC, Tan AL, Fukami K, Thallas-Bonke V, Nawroth PP, Brownlee M, Bierhaus A, Cooper ME, Forbes JM. RAGE-induced cytosolic ROS promote mitochondrial superoxide generation in diabetes. J Am Soc Nephrol. 2009 Apr;20(4):742-52. doi: 10.1681/ASN.2008050514. Epub 2009 Jan 21. PMID: 19158353; PMCID: PMC2663823.

Craft S, Watson GS. Insulin and neurodegenerative disease: shared and specific mechanisms. Lancet Neurol. 2004 Mar;3(3):169-78. doi: 10.1016/S1474-4422(04)00681-7. PMID: 14980532.

Crane PK, Walker R, Hubbard RA, Li G, Nathan DM, Zheng H, Haneuse S, Craft S, Montine TJ, Kahn SE, McCormick W, McCurry SM, Bowen JD, Larson EB. Glucose levels and risk of dementia. N Engl J Med. 2013 Aug 8;369(6):540-8. doi: 10.1056/NEJMoa1215740. Erratum in: N Engl J Med. 2013 Oct 10;369(15):1476. PMID: 23924004; PMCID: PMC3955123.

Croft CL, Futch HS, Moore BD, Golde TE. Organotypic brain slice cultures to model neurodegenerative proteinopathies. Mol Neurodegener. 2019 Dec 2;14(1):45. doi: 10.1186/s13024-019-0346-0. PMID: 31791377; PMCID: PMC6889333.

Cruts M, Theuns J, Van Broeckhoven C. Locus-specific mutation databases for neurodegenerative brain diseases. Hum Mutat. 2012 Sep;33(9):1340-4. doi: 10.1002/humu.22117. Epub 2012 Jul 2. PMID: 22581678; PMCID: PMC3465795.

Császár E, Lénárt N, Cserép C, Környei Z, Fekete R, Pósfai B, Balázsfi D, Hangya B, Schwarcz AD, Szabadits E, Szöllősi D, Szigeti K, Máthé D, West BL, Sviatkó K, Brás AR, Mariani JC, Kliewer A, Lenkei Z, Hricisák L, Benyó Z, Baranyi M, Sperlágh B, Menyhárt Á, Farkas E, Dénes Á. Microglia modulate blood flow, neurovascular coupling, and hypoperfusion via purinergic actions. J Exp Med. 2022 Mar 7;219(3):e20211071. doi: 10.1084/jem.20211071. Epub 2022 Feb 24. PMID: 35201268; PMCID: PMC8932534.

Cuccaro ML, Carney RM, Zhang Y, Bohm C, Kunkle BW, Vardarajan BN, Whitehead PL, Cukier HN, Mayeux R, St George-Hyslop P, Pericak-Vance MA. *SORL1* mutations in early- and late-onset Alzheimer disease. Neurol Genet. 2016 Oct 26;2(6):e116. doi: 10.1212/NXG.0000000000000116. PMID: 27822510; PMCID: PMC5082932.

Cukierman T, Gerstein HC, Williamson JD. Cognitive decline and dementia in diabetes--systematic overview of prospective observational studies. Diabetologia. 2005 Dec;48(12):2460-9. doi: 10.1007/s00125-005-0023-4. Epub 2005 Nov 8. PMID: 16283246

Cummings J. Anti-Amyloid Monoclonal Antibodies are Transformative Treatments that Redefine Alzheimer's Disease Therapeutics. Drugs. 2023 May;83(7):569-576. doi: 10.1007/s40265-023-01858-9. Epub 2023 Apr 15. PMID: 37060386; PMCID: PMC10195708.

Cummings JL. Alzheimer's disease. N Engl J Med. 2004 Jul 1;351(1):56-67. doi: 10.1056/NEJMra040223. PMID: 15229308.

Cunha SA, Borges S, Baptista-Silva S, Ribeiro T, Oliveira-Silva P, Pintado M, Batista P. Astaxanthin impact on brain: health potential and market perspective. Crit Rev

Food Sci Nutr. 2023 Jul 7:1-24. doi: 10.1080/10408398.2023.2232866. Epub ahead of print. PMID: 37417323.

Cynis H, Scheel E, Saido TC, Schilling S, Demuth HU. Amyloidogenic processing of amyloid precursor protein: evidence of a pivotal role of glutaminyl cyclase in generation of pyroglutamate-modified amyloid-beta. Biochemistry. 2008 Jul 15;47(28):7405-13. doi: 10.1021/bi800250p. Epub 2008 Jun 21. PMID: 18570439.

Cynis H, Schilling S, Bodnár M, Hoffmann T, Heiser U, Saido TC, Demuth HU. Inhibition of glutaminyl cyclase alters pyroglutamate formation in mammalian cells. Biochim Biophys Acta. 2006 Oct;1764(10):1618-25. doi: 10.1016/j.bbapap.2006.08.003. Epub 2006 Aug 16. PMID: 17005457.

Dalfrà MG, Burlina S, Del Vescovo GG, Lapolla A. Genetics and Epigenetics: New Insight on Gestational Diabetes Mellitus. Front Endocrinol (Lausanne). 2020 Dec 1; 11:602477. doi: 10.3389/fendo.2020.602477. PMID: 33335512; PMCID: PMC7736606.

Dam T, Boxer AL, Golbe LI, Höglinger GU, Morris HR, Litvan I, Lang AE, Corvol JC, Aiba I, Grundman M, Yang L, Tidemann-Miller B, Kupferman J, Harper K, Kamisoglu K, Wald MJ, Graham DL, Gedney L, O'Gorman J, Haeberlein SB; PASSPORT Study Group. Safety and efficacy of anti-tau monoclonal antibody gosuranemab in progressive supranuclear palsy: a phase 2, randomized, placebo-controlled trial. Nat Med. 2021 Aug;27(8):1451-1457. doi: 10.1038/s41591-021-01455-x. Epub 2021 Aug 12. Erratum in: Nat Med. 2022 Oct 17; PMID: 34385707.

Daneman R, Prat A. The blood-brain barrier. Cold Spring Harb Perspect Biol. 2015 Jan 5;7(1): a020412. doi: 10.1101/cshperspect. a020412. PMID: 25561720; PMCID: PMC4292164.

Daneman R, Zhou L, Kebede AA, Barres BA. Pericytes are required for blood-brain barrier integrity during embryogenesis. Nature. 2010 Nov 25;468(7323):562-6. doi: 10.1038/nature09513. Epub 2010 Oct 13. PMID: 20944625; PMCID: PMC3241506.

D'Arrigo C, Tabaton M, Perico A. N-terminal truncated pyroglutamyl beta amyloid peptide Abetapy3-42 shows a faster aggregation kinetics than the full-length Abeta1-42. Biopolymers. 2009 Oct;91(10):861-73. doi: 10.1002/bip.21271. PMID: 19562755.

de Boer AG, van der Sandt IC, Gaillard PJ. The role of drug transporters at the blood-brain barrier. Annu Rev Pharmacol Toxicol. 2003; 43:629-56. doi: 10.1146/annurev.pharmtox.43.100901.140204. Epub 2002 Jan 10. PMID: 12415123.

De Felice FG. Alzheimer's disease and insulin resistance: translating basic science into clinical applications. J Clin Invest. 2013 Feb;123(2):531-9. doi: 10.1172/JCI64595. Epub 2013 Feb 1. PMID: 23485579; PMCID: PMC3561831.

de Heus RAA, Olde Rikkert MGM, Tully PJ, Lawlor BA, Claassen JAHR; NILVAD Study Group. Blood Pressure Variability and Progression of Clinical Alzheimer Disease. Hypertension. 2019 Nov;74(5):1172-1180. doi: 10.1161/HYPERTENSIONAHA.119.13664. Epub 2019 Sep 23. PMID: 31542965.

de la Cueva M, Antequera D, Ordoñez-Gutierrez L, Wandosell F, Camins A, Carro E, Bartolome F. Amyloid-β impairs mitochondrial dynamics and autophagy in Alzheimer's disease experimental models. Sci Rep. 2022 Jun 16;12(1):10092. doi: 10.1038/s41598-022-13683-3. Erratum in: Sci Rep. 2023 Nov 7;13(1):19303. PMID: 35710783; PMCID: PMC9203760.

de la Monte SM. Relationships between diabetes and cognitive impairment. Endocrinol Metab Clin North Am. 2014 Mar;43(1):245-67. doi: 10.1016/j.ecl.2013.09.006. Epub 2013 Dec 12. PMID: 24582101; PMCID: PMC4978517.

de la Monte SM. The Full Spectrum of Alzheimer's Disease Is Rooted in Metabolic Derangements That Drive Type 3 Diabetes. Adv Exp Med Biol. 2019; 1128:45-83. doi: 10.1007/978-981-13-3540-2_4. PMID: 31062325; PMCID: PMC9996398.

de la Torre JC. Vascular risk factor detection and control may prevent Alzheimer's disease. Ageing Res Rev. 2010 Jul;9(3):218-25. doi: 10.1016/j.arr.2010.04.002. Epub 2010 Apr 10. PMID: 20385255

De Souza EB. Corticotropin-releasing factor receptors: physiology, pharmacology, biochemistry and role in central nervous system and immune disorders. Psychoneuroendocrinology. 1995;20(8):789-819. doi: 10.1016/0306-4530(95)00011-9. PMID: 8834089.

Deane R, Singh I, Sagare AP, Bell RD, Ross NT, LaRue B, Love R, Perry S, Paquette N, Deane RJ, Thiyagarajan M, Zarcone T, Fritz G, Friedman AE, Miller BL,

Zlokovic BV. A multimodal RAGE-specific inhibitor reduces amyloid β-mediated brain disorder in a mouse model of Alzheimer disease. J Clin Invest. 2012 Apr;122(4):1377-92. doi: 10.1172/JCI58642. Epub 2012 Mar 12. PMID: 22406537; PMCID: PMC3314449.

Deane R, Wu Z, Sagare A, Davis J, Du Yan S, Hamm K, Xu F, Parisi M, LaRue B, Hu HW, Spijkers P, Guo H, Song X, Lenting PJ, Van Nostrand WE, Zlokovic BV. LRP/amyloid beta-peptide interaction mediates differential brain efflux of Abeta isoforms. Neuron. 2004 Aug 5;43(3):333-44. doi: 10.1016/j.neuron.2004.07.017. PMID: 15294142.

Delbridge ARD, Huh D, Brickelmaier M, Burns JC, Roberts C, Challa R, Raymond N, Cullen P, Carlile TM, Ennis KA, Liu M, Sun C, Allaire NE, Foos M, Tsai HH, Franchimont N, Ransohoff RM, Butts C, Mingueneau M. Organotypic Brain Slice Culture Microglia Exhibit Molecular Similarity to Acutely Isolated Adult Microglia and Provide a Platform to Study Neuroinflammation. Front Cell Neurosci. 2020 Dec 21;14: 592005. doi: 10.3389/fncel.2020.592005. PMID: 33473245; PMCID: PMC7812919.

Deplanque D, Gelé P, Pétrault O, Six I, Furman C, Bouly M, Nion S, Dupuis B, Leys D, Fruchart JC, Cecchelli R, Staels B, Duriez P, Bordet R. Peroxisome proliferator-activated receptor-alpha activation as a mechanism of preventive neuroprotection induced by chronic fenofibrate treatment. J Neurosci. 2003 Jul 16;23(15):6264-71. doi: 10.1523/JNEUROSCI.23-15-06264.2003. PMID: 12867511; PMCID: PMC6740545.

Di Battista AM, Heinsinger NM, Rebeck GW. Alzheimer's Disease Genetic Risk Factor APOE-ε4 Also Affects Normal Brain Function. Curr Alzheimer Res. 2016;13(11):1200-1207. doi: 10.2174/1567205013666160401115127. PMID: 27033053; PMCID: PMC5839141.

Di Domenico F, Perluigi M, Butterfield DA, Cornelius C, Calabrese V. Oxidative damage in rat brain during aging: interplay between energy and metabolic key target proteins. Neurochem Res. 2010 Dec;35(12):2184-92. doi: 10.1007/s11064-010-0295-z. Epub 2010 Oct 21. PMID: 20963486.

Dina Dakkak, Saskia Pollack, Tong Guo et al. Truncated tau disrupts autophagy and lysosomal biogenesis, 11 April 2022, PREPRINT (Version 1) available at Research Square [https://doi.org/10.21203/rs.3.rs-1522321/v1]

Dirkx R Jr, Solimena M. Cholesterol-enriched membrane rafts and insulin secretion. J Diabetes Investig. 2012 Aug 20;3(4):339-46. doi: 10.1111/j.2040-1124.2012.00200.x. PMID: 24843586; PMCID: PMC4019251.

Donahue JE, Flaherty SL, Johanson CE, Duncan JA 3rd, Silverberg GD, Miller MC, Tavares R, Yang W, Wu Q, Sabo E, Hovanesian V, Stopa EG. RAGE, LRP1, and amyloid-beta protein in Alzheimer's disease. Acta Neuropathol. 2006 Oct;112(4):405-15. doi: 10.1007/s00401-006-0115-3. Epub 2006 Jul 25. PMID: 16865397.

Dong J, Atwood CS, Anderson VE, Siedlak SL, Smith MA, Perry G, Carey PR. Metal binding and oxidation of amyloid-beta within isolated senile plaque cores: Raman microscopic evidence. Biochemistry. 2003 Mar 18;42(10):2768-73. doi: 10.1021/bi0272151. PMID: 12627941.

Dorrier CE, Jones HE, Pintarić L, Siegenthaler JA, Daneman R. Emerging roles for CNS fibroblasts in health, injury and disease. Nat Rev Neurosci. 2022 Jan;23(1):23-34. doi: 10.1038/s41583-021-00525-w. Epub 2021 Oct 20. PMID: 34671105; PMCID: PMC8527980.

Dubois B, Hampel H, Feldman HH, Scheltens P, Aisen P, Andrieu S, Bakardjian H, Benali H, Bertram L, Blennow K, Broich K, Cavedo E, Crutch S, Dartigues JF, Duyckaerts C, Epelbaum S, Frisoni GB, Gauthier S, Genthon R, Gouw AA, Habert MO, Holtzman DM, Kivipelto M, Lista S, Molinuevo JL, O'Bryant SE, Rabinovici GD, Rowe C, Salloway S, Schneider LS, Sperling R, Teichmann M, Carrillo MC, Cummings J, Jack CR Jr; Proceedings of the Meeting of the International Working Group (IWG) and the American Alzheimer's Association on “The Preclinical State of AD”; July 23, 2015; Washington DC, USA. Preclinical Alzheimer's disease: Definition, natural history, and diagnostic criteria. Alzheimers Dement. 2016 Mar;12(3):292-323. doi: 10.1016/j.jalz.2016.02.002. PMID: 27012484; PMCID: PMC6417794.

Dumitrescu L, Barnes LL, Thambisetty M, Beecham G, Kunkle B, Bush WS, Gifford KA, Chibnik LB, Mukherjee S, De Jager PL, Kukull W, Crane PK, Resnick SM, Keene CD, Montine TJ, Schellenberg GD, Deming Y, Chao MJ, Huentelman M, Martin ER, Hamilton-Nelson K, Shaw LM, Trojanowski JQ, Peskind ER, Cruchaga C, Pericak-

Vance MA, Goate AM, Cox NJ, Haines JL, Zetterberg H, Blennow K, Larson EB, Johnson SC, Albert M; Alzheimer's Disease Genetics Consortium and the Alzheimer's Disease Neuroimaging Initiative; Bennett DA, Schneider JA, Jefferson AL, Hohman TJ. Sex differences in the genetic predictors of Alzheimer's pathology. Brain. 2019 Sep 1;142(9):2581-2589. doi: 10.1093/brain/awz206. PMID: 31497858; PMCID: PMC6736148.

Dzamba D, Harantova L, Butenko O, Anderova M. Glial Cells - The Key Elements of Alzheimer´s Disease. Curr Alzheimer Res. 2016;13(8):894-911. doi: 10.2174/1567205013666160129095924. PMID: 26825092.

ElAli A, Hermann DM. ATP-binding cassette transporters and their roles in protecting the brain. Neuroscientist. 2011 Aug;17(4):423-36. doi: 10.1177/1073858410391270. Epub 2011 Apr 25. PMID: 21518814.

Engelhardt B, Vajkoczy P, Weller RO. The movers and shapers in immune privilege of the CNS. Nat Immunol. 2017 Feb;18(2):123-131. doi: 10.1038/ni.3666. Epub 2017 Jan 16. PMID: 28092374.

Erickson MA, Banks WA. Neuroimmune Axes of the Blood-Brain Barriers and Blood-Brain Interfaces: Bases for Physiological Regulation, Disease States, and Pharmacological Interventions. Pharmacol Rev. 2018 Apr;70(2):278-314. doi: 10.1124/pr.117.014647. PMID: 29496890; PMCID: PMC5833009.

Estall JL, Kahn M, Cooper MP, Fisher FM, Wu MK, Laznik D, Qu L, Cohen DE, Shulman GI, Spiegelman BM. Sensitivity of lipid metabolism and insulin signaling to genetic alterations in hepatic peroxisome proliferator-activated receptor-gamma coactivator-1alpha expression. Diabetes. 2009 Jul;58(7):1499-508. doi: 10.2337/db08-1571. Epub 2009 Apr 14. PMID: 19366863; PMCID: PMC2699879.

Ettcheto M, Petrov D, Pedrós I, Alva N, Carbonell T, Beas-Zarate C, Pallas M, Auladell C, Folch J, Camins A. Evaluation of Neuropathological Effects of a High-Fat Diet in a Presymptomatic Alzheimer's Disease Stage in APP/PS1 Mice. J Alzheimers Dis. 2016 Jul 14;54(1):233-51. doi: 10.3233/JAD-160150. PMID: 27567882.

Evrard C, Kienlen-Campard P, Coevoet M, Opsomer R, Tasiaux B, Melnyk P, Octave JN, Buée L, Sergeant N, Vingtdeux V. Contribution of the Endosomal-Lysosomal and Proteasomal Systems in Amyloid-β Precursor Protein Derived Fragments

Processing. Front Cell Neurosci. 2018 Nov 22; 12:435. doi: 10.3389/fncel.2018.00435. PMID: 30524243; PMCID: PMC6263093.

Faber OK, Hagen C, Binder C, Markussen J, Naithani VK, Blix PM, Kuzuya H, Horwitz DL, Rubenstein AH, Rossing N. Kinetics of human connecting peptide in normal and diabetic subjects. J Clin Invest. 1978 Jul;62(1):197-203. doi: 10.1172/JCI109106. PMID: 659633; PMCID: PMC371754.

Fabian H, Szendrei GI, Mantsch HH, Greenberg BD, Otvös L Jr. Synthetic post-translationally modified human A beta peptide exhibits a markedly increased tendency to form beta-pleated sheets in vitro. Eur J Biochem. 1994 May 1;221(3):959-64. doi: 10.1111/j.1432-1033. 1994.tb18811. x. PMID: 8181478.

Fakhri S, Abbaszadeh F, Dargahi L, Jorjani M. Astaxanthin: A mechanistic review on its biological activities and health benefits. Pharmacol Res. 2018 Oct; 136:1-20. doi: 10.1016/j.phrs.2018.08.012. Epub 2018 Aug 17. PMID: 30121358.

Fakhri S, Aneva IY, Farzaei MH, Sobarzo-Sánchez E. The Neuroprotective Effects of Astaxanthin: Therapeutic Targets and Clinical Perspective. Molecules. 2019 Jul 20;24(14):2640. doi: 10.3390/molecules24142640. PMID: 31330843; PMCID: PMC6680436.

Fang F, Yu Q, Arancio O, Chen D, Gore SS, Yan SS, Yan SF. RAGE mediates Aβ accumulation in a mouse model of Alzheimer's disease via modulation of β- and γ-secretase activity. Hum Mol Genet. 2018 Mar 15;27(6):1002-1014. doi: 10.1093/hmg/ddy017. PMID: 29329433; PMCID: PMC6075512

Farrer LA, Cupples LA, Haines JL, Hyman B, Kukull WA, Mayeux R, Myers RH, Pericak-Vance MA, Risch N, van Duijn CM. Effects of age, sex, and ethnicity on the association between apolipoprotein E genotype and Alzheimer disease. A meta-analysis. APOE and Alzheimer Disease Meta Analysis Consortium. JAMA. 1997 Oct 22-29;278(16):1349-56. PMID: 9343467.

Feng T, Tammineni P, Agrawal C, Jeong YY, Cai Q. Autophagy-mediated Regulation of BACE1 Protein Trafficking and Degradation. J Biol Chem. 2017 Feb 3;292(5):1679-1690. doi: 10.1074/jbc.M116.766584. Epub 2016 Dec 27. PMID: 28028177; PMCID: PMC5290944.

Ferrannini E, Wahren J, Faber OK, Felig P, Binder C, DeFronzo RA. Splanchnic and renal metabolism of insulin in human subjects: a dose-response study. Am J Physiol. 1983 Jun;244(6): E517-27. doi: 10.1152/ajpendo.1983.244.6. E517. PMID: 6344651.

Ferretti MT, Iulita MF, Cavedo E, Chiesa PA, Schumacher Dimech A, Santuccione Chadha A, Baracchi F, Girouard H, Misoch S, Giacobini E, Depypere H, Hampel H; Women's Brain Project and the Alzheimer Precision Medicine Initiative. Sex differences in Alzheimer disease - the gateway to precision medicine. Nat Rev Neurol. 2018 Aug;14(8):457-469. doi: 10.1038/s41582-018-0032-9. PMID: 29985474.

Figlewicz DP. Insulin, food intake, and reward. Semin Clin Neuropsychiatry. 2003 Apr;8(2):82-93. doi: 10.1053/scnp.2003.50012. PMID: 12728408.

Fillit H, Nash DT, Rundek T, Zuckerman A. Cardiovascular risk factors and dementia. Am J Geriatr Pharmacother. 2008 Jun;6(2):100-18. doi: 10.1016/j.amjopharm.2008.06.004. PMID: 18675769.

Finck BN, Kelly DP. PGC-1 coactivators: inducible regulators of energy metabolism in health and disease. J Clin Invest. 2006 Mar;116(3):615-22. doi: 10.1172/JCI27794. PMID: 16511594; PMCID: PMC1386111.

Fishel MA, Watson GS, Montine TJ, Wang Q, Green PS, Kulstad JJ, Cook DG, Peskind ER, Baker LD, Goldgaber D, Nie W, Asthana S, Plymate SR, Schwartz MW, Craft S. Hyperinsulinemia provokes synchronous increases in central inflammation and beta-amyloid in normal adults. Arch Neurol. 2005 Oct;62(10):1539-44. doi: 10.1001/archneur.62.10. noc50112. PMID: 16216936.

Fisher DW, Bennett DA, Dong H. Sexual dimorphism in predisposition to Alzheimer's disease. Neurobiol Aging. 2018 Oct; 70:308-324. doi: 10.1016/j.neurobiolaging.2018.04.004. Epub 2018 Apr 17. PMID: 29754747; PMCID: PMC6368179.

Fisher FM, Chui PC, Antonellis PJ, Bina HA, Kharitonenkov A, Flier JS, Maratos-Flier E. Obesity is a fibroblast growth factor 21 (FGF21)-resistant state. Diabetes. 2010 Nov;59(11):2781-9. doi: 10.2337/db10-0193. Epub 2010 Aug 3. PMID: 20682689; PMCID: PMC2963536.

Fisher FM, Chui PC, Nasser IA, Popov Y, Cunniff JC, Lundasen T, Kharitonenkov A, Schuppan D, Flier JS, Maratos-Flier E. Fibroblast growth factor 21 limits lipotoxicity

by promoting hepatic fatty acid activation in mice on methionine and choline-deficient diets. Gastroenterology. 2014 Nov;147(5):1073-83. e 6. doi: 10.1053/j.gastro.2014.07.044. Epub 2014 Jul 30. PMID: 25083607; PMCID: PMC4570569.

Fitz NF, Cronican A, Pham T, Fogg A, Fauq AH, Chapman R, Lefterov I, Koldamova R. Liver X receptor agonist treatment ameliorates amyloid pathology and memory deficits caused by high-fat diet in APP23 mice. J Neurosci. 2010 May 19;30(20):6862-72. doi: 10.1523/JNEUROSCI.1051-10.2010. PMID: 20484628; PMCID: PMC2883862.

Fitzpatrick AL, Kuller LH, Ives DG, Lopez OL, Jagust W, Breitner JC, Jones B, Lyketsos C, Dulberg C. Incidence and prevalence of dementia in the Cardiovascular Health Study. J Am Geriatr Soc. 2004 Feb;52(2):195-204. doi: 10.1111/j.1532-5415.2004.52058. x. PMID: 14728627.

FitzPatrick LM, Hawkins KE, Delhove JMKM, Fernandez E, Soldati C, Bullen LF, Nohturfft A, Waddington SN, Medina DL, Bolaños JP, McKay TR. NF-κB Activity Initiates Human ESC-Derived Neural Progenitor Cell Differentiation by Inducing a Metabolic Maturation Program. Stem Cell Reports. 2018 Jun 5;10(6):1766-1781. doi: 10.1016/j.stemcr.2018.03.015. Epub 2018 Apr 19. PMID: 29681545; PMCID: PMC5989595.

Fonseca AC, Ferreiro E, Oliveira CR, Cardoso SM, Pereira CF. Activation of the endoplasmic reticulum stress response by the amyloid-beta 1-40 peptide in brain endothelial cells. Biochim Biophys Acta. 2013 Dec;1832(12):2191-203. doi: 10.1016/j.bbadis.2013.08.007. Epub 2013 Aug 28. PMID: 23994613.

Francis PT, Palmer AM, Snape M, Wilcock GK. The cholinergic hypothesis of Alzheimer's disease: a review of progress. J Neurol Neurosurg Psychiatry. 1999 Feb;66(2):137-47. doi: 10.1136/jnnp.66.2.137. PMID: 10071091; PMCID: PMC1736202.

Franke H, Galla H, Beuckmann CT. Primary cultures of brain microvessel endothelial cells: a valid and flexible model to study drug transport through the blood-brain barrier *in vitro*. Brain Res Brain Res Protoc. 2000 Jul;5(3):248-56. doi: 10.1016/s1385-299x (00)00020-9. PMID: 10906490.

Freiherr J, Hallschmid M, Frey WH 2nd, Brünner YF, Chapman CD, Hölscher C, Craft S, De Felice FG, Benedict C. Intranasal insulin as a treatment for Alzheimer's disease: a review of basic research and clinical evidence. CNS Drugs. 2013 Jul;27(7):505-14. doi: 10.1007/s40263-013-0076-8. PMID: 23719722; PMCID: PMC3709085.

Friedman BA, Srinivasan K, Ayalon G, Meilandt WJ, Lin H, Huntley MA, Cao Y, Lee SH, Haddick PCG, Ngu H, Modrusan Z, Larson JL, Kaminker JS, van der Brug MP, Hansen DV. Diverse Brain Myeloid Expression Profiles Reveal Distinct Microglial Activation States and Aspects of Alzheimer's Disease Not Evident in Mouse Models. Cell Rep. 2018 Jan 16;22(3):832-847. doi: 10.1016/j.celrep.2017.12.066. PMID: 29346778.

Fruchart JC, Duriez P, Staels B. Peroxisome proliferator-activated receptor-alpha activators regulate genes governing lipoprotein metabolism, vascular inflammation and atherosclerosis. Curr Opin Lipidol. 1999 Jun;10(3):245-57. doi: 10.1097/00041433-199906000-00007. PMID: 10431661.

Fukuchi K, Hart M, Yan Z, Hassell JR, Li L. Transgenic mice overexpressing both amyloid beta-protein and perlecan in pancreatic acinar cells. Histol Histopathol. 2004 Jul;19(3):845-52. doi: 10.14670/HH-19.845. PMID: 15168347.

Galasso C, Orefice I, Pellone P, Cirino P, Miele R, Ianora A, Brunet C, Sansone C. On the Neuroprotective Role of Astaxanthin: New Perspectives? Mar Drugs. 2018 Jul 24;16(8):247. doi: 10.3390/md16080247. PMID: 30042358; PMCID: PMC6117702.

Gali CC, Fanaee-Danesh E, Zandl-Lang M, Albrecher NM, Tam-Amersdorfer C, Stracke A, Sachdev V, Reichmann F, Sun Y, Avdili A, Reiter M, Kratky D, Holzer P, Lass A, Kandimalla KK, Panzenboeck U. Amyloid-beta impairs insulin signaling by accelerating autophagy-lysosomal degradation of LRP1 and IR-β in blood-brain barrier endothelial cells in vitro and in 3XTg-AD mice. Mol Cell Neurosci. 2019 Sep; 99:103390. doi: 10.1016/j.mcn.2019.103390. Epub 2019 Jul 2. PMID: 31276749; PMCID: PMC6897558.

Gallart-Palau X, Lee BS, Adav SS, Qian J, Serra A, Park JE, Lai MK, Chen CP, Kalaria RN, Sze SK. Gender differences in white matter pathology and mitochondrial dysfunction in Alzheimer's disease with cerebrovascular disease. Mol Brain. 2016

Mar 17; 9:27. doi: 10.1186/s13041-016-0205-7. PMID: 26983404; PMCID: PMC4794845.

Ganguli M, Dodge HH, Shen C, Pandav RS, DeKosky ST. Alzheimer disease and mortality: a 15-year epidemiological study. Arch Neurol. 2005 May;62(5):779-84. doi: 10.1001/archneur.62.5.779. PMID: 15883266.

Gao Y, Yan Y, Fang Q, Zhang N, Kumar G, Zhang J, Song LJ, Yu J, Zhao L, Zhang HT, Ma CG. The Rho kinase inhibitor fasudil attenuates $A\beta_{1-42}$-induced apoptosis via the ASK1/JNK signal pathway in primary cultures of hippocampal neurons. Metab Brain Dis. 2019 Dec;34(6):1787-1801. doi: 10.1007/s11011-019-00487-0. Epub 2019 Sep 3. PMID: 31482248.

García-Fernández P, Üçeyler N, Sommer C. From the low-density lipoprotein receptor-related protein 1 to neuropathic pain: a potentially novel target. Pain Rep. 2021 Mar 9;6(1):e898. doi: 10.1097/PR9.0000000000000898. PMID: 33981930; PMCID: PMC8108589.

GBD 2021 Diabetes Collaborators. Global, regional, and national burden of diabetes from 1990 to 2021, with projections of prevalence to 2050: a systematic analysis for the Global Burden of Disease Study 2021. Lancet. 2023 Jul 15;402(10397):203-234. doi: 10.1016/S0140-6736(23)01301-6. Epub 2023 Jun 22. PMID: 37356446; PMCID: PMC10364581.

Ghasemi R, Haeri A, Dargahi L, Mohamed Z, Ahmadiani A. Insulin in the brain: sources, localization and functions. Mol Neurobiol. 2013 Feb;47(1):145-71. doi: 10.1007/s12035-012-8339-9. Epub 2012 Sep 7. PMID: 22956272.

Ghiso J, Shayo M, Calero M, Ng D, Tomidokoro Y, Gandy S, Rostagno A, Frangione B. Systemic catabolism of Alzheimer's Abeta40 and Abeta42. J Biol Chem. 2004 Oct 29;279(44):45897-908. doi: 10.1074/jbc.M407668200. Epub 2004 Aug 20. PMID: 15322125.

Ghosh A, Pahan K. PPARα in lysosomal biogenesis: A perspective. Pharmacol Res. 2016 Jan; 103:144-8. doi: 10.1016/j.phrs.2015.11.011. Epub 2015 Nov 24. PMID: 26621249; PMCID: PMC4861553.

Giannakopoulos P, Herrmann FR, Bussière T, Bouras C, Kövari E, Perl DP, Morrison JH, Gold G, Hof PR. Tangle and neuron numbers, but not amyloid load, predict

cognitive status in Alzheimer's disease. Neurology. 2003 May 13;60(9):1495-500. doi: 10.1212/01.wnl.0000063311.58879.01. PMID: 12743238.

Giannini EG, Testa R, Savarino V. Liver enzyme alteration: a guide for clinicians. CMAJ. 2005 Feb 1;172(3):367-79. doi: 10.1503/cmaj.1040752. PMID: 15684121; PMCID: PMC545762.

Glenner GG, Wong CW. Alzheimer's disease: initial report of the purification and characterization of a novel cerebrovascular amyloid protein. Biochem Biophys Res Commun. 1984 May 16;120(3):885-90. doi: 10.1016/s0006-291x (84)80190-4. PMID: 6375662.

Goldstein BJ. Insulin resistance as the core defect in type 2 diabetes mellitus. Am J Cardiol. 2002 Sep 5;90(5A):3G-10G. doi: 10.1016/s0002-9149(02)02553-5. PMID: 12231073.

Gómez-Isla T, Price JL, McKeel DW Jr, Morris JC, Growdon JH, Hyman BT. Profound loss of layer II entorhinal cortex neurons occurs in very mild Alzheimer's disease. J Neurosci. 1996 Jul 15;16(14):4491-500. doi: 10.1523/JNEUROSCI.16-14-04491.1996. PMID: 8699259; PMCID: PMC6578866.

Gonçalves NP, Vægter CB, Andersen H, Østergaard L, Calcutt NA, Jensen TS. Schwann cell interactions with axons and microvessels in diabetic neuropathy. Nat Rev Neurol. 2017 Mar;13(3):135-147. doi: 10.1038/nrneurol.2016.201. Epub 2017 Jan 30. PMID: 28134254; PMCID: PMC7391875.

Gonias SL, Campana WM. LDL receptor-related protein-1: a regulator of inflammation in atherosclerosis, cancer, and injury to the nervous system. Am J Pathol. 2014 Jan;184(1):18-27. doi: 10.1016/j.ajpath.2013.08.029. Epub 2013 Oct 12. PMID: 24128688; PMCID: PMC3873482.

Gordon BA, Blazey TM, Su Y, Hari-Raj A, Dincer A, Flores S, Christensen J, McDade E, Wang G, Xiong C, Cairns NJ, Hassenstab J, Marcus DS, Fagan AM, Jack CR Jr, Hornbeck RC, Paumier KL, Ances BM, Berman SB, Brickman AM, Cash DM, Chhatwal JP, Correia S, Förster S, Fox NC, Graff-Radford NR, la Fougère C, Levin J, Masters CL, Rossor MN, Salloway S, Saykin AJ, Schofield PR, Thompson PM, Weiner MM, Holtzman DM, Raichle ME, Morris JC, Bateman RJ, Benzinger TLS. Spatial patterns of neuroimaging biomarker change in individuals from families with

autosomal dominant Alzheimer's disease: a longitudinal study. Lancet Neurol. 2018 Mar;17(3):241-250. doi: 10.1016/S1474-4422(18)30028-0. Epub 2018 Feb 1. PMID: 29397305; PMCID: PMC5816717.

Goyal R, Singhal M, Jialal I. Type 2 Diabetes. [Updated 2023 Jun 23]. In: StatPearls [Internet]. Treasure Island (FL): StatPearls Publishing; 2023 Jan-. Available from: https://www.ncbi.nlm.nih.gov/books/NBK513253/

Gratuze M, Julien J, Petry FR, Morin F, Planel E. Insulin deprivation induces PP2A inhibition and tau hyperphosphorylation in hTau mice, a model of Alzheimer's disease-like tau pathology. Sci Rep. 2017 Apr 12; 7:46359. doi: 10.1038/srep46359. PMID: 28402338; PMCID: PMC5389355.

Graves SI, Baker DJ. Implicating endothelial cell senescence to dysfunction in the ageing and diseased brain. Basic Clin Pharmacol Toxicol. 2020 Aug;127(2):102-110. doi: 10.1111/bcpt.13403. Epub 2020 Mar 23. PMID: 32162446; PMCID: PMC7384943.

Griffin WS, Stanley LC, Ling C, White L, MacLeod V, Perrot LJ, White CL 3rd, Araoz C. Brain interleukin 1 and S-100 immunoreactivity are elevated in Down syndrome and Alzheimer disease. Proc Natl Acad Sci U S A. 1989 Oct;86(19):7611-5. doi: 10.1073/pnas.86.19.7611. PMID: 2529544; PMCID: PMC298116.

Grillo CA, Piroli GG, Hendry RM, Reagan LP. Insulin-stimulated translocation of GLUT4 to the plasma membrane in rat hippocampus is PI3-kinase dependent. Brain Res. 2009 Nov 3; 1296:35-45. doi: 10.1016/j.brainres.2009.08.005. Epub 2009 Aug 11. PMID: 19679110; PMCID: PMC2997526.

Grodstein F, Chen J, Wilson RS, Manson JE; Nurses' Health Study. Type 2 diabetes and cognitive function in community-dwelling elderly women. Diabetes Care. 2001 Jun;24(6):1060-5. doi: 10.2337/diacare.24.6.1060. PMID: 11375371

Guerreiro R, Wojtas A, Bras J, Carrasquillo M, Rogaeva E, Majounie E, Cruchaga C, Sassi C, Kauwe JS, Younkin S, Hazrati L, Collinge J, Pocock J, Lashley T, Williams J, Lambert JC, Amouyel P, Goate A, Rademakers R, Morgan K, Powell J, St George-Hyslop P, Singleton A, Hardy J; Alzheimer Genetic Analysis Group. TREM2 variants in Alzheimer's disease. N Engl J Med. 2013 Jan 10;368(2):117-27. doi:

10.1056/NEJMoa1211851. Epub 2012 Nov 14. PMID: 23150934; PMCID: PMC3631573.

Güntert A, Döbeli H, Bohrmann B. High sensitivity analysis of amyloid-beta peptide composition in amyloid deposits from human and PS2APP mouse brain. Neuroscience. 2006 Dec 1;143(2):461-75. doi: 10.1016/j.neuroscience.2006.08.027. Epub 2006 Sep 27. PMID: 17008022.

Gür E, Fertan E, Kosel F, Wong AA, Balcı F, Brown RE. Sex differences in the timing behavior performance of 3xTg-AD and wild-type mice in the peak interval procedure. Behav Brain Res. 2019 Mar 15; 360:235-243. doi: 10.1016/j.bbr.2018.11.047. Epub 2018 Nov 30. PMID: 30508608.

Haass C. Take five--BACE and the gamma-secretase quartet conduct Alzheimer's amyloid beta-peptide generation. EMBO J. 2004 Feb 11;23(3):483-8. doi: 10.1038/sj.emboj.7600061. Epub 2004 Jan 29. PMID: 14749724; PMCID: PMC1271800.

Halder SK, Sapkota A, Milner R. The impact of genetic manipulation of laminin and integrins at the blood-brain barrier. Fluids Barriers CNS. 2022 Jun 11;19(1):50. doi: 10.1186/s12987-022-00346-8. PMID: 35690759; PMCID: PMC9188059.

Hale C, Chen MM, Stanislaus S, Chinookoswong N, Hager T, Wang M, Véniant MM, Xu J. Lack of overt FGF21 resistance in two mouse models of obesity and insulin resistance. Endocrinology. 2012 Jan;153(1):69-80. doi: 10.1210/en.2010-1262. Epub 2011 Nov 8. PMID: 22067317.

Hampel H, Hardy J, Blennow K, Chen C, Perry G, Kim SH, Villemagne VL, Aisen P, Vendruscolo M, Iwatsubo T, Masters CL, Cho M, Lannfelt L, Cummings JL, Vergallo A. The Amyloid-β Pathway in Alzheimer's Disease. Mol Psychiatry. 2021 Oct;26(10):5481-5503. doi: 10.1038/s41380-021-01249-0. Epub 2021 Aug 30. PMID: 34456336; PMCID: PMC8758495.

Handschin C, Choi CS, Chin S, Kim S, Kawamori D, Kurpad AJ, Neubauer N, Hu J, Mootha VK, Kim YB, Kulkarni RN, Shulman GI, Spiegelman BM. Abnormal glucose homeostasis in skeletal muscle-specific PGC-1alpha knockout mice reveals skeletal muscle-pancreatic beta cell crosstalk. J Clin Invest. 2007 Nov;117(11):3463-74. doi: 10.1172/JCI31785. PMID: 17932564; PMCID: PMC2000810.

Hanley AJ, Williams K, Festa A, Wagenknecht LE, D'Agostino RB Jr, Kempf J, Zinman B, Haffner SM; insulin resistance atherosclerosis study. Elevations in markers of liver injury and risk of type 2 diabetes: the insulin resistance atherosclerosis study. Diabetes. 2004 Oct;53(10):2623-32. doi: 10.2337/diabetes.53.10.2623. PMID: 15448093.

Hao M, Head WS, Gunawardana SC, Hasty AH, Piston DW. Direct effect of cholesterol on insulin secretion: a novel mechanism for pancreatic beta-cell dysfunction. Diabetes. 2007 Sep;56(9):2328-38. doi: 10.2337/db07-0056. Epub 2007 Jun 15. PMID: 17575085.

Harano Y, Yasui K, Toyama T, Nakajima T, Mitsuyoshi H, Mimani M, Hirasawa T, Itoh Y, Okanoue T. Fenofibrate, a peroxisome proliferator-activated receptor alpha agonist, reduces hepatic steatosis and lipid peroxidation in fatty liver Shionogi mice with hereditary fatty liver. Liver Int. 2006 Jun;26(5):613-20. doi: 10.1111/j.1478-3231.2006.01265. x. PMID: 16762007.

Hardy J, Selkoe DJ. The amyloid hypothesis of Alzheimer's disease: progress and problems on the road to therapeutics. Science. 2002 Jul 19;297(5580):353-6. doi: 10.1126/science.1072994. Erratum in: Science 2002 Sep 27;297(5590):2209. PMID: 12130773.

Hardy J, Selkoe DJ. The amyloid hypothesis of Alzheimer's disease: progress and problems on the road to therapeutics. Science. 2002 Jul 19;297(5580):353-6. doi: 10.1126/science.1072994. Erratum in: Science 2002 Sep 27;297(5590):2209. PMID: 12130773.

Härtig W, Goldhammer S, Bauer U, Wegner F, Wirths O, Bayer TA, Grosche J. Concomitant detection of beta-amyloid peptides with N-terminal truncation and different C-terminal endings in cortical plaques from cases with Alzheimer's disease, senile monkeys and triple transgenic mice. J Chem Neuroanat. 2010 Sep;40(1):82-92. doi: 10.1016/j.jchemneu.2010.03.006. Epub 2010 Mar 25. PMID: 20347032.

Hartley D, Blumenthal T, Carrillo M, DiPaolo G, Esralew L, Gardiner K, Granholm AC, Iqbal K, Krams M, Lemere C, Lott I, Mobley W, Ness S, Nixon R, Potter H, Reeves R, Sabbagh M, Silverman W, Tycko B, Whitten M, Wisniewski T. Down syndrome and Alzheimer's disease: Common pathways, common goals. Alzheimers Dement. 2015

Jun;11(6):700-9. doi: 10.1016/j.jalz.2014.10.007. Epub 2014 Dec 12. PMID: 25510383; PMCID: PMC4817997.

Haruwaka K, Ikegami A, Tachibana Y, Ohno N, Konishi H, Hashimoto A, Matsumoto M, Kato D, Ono R, Kiyama H, Moorhouse AJ, Nabekura J, Wake H. Dual microglia effects on blood brain barrier permeability induced by systemic inflammation. Nat Commun. 2019 Dec 20;10(1):5816. doi: 10.1038/s41467-019-13812-z. PMID: 31862977; PMCID: PMC6925219.

He W, Barrow CJ. The A beta 3-pyroglutamyl and 11-pyroglutamyl peptides found in senile plaque have greater beta-sheet forming and aggregation propensities in vitro than full-length A beta. Biochemistry. 1999 Aug 17;38(33):10871-7. doi: 10.1021/bi990563r. PMID: 10451383.

Hebert LE, Scherr PA, McCann JJ, Beckett LA, Evans DA. Is the risk of developing Alzheimer's disease greater for women than for men? Am J Epidemiol. 2001 Jan 15;153(2):132-6. doi: 10.1093/aje/153.2.132. PMID: 11159157.

Heithoff BP, George KK, Phares AN, Zuidhoek IA, Munoz-Ballester C, Robel S. Astrocytes are necessary for blood-brain barrier maintenance in the adult mouse brain. Glia. 2021 Feb;69(2):436-472. doi: 10.1002/glia.23908. Epub 2020 Sep 21. PMID: 32955153; PMCID: PMC7736206.

Helzner EP, Scarmeas N, Cosentino S, Tang MX, Schupf N, Stern Y. Survival in Alzheimer disease: a multiethnic, population-based study of incident cases. Neurology. 2008 Nov 4;71(19):1489-95. doi: 10.1212/01.wnl.0000334278.11022.42. Erratum in: Neurology. 2009 Mar 3;72(9):861. PMID: 18981370; PMCID: PMC2843528.

Hendriks S, Peetoom K, Bakker C, van der Flier WM, Papma JM, Koopmans R, Verhey FRJ, de Vugt M, Köhler S; Young-Onset Dementia Epidemiology Study Group; Withall A, Parlevliet JL, Uysal-Bozkir Ö, Gibson RC, Neita SM, Nielsen TR, Salem LC, Nyberg J, Lopes MA, Dominguez JC, De Guzman MF, Egeberg A, Radford K, Broe T, Subramaniam M, Abdin E, Bruni AC, Di Lorenzo R, Smith K, Flicker L, Mol MO, Basta M, Yu D, Masika G, Petersen MS, Ruano L. Global Prevalence of Young-Onset Dementia: A Systematic Review and Meta-analysis. JAMA Neurol. 2021 Sep 1;78(9):1080-1090. doi: 10.1001/jamaneurol.2021.2161. PMID: 34279544; PMCID: PMC8290331.

Heneka MT, Carson MJ, El Khoury J, Landreth GE, Brosseron F, Feinstein DL, Jacobs AH, Wyss-Coray T, Vitorica J, Ransohoff RM, Herrup K, Frautschy SA, Finsen B, Brown GC, Verkhratsky A, Yamanaka K, Koistinaho J, Latz E, Halle A, Petzold GC, Town T, Morgan D, Shinohara ML, Perry VH, Holmes C, Bazan NG, Brooks DJ, Hunot S, Joseph B, Deigendesch N, Garaschuk O, Boddeke E, Dinarello CA, Breitner JC, Cole GM, Golenbock DT, Kummer MP. Neuroinflammation in Alzheimer's disease. Lancet Neurol. 2015 Apr;14(4):388-405. doi: 10.1016/S1474-4422(15)70016-5. PMID: 25792098; PMCID: PMC5909703.

Ho L, Qin W, Pompl PN, Xiang Z, lawaJ, Zhao Z, Peng Y, Cambareri G, Rocher A, Mobbs CV, Hof PR, Pasinetti GM. Diet-induced insulin resistance promotes amyloidosis in a transgenic mouse model of Alzheimer's disease. FASEB J. 2004 May;18(7):902-4. doi: 10.1096/fj.03-0978fje. Epub 2004 Mar 19. PMID: 15033922.

Hof PR, Cox K, Morrison JH. Quantitative analysis of a vulnerable subset of pyramidal neurons in Alzheimer's disease: I. Superior frontal and inferior temporal cortex. J Comp Neurol. 1990 Nov 1;301(1):44-54. doi: 10.1002/cne.903010105. PMID: 2127598.

Höglinger GU, Litvan I, Mendonca N, Wang D, Zheng H, Rendenbach-Mueller B, Lon HK, Jin Z, Fisseha N, Budur K, Gold M, Ryman D, Florian H; Arise Investigators. Safety and efficacy of tilavonemab in progressive supranuclear palsy: a phase 2, randomised, placebo-controlled trial. Lancet Neurol. 2021 Mar;20(3):182-192. doi: 10.1016/S1474-4422(20)30489-0. PMID: 33609476.

Hone E, Martins IJ, Fonte J, Martins RN. Apolipoprotein E influences amyloid-beta clearance from the murine periphery. J Alzheimers Dis. 2003 Feb;5(1):1-8. doi: 10.3233/jad-2003-5101. PMID: 12590160.

Hooli BV, Mohapatra G, Mattheisen M, Parrado AR, Roehr JT, Shen Y, Gusella JF, Moir R, Saunders AJ, Lange C, Tanzi RE, Bertram L. Role of common and rare APP DNA sequence variants in Alzheimer disease. Neurology. 2012 Apr 17;78(16):1250-7. doi: 10.1212/WNL.0b013e3182515972. Epub 2012 Apr 4. PMID: 22491860; PMCID: PMC3324321.

Horton JD, Goldstein JL, Brown MS. SREBPs: activators of the complete program of cholesterol and fatty acid synthesis in the liver. J Clin Invest. 2002 May;109(9):1125-31. doi: 10.1172/JCI15593. PMID: 11994399; PMCID: PMC150968.

Hosaka Y, Araya J, Fujita Y, Kuwano K. Role of chaperone-mediated autophagy in the pathophysiology including pulmonary disorders. Inflamm Regen. 2021 Oct 1;41(1):29. doi: 10.1186/s41232-021-00180-9. PMID: 34593046; PMCID: PMC8485456.

Hull RL, Westermark GT, Westermark P, Kahn SE. Islet amyloid: a critical entity in the pathogenesis of type 2 diabetes. J Clin Endocrinol Metab. 2004 Aug;89(8):3629-43. doi: 10.1210/jc.2004-0405. PMID: 15292279

Hunter SJ, Boyd AC, O'Harte FP, McKillop AM, Wiggam MI, Mooney MH, McCluskey JT, Lindsay JR, Ennis CN, Gamble R, Sheridan B, Barnett CR, McNulty H, Bell PM, Flatt PR. Demonstration of glycated insulin in human diabetic plasma and decreased biological activity assessed by euglycemic-hyperinsulinemic clamp technique in humans. Diabetes. 2003 Feb;52(2):492-8. doi: 10.2337/diabetes.52.2.492. PMID: 12540 Miranda-Díaz AG, Pazarín-Villaseñor L, Yanowsky-Escatell FG, Andrade-Sierra J. Oxidative Stress in Diabetic Nephropathy with Early Chronic Kidney Disease. J Diabetes Res. 2016; 2016:7047238. doi: 10.1155/2016/7047238. Epub 2016 Jul 20. PMID: 27525285; PMCID: PMC4971321.626.

Iadecola C, Davisson RL. Hypertension and cerebrovascular dysfunction. Cell Metab. 2008 Jun;7(6):476-84. doi: 10.1016/j.cmet.2008.03.010. PMID: 18522829; PMCID: PMC2475602.

Infante-Garcia C, Ramos-Rodriguez JJ, Galindo-Gonzalez L, Garcia-Alloza M. Long-term central pathology and cognitive impairment are exacerbated in a mixed model of Alzheimer's disease and type 2 diabetes. Psychoneuroendocrinology. 2016 Mar; 65:15-25. doi: 10.1016/j.psyneuen.2015.12.001. Epub 2015 Dec 3. PMID: 26708068.

Iqbal K, Grundke-Iqbal I. Alzheimer neurofibrillary degeneration: significance, etiopathogenesis, therapeutics and prevention. J Cell Mol Med. 2008 Jan-Feb;12(1):38-55. doi: 10.1111/j.1582-4934.2008.00225. x. Epub 2007 Jan 9. PMID: 18194444; PMCID: PMC3139457

Iroz A, Montagner A, Benhamed F, Levavasseur F, Polizzi A, Anthony E, Régnier M, Fouché E, Lukowicz C, Cauzac M, Tournier E, Do-Cruzeiro M, Daujat-Chavanieu M, Gerbal-Chalouin S, Fauveau V, Marmier S, Burnol AF, Guilmeau S, Lippi Y, Girard J, Wahli W, Dentin R, Guillou H, Postic C. A Specific ChREBP and PPARα Cross-Talk Is Required for the Glucose-Mediated FGF21 Response. Cell Rep. 2017 Oct

10;21(2):403-416. doi: 10.1016/j.celrep.2017.09.065. PMID: 29020627; PMCID: PMC5643524.

Islam S, Rahman S, Haque T, Sumon AH, Ahmed AM, Ali N. Prevalence of elevated liver enzymes and its association with type 2 diabetes: A cross-sectional study in Bangladeshi adults. Endocrinol Diabetes Metab. 2020 Feb 12;3(2): e00116. doi: 10.1002/edm2.116. PMID: 32318634; PMCID: PMC7170449.

Ito N, Saito H, Seki S, Ueda F, Asada T. Effects of Composite Supplement Containing Astaxanthin and Sesamin on Cognitive Functions in People with Mild Cognitive Impairment: A Randomized, Double-Blind, Placebo-Controlled Trial. J Alzheimers Dis. 2018;62(4):1767-1775. doi: 10.3233/JAD-170969. Erratum in: J Alzheimers Dis. 2019;68(2):839. PMID: 29614679; PMCID: PMC5900571.

Ito S, Kimura K, Haneda M, Ishida Y, Sawada M, Isobe K. Induction of matrix metalloproteinases (MMP3, MMP12 and MMP13) expression in the microglia by amyloid-beta stimulation via the PI3K/Akt pathway. Exp Gerontol. 2007 Jun;42(6):532-7. doi: 10.1016/j.exger.2006.11.012. Epub 2007 Jan 2. PMID: 17198748.

Ito S, Sawada M, Haneda M, Ishida Y, Isobe K. Amyloid-beta peptides induce several chemokine mRNA expressions in the primary microglia and Ra2 cell line via the PI3K/Akt and/or ERK pathway. Neurosci Res. 2006 Nov;56(3):294-9. doi: 10.1016/j.neures.2006.07.009. Epub 2006 Sep 15. PMID: 16978723.

Itoh N, Sakaue S, Nakagawa H, Kurogochi M, Ohira H, Deguchi K, et al. Analysis of N-glycan in serum glycoproteins from db/db mice and humans with type 2 diabetes. American journal of physiology. 2007; 293(4): E1069–77. https://doi.org/10.1152/ajpendo.00182.2007 PMID: 17666489.

Ittner LM, Götz J. Amyloid-β and tau--a toxic pas de deux in Alzheimer's disease. Nat Rev Neurosci. 2011 Feb;12(2):65-72. doi: 10.1038/nrn2967. Epub 2010 Dec 31. PMID: 21193853.

Jack CR Jr, Albert MS, Knopman DS, McKhann GM, Sperling RA, Carrillo MC, Thies B, Phelps CH. Introduction to the recommendations from the National Institute on Aging-Alzheimer's Association workgroups on diagnostic guidelines for Alzheimer's

disease. Alzheimers Dement. 2011 May;7(3):257-62. doi: 10.1016/j.jalz.2011.03.004. Epub 2011 Apr 21. PMID: 21514247; PMCID: PMC3096735.

Jack CR Jr, Bennett DA, Blennow K, Carrillo MC, Dunn B, Haeberlein SB, Holtzman DM, Jagust W, Jessen F, Karlawish J, Liu E, Molinuevo JL, Montine T, Phelps C, Rankin KP, Rowe CC, Scheltens P, Siemers E, Snyder HM, Sperling R; Contributors. NIA-AA Research Framework: Toward a biological definition of Alzheimer's disease. Alzheimers Dement. 2018 Apr;14(4):535-562. doi: 10.1016/j.jalz.2018.02.018. PMID: 29653606; PMCID: PMC5958625.

Jack CR Jr, Lowe VJ, Weigand SD, Wiste HJ, Senjem ML, Knopman DS, Shiung MM, Gunter JL, Boeve BF, Kemp BJ, Weiner M, Petersen RC; Alzheimer's Disease Neuroimaging Initiative. Serial PIB and MRI in normal, mild cognitive impairment and Alzheimer's disease: implications for sequence of pathological events in Alzheimer's disease. Brain. 2009 May;132(Pt 5):1355-65. doi: 10.1093/brain/awp062. Epub 2009 Mar 31. PMID: 19339253; PMCID: PMC2677798.

Jackson RJ, Meltzer JC, Nguyen H, Commins C, Bennett RE, Hudry E, Hyman BT. APOE4 derived from astrocytes leads to blood-brain barrier impairment. Brain. 2022 Oct 21;145(10):3582-3593. doi: 10.1093/brain/awab478. PMID: 34957486; PMCID: PMC9586546.

Jaeger LB, Dohgu S, Sultana R, Lynch JL, Owen JB, Erickson MA, Shah GN, Price TO, Fleegal-Demotta MA, Butterfield DA, Banks WA. Lipopolysaccharide alters the blood-brain barrier transport of amyloid beta protein: a mechanism for inflammation in the progression of Alzheimer's disease. Brain Behav Immun. 2009 May;23(4):507-17. doi: 10.1016/j.bbi.2009.01.017. Epub 2009 Feb 6. Erratum in: Brain Behav Immun. 2011 Nov;25(8):1737. Butterfiled, D Allan [corrected to Butterfield, D Allan]. PMID: 19486646; PMCID: PMC2783557.

Jagusch W, Voncramon DY, Renner R, Hepp KD (1992) Cognitive function and metabolic state in elderly diabetic patients. Diabetes Nutrition & Metabolism 5: 265–274.

Janson J, Laedtke T, Parisi JE, O'Brien P, Petersen RC, Butler PC. Increased risk of type 2 diabetes in Alzheimer disease. Diabetes. 2004 Feb;53(2):474-81. doi: 10.2337/diabetes.53.2.474. PMID: 14747300.

Janson J, Laedtke T, Parisi JE, O'Brien P, Petersen RC, Butler PC. Increased risk of type 2 diabetes in Alzheimer disease. Diabetes. 2004 Feb;53(2):474-81. doi: 10.2337/diabetes.53.2.474. PMID: 14747300.

Jawhar S, Wirths O, Bayer TA. Pyroglutamate amyloid-β (Aβ): a hatchet man in Alzheimer disease. J Biol Chem. 2011 Nov 11;286(45):38825-32. doi: 10.1074/jbc. R111.288308. Epub 2011 Sep 29. PMID: 21965666; PMCID: PMC3234707.

Jawhar S, Wirths O, Schilling S, Graubner S, Demuth HU, Bayer TA (2011) Overexpression of glutaminyl cyclase, the enzyme responsible for pyroglutamate Abeta formation, induces behavioral deficits, and glutaminyl cyclase knock-out rescues the behavioral phenotype in 5XFAD mice. J Biol Chem 286, 4454-4460

Jay TR, Miller CM, Cheng PJ, Graham LC, Bemiller S, Broihier ML, Xu G, Margevicius D, Karlo JC, Sousa GL, Cotleur AC, Butovsky O, Bekris L, Staugaitis SM, Leverenz JB, Pimplikar SW, Landreth GE, Howell GR, Ransohoff RM, Lamb BT. TREM2 deficiency eliminates TREM2+ inflammatory macrophages and ameliorates pathology in Alzheimer's disease mouse models. J Exp Med. 2015 Mar 9;212(3):287-95. doi: 10.1084/jem.20142322. Epub 2015 Mar 2. PMID: 25732305; PMCID: PMC4354365.

Ji J, Petropavlovskaia M, Khatchadourian A, Patapas J, Makhlin J, Rosenberg L, Maysinger D. Type 2 diabetes is associated with suppression of autophagy and lipid accumulation in β-cells. J Cell Mol Med. 2019 Apr;23(4):2890-2900. doi: 10.1111/jcmm.14172. Epub 2019 Feb 1. PMID: 30710421; PMCID: PMC6433726.

Jia Y, Kim JY, Jun HJ, Kim SJ, Lee JH, Hoang MH, Hwang KY, Um SJ, Chang HI, Lee SJ. The natural carotenoid astaxanthin, a PPAR-α agonist and PPAR-γ antagonist, reduces hepatic lipid accumulation by rewiring the transcriptome in lipid-loaded hepatocytes. Mol Nutr Food Res. 2012 Jun;56(6):878-88. doi: 10.1002/mnfr.201100798. PMID: 22707263.

Jia Y, Wu C, Kim J, Kim B, Lee SJ. Astaxanthin reduces hepatic lipid accumulations in high-fat-fed C57BL/6J mice via activation of peroxisome proliferator-activated receptor (PPAR) alpha and inhibition of PPAR gamma and Akt. J Nutr Biochem. 2016 Feb; 28:9-18. doi: 10.1016/j.jnutbio.2015.09.015. Epub 2015 Sep 30. PMID: 26878778.

Johnson DG, Alberti KG, Faber OK, Binder C. Hyperinsulinism of hepatic cirrhosis: Diminished degradation or hypersecretion? Lancet. 1977 Jan 1;1(8001):10-3. doi: 10.1016/s0140-6736(77)91652-x. PMID: 63654.

Jolivalt CG, Hurford R, Lee CA, Dumaop W, Rockenstein E, Masliah E. Type 1 diabetes exaggerates features of Alzheimer's disease in APP transgenic mice. Exp Neurol. 2010 Jun;223(2):422-31. doi: 10.1016/j.expneurol.2009.11.005. Epub 2009 Nov 18. PMID: 19931251; PMCID: PMC2864332.

Jonsson T, Stefansson H, Steinberg S, Jonsdottir I, Jonsson PV, Snaedal J, Bjornsson S, Huttenlocher J, Levey AI, Lah JJ, Rujescu D, Hampel H, Giegling I, Andreassen OA, Engedal K, Ulstein I, Djurovic S, Ibrahim-Verbaas C, Hofman A, Ikram MA, van Duijn CM, Thorsteinsdottir U, Kong A, Stefansson K. Variant of TREM2 associated with the risk of Alzheimer's disease. N Engl J Med. 2013 Jan 10;368(2):107-16. doi: 10.1056/NEJMoa1211103. Epub 2012 Nov 14. PMID: 23150908; PMCID: PMC3677583.

Julien C, Tremblay C, Phivilay A, Berthiaume L, Emond V, Julien P, Calon F. High-fat diet aggravates amyloid-beta and tau pathologies in the 3xTg-AD mouse model. Neurobiol Aging. 2010 Sep;31(9):1516-31. doi: 10.1016/j.neurobiolaging.2008.08.022. Epub 2008 Oct 15. PMID: 18926603.

Jurgens CA, Toukatly MN, Fligner CL, Udayasankar J, Subramanian SL, Zraika S, Aston-Mourney K, Carr DB, Westermark P, Westermark GT, Kahn SE, Hull RL. β-cell loss and β-cell apoptosis in human type 2 diabetes are related to islet amyloid deposition. Am J Pathol. 2011 Jun;178(6):2632-40. doi: 10.1016/j.ajpath.2011.02.036. Erratum in: Am J Pathol. 2011 Jul;179(1):537-8. PMID: 21641386; PMCID: PMC3123989.

Kabeya Y, Mizushima N, Ueno T, Yamamoto A, Kirisako T, Noda T, Kominami E, Ohsumi Y, Yoshimori T. LC3, a mammalian homologue of yeast Apg8p, is localized in autophagosome membranes after processing. EMBO J. 2000 Nov 1;19(21):5720-8. doi: 10.1093/emboj/19.21.5720. Erratum in: EMBO J. 2003 Sep 1;22(17):4577. PMID: 11060023; PMCID: PMC305793.

Kahn SE. The relative contributions of insulin resistance and beta-cell dysfunction to the pathophysiology of Type 2 diabetes. Diabetologia. 2003 Jan;46(1):3-19. doi: 10.1007/s00125-002-1009-0. Epub 2003 Jan 11. PMID: 12637977.

Kang DE, Pietrzik CU, Baum L, Chevallier N, Merriam DE, Kounnas MZ, Wagner SL, Troncoso JC, Kawas CH, Katzman R, Koo EH. Modulation of amyloid beta-protein clearance and Alzheimer's disease susceptibility by the LDL receptor-related protein pathway. J Clin Invest. 2000 Nov;106(9):1159-66. doi: 10.1172/JCI11013. PMID: 11067868; PMCID: PMC301422.

Kang S, Kim CH, Jung H, Kim E, Song HT, Lee JE. Agmatine ameliorates type 2 diabetes induced-Alzheimer's disease-like alterations in high-fat diet-fed mice via reactivation of blunted insulin signalling. Neuropharmacology. 2017 Feb;113(Pt A):467-479. doi: 10.1016/j.neuropharm.2016.10.029. Epub 2016 Oct 31. PMID: 27810390.

Karch CM, Goate AM. Alzheimer's disease risk genes and mechanisms of disease pathogenesis. Biol Psychiatry. 2015 Jan 1;77(1):43-51. doi: 10.1016/j.biopsych.2014.05.006. Epub 2014 May 17. PMID: 24951455; PMCID: PMC4234692.

Katagiri M, Satoh A, Tsuji S, Shirasawa T. Effects of astaxanthin-rich Haematococcus pluvialis extract on cognitive function: a randomised, double-blind, placebo-controlled study. J Clin Biochem Nutr. 2012 Sep;51(2):102-7. doi: 10.3164/jcbn. D-11-00017. Epub 2012 Mar 30. PMID: 22962526; PMCID: PMC3432818.

Kaushik S, Cuervo AM. The coming of age of chaperone-mediated autophagy. Nat Rev Mol Cell Biol. 2018 Jun;19(6):365-381. doi: 10.1038/s41580-018-0001-6. PMID: 29626215; PMCID: PMC6399518.

Kawada T. [Lipid metabolism related nuclear receptor--the structure, function, expression and classification of peroxisome proliferation-activated receptor (PPAR)]. Nihon Rinsho. 1998 Jul;56(7):1722-8. Japanese. PMID: 9702044.

Ke YD, Delerue F, Gladbach A, Götz J, Ittner LM. Experimental diabetes mellitus exacerbates tau pathology in a transgenic mouse model of Alzheimer's disease. PLoS One. 2009 Nov 19;4(11): e7917. doi: 10.1371/journal.pone.0007917. PMID: 19936237; PMCID: PMC2775636.

Keep RF, Jones HC, Hamilton MG, Drewes LR. A year in review: brain barriers and brain fluids research in 2022. Fluids Barriers CNS. 2023 Apr 21;20(1):30. doi: 10.1186/s12987-023-00429-0. PMID: 37085841; PMCID: PMC10120509

Kellar D, Craft S. Brain insulin resistance in Alzheimer's disease and related disorders: mechanisms and therapeutic approaches. Lancet Neurol. 2020 Sep;19(9):758-766. doi: 10.1016/S1474-4422(20)30231-3. Epub 2020 Jul 27. PMID: 32730766; PMCID: PMC9661919.

Kennelly S, Collins O. Walking the cognitive "minefield" between high and low blood pressure. J Alzheimers Dis. 2012;32(3):609-21. doi: 10.3233/JAD-2012-120748. PMID: 22810098.

Kepp KP, Robakis NK, Høilund-Carlsen PF, Sensi SL, Vissel B. The amyloid cascade hypothesis: an updated critical review. Brain. 2023 May 15: awad159. doi: 10.1093/brain/awad159. Epub ahead of print. PMID: 37183523.

Keren-Shaul H, Spinrad A, Weiner A, Matcovitch-Natan O, Dvir-Szternfeld R, Ulland TK, David E, Baruch K, Lara-Astaiso D, Toth B, Itzkovitz S, Colonna M, Schwartz M, Amit I. A Unique Microglia Type Associated with Restricting Development of Alzheimer's Disease. Cell. 2017 Jun 15;169(7):1276-1290.e17. doi: 10.1016/j.cell.2017.05.018. Epub 2017 Jun 8. PMID: 28602351.

Kim SH, Kim H. Astaxanthin Modulation of Signaling Pathways That Regulate Autophagy. Mar Drugs. 2019 Sep 23;17(10):546. doi: 10.3390/md17100546. PMID: 31547619; PMCID: PMC6836186.

Kim YJ, Kim YA, Yokozawa T. Protection against oxidative stress, inflammation, and apoptosis of high-glucose-exposed proximal tubular epithelial cells by astaxanthin. J Agric Food Chem. 2009 Oct 14;57(19):8793-7. doi: 10.1021/jf9019745. PMID: 19731916.

Kirchner H, Sinha I, Gao H, Ruby MA, Schönke M, Lindvall JM, Barrès R, Krook A, Näslund E, Dahlman-Wright K, Zierath JR. Altered DNA methylation of glycolytic and lipogenic genes in liver from obese and type 2 diabetic patients. Mol Metab. 2016 Jan 2;5(3):171-183. doi: 10.1016/j.molmet.2015.12.004. PMID: 26977391; PMCID: PMC4770265.

Kivipelto M, Helkala EL, Hänninen T, Laakso MP, Hallikainen M, Alhainen K, Soininen H, Tuomilehto J, Nissinen A. Midlife vascular risk factors and late-life mild cognitive impairment: A population-based study. Neurology. 2001 Jun 26;56(12):1683-9. doi: 10.1212/wnl.56.12.1683. PMID: 11425934.

Klegeris A, McGeer PL. Complement activation by islet amyloid polypeptide (IAPP) and alpha-synuclein 112. Biochem Biophys Res Commun. 2007 Jun 15;357(4):1096-9. doi: 10.1016/j.bbrc.2007.04.055. Epub 2007 Apr 18. PMID: 17459337.

Kleiner S, Mepani RJ, Laznik D, Ye L, Jurczak MJ, Jornayvaz FR, Estall JL, Chatterjee Bhowmick D, Shulman GI, Spiegelman BM. Development of insulin resistance in mice lacking PGC-1α in adipose tissues. Proc Natl Acad Sci U S A. 2012 Jun 12;109(24):9635-40. doi: 10.1073/pnas.1207287109. Epub 2012 May 29. PMID: 22645355; PMCID: PMC3386123.

Kling MA, Trojanowski JQ, Wolk DA, Lee VM, Arnold SE. Vascular disease and dementias: paradigm shifts to drive research in new directions. Alzheimers Dement. 2013 Jan;9(1):76-92. doi: 10.1016/j.jalz.2012.02.007. Epub 2012 Nov 22. PMID: 23183137; PMCID: PMC3640817

Knight EM, Martins IV, Gümüsgöz S, Allan SM, Lawrence CB. High-fat diet-induced memory impairment in triple-transgenic Alzheimer's disease (3xTgAD) mice is independent of changes in amyloid and tau pathology. Neurobiol Aging. 2014 Aug;35(8):1821-32. doi: 10.1016/j.neurobiolaging.2014.02.010. Epub 2014 Feb 15. PMID: 24630364; PMCID: PMC4024197.

Knopman DS, Roberts R. Vascular risk factors: imaging and neuropathologic correlates. J Alzheimers Dis. 2010;20(3):699-709. doi: 10.3233/JAD-2010-091555. PMID: 20182020; PMCID: PMC2883660.

Knopp RC, Banks WA, Erickson MA. Physical associations of microglia and the vascular blood-brain barrier and their importance in development, health, and disease. Curr Opin Neurobiol. 2022 Dec; 77:102648. doi: 10.1016/j.conb.2022.102648. Epub 2022 Nov 5. PMID: 36347075.

Kopf D, Frölich L. Risk of incident Alzheimer's disease in diabetic patients: a systematic review of prospective trials. J Alzheimers Dis. 2009;16(4):677-85. doi: 10.3233/JAD-2009-1011. PMID: 19387104.

Koran MEI, Wagener M, Hohman TJ; Alzheimer's Neuroimaging Initiative. Sex differences in the association between AD biomarkers and cognitive decline. Brain Imaging Behav. 2017 Feb;11(1):205-213. doi: 10.1007/s11682-016-9523-8. PMID: 26843008; PMCID: PMC4972701.

Korvatska O, Leverenz JB, Jayadev S, McMillan P, Kurtz I, Guo X, Rumbaugh M, Matsushita M, Girirajan S, Dorschner MO, Kiianitsa K, Yu CE, Brkanac Z, Garden GA, Raskind WH, Bird TD. R47H Variant of TREM2 Associated with Alzheimer Disease in a Large Late-Onset Family: Clinical, Genetic, and Neuropathological Study. JAMA Neurol. 2015 Aug;72(8):920-7. doi: 10.1001/jamaneurol.2015.0979. PMID: 26076170; PMCID: PMC4825672.

Kruit JK, Wijesekara N, Fox JE, Dai XQ, Brunham LR, Searle GJ, Morgan GP, Costin AJ, Tang R, Bhattacharjee A, Johnson JD, Light PE, Marsh BJ, Macdonald PE, Verchere CB, Hayden MR. Islet cholesterol accumulation due to loss of ABCA1 leads to impaired exocytosis of insulin granules. Diabetes. 2011 Dec;60(12):3186-96. doi: 10.2337/db11-0081. Epub 2011 Oct 12. PMID: 21998401; PMCID: PMC3219942.

Kruyer A, Soplop N, Strickland S, Norris EH. Chronic Hypertension Leads to Neurodegeneration in the TgSwDI Mouse Model of Alzheimer's Disease. Hypertension. 2015 Jul;66(1):175-82. doi: 10.1161/HYPERTENSIONAHA.115.05524. Epub 2015 May 4. PMID: 25941345; PMCID: PMC4465852.

Kukull WA, Higdon R, Bowen JD, McCormick WC, Teri L, Schellenberg GD, van Belle G, Jolley L, Larson EB. Dementia and Alzheimer disease incidence: a prospective cohort study. Arch Neurol. 2002 Nov;59(11):1737-46. doi: 10.1001/archneur.59.11.1737. PMID: 12433261.

Kumar S, Rezaei-Ghaleh N, Terwel D, Thal DR, Richard M, Hoch M, Mc Donald JM, Wüllner U, Glebov K, Heneka MT, Walsh DM, Zweckstetter M, Walter J. Extracellular phosphorylation of the amyloid β-peptide promotes formation of toxic aggregates during the pathogenesis of Alzheimer's disease. EMBO J. 2011 Jun 1;30(11):2255-65. doi: 10.1038/emboj.2011.138. Epub 2011 Apr 28. PMID: 21527912; PMCID: PMC3117653.

Kuo YM, Emmerling MR, Woods AS, Cotter RJ, Roher AE. Isolation, chemical characterization, and quantitation of A beta 3-pyroglutamyl peptide from neuritic

plaques and vascular amyloid deposits. Biochem Biophys Res Commun. 1997 Aug 8;237(1):188-91. doi: 10.1006/bbrc.1997.7083. PMID: 9266855.

Kuo YM, Kokjohn TA, Beach TG, Sue LI, Brune D, Lopez JC, Kalback WM, Abramowski D, Sturchler-Pierrat C, Staufenbiel M, Roher AE. Comparative analysis of amyloid-beta chemical structure and amyloid plaque morphology of transgenic mouse and Alzheimer's disease brains. J Biol Chem. 2001 Apr 20;276(16):12991-8. doi: 10.1074/jbc.M007859200. Epub 2001 Jan 10. PMID: 11152675.

Kuriakose A, Chirmule N, Nair P. Immunogenicity of Biotherapeutics: Causes and Association with Posttranslational Modifications. J Immunol Res. 2016; 2016:1298473. doi: 10.1155/2016/1298473. Epub 2016 Jun 29. PMID: 27437405; PMCID: PMC4942633

Kuusisto J, Koivisto K, Mykkänen L, Helkala EL, Vanhanen M, Hänninen T, Kervinen K, Kesäniemi YA, Riekkinen PJ, Laakso M. Association between features of the insulin resistance syndrome and Alzheimer's disease independently of apolipoprotein E4 phenotype: cross sectional population-based study. BMJ. 1997 Oct 25;315(7115):1045-9. doi: 10.1136/bmj.315.7115.1045. PMID: 9366728; PMCID: PMC2127678.

Lachance V, Wang Q, Sweet E, Choi I, Cai CZ, Zhuang XX, Zhang Y, Jiang JL, Blitzer RD, Bozdagi-Gunal O, Zhang B, Lu JH, Yue Z. Autophagy protein NRBF2 has reduced expression in Alzheimer's brains and modulates memory and amyloid-beta homeostasis in mice. Mol Neurodegener. 2019 Nov 27;14(1):43. doi: 10.1186/s13024-019-0342-4. PMID: 31775806; PMCID: PMC6882183.

Lacorte E, Ancidoni A, Zaccaria V, Remoli G, Tariciotti L, Bellomo G, Sciancalepore F, Corbo M, Lombardo FL, Bacigalupo I, Canevelli M, Piscopo P, Vanacore N. Safety and Efficacy of Monoclonal Antibodies for Alzheimer's Disease: A Systematic Review and Meta-Analysis of Published and Unpublished Clinical Trials. J Alzheimers Dis. 2022;87(1):101-129. doi: 10.3233/JAD-220046. PMID: 35275549; PMCID: PMC9198746.

Lambert JC, Ibrahim-Verbaas CA, Harold D, Naj AC, Sims R, Bellenguez C, DeStafano AL, Bis JC, Beecham GW, Grenier-Boley B, Russo G, Thorton-Wells TA, Jones N, Smith AV, Chouraki V, Thomas C, Ikram MA, Zelenika D, Vardarajan BN, Kamatani Y, Lin CF, Gerrish A, Schmidt H, Kunkle B, Dunstan ML, Ruiz A, Bihoreau

MT, Choi SH, Reitz C, Pasquier F, Cruchaga C, Craig D, Amin N, Berr C, Lopez OL, De Jager PL, Deramecourt V, Johnston JA, Evans D, Lovestone S, Letenneur L, Morón FJ, Rubinsztein DC, Eiriksdottir G, Sleegers K, Goate AM, Fiévet N, Huentelman MW, Gill M, Brown K, Kamboh MI, Keller L, Barberger-Gateau P, McGuiness B, Larson EB, Green R, Myers AJ, Dufouil C, Todd S, Wallon D, Love S, Rogaeva E, Gallacher J, St George-Hyslop P, Clarimon J, Lleo A, Bayer A, Tsuang DW, Yu L, Tsolaki M, Bossù P, Spalletta G, Proitsi P, Collinge J, Sorbi S, Sanchez-Garcia F, Fox NC, Hardy J, Deniz Naranjo MC, Bosco P, Clarke R, Brayne C, Galimberti D, Mancuso M, Matthews F; European Alzheimer's Disease Initiative (EADI); Genetic and Environmental Risk in Alzheimer's Disease; Alzheimer's Disease Genetic Consortium; Cohorts for Heart and Aging Research in Genomic Epidemiology; Moebus S, Mecocci P, Del Zompo M, Maier W, Hampel H, Pilotto A, Bullido M, Panza F, Caffarra P, Nacmias B, Gilbert JR, Mayhaus M, Lannefelt L, Hakonarson H, Pichler S, Carrasquillo MM, Ingelsson M, Beekly D, Alvarez V, Zou F, Valladares O, Younkin SG, Coto E, Hamilton-Nelson KL, Gu W, Razquin C, Pastor P, Mateo I, Owen MJ, Faber KM, Jonsson PV, Combarros O, O'Donovan MC, Cantwell LB, Soininen H, Blacker D, Mead S, Mosley TH Jr, Bennett DA, Harris TB, Fratiglioni L, Holmes C, de Bruijn RF, Passmore P, Montine TJ, Bettens K, Rotter JI, Brice A, Morgan K, Foroud TM, Kukull WA, Hannequin D, Powell JF, Nalls MA, Ritchie K, Lunetta KL, Kauwe JS, Boerwinkle E, Riemenschneider M, Boada M, Hiltuenen M, Martin ER, Schmidt R, Rujescu D, Wang LS, Dartigues JF, Mayeux R, Tzourio C, Hofman A, Nöthen MM, Graff C, Psaty BM, Jones L, Haines JL, Holmans PA, Lathrop M, Pericak-Vance MA, Launer LJ, Farrer LA, van Duijn CM, Van Broeckhoven C, Moskvina V, Seshadri S, Williams J, Schellenberg GD, Amouyel P. Meta-analysis of 74,046 individuals identifies 11 new susceptibility loci for Alzheimer's disease. Nat Genet. 2013 Dec;45(12):1452-8. doi: 10.1038/ng.2802. Epub 2013 Oct 27. PMID: 24162737; PMCID: PMC3896259.

Lanoiselée HM, Nicolas G, Wallon D, Rovelet-Lecrux A, Lacour M, Rousseau S, Richard AC, Pasquier F, Rollin-Sillaire A, Martinaud O, Quillard-Muraine M, de la Sayette V, Boutoleau-Bretonniere C, Etcharry-Bouyx F, Chauviré V, Sarazin M, le Ber I, Epelbaum S, Jonveaux T, Rouaud O, Ceccaldi M, Félician O, Godefroy O, Formaglio M, Croisile B, Auriacombe S, Chamard L, Vincent JL, Sauvée M, Marelli-Tosi C, Gabelle A, Ozsancak C, Pariente J, Paquet C, Hannequin D, Campion D; collaborators of the CNR-MAJ project. APP, PSEN1, and PSEN2 mutations in early-

onset Alzheimer disease: A genetic screening study of familial and sporadic cases. PLoS Med. 2017 Mar 28;14(3): e1002270. doi: 10.1371/journal.pmed.1002270. PMID: 28350801; PMCID: PMC5370101.

Larson EB, Shadlen MF, Wang L, McCormick WC, Bowen JD, Teri L, Kukull WA. Survival after initial diagnosis of Alzheimer disease. Ann Intern Med. 2004 Apr 6;140(7):501-9. doi: 10.7326/0003-4819-140-7-200404060-00008. PMID: 15068977.

Lawal SK, Olojede SO, Dare A, Faborode OS, Naidu ECS, Rennie CO, Azu OO. Silver Nanoparticles Conjugate Attenuates Highly Active Antiretroviral Therapy-Induced Hippocampal Nissl Substance and Cognitive Deficits in Diabetic Rats. J Diabetes Res. 2021 Nov 19; 2021:2118538. doi: 10.1155/2021/2118538. PMID: 34840987; PMCID: PMC8626174.

Laws KR, Irvine K, Gale TM. Sex differences in Alzheimer's disease. Curr Opin Psychiatry. 2018 Mar;31(2):133-139. doi: 10.1097/YCO.0000000000000401. PMID: 29324460.

Lazarov O, Hollands C. Hippocampal neurogenesis: Learning to remember. Prog Neurobiol. 2016 Mar-May;138-140:1-18. doi: 10.1016/j.pneurobio.2015.12.006. Epub 2016 Feb 6. PMID: 26855369; PMCID: PMC4828289.

Leclerc M, Bourassa P, Tremblay C, Caron V, Sugère C, Emond V, Bennett DA, Calon F. Cerebrovascular insulin receptors are defective in Alzheimer's disease. Brain. 2023 Jan 5;146(1):75-90. doi: 10.1093/brain/awac309. PMID: 36280236; PMCID: PMC9897197.

Lee H, Lim JW, Kim H. Effect of Astaxanthin on Activation of Autophagy and Inhibition of Apoptosis in *Helicobacter pylori*-Infected Gastric Epithelial Cell Line AGS. Nutrients. 2020 Jun 11;12(6):1750. doi: 10.3390/nu12061750. PMID: 32545395; PMCID: PMC7353244.

Lee JA, Gao FB. Regulation of Abeta pathology by beclin 1: a protective role for autophagy? J Clin Invest. 2008 Jun;118(6):2015-8. doi: 10.1172/JCI35662. PMID: 18497881; PMCID: PMC2391068

Lee JH, Yang DS, Goulbourne CN, Im E, Stavrides P, Pensalfini A, Chan H, Bouchet-Marquis C, Bleiwas C, Berg MJ, Huo C, Peddy J, Pawlik M, Levy E, Rao M, Staufenbiel M, Nixon RA. Faulty autolysosome acidification in Alzheimer's disease

mouse models induces autophagic build-up of Aβ in neurons, yielding senile plaques. Nat Neurosci. 2022 Jun;25(6):688-701. doi: 10.1038/s41593-022-01084-8. Epub 2022 Jun 2. PMID: 35654956; PMCID: PMC9174056.

Leibson CL, Rocca WA, Hanson VA, Cha R, Kokmen E, O'Brien PC, Palumbo PJ. The risk of dementia among persons with diabetes mellitus: a population-based cohort study. Ann N Y Acad Sci. 1997 Sep 26; 826:422-7. doi: 10.1111/j.1749-6632. 1997.tb48496. x. PMID: 9329716.

Li R, Singh M. Sex differences in cognitive impairment and Alzheimer's disease. Front Neuroendocrinol. 2014 Aug;35(3):385-403. doi: 10.1016/j.yfrne.2014.01.002. Epub 2014 Jan 13. PMID: 24434111; PMCID: PMC4087048.

Li W, Yang Q, Mao Z. Chaperone-mediated autophagy: machinery, regulation and biological consequences. Cell Mol Life Sci. 2011 Mar;68(5):749-63. doi: 10.1007/s00018-010-0565-6. Epub 2010 Oct 26. PMID: 20976518.

Li X, Qi Z, Zhao L, Yu Z. Astaxanthin reduces type 2 diabetic-associated cognitive decline in rats via activation of PI3K/Akt and attenuation of oxidative stress. Mol Med Rep. 2016 Jan;13(1):973-9. doi: 10.3892/mmr.2015.4615. Epub 2015 Nov 25. PMID: 26648531.

Li ZG, Zhang W, Sima AA. Alzheimer-like changes in rat models of spontaneous diabetes. Diabetes. 2007 Jul;56(7):1817-24. doi: 10.2337/db07-0171. Epub 2007 Apr 24. Erratum in: Diabetes. 2007 Oct;56(10):2650. PMID: 17456849.

Liesinger AM, Graff-Radford NR, Duara R, Carter RE, Hanna Al-Shaikh FS, Koga S, Hinkle KM, DiLello SK, Johnson MF, Aziz A, Ertekin-Taner N, Ross OA, Dickson DW, Murray ME. Sex and age interact to determine clinicopathologic differences in Alzheimer's disease. Acta Neuropathol. 2018 Dec;136(6):873-885. doi: 10.1007/s00401-018-1908-x. Epub 2018 Sep 15. PMID: 30219939; PMCID: PMC6280837.

Ling C, Del Guerra S, Lupi R, Rönn T, Granhall C, Luthman H, Masiello P, Marchetti P, Groop L, Del Prato S. Epigenetic regulation of PPARGC1A in human type 2 diabetic islets and effect on insulin secretion. Diabetologia. 2008 Apr;51(4):615-22. doi: 10.1007/s00125-007-0916-5. Epub 2008 Feb 13. PMID: 18270681; PMCID: PMC2270364.

Ling C, Del Guerra S, Lupi R, Rönn T, Granhall C, Luthman H, Masiello P, Marchetti P, Groop L, Del Prato S. Epigenetic regulation of PPARGC1A in human type 2 diabetic islets and effect on insulin secretion. Diabetologia. 2008 Apr;51(4):615-22. doi: 10.1007/s00125-007-0916-5. Epub 2008 Feb 13. PMID: 18270681; PMCID: PMC2270364.

Liu C, Lin JD. PGC-1 coactivators in the control of energy metabolism. Acta Biochim Biophys Sin (Shanghai). 2011 Apr;43(4):248-57. doi: 10.1093/abbs/gmr007. Epub 2011 Feb 16. PMID: 21325336; PMCID: PMC3063079.

Liu CC, Hu J, Tsai CW, Yue M, Melrose HL, Kanekiyo T, Bu G. Neuronal LRP1 regulates glucose metabolism and insulin signaling in the brain. J Neurosci. 2015 Apr 8;35(14):5851-9. doi: 10.1523/JNEUROSCI.5180-14.2015. PMID: 25855193; PMCID: PMC4388937.

Liu CC, Liu CC, Kanekiyo T, Xu H, Bu G. Apolipoprotein E and Alzheimer disease: risk, mechanisms and therapy. Nat Rev Neurol. 2013 Feb;9(2):106-18. doi: 10.1038/nrneurol.2012.263. Epub 2013 Jan 8. Erratum in: Nat Rev Neurol. 2013. doi: 10.1038/nmeurol.2013.32. Liu, Chia-Chan [corrected to Liu, Chia-Chen]. PMID: 23296339; PMCID: PMC3726719.

Liu CC, Zhao J, Fu Y, Inoue Y, Ren Y, Chen Y, Doss SV, Shue F, Jeevaratnam S, Bastea L, Wang N, Martens YA, Qiao W, Wang M, Zhao N, Jia L, Yamazaki Y, Yamazaki A, Rosenberg CL, Wang Z, Kong D, Li Z, Kuchenbecker LA, Trottier ZA, Felton L, Rogers J, Quicksall ZS, Linares C, Knight J, Chen Y, Kurti A, Kanekiyo T, Fryer JD, Asmann YW, Storz P, Wang X, Peng J, Zhang B, Kim BYS, Bu G. Peripheral apoE4 enhances Alzheimer's pathology and impairs cognition by compromising cerebrovascular function. Nat Neurosci. 2022 Aug;25(8):1020-1033. doi: 10.1038/s41593-022-01127-0. Epub 2022 Aug 1. PMID: 35915180; PMCID: PMC10009873.

Liu W, Wong A, Law AC, Mok VC. Cerebrovascular disease, amyloid plaques, and dementia. Stroke. 2015 May;46(5):1402-7. doi: 10.1161/STROKEAHA.114.006571. Epub 2015 Mar 12. PMID: 25765727

Liu Y, Liu F, Grundke-Iqbal I, Iqbal K, Gong CX. Deficient brain insulin signalling pathway in Alzheimer's disease and diabetes. J Pathol. 2011 Sep;225(1):54-62. doi: 10.1002/path.2912. Epub 2011 May 19. PMID: 21598254; PMCID: PMC4484598.

Livingston G, Huntley J, Sommerlad A, Ames D, Ballard C, Banerjee S, Brayne C, Burns A, Cohen-Mansfield J, Cooper C, Costafreda SG, Dias A, Fox N, Gitlin LN, Howard R, Kales HC, Kivimäki M, Larson EB, Ogunniyi A, Orgeta V, Ritchie K, Rockwood K, Sampson EL, Samus Q, Schneider LS, Selbæk G, Teri L, Mukadam N. Dementia prevention, intervention, and care: 2020 report of the Lancet Commission. Lancet. 2020 Aug 8;396(10248):413-446. doi: 10.1016/S0140-6736(20)30367-6. Epub 2020 Jul 30. PMID: 32738937; PMCID: PMC7392084.

Lobos P, Bruna B, Cordova A, Barattini P, Galáz JL, Adasme T, Hidalgo C, Muñoz P, Paula-Lima A. Astaxanthin Protects Primary Hippocampal Neurons against Noxious Effects of Aβ-Oligomers. Neural Plast. 2016; 2016:3456783. doi: 10.1155/2016/3456783. Epub 2016 Mar 1. PMID: 27034843; PMCID: PMC4791503.

Loewith R, Jacinto E, Wullschleger S, Lorberg A, Crespo JL, Bonenfant D, Oppliger W, Jenoe P, Hall MN. Two TOR complexes, only one of which is rapamycin sensitive, have distinct roles in cell growth control. Mol Cell. 2002 Sep;10(3):457-68. doi: 10.1016/s1097-2765(02)00636-6. PMID: 12408816.

Lopes DH, Colin C, Degaki TL, de Sousa AC, Vieira MN, Sebollela A, Martinez AM, Bloch C Jr, Ferreira ST, Sogayar MC. Amyloidogenicity and cytotoxicity of recombinant mature human islet amyloid polypeptide (rhIAPP). J Biol Chem. 2004 Oct 8;279(41):42803-10. doi: 10.1074/jbc.M406108200. Epub 2004 Jul 28. PMID: 15292167.

López-Otín C, Blasco MA, Partridge L, Serrano M, Kroemer G. The hallmarks of aging. Cell. 2013 Jun 6;153(6):1194-217. doi: 10.1016/j.cell.2013.05.039. PMID: 23746838; PMCID: PMC3836174.

Löscher W, Potschka H. Blood-brain barrier active efflux transporters: ATP-binding cassette gene family. NeuroRx. 2005 Jan;2(1):86-98. doi: 10.1602/neurorx.2.1.86. PMID: 15717060; PMCID: PMC539326.

Loukovaara M, Leinonen P, Teramo K, Nurminen E, Andersson S, Rutanen EM. Effect of maternal diabetes on phosphorylation of insulin-like growth factor binding protein-1 in cord serum. Diabet Med. 2005; 22(4):434–9. https://doi.org/10.1111/j.1464-5491.2005.01430.x PMID: 15787669.

Luchsinger JA, Reitz C, Patel B, Tang MX, Manly JJ, Mayeux R. Relation of diabetes to mild cognitive impairment. Arch Neurol. 2007 Apr;64(4):570-5. doi: 10.1001/archneur.64.4.570. PMID: 17420320.

Ma L, Allen M, Sakae N, Ertekin-Taner N, Graff-Radford NR, Dickson DW, Younkin SG, Sevlever D. Expression and processing analyses of wild type and p.R47H TREM2 variant in Alzheimer's disease brains. Mol Neurodegener. 2016 Nov 25;11(1):72. doi: 10.1186/s13024-016-0137-9. PMID: 27887626; PMCID: PMC5124229.

Ma QL, Yang F, Rosario ER, Ubeda OJ, Beech W, Gant DJ, Chen PP, Hudspeth B, Chen C, Zhao Y, Vinters HV, Frautschy SA, Cole GM. Beta-amyloid oligomers induce phosphorylation of tau and inactivation of insulin receptor substrate via c-Jun N-terminal kinase signaling: suppression by omega-3 fatty acids and curcumin. J Neurosci. 2009 Jul 15;29(28):9078-89. doi: 10.1523/JNEUROSCI.1071-09.2009. PMID: 19605645; PMCID: PMC3849615.

Ma T, Hoeffer CA, Capetillo-Zarate E, Yu F, Wong H, Lin MT, Tampellini D, Klann E, Blitzer RD, Gouras GK. Dysregulation of the mTOR pathway mediates impairment of synaptic plasticity in a mouse model of Alzheimer's disease. PLoS One. 2010 Sep 20;5(9): e12845. doi: 10.1371/journal.pone.0012845. PMID: 20862226; PMCID: PMC2942840.

Machado A, Herrera AJ, de Pablos RM, Espinosa-Oliva AM, Sarmiento M, Ayala A, Venero JL, Santiago M, Villarán RF, Delgado-Cortés MJ, Argüelles S, Cano J. Chronic stress as a risk factor for Alzheimer's disease. Rev Neurosci. 2014;25(6):785-804. doi: 10.1515/revneuro-2014-0035. PMID: 25178904.

Manly JJ, Jones RN, Langa KM, Ryan LH, Levine DA, McCammon R, Heeringa SG, Weir D. Estimating the Prevalence of Dementia and Mild Cognitive Impairment in the US: The 2016 Health and Retirement Study Harmonized Cognitive Assessment Protocol Project. JAMA Neurol. 2022 Dec 1;79(12):1242-1249. doi: 10.1001/jamaneurol.2022.3543. PMID: 36279130; PMCID: PMC9593315.

Maoz BM, Herland A, FitzGerald EA, Grevesse T, Vidoudez C, Pacheco AR, Sheehy SP, Park TE, Dauth S, Mannix R, Budnik N, Shores K, Cho A, Nawroth JC, Segrè D, Budnik B, Ingber DE, Parker KK. A linked organ-on-chip model of the human neurovascular unit reveals the metabolic coupling of endothelial and neuronal cells.

Nat Biotechnol. 2018 Oct;36(9):865-874. doi: 10.1038/nbt.4226. Epub 2018 Aug 20. PMID: 30125269; PMCID: PMC9254231.

Marchesi VT. Alzheimer's dementia begins as a disease of small blood vessels, damaged by oxidative-induced inflammation and dysregulated amyloid metabolism: implications for early detection and therapy. FASEB J. 2011 Jan;25(1):5-13. doi: 10.1096/fj.11-0102ufm. PMID: 21205781

Marchi N, Banjara M, Janigro D. Blood-brain barrier, bulk flow, and interstitial clearance in epilepsy. J Neurosci Methods. 2016 Feb 15; 260:118-24. doi: 10.1016/j.jneumeth.2015.06.011. Epub 2015 Jun 18. PMID: 26093166; PMCID: PMC4835226.

Mathys H, Davila-Velderrain J, Peng Z, Gao F, Mohammadi S, Young JZ, Menon M, He L, Abdurrob F, Jiang X, Martorell AJ, Ransohoff RM, Hafler BP, Bennett DA, Kellis M, Tsai LH. Single-cell transcriptomic analysis of Alzheimer's disease. Nature. 2019 Jun;570(7761):332-337. doi: 10.1038/s41586-019-1195-2. Epub 2019 May 1. Erratum in: Nature. 2019 Jun 17; PMID: 31042697; PMCID: PMC6865822.

Matsuo M, Campenot RB, Vance DE, Ueda K, Vance JE. Involvement of low-density lipoprotein receptor-related protein and ABCG1 in stimulation of axonal extension by apoE-containing lipoproteins. Biochim Biophys Acta. 2011 Jan;1811(1):31-8. doi: 10.1016/j.bbalip.2010.10.004. Epub 2010 Oct 30. PMID: 21040802.

Matyi J, Tschanz JT, Rattinger GB, Sanders C, Vernon EK, Corcoran C, Kauwe JSK, Buhusi M. Sex Differences in Risk for Alzheimer's Disease Related to Neurotrophin Gene Polymorphisms: The Cache County Memory Study. J Gerontol A Biol Sci Med Sci. 2017 Nov 9;72(12):1607-1613. doi: 10.1093/gerona/glx092. Erratum in: J Gerontol A Biol Sci Med Sci. 2018 Mar 2;73(3):311. PMID: 28498887; PMCID: PMC5861928.

Mawuenyega KG, Sigurdson W, Ovod V, Munsell L, Kasten T, Morris JC, Yarasheski KE, Bateman RJ. Decreased clearance of CNS beta-amyloid in Alzheimer's disease. Science. 2010 Dec 24;330(6012):1774. doi: 10.1126/science.1197623. Epub 2010 Dec 9. PMID: 21148344; PMCID: PMC3073454.

Mazzei G, Ikegami R, Abolhassani N, Haruyama N, Sakumi K, Saito T, Saido TC, Nakabeppu Y. A high-fat diet exacerbates the Alzheimer's disease pathology in the

hippocampus of the App$^{NL-F/NL-F}$ knock-in mouse model. Aging Cell. 2021 Aug;20(8): e13429. doi: 10.1111/acel.13429. Epub 2021 Jul 10. PMID: 34245097; PMCID: PMC8373331.

McColl G, Roberts BR, Gunn AP, Perez KA, Tew DJ, Masters CL, Barnham KJ, Cherny RA, Bush AI. The Caenorhabditis elegans A beta 1-42 model of Alzheimer disease predominantly expresses A beta 3-42. J Biol Chem. 2009 Aug 21;284(34):22697-702. doi: 10.1074/jbc.C109.028514. Epub 2009 Jul 2. PMID: 19574211; PMCID: PMC2755678.

McGeer PL, Itagaki S, Tago H, McGeer EG. Reactive microglia in patients with senile dementia of the Alzheimer type are positive for the histocompatibility glycoprotein HLA-DR. Neurosci Lett. 1987 Aug 18;79(1-2):195-200. doi: 10.1016/0304-3940(87)90696-3. PMID: 3670729.

McGeer PL, McGeer EG. Local neuroinflammation and the progression of Alzheimer's disease. J Neurovirol. 2002 Dec;8(6):529-38. doi: 10.1080/13550280290100969. PMID: 12476347.

McGeer PL, McGeer EG. Polymorphisms in inflammatory genes and the risk of Alzheimer disease. Arch Neurol. 2001 Nov;58(11):1790-2. doi: 10.1001/archneur.58.11.1790. PMID: 11708985

McGeer PL, McGeer EG. The possible role of complement activation in Alzheimer disease. Trends Mol Med. 2002 Nov;8(11):519-23. doi: 10.1016/s1471-4914(02)02422-x. PMID: 12421685.

McGeer PL, Rogers J. Anti-inflammatory agents as a therapeutic approach to Alzheimer's disease. Neurology. 1992 Feb;42(2):447-9. doi: 10.1212/wnl.42.2.447. PMID: 1736183.

McKhann GM, Knopman DS, Chertkow H, Hyman BT, Jack CR Jr, Kawas CH, Klunk WE, Koroshetz WJ, Manly JJ, Mayeux R, Mohs RC, Morris JC, Rossor MN, Scheltens P, Carrillo MC, Thies B, Weintraub S, Phelps CH. The diagnosis of dementia due to Alzheimer's disease: recommendations from the National Institute on Aging-Alzheimer's Association workgroups on diagnostic guidelines for Alzheimer's disease. Alzheimers Dement. 2011 May;7(3):263-9. doi:

10.1016/j.jalz.2011.03.005. Epub 2011 Apr 21. PMID: 21514250; PMCID: PMC3312024.

McMillan DE. Elevation of glycoprotein fucose in diabetes mellitus. Diabetes. 1972; 21(8):863–71. PMID: 4114640.

McShane R, Areosa Sastre A, Minakaran N. Memantine for dementia. Cochrane Database Syst Rev. 2006 Apr 19;(2):CD003154. doi: 10.1002/14651858.CD003154.pub5. Update in: Cochrane Database Syst Rev. 2019 Mar 20;3:CD003154. PMID: 16625572

Meilandt WJ, Ngu H, Gogineni A, Lalehzadeh G, Lee SH, Srinivasan K, Imperio J, Wu T, Weber M, Kruse AJ, Stark KL, Chan P, Kwong M, Modrusan Z, Friedman BA, Elstrott J, Foreman O, Easton A, Sheng M, Hansen DV. Trem2 Deletion Reduces Late-Stage Amyloid Plaque Accumulation, Elevates the Aβ42: Aβ40 Ratio, and Exacerbates Axonal Dystrophy and Dendritic Spine Loss in the PS2APP Alzheimer's Mouse Model. J Neurosci. 2020 Feb 26;40(9):1956-1974. doi: 10.1523/JNEUROSCI.1871-19.2019. Epub 2020 Jan 24. PMID: 31980586; PMCID: PMC7046459.

Mejlvang J, Olsvik H, Svenning S, Bruun JA, Abudu YP, Larsen KB, Brech A, Hansen TE, Brenne H, Hansen T, Stenmark H, Johansen T. Starvation induces rapid degradation of selective autophagy receptors by endosomal microautophagy. J Cell Biol. 2018 Oct 1;217(10):3640-3655. doi: 10.1083/jcb.201711002. Epub 2018 Jul 17. PMID: 30018090; PMCID: PMC6168274.

Meraz-Ríos MA, Toral-Rios D, Franco-Bocanegra D, Villeda-Hernández J, Campos-Peña V. Inflammatory process in Alzheimer's Disease. Front Integr Neurosci. 2013 Aug 13; 7:59. doi: 10.3389/fnint.2013.00059. PMID: 23964211; PMCID: PMC3741576.

Metaxakis A, Ploumi C, Tavernarakis N. Autophagy in Age-Associated Neurodegeneration. Cells. 2018 May 5;7(5):37. doi: 10.3390/cells7050037. PMID: 29734735; PMCID: PMC5981261.

Michalik L, Auwerx J, Berger JP, Chatterjee VK, Glass CK, Gonzalez FJ, Grimaldi PA, Kadowaki T, Lazar MA, O'Rahilly S, Palmer CN, Plutzky J, Reddy JK, Spiegelman BM, Staels B, Wahli W. International Union of Pharmacology. LXI.

Peroxisome proliferator-activated receptors. Pharmacol Rev. 2006 Dec;58(4):726-41. doi: 10.1124/pr.58.4.5. PMID: 17132851.

Miech RA, Breitner JC, Zandi PP, Khachaturian AS, Anthony JC, Mayer L. Incidence of AD may decline in the early 90s for men, later for women: The Cache County study. Neurology. 2002 Jan 22;58(2):209-18. doi: 10.1212/wnl.58.2.209. PMID: 11805246.

Miedema K. Standardization of HbA1c and optimal range of monitoring. Scandinavian journal of clinical and laboratory investigation. 2005; 65(sup240):61–72. https://doi.org/10.1080/00365510500236143 PMID: 16112961.

Mielke MM, Milic NM, Weissgerber TL, White WM, Kantarci K, Mosley TH, Windham BG, Simpson BN, Turner ST, Garovic VD. Impaired Cognition and Brain Atrophy Decades After Hypertensive Pregnancy Disorders. Circ Cardiovasc Qual Outcomes. 2016 Feb;9(2 Suppl 1): S70-6. doi: 10.1161/CIRCOUTCOMES.115.002461. PMID: 26908863; PMCID: PMC4770570.

Mielke MM, Vemuri P, Rocca WA. Clinical epidemiology of Alzheimer's disease: assessing sex and gender differences. Clin Epidemiol. 2014 Jan 8; 6:37-48. doi: 10.2147/CLEP.S37929. PMID: 24470773; PMCID: PMC3891487.

Miklossy J, McGeer PL. Common mechanisms involved in Alzheimer's disease and type 2 diabetes: a key role of chronic bacterial infection and inflammation. Aging (Albany NY). 2016 Apr;8(4):575-88. doi: 10.18632/aging.100921. PMID: 26961231; PMCID: PMC4925815.

Miklossy J, Qing H, Radenovic A, Kis A, Vileno B, Làszló F, Miller L, Martins RN, Waeber G, Mooser V, Bosman F, Khalili K, Darbinian N, McGeer PL. Beta amyloid and hyperphosphorylated tau deposits in the pancreas in type 2 diabetes. Neurobiol Aging. 2010 Sep;31(9):1503-15. doi: 10.1016/j.neurobiolaging.2008.08.019. Epub 2008 Oct 23. PMID: 18950899; PMCID: PMC4140193.

Miller DL, Papayannopoulos IA, Styles J, Bobin SA, Lin YY, Biemann K, Iqbal K. Peptide compositions of the cerebrovascular and senile plaque core amyloid deposits of Alzheimer's disease. Arch Biochem Biophys. 1993 Feb 15;301(1):41-52. doi: 10.1006/abbi.1993.1112. PMID: 8442665.

Millucci L, Ghezzi L, Bernardini G, Santucci A. Conformations and biological activities of amyloid beta peptide 25-35. Curr Protein Pept Sci. 2010 Feb;11(1):54-67. doi: 10.2174/138920310790274626. PMID: 20201807.

Milton NG. Phosphorylated amyloid-beta: the toxic intermediate in alzheimer's disease neurodegeneration. Subcell Biochem. 2005; 38:381-402. doi: 10.1007/0-387-23226-5_20. PMID: 15709490.

Milton NG. Phosphorylation of amyloid-beta at the serine 26 residue by human cdc2 kinase. Neuroreport. 2001 Dec 4;12(17):3839-44. doi: 10.1097/00001756-200112040-00047. PMID: 11726805.

Mintun MA, Lo AC, Duggan Evans C, Wessels AM, Ardayfio PA, Andersen SW, Shcherbinin S, Sparks J, Sims JR, Brys M, Apostolova LG, Salloway SP, Skovronsky DM. Donanemab in Early Alzheimer's Disease. N Engl J Med. 2021 May 6;384(18):1691-1704. doi: 10.1056/NEJMoa2100708. Epub 2021 Mar 13. PMID: 33720637.

Miragliotta G, Del Prete R, Mosca A. Helicobacter pylori infection and coronary heart disease. Lancet. 1994 Sep 10;344(8924):751. doi: 10.1016/s0140-6736(94)92240-3. PMID: 7915795.

Miranda-Díaz AG, Pazarín-Villaseñor L, Yanowsky-Escatell FG, Andrade-Sierra J. Oxidative Stress in Diabetic Nephropathy with Early Chronic Kidney Disease. J Diabetes Res. 2016; 2016:7047238. doi: 10.1155/2016/7047238. Epub 2016 Jul 20. PMID: 27525285; PMCID: PMC4971321.

Miravalle L, Calero M, Takao M, Roher AE, Ghetti B, Vidal R. Amino-terminally truncated Abeta peptide species are the main component of cotton wool plaques. Biochemistry. 2005 Aug 16;44(32):10810-21. doi: 10.1021/bi0508237. PMID: 16086583.

Mizushima N. Autophagy: process and function. Genes Dev. 2007 Nov 15;21(22):2861-73. doi: 10.1101/gad.1599207. PMID: 18006683.

Montagne A, Barnes SR, Sweeney MD, Halliday MR, Sagare AP, Zhao Z, Toga AW, Jacobs RE, Liu CY, Amezcua L, Harrington MG, Chui HC, Law M, Zlokovic BV. Blood-brain barrier breakdown in the aging human hippocampus. Neuron. 2015 Jan

21;85(2):296-302. doi: 10.1016/j.neuron.2014.12.032. PMID: 25611508; PMCID: PMC4350773.

Monteiro C, Toth B, Wildsmith K, Sanabria-Bohorquez S, Brunstein F, Madsen A, Dolton M, Ramakrishnan V, Abramzon D, Teng E. Phase 2 trial of semorinemab in mild-to-moderate Alzheimer's disease (LAURIET): topline results. J Prev Alzheimers Dis. 2021;8(Suppl 1): S11.

Mootha VK, Lindgren CM, Eriksson KF, Subramanian A, Sihag S, Lehar J, Puigserver P, Carlsson E, Ridderstråle M, Laurila E, Houstis N, Daly MJ, Patterson N, Mesirov JP, Golub TR, Tamayo P, Spiegelman B, Lander ES, Hirschhorn JN, Altshuler D, Groop LC. PGC-1alpha-responsive genes involved in oxidative phosphorylation are coordinately downregulated in human diabetes. Nat Genet. 2003 Jul;34(3):267-73. doi: 10.1038/ng1180. PMID: 12808457.

Moran C, Beare R, Wang W, Callisaya M, Srikanth V; Alzheimer's Disease Neuroimaging Initiative (ADNI). Type 2 diabetes mellitus, brain atrophy, and cognitive decline. Neurology. 2019 Feb 19;92(8): e823-e830. doi: 10.1212/WNL.0000000000006955. Epub 2019 Jan 23. PMID: 30674592; PMCID: PMC7987953.

Morán-Salvador E, López-Parra M, García-Alonso V, Titos E, Martínez-Clemente M, González-Périz A, López-Vicario C, Barak Y, Arroyo V, Clària J. Role for PPARγ in obesity-induced hepatic steatosis as determined by hepatocyte- and macrophage-specific conditional knockouts. FASEB J. 2011 Aug;25(8):2538-50. doi: 10.1096/fj.10-173716. Epub 2011 Apr 19. PMID: 21507897.

Mori H, Ishii K, Tomiyama T, Furiya Y, Sahara N, Asano S, Endo N, Shirasawa T, Takio K. Racemization: its biological significance on neuropathogenesis of Alzheimer's disease. Tohoku J Exp Med. 1994 Nov;174(3):251-62. doi: 10.1620/tjem.174.251. PMID: 7761990.

Morris R. Developments of a water-maze procedure for studying spatial learning in the rat. J Neurosci Methods. 1984 May;11(1):47-60. doi: 10.1016/0165-0270(84)90007-4. PMID: 6471907.

Mosconi L, Berti V, Quinn C, McHugh P, Petrongolo G, Varsavsky I, Osorio RS, Pupi A, Vallabhajosula S, Isaacson RS, de Leon MJ, Brinton RD. Sex differences in

Alzheimer risk: Brain imaging of endocrine vs chronologic aging. Neurology. 2017 Sep 26;89(13):1382-1390. doi: 10.1212/WNL.0000000000004425. Epub 2017 Aug 30. PMID: 28855400; PMCID: PMC5652968.

Mraz M, Bartlova M, Lacinova Z, Michalsky D, Kasalicky M, Haluzikova D, Matoulek M, Dostalova I, Humenanska V, Haluzik M. Serum concentrations and tissue expression of a novel endocrine regulator fibroblast growth factor-21 in patients with type 2 diabetes and obesity. Clin Endocrinol (Oxf). 2009 Sep;71(3):369-75. doi: 10.1111/j.1365-2265.2008.03502. x. Epub 2008 Dec 11. PMID: 19702724.

Mrdjen D, Pavlovic A, Hartmann FJ, Schreiner B, Utz SG, Leung BP, Lelios I, Heppner FL, Kipnis J, Merkler D, Greter M, Becher B. High-Dimensional Single-Cell Mapping of Central Nervous System Immune Cells Reveals Distinct Myeloid Subsets in Health, Aging, and Disease. Immunity. 2018 Feb 20;48(2):380-395.e6. doi: 10.1016/j.immuni.2018.01.011. Epub 2018 Feb 6. Erratum in: Immunity. 2018 Mar 20;48(3):599. PMID: 29426702.

Mudher A, Lovestone S. Alzheimer's disease-do tauists and baptists finally shake hands? Trends Neurosci. 2002 Jan;25(1):22-6. doi: 10.1016/s0166-2236(00)02031-2. PMID: 11801334

Mukherjee A, Morales-Scheihing D, Salvadores N, Moreno-Gonzalez I, Gonzalez C, Taylor-Presse K, Mendez N, Shahnawaz M, Gaber AO, Sabek OM, Fraga DW, Soto C. Induction of IAPP amyloid deposition and associated diabetic abnormalities by a prion-like mechanism. J Exp Med. 2017 Sep 4;214(9):2591-2610. doi: 10.1084/jem.20161134. Epub 2017 Aug 1. PMID: 28765400; PMCID: PMC5584114.

Mullard A. Failure of first anti-tau antibody in Alzheimer disease highlights risks of history repeating. Nat Rev Drug Discov. 2021 Jan;20(1):3-5. doi: 10.1038/d41573-020-00217-7. PMID: 33303932

Murakami K, Uno M, Masuda Y, Shimizu T, Shirasawa T, Irie K. Isomerization and/or racemization at Asp23 of Abeta42 do not increase its aggregative ability, neurotoxicity, and radical productivity in vitro. Biochem Biophys Res Commun. 2008 Feb 15;366(3):745-51. doi: 10.1016/j.bbrc.2007.12.009. Epub 2007 Dec 17. PMID: 18078812.

Nakae J, Biggs WH 3rd, Kitamura T, Cavenee WK, Wright CV, Arden KC, Accili D. Regulation of insulin action and pancreatic beta-cell function by mutated alleles of the

gene encoding forkhead transcription factor Foxo1. Nat Genet. 2002 Oct;32(2):245-53. doi: 10.1038/ng890. Epub 2002 Sep 3. PMID: 12219087.

Nakajima C, Haffner P, Goerke SM, Zurhove K, Adelmann G, Frotscher M, Herz J, Bock HH, May P. The lipoprotein receptor LRP1 modulates sphingosine-1-phosphate signaling and is essential for vascular development. Development. 2014 Dec;141(23):4513-25. doi: 10.1242/dev.109124. Epub 2014 Nov 5. PMID: 25377550; PMCID: PMC4302929.

Nakatogawa H. Mechanisms governing autophagosome biogenesis. Nat Rev Mol Cell Biol. 2020 Aug;21(8):439-458. doi: 10.1038/s41580-020-0241-0. Epub 2020 May 5. PMID: 32372019.

Natunen T, Martiskainen H, Sarajärvi T, Helisalmi S, Pursiheimo JP, Viswanathan J, Laitinen M, Mäkinen P, Kauppinen T, Rauramaa T, Leinonen V, Alafuzoff I, Haapasalo A, Soininen H, Hiltunen M. Effects of NR1H3 genetic variation on the expression of liver X receptor α and the progression of Alzheimer's disease. PLoS One. 2013 Nov 20;8(11):e80700. doi: 10.1371/journal.pone.0080700. PMID: 24278306; PMCID: PMC3835410

Nguyen AT, Wang K, Hu G, Wang X, Miao Z, Azevedo JA, Suh E, Van Deerlin VM, Choi D, Roeder K, Li M, Lee EB. APOE and TREM2 regulate amyloid-responsive microglia in Alzheimer's disease. Acta Neuropathol. 2020 Oct;140(4):477-493. doi: 10.1007/s00401-020-02200-3. Epub 2020 Aug 25. Erratum in: Acta Neuropathol. 2023 Aug 17; PMID: 32840654; PMCID: PMC7520051.

Nho K, Kueider-Paisley A, Ahmad S, Mahmoudian Dehkordi S, Arnold M, Risacher SL, Louie G, Blach C, Baillie R, Han X, Kastenmüller G, Trojanowski JQ, Shaw LM, Weiner MW, Doraiswamy PM, van Duijn C, Saykin AJ, Kaddurah-Daouk R; Alzheimer’s Disease Neuroimaging Initiative and the Alzheimer Disease Metabolomics Consortium. Association of Altered Liver Enzymes with Alzheimer Disease Diagnosis, Cognition, Neuroimaging Measures, and Cerebrospinal Fluid Biomarkers. JAMA Netw Open. 2019 Jul 3;2(7): e197978. doi: 10.1001/jamanetworkopen.2019.7978. PMID: 31365104; PMCID: PMC6669786.

Ni Y, Nagashimada M, Zhuge F, Zhan L, Nagata N, Tsutsui A, Nakanuma Y, Kaneko S, Ota T. Astaxanthin prevents and reverses diet-induced insulin resistance and

steatohepatitis in mice: A comparison with vitamin E. Sci Rep. 2015 Nov 25;5:17192. doi: 10.1038/srep17192. PMID: 26603489; PMCID: PMC4658633

Nicolau C, Greferath R, Balaban TS, Lazarte JE, Hopkins RJ. A liposome-based therapeutic vaccine against beta -amyloid plaques on the pancreas of transgenic NORBA mice. Proc Natl Acad Sci U S A. 2002 Feb 19;99(4):2332-7. doi: 10.1073/pnas.022627199. Epub 2002 Feb 12. PMID: 11842183; PMCID: PMC122365.

Nicolazzo JA, Mehta DC. Transport of drugs across the blood-brain barrier in Alzheimer's disease. Ther Deliv. 2010 Oct;1(4):595-611. doi: 10.4155/tde.10.41. PMID: 22833970.

Niikura T, TaGma H, Kita Y. Neuronal cell death in Alzheimer's disease and a neuroprotective factor, humanin. Curr Neuropharmacol. 2006 Apr;4(2):139-47. doi: 10.2174/157015906776359577. PMID: 18615127; PMCID: PMC2430668.

Nilsson E, Jansson PA, Perfilyev A, Volkov P, Pedersen M, Svensson MK, Poulsen P, Ribel-Madsen R, Pedersen NL, Almgren P, Fadista J, Rönn T, Klarlund Pedersen B, Scheele C, Vaag A, Ling C. Altered DNA methylation and differential expression of genes influencing metabolism and inflammation in adipose tissue from subjects with type 2 diabetes. Diabetes. 2014 Sep;63(9):2962-76. doi: 10.2337/db13-1459. Epub 2014 May 8. PMID: 24812430.

Nilsson E, Matte A, Perfilyev A, de Mello VD, Käkelä P, Pihlajamäki J, Ling C. Epigenetic Alterations in Human Liver from Subjects with Type 2 Diabetes in Parallel With Reduced Folate Levels. J Clin Endocrinol Metab. 2015 Nov;100(11): E1491-501. doi: 10.1210/jc.2015-3204. Epub 2015 Sep 29. PMID: 26418287; PMCID: PMC4702449.

Nitert MD, Dayeh T, Volkov P, Elgzyri T, Hall E, Nilsson E, Yang BT, Lang S, Parikh H, Wessman Y, Weishaupt H, Attema J, Abels M, Wierup N, Almgren P, Jansson PA, Rönn T, Hansson O, Eriksson KF, Groop L, Ling C. Impact of an exercise intervention on DNA methylation in skeletal muscle from first-degree relatives of patients with type 2 diabetes. Diabetes. 2012 Dec;61(12):3322-32. doi: 10.2337/db11-1653. Epub 2012 Oct 1. PMID: 23028138; PMCID: PMC3501844.

Nixon RA, Wegiel J, Kumar A, Yu WH, Peterhoff C, Cataldo A, Cuervo AM. Extensive involvement of autophagy in Alzheimer disease: an immuno-electron microscopy study. J Neuropathol Exp Neurol. 2005 Feb;64(2):113-22. doi: 10.1093/jnen/64.2.113. PMID: 15751225.

Nixon RA. Amyloid precursor protein and endosomal-lysosomal dysfunction in Alzheimer's disease: inseparable partners in a multifactorial disease. FASEB J. 2017 Jul;31(7):2729-2743. doi: 10.1096/fj.201700359. PMID: 28663518; PMCID: PMC6137496.

Noroozi Karimabad M, Khalili P, Ayoobi F, Esmaeili-Nadimi A, La Vecchia C, Jamali Z. Serum liver enzymes and diabetes from the Rafsanjan cohort study. BMC Endocr Disord. 2022 May 12;22(1):127. doi: 10.1186/s12902-022-01042-2. PMID: 35549705; PMCID: PMC9102258.

Norton L, Shannon CE, Fourcaudot M, Hu C, Wang N, Ren W, Song J, Abdul-Ghani M, DeFronzo RA, Ren J, Jia W. Sodium-glucose co-transporter (SGLT) and glucose transporter (GLUT) expression in the kidney of type 2 diabetic subjects. Diabetes Obes Metab. 2017 Sep;19(9):1322-1326. doi: 10.1111/dom.13003. Epub 2017 Jul 13. PMID: 28477418.

O'Brien JA, Patrick AR, Caro J. Estimates of direct medical costs for microvascular and macrovascular complications resulting from type 2 diabetes mellitus in the United States in 2000. Clin Ther. 2003; 25:1017-1038

Oddo S. The role of mTOR signaling in Alzheimer disease. Front Biosci (Schol Ed). 2012 Jan 1;4(3):941-52. doi: 10.2741/s310. PMID: 22202101; PMCID: PMC4111148.

Orihuela R, McPherson CA, Harry GJ. Microglial M1/M2 polarization and metabolic states. Br J Pharmacol. 2016 Feb;173(4):649-65. doi: 10.1111/bph.13139. Epub 2015 May 11. PMID: 25800044; PMCID: PMC4742299.

Ott A, Stolk RP, van Harskamp F, Pols HA, Hofman A, Breteler MM. Diabetes mellitus and the risk of dementia: The Rotterdam Study. Neurology. 1999 Dec 10;53(9):1937-42. doi: 10.1212/wnl.53.9.1937. PMID: 10599761.

P X, Zz L, Gg J, Lp W, Cm B, Yl W, Chen MF, W L. The role of LRP1 in Aβ efflux transport across the blood-brain barrier and cognitive dysfunction in diabetes

mellitus. Neurochem Int. 2022 Nov; 160:105417. doi: 10.1016/j.neuint.2022.105417. Epub 2022 Sep 5. PMID: 36067928.

Papageorgiou IE, Lewen A, Galow LV, Cesetti T, Scheffel J, Regen T, Hanisch UK, Kann O. TLR4-activated microglia require IFN-γ to induce severe neuronal dysfunction and death in situ. Proc Natl Acad Sci U S A. 2016 Jan 5;113(1):212-7. doi: 10.1073/pnas.1513853113. Epub 2015 Dec 22. PMID: 26699475; PMCID: PMC4711883.

Parzych KR, Klionsky DJ. An overview of autophagy: morphology, mechanism, and regulation. Antioxid Redox Signal. 2014 Jan 20;20(3):460-73. doi: 10.1089/ars.2013.5371. Epub 2013 Aug 2. PMID: 23725295; PMCID: PMC3894687

Patabendige A, Janigro D. The role of the blood-brain barrier during neurological disease and infection. Biochem Soc Trans. 2023 Apr 26;51(2):613-626. doi: 10.1042/BST20220830. PMID: 36929707; PMCID: PMC10212550.

Patti ME, Butte AJ, Crunkhorn S, Cusi K, Berria R, Kashyap S, Miyazaki Y, Kohane I, Costello M, Saccone R, Landaker EJ, Goldfine AB, Mun E, DeFronzo R, Finlayson J, Kahn CR, Mandarino LJ. Coordinated reduction of genes of oxidative metabolism in humans with insulin resistance and diabetes: Potential role of PGC1 and NRF1. Proc Natl Acad Sci U S A. 2003 Jul 8;100(14):8466-71. doi: 10.1073/pnas.1032913100. Epub 2003 Jun 27. PMID: 12832613; PMCID: PMC166252.

Paxinos, G. and Franklin, K.B.J. (2001) The Mouse Brain in Stereotaxic Coordinates. 2nd Edition, Academic Press, San Diego.

Pei JJ, Braak E, Braak H, Grundke-Iqbal I, Iqbal K, Winblad B, Cowburn RF. Distribution of active glycogen synthase kinase 3beta (GSK-3beta) in brains staged for Alzheimer disease neurofibrillary changes. J Neuropathol Exp Neurol. 1999 Sep;58(9):1010-9. doi: 10.1097/00005072-199909000-00011. PMID: 10499443.

Peila R, Rodriguez BL, Launer LJ; Honolulu-Asia Aging Study. Type 2 diabetes, APOE gene, and the risk for dementia and related pathologies: The Honolulu-Asia Aging Study. Diabetes. 2002 Apr;51(4):1256-62. doi: 10.2337/diabetes.51.4.1256. PMID: 11916953.

Pereira CD, Martins F, Wiltfang J, da Cruz E Silva OAB, Rebelo S. ABC Transporters Are Key Players in Alzheimer's Disease. J Alzheimers Dis. 2018;61(2):463-485. doi: 10.3233/JAD-170639. PMID: 29171999.

Pereyra M, Katche C, de Landeta AB, Medina JH. mTORC1 controls long-term memory retrieval. Sci Rep. 2018 Jun 8;8(1):8759. doi: 10.1038/s41598-018-27053-5. PMID: 29884898; PMCID: PMC5993780.

Perlmuter LC, Hakami MK, Hodgson-Harrington C, Ginsberg J, Katz J, Singer DE, Nathan DM. Decreased cognitive function in aging non-insulin-dependent diabetic patients. Am J Med. 1984 Dec;77(6):1043-8. doi: 10.1016/0002-9343(84)90186-4. PMID: 6334441.

Pflanzner T, Kuhlmann CR, Pietrzik CU. Blood-brain-barrier models for the investigation of transporter- and receptor-mediated amyloid-β clearance in Alzheimer's disease. Curr Alzheimer Res. 2010 Nov;7(7):578-90. doi: 10.2174/156720510793499066. PMID: 20704558.

Piaceri I, Nacmias B, Sorbi S. Genetics of familial and sporadic Alzheimer's disease. Front Biosci (Elite Ed). 2013 Jan 1;5(1):167-77. doi: 10.2741/e605. PMID: 23276979.

Piccini A, Russo C, Gliozzi A, Relini A, Vitali A, Borghi R, Giliberto L, Armirotti A, D'Arrigo C, Bachi A, Cattaneo A, Canale C, Torrassa S, Saido TC, Markesbery W, Gambetti P, Tabaton M. beta-amyloid is different in normal aging and in Alzheimer disease. J Biol Chem. 2005 Oct 7;280(40):34186-92. doi: 10.1074/jbc.M501694200. Epub 2005 Aug 15. PMID: 16103127.

Pickford F, Masliah E, Britschgi M, Lucin K, Narasimhan R, Jaeger PA, Small S, Spencer B, Rockenstein E, Levine B, Wyss-Coray T. The autophagy-related protein beclin 1 shows reduced expression in early Alzheimer disease and regulates amyloid beta accumulation in mice. J Clin Invest. 2008 Jun;118(6):2190-9. doi: 10.1172/JCI33585. PMID: 18497889; PMCID: PMC2391284.

Pike CJ. Sex and the development of Alzheimer's disease. J Neurosci Res. 2017 Jan 2;95(1-2):671-680. doi: 10.1002/jnr.23827. PMID: 27870425; PMCID: PMC5120614.

Plassman BL, Langa KM, Fisher GG, Heeringa SG, Weir DR, Ofstedal MB, Burke JR, Hurd MD, Potter GG, Rodgers WL, Steffens DC, Willis RJ, Wallace RB. Prevalence of dementia in the United States: the aging, demographics, and memory

study. Neuroepidemiology. 2007;29(1-2):125-32. doi: 10.1159/000109998. Epub 2007 Oct 29. PMID: 17975326; PMCID: PMC2705925.

Plata-Salamán CR, ffrench-Mullen JM. Interleukin-1 beta inhibits Ca2+ channel currents in hippocampal neurons through protein kinase C. Eur J Pharmacol. 1994 Jan 1;266(1):1-10. doi: 10.1016/0922-4106(94)90202-x. PMID: 8137877.

Poling MC, Kauffman AS. Organizational and activational effects of sex steroids on kisspeptin neuron development. Front Neuroendocrinol. 2013 Jan;34(1):3-17. doi: 10.1016/j.yfrne.2012.06.001. Epub 2012 Jun 19. PMID: 22728025; PMCID: PMC3725275.

Polonsky KS. Dynamics of insulin secretion in obesity and diabetes. Int J Obes Relat Metab Disord. 2000 Jun;24 Suppl 2: S29-31. doi: 10.1038/sj.ijo.0801273. PMID: 10997604.

Porte D Jr, Seeley RJ, Woods SC, Baskin DG, Figlewicz DP, Schwartz MW. Obesity, diabetes and the central nervous system. Diabetologia. 1998 Aug;41(8):863-81. doi: 10.1007/s001250051002. PMID: 9726588.

Portelius E, Bogdanovic N, Gustavsson MK, Volkmann I, Brinkmalm G, Zetterberg H, Winblad B, Blennow K. Mass spectrometric characterization of brain amyloid beta isoform signatures in familial and sporadic Alzheimer's disease. Acta Neuropathol. 2010 Aug;120(2):185-93. doi: 10.1007/s00401-010-0690-1. Epub 2010 Apr 24. PMID: 20419305; PMCID: PMC3568930.

Postma IR, Bouma A, Ankersmit IF, Zeeman GG. Neurocognitive functioning following preeclampsia and eclampsia: a long-term follow-up study. Am J Obstet Gynecol. 2014 Jul;211(1):37.e1-9. doi: 10.1016/j.ajog.2014.01.042. Epub 2014 Feb 1. PMID: 24495666.

Pradeepkiran JA, Baig J, Selman A, Reddy PH. Mitochondria in Aging and Alzheimer's Disease: Focus on Mitophagy. Neuroscientist. 2023 Jan 3:10738584221139761. doi: 10.1177/10738584221139761. Epub ahead of print. PMID: 36597577.

Pradhan LK, Sahoo PK, Chauhan S, Das SK. Recent Advances Towards Diagnosis and Therapeutic Fingerprinting for Alzheimer's Disease. J Mol Neurosci. 2022

Jun;72(6):1143-1165. doi: 10.1007/s12031-022-02009-7. Epub 2022 May 12. PMID: 35553375

Qian M, Fang X, Wang X. Autophagy and inflammation. Clin Transl Med. 2017 Dec;6(1):24. doi: 10.1186/s40169-017-0154-5. Epub 2017 Jul 26. PMID: 28748360; PMCID: PMC5529308

Qinna NA, Badwan AA. Impact of streptozotocin on altering normal glucose homeostasis during insulin testing in diabetic rats compared to normoglycemic rats. Drug design, development and therapy. 2015; 9:2515. https://doi.org/10.2147/DDDT.S79885 PMID: 26005328.

Qosa H, Miller DS, Pasinelli P, Trotti D. Regulation of ABC efflux transporters at blood-brain barrier in health and neurological disorders. Brain Res. 2015 Dec 2;1628(Pt B):298-316. doi: 10.1016/j.brainres.2015.07.005. Epub 2015 Jul 15. PMID: 26187753; PMCID: PMC4681613.

Querfurth HW, LaFerla FM. Alzheimer's disease. N Engl J Med. 2010 Jan 28;362(4):329-44. doi: 10.1056/NEJMra0909142. Erratum in: N Engl J Med. 2011 Feb 10;364(6):588. PMID: 20107219.

Quiroz YT, Zetterberg H, Reiman EM, Chen Y, Su Y, Fox-Fuller JT, Garcia G, Villegas A, Sepulveda-Falla D, Villada M, Arboleda-Velasquez JF, Guzmán-Vélez E, Vila-Castelar C, Gordon BA, Schultz SA, Protas HD, Ghisays V, Giraldo M, Tirado V, Baena A, Munoz C, Rios-Romenets S, Tariot PN, Blennow K, Lopera F. Plasma neurofilament light chain in the presenilin 1 E280A autosomal dominant Alzheimer's disease kindred: a cross-sectional and longitudinal cohort study. Lancet Neurol. 2020 Jun;19(6):513-521. doi: 10.1016/S1474-4422(20)30137-X. Epub 2020 May 26. PMID: 32470423; PMCID: PMC7417082.

Rahman SO, Panda BP, Parvez S, Kaundal M, Hussain S, Akhtar M, Najmi AK. Neuroprotective role of astaxanthin in hippocampal insulin resistance induced by Aβ peptides in animal model of Alzheimer's disease. Biomed Pharmacother. 2019 Feb; 110:47-58. doi: 10.1016/j.biopha.2018.11.043. Epub 2018 Nov 18. PMID: 30463045.

Rains JL, Jain SK. Oxidative stress, insulin signaling, and diabetes. Free Radic Biol Med. 2011 Mar 1;50(5):567-75. doi: 10.1016/j.freeradbiomed.2010.12.006. Epub 2010 Dec 13. PMID: 21163346; PMCID: PMC3557825.

Rajan KB, Weuve J, Barnes LL, McAninch EA, Wilson RS, Evans DA. Population estimate of people with clinical Alzheimer's disease and mild cognitive impairment in the United States (2020-2060). Alzheimers Dement. 2021 Dec;17(12):1966-1975. doi: 10.1002/alz.12362. Epub 2021 May 27. PMID: 34043283; PMCID: PMC9013315.

Rajendran L, Honsho M, Zahn TR, Keller P, Geiger KD, Verkade P, Simons K. Alzheimer's disease beta-amyloid peptides are released in association with exosomes. Proc Natl Acad Sci U S A. 2006 Jul 25;103(30):11172-7. doi: 10.1073/pnas.0603838103. Epub 2006 Jul 12. PMID: 16837572; PMCID: PMC1544060

Ramos-Rodriguez JJ, Jimenez-Palomares M, Murillo-Carretero MI, Infante-Garcia C, Berrocoso E, Hernandez-Pacho F, Lechuga-Sancho AM, Cozar-Castellano I, Garcia-Alloza M. Central vascular disease and exacerbated pathology in a mixed model of type 2 diabetes and Alzheimer's disease. Psychoneuroendocrinology. 2015 Dec; 62:69-79. doi: 10.1016/j.psyneuen.2015.07.606. Epub 2015 Jul 26. PMID: 26254770.

Rapposelli S, Digiacomo M, Balsamo A. P-gp transporter and its role in neurodegenerative diseases. Curr Top Med Chem. 2009;9(2):209-17. doi: 10.2174/156802609787521544. PMID: 19200006.

Raz L, Knoefel J, Bhaskar K. The neuropathology and cerebrovascular mechanisms of dementia. J Cereb Blood Flow Metab. 2016 Jan;36(1):172-86. doi: 10.1038/jcbfm.2015.164. PMID: 26174330; PMCID: PMC4758551.

Razay G, Vreugdenhil A, Wilcock G. The metabolic syndrome and Alzheimer disease. Arch Neurol. 2007 Jan;64(1):93-6. doi: 10.1001/archneur.64.1.93. PMID: 17210814.

Reiman EM, Quiroz YT, Fleisher AS, Chen K, Velez-Pardo C, Jimenez-Del-Rio M, Fagan AM, Shah AR, Alvarez S, Arbelaez A, Giraldo M, Acosta-Baena N, Sperling RA, Dickerson B, Stern CE, Tirado V, Munoz C, Reiman RA, Huentelman MJ, Alexander GE, Langbaum JB, Kosik KS, Tariot PN, Lopera F. Brain imaging and fluid biomarker analysis in young adults at genetic risk for autosomal dominant Alzheimer's disease in the presenilin 1 E280A kindred: a case-control study. Lancet Neurol. 2012 Dec;11(12):1048-56. doi: 10.1016/S1474-4422(12)70228-4. Epub 2012 Nov 6. PMID: 23137948; PMCID: PMC4181671.

Reitz C, Cheng R, Rogaeva E, Lee JH, Tokuhiro S, Zou F, Bettens K, Sleegers K, Tan EK, Kimura R, Shibata N, Arai H, Kamboh MI, Prince JA, Maier W, Riemenschneider M, Owen M, Harold D, Hollingworth P, Cellini E, Sorbi S, Nacmias B, Takeda M, Pericak-Vance MA, Haines JL, Younkin S, Williams J, van Broeckhoven C, Farrer LA, St George-Hyslop PH, Mayeux R; Genetic and Environmental Risk in Alzheimer Disease 1 Consortium. Meta-analysis of the association between variants in SORL1 and Alzheimer disease. Arch Neurol. 2011 Jan;68(1):99-106. doi: 10.1001/archneurol.2010.346. Erratum in: Arch Neurol. 2011 Mar;68(3):293. PMID: 21220680; PMCID: PMC3086666.

Renna M, Jimenez-Sanchez M, Sarkar S, Rubinsztein DC. Chemical inducers of autophagy that enhance the clearance of mutant proteins in neurodegenerative diseases. J Biol Chem. 2010 Apr 9;285(15):11061-7. doi: 10.1074/jbc. R109.072181. Epub 2010 Feb 10. PMID: 20147746; PMCID: PMC2856980.

Rhea EM, Banks WA, Raber J. Insulin Resistance in Peripheral Tissues and the Brain: A Tale of Two Sites. Biomedicines. 2022 Jul 2;10(7):1582. doi: 10.3390/biomedicines10071582. PMID: 35884888; PMCID: PMC9312939.

Ribel-Madsen R, Fraga MF, Jacobsen S, Bork-Jensen J, Lara E, Calvanese V, Fernandez AF, Friedrichsen M, Vind BF, Højlund K, Beck-Nielsen H, Esteller M, Vaag A, Poulsen P. Genome-wide analysis of DNA methylation differences in muscle and fat from monozygotic twins discordant for type 2 diabetes. PLoS One. 2012;7(12): e51302. doi: 10.1371/journal.pone.0051302. Epub 2012 Dec 10. PMID: 23251491; PMCID: PMC3519577.

Rickle A, Bogdanovic N, Volkman I, Winblad B, Ravid R, Cowburn RF. Akt activity in Alzheimer's disease and other neurodegenerative disorders. Neuroreport. 2004 Apr 29;15(6):955-9. doi: 10.1097/00001756-200404290-00005. PMID: 15076714.

Rius-Pérez S, Tormos AM, Pérez S, Taléns-Visconti R. Vascular pathology: Cause or effect in Alzheimer disease? Neurologia (Engl Ed). 2018 Mar;33(2):112-120. English, Spanish. doi: 10.1016/j.nrl.2015.07.010. Epub 2015 Sep 16. PMID: 26385017.

Rivera EJ, Goldin A, Fulmer N, Tavares R, Wands JR, de la Monte SM. Insulin and insulin-like growth factor expression and function deteriorate with progression of Alzheimer's disease: link to brain reductions in acetylcholine. J Alzheimers Dis. 2005 Dec;8(3):247-68. doi: 10.3233/jad-2005-8304. PMID: 16340083.

Roduit R, Morin J, Massé F, Segall L, Roche E, Newgard CB, Assimacopoulos-Jeannet F, Prentki M. Glucose down-regulates the expression of the peroxisome proliferator-activated receptor-alpha gene in the pancreatic beta -cell. J Biol Chem. 2000 Nov 17;275(46):35799-806. doi: 10.1074/jbc.M006001200. PMID: 10967113.

Rogaeva E, Meng Y, Lee JH, Gu Y, Kawarai T, Zou F, Katayama T, Baldwin CT, Cheng R, Hasegawa H, Chen F, Shibata N, Lunetta KL, Pardossi-Piquard R, Bohm C, Wakutani Y, Cupples LA, Cuenco KT, Green RC, Pinessi L, Rainero I, Sorbi S, Bruni A, Duara R, Friedland RP, Inzelberg R, Hampe W, Bujo H, Song YQ, Andersen OM, Willnow TE, Graff-Radford N, Petersen RC, Dickson D, Der SD, Fraser PE, Schmitt-Ulms G, Younkin S, Mayeux R, Farrer LA, St George-Hyslop P. The neuronal sortilin-related receptor SORL1 is genetically associated with Alzheimer disease. Nat Genet. 2007 Feb;39(2):168-77. doi: 10.1038/ng1943. Epub 2007 Jan 14. PMID: 17220890; PMCID: PMC2657343.

Rosario ER, Chang L, Head EH, Stanczyk FZ, Pike CJ. Brain levels of sex steroid hormones in men and women during normal aging and in Alzheimer's disease. Neurobiol Aging. 2011 Apr;32(4):604-13. doi: 10.1016/j.neurobiolaging.2009.04.008. Epub 2009 May 9. PMID: 19428144; PMCID: PMC2930132.

Rössler K, Neuchrist C, Kitz K, Scheiner O, Kraft D, Lassmann H. Expression of leucocyte adhesion molecules at the human blood-brain barrier (BBB). J Neurosci Res. 1992 Feb;31(2):365-74. doi: 10.1002/jnr.490310219. PMID: 1374132.

Rotermund C, Truckenmüller FM, Schell H, Kahle PJ. Diet-induced obesity accelerates the onset of terminal phenotypes in α-synuclein transgenic mice. J Neurochem. 2014 Dec;131(6):848-58. doi: 10.1111/jnc.12813. Epub 2014 Aug 11. PMID: 24995537.

Rui L. Energy metabolism in the liver. Compr Physiol. 2014 Jan;4(1):177-97. doi: 10.1002/cphy.c130024. PMID: 24692138; PMCID: PMC4050641.

Ruiz R, Jideonwo V, Ahn M, Surendran S, Tagliabracci VS, Hou Y, Gamble A, Kerner J, Irimia-Dominguez JM, Puchowicz MA, DePaoli-Roach A, Hoppel C, Roach P, Morral N. Sterol regulatory element-binding protein-1 (SREBP-1) is required to regulate glycogen synthesis and gluconeogenic gene expression in mouse liver. J Biol Chem. 2014 Feb 28;289(9):5510-7. doi: 10.1074/jbc.M113.541110. Epub 2014 Jan 7. PMID: 24398675; PMCID: PMC3937627.

Russo C, Schettini G, Saido TC, Hulette C, Lippa C, Lannfelt L, Ghetti B, Gambetti P, Tabaton M, Teller JK. Presenilin-1 mutations in Alzheimer's disease. Nature. 2000 Jun 1;405(6786):531-2. doi: 10.1038/35014735. PMID: 10850703.

Russo C, Violani E, Salis S, Venezia V, Dolcini V, Damonte G, Benatti U, D'Arrigo C, Patrone E, Carlo P, Schettini G. Pyroglutamate-modified amyloid beta-peptides--AbetaN3(pE)--strongly affect cultured neuron and astrocyte survival. J Neurochem. 2002 Sep;82(6):1480-9. doi: 10.1046/j.1471-4159.2002.01107. x. PMID: 12354296.

Ruud J, Steculorum SM, Brüning JC. Neuronal control of peripheral insulin sensitivity and glucose metabolism. Nat Commun. 2017 May 4; 8:15259. doi: 10.1038/ncomms15259. PMID: 28469281; PMCID: PMC5418592.

Saddiki H, Fayosse A, Cognat E, Sabia S, Engelborghs S, Wallon D, Alexopoulos P, Blennow K, Zetterberg H, Parnetti L, Zerr I, Hermann P, Gabelle A, Boada M, Orellana A, de Rojas I, Lilamand M, Bjerke M, Van Broeckhoven C, Farotti L, Salvadori N, Diehl-Schmid J, Grimmer T, Hourregue C, Dugravot A, Nicolas G, Laplanche JL, Lehmann S, Bouaziz-Amar E; Alzheimer's Disease Neuroimaging Initiative; Hugon J, Tzourio C, Singh-Manoux A, Paquet C, Dumurgier J. Age and the association between apolipoprotein E genotype and Alzheimer disease: A cerebrospinal fluid biomarker-based case-control study. PLoS Med. 2020 Aug 20;17(8): e1003289. doi: 10.1371/journal.pmed.1003289. PMID: 32817639; PMCID: PMC7446786.

Sagare AP, Bell RD, Zlokovic BV. Neurovascular dysfunction and faulty amyloid β-peptide clearance in Alzheimer disease. Cold Spring Harb Perspect Med. 2012 Oct 1;2(10): a011452. doi: 10.1101/cshperspect. a011452. PMID: 23028132; PMCID: PMC3475405.

Sah SK, Lee C, Jang JH, Park GH. Effect of high-fat diet on cognitive impairment in triple-transgenic mice model of Alzheimer's disease. Biochem Biophys Res Commun. 2017 Nov 4;493(1):731-736. doi: 10.1016/j.bbrc.2017.08.122. Epub 2017 Sep 1. PMID: 28865961.

Saido TC, Iwatsubo T, Mann DM, Shimada H, Ihara Y, Kawashima S. Dominant and differential deposition of distinct beta-amyloid peptide species, A beta N3(pE), in senile plaques. Neuron. 1995 Feb;14(2):457-66. doi: 10.1016/0896-6273(95)90301-1. PMID: 7857653.

Saido TC, Yamao-Harigaya W, Iwatsubo T, Kawashima S. Amino- and carboxyl-terminal heterogeneity of beta-amyloid peptides deposited in human brain. Neurosci Lett. 1996 Sep 13;215(3):173-6. doi: 10.1016/0304-3940(96)12970-0. PMID: 8899741.

Saido TC. Alzheimer's disease as proteolytic disorders: anabolism and catabolism of beta-amyloid. Neurobiol Aging. 1998 Jan-Feb;19(1 Suppl): S69-75. doi: 10.1016/s0197-4580(98)00033-5. PMID: 9562472.

Saito T, Takaki Y, Iwata N, Trojanowski J, Saido TC. Alzheimer's disease, neuropeptides, neuropeptidase, and amyloid-beta peptide metabolism. Sci Aging Knowledge Environ. 2003 Jan 22;2003(3):PE1. doi: 10.1126/sageke.2003.3.pe1. PMID: 12844556.

Salas IH, Weerasekera A, Ahmed T, Callaerts-Vegh Z, Himmelreich U, D'Hooge R, Balschun D, Saido TC, De Strooper B, Dotti CG. High fat diet treatment impairs hippocampal long-term potentiation without alterations of the core neuropathological features of Alzheimer disease. Neurobiol Dis. 2018 May; 113:82-96. doi: 10.1016/j.nbd.2018.02.001. Epub 2018 Feb 7. PMID: 29427755.

Sando SB, Melquist S, Cannon A, Hutton M, Sletvold O, Saltvedt I, White LR, Lydersen S, Aasly J. Risk-reducing effect of education in Alzheimer's disease. Int J Geriatr Psychiatry. 2008 Nov;23(11):1156-62. doi: 10.1002/gps.2043. PMID: 18484674.

Sankar SB, Infante-Garcia C, Weinstock LD, Ramos-Rodriguez JJ, Hierro-Bujalance C, Fernandez-Ponce C, Wood LB, Garcia-Alloza M. Amyloid beta and diabetic pathology cooperatively stimulate cytokine expression in an Alzheimer's mouse model. J Neuroinflammation. 2020 Jan 28;17(1):38. doi: 10.1186/s12974-020-1707-x. PMID: 31992349; PMCID: PMC6988295

Sano O, Tsujita M, Shimizu Y, Kato R, Kobayashi A, Kioka N, Remaley AT, Michikawa M, Ueda K, Matsuo M. ABCG1 and ABCG4 Suppress γ-Secretase Activity and Amyloid β Production. PLoS One. 2016 May 19;11(5): e0155400. doi: 10.1371/journal.pone.0155400. PMID: 27196068; PMCID: PMC4872999.

Santa-Maria AR, Walter FR, Figueiredo R, Kincses A, Vigh JP, Heymans M, Culot M, Winter P, Gosselet F, Dér A, Deli MA. Flow induces barrier and glycocalyx-related

genes and negative surface charge in a lab-on-a-chip human blood-brain barrier model. J Cereb Blood Flow Metab. 2021 Sep;41(9):2201-2215. doi: 10.1177/0271678X21992638. Epub 2021 Feb 9. PMID: 33563079; PMCID: PMC8393308.

Santos CY, Snyder PJ, Wu WC, Zhang M, Echeverria A, Alber J. Pathophysiologic relationship between Alzheimer's disease, cerebrovascular disease, and cardiovascular risk: A review and synthesis. Alzheimers Dement (Amst). 2017 Feb 9; 7:69-87. doi: 10.1016/j.dadm.2017.01.005. PMID: 28275702; PMCID: PMC5328683.

Sasahara K, Morigaki K, Shinya K. Effects of membrane interaction and aggregation of amyloid β-peptide on lipid mobility and membrane domain structure. Phys Chem Chem Phys. 2013 Jun 21;15(23):8929-39. doi: 10.1039/c3cp44517h. Epub 2013 Mar 21. PMID: 23515399.

Saunders NR, Habgood MD, Møllgård K, Dziegielewska KM. The biological significance of brain barrier mechanisms: help or hindrance in drug delivery to the central nervous system? F1000Res. 2016 Mar 10;5: F1000 Faculty Rev-313. doi: 10.12688/f1000research.7378.1. PMID: 26998242; PMCID: PMC4786902.

Schiera G, Bono E, Raffa MP, Gallo A, Pitarresi GL, Di Liegro I, Savettieri G. Synergistic effects of neurons and astrocytes on the differentiation of brain capillary endothelial cells in culture. J Cell Mol Med. 2003 Apr-Jun;7(2):165-70. doi: 10.1111/j.1582-4934. 2003.tb00215. x. PMID: 12927055; PMCID: PMC6740229.

Schilling S, Appl T, Hoffmann T, Cynis H, Schulz K, Jagla W, Friedrich D, Wermann M, Buchholz M, Heiser U, von Hörsten S, Demuth HU. Inhibition of glutaminyl cyclase prevents pGlu-Abeta formation after intracortical/hippocampal microinjection in vivo/in situ. J Neurochem. 2008 Aug;106(3):1225-36. doi: 10.1111/j.1471-4159.2008.05471. x. Epub 2008 Jul 8. PMID: 18627432.

Schilling S, Hoffmann T, Manhart S, Hoffmann M, Demuth HU. Glutaminyl cyclases unfold glutamyl cyclase activity under mild acid conditions. FEBS Lett. 2004 Apr 9;563(1-3):191-6. doi: 10.1016/S0014-5793(04)00300-X. PMID: 15063747.

Schilling S, Lauber T, Schaupp M, Manhart S, Scheel E, Böhm G, Demuth HU. On the seeding and oligomerization of pGlu-amyloid peptides (in vitro). Biochemistry. 2006 Oct 17;45(41):12393-9. doi: 10.1021/bi0612667. PMID: 17029395.

Schilling S, Lauber T, Schaupp M, Manhart S, Scheel E, Böhm G, Demuth HU. On the seeding and oligomerization of pGlu-amyloid peptides (in vitro). Biochemistry. 2006 Oct 17;45(41):12393-9. doi: 10.1021/bi0612667. PMID: 17029395.

Schilling S, Zeitschel U, Hoffmann T, Heiser U, Francke M, Kehlen A, Holzer M, Hutter-Paier B, Prokesch M, Windisch M, Jagla W, Schlenzig D, Lindner C, Rudolph T, Reuter G, Cynis H, Montag D, Demuth HU, Rossner S. Glutaminyl cyclase inhibition attenuates pyroglutamate Abeta and Alzheimer's disease-like pathology. Nat Med. 2008 Oct;14(10):1106-11. doi: 10.1038/nm.1872. Epub 2008 Sep 28. PMID: 18836460.

Schlenzig D, Manhart S, Cinar Y, Kleinschmidt M, Hause G, Willbold D, Funke SA, Schilling S, Demuth HU. Pyroglutamate formation influences solubility and amyloidogenicity of amyloid peptides. Biochemistry. 2009 Jul 28;48(29):7072-8. doi: 10.1021/bi900818a. PMID: 19518051.

Schmidt R, Hofer E, Bouwman FH, Buerger K, Cordonnier C, Fladby T, Galimberti D, Georges J, Heneka MT, Hort J, Laczó J, Molinuevo JL, O'Brien JT, Religa D, Scheltens P, Schott JM, Sorbi S. EFNS-ENS/EAN Guideline on concomitant use of cholinesterase inhibitors and memantine in moderate to severe Alzheimer's disease. Eur J Neurol. 2015 Jun;22(6):889-98. doi: 10.1111/ene.12707. Epub 2015 Mar 25. PMID: 25808982.

Schmitz G, Orsó E. Intracellular cholesterol and phospholipid trafficking: comparable mechanisms in macrophages and neuronal cells. Neurochem Res. 2001 Sep;26(8-9):1045-68. doi: 10.1023/a:1012357106398. PMID: 11699932.

Schreiner TG, Popescu BO. Amyloid Beta Dynamics in Biological Fluids-Therapeutic Impact. J Clin Med. 2021 Dec 20;10(24):5986. doi: 10.3390/jcm10245986. PMID: 34945282; PMCID: PMC8706225.

Schuck S. Microautophagy - distinct molecular mechanisms handle cargoes of many sizes. J Cell Sci. 2020 Sep 9;133(17):jcs246322. doi: 10.1242/jcs.246322. PMID: 32907930.

Sczelecki S, Besse-Patin A, Abboud A, Kleiner S, Laznik-Bogoslavski D, Wrann CD, Ruas JL, Haibe-Kains B, Estall JL. Loss of Pgc-1α expression in aging mouse muscle potentiates glucose intolerance and systemic inflammation. Am J Physiol

Endocrinol Metab. 2014 Jan 15;306(2): E157-67. doi: 10.1152/ajpendo.00578.2013. Epub 2013 Nov 26. PMID: 24280126; PMCID: PMC4073996.

Selkoe DJ, Hardy J. The amyloid hypothesis of Alzheimer's disease at 25 years. EMBO Mol Med. 2016 Jun 1;8(6):595-608. doi: 10.15252/emmm.201606210. PMID: 27025652; PMCID: PMC4888851.

Selkoe DJ. Alzheimer's disease is a synaptic failure. Science. 2002 Oct 25;298(5594):789-91. doi: 10.1126/science.1074069. PMID: 12399581.

Seo MH, Bae JC, Park SE, Rhee EJ, Park CY, Oh KW, Park SW, Kim SW, Lee WY. Association of lipid and lipoprotein profiles with future development of type 2 diabetes in nondiabetic Korean subjects: a 4-year retrospective, longitudinal study. J Clin Endocrinol Metab. 2011 Dec;96(12): E2050-4. doi: 10.1210/jc.2011-1857. Epub 2011 Oct 12. PMID: 21994961.

Sergeant N, Bombois S, Ghestem A, Drobecq H, Kostanjevecki V, Missiaen C, Wattez A, David JP, Vanmechelen E, Sergheraert C, Delacourte A. Truncated beta-amyloid peptide species in pre-clinical Alzheimer's disease as new targets for the vaccination approach. J Neurochem. 2003 Jun;85(6):1581-91. doi: 10.1046/j.1471-4159.2003.01818. x. PMID: 12787077.

Sevalle J, Amoyel A, Robert P, Fournié-Zaluski MC, Roques B, Checler F. Aminopeptidase A contributes to the N-terminal truncation of amyloid beta-peptide. J Neurochem. 2009 Apr;109(1):248-56. doi: 10.1111/j.1471-4159.2009.05950. x. Epub 2009 Feb 23. PMID: 19187443.

Shackleton B, Crawford F, Bachmeier C. Inhibition of ADAM10 promotes the clearance of Aβ across the BBB by reducing LRP1 ectodomain shedding. Fluids Barriers CNS. 2016 Aug 8;13(1):14. doi: 10.1186/s12987-016-0038-x. PMID: 27503326; PMCID: PMC4977753.

Shao Y, Chen J, Dong LJ, He X, Cheng R, Zhou K, Liu J, Qiu F, Li XR, Ma JX. A Protective Effect of PPARα in Endothelial Progenitor Cells Through Regulating Metabolism. Diabetes. 2019 Nov;68(11):2131-2142. doi: 10.2337/db18-1278. Epub 2019 Aug 26. PMID: 31451517; PMCID: PMC6804623.

Shen M, Chen K, Lu J, Cheng P, Xu L, Dai W, Wang F, He L, Zhang Y, Chengfen W, Li J, Yang J, Zhu R, Zhang H, Zheng Y, Zhou Y, Guo C. Protective effect of

astaxanthin on liver fibrosis through modulation of TGF-β1 expression and autophagy. Mediators Inflamm. 2014; 2014:954502. doi: 10.1155/2014/954502. Epub 2014 Apr 17. PMID: 24860243; PMCID: PMC4016904.

Sherrington R, Froelich S, Sorbi S, Campion D, Chi H, Rogaeva EA, Levesque G, Rogaev EI, Lin C, Liang Y, Ikeda M, Mar L, Brice A, Agid Y, Percy ME, Clerget-Darpoux F, Piacentini S, Marcon G, Nacmias B, Amaducci L, Frebourg T, Lannfelt L, Rommens JM, St George-Hyslop PH. Alzheimer's disease associated with mutations in presenilin 2 is rare and variably penetrant. Hum Mol Genet. 1996 Jul;5(7):985-8. doi: 10.1093/hmg/5.7.985. PMID: 8817335.

Shibata M, Yamada S, Kumar SR, Calero M, Bading J, Frangione B, Holtzman DM, Miller CA, Strickland DK, Ghiso J, Zlokovic BV. Clearance of Alzheimer's amyloid-ss (1-40) peptide from brain by LDL receptor-related protein-1 at the blood-brain barrier. J Clin Invest. 2000 Dec;106(12):1489-99. doi: 10.1172/JCI10498. PMID: 11120756; PMCID: PMC387254.

Shimizu T, Watanabe A, Ogawara M, Mori H, Shirasawa T. Isoaspartate formation and neurodegeneration in Alzheimer's disease. Arch Biochem Biophys. 2000 Sep 15;381(2):225-34. doi: 10.1006/abbi.2000.1955. PMID: 11032409.

Shimomura I, Bashmakov Y, Horton JD. Increased levels of nuclear SREBP-1c associated with fatty livers in two mouse models of diabetes mellitus. J Biol Chem. 1999 Oct 15;274(42):30028-32. doi: 10.1074/jbc.274.42.30028. PMID: 10514488.

Shinohara M, Tachibana M, Kanekiyo T, Bu G. Role of LRP1 in the pathogenesis of Alzheimer's disease: evidence from clinical and preclinical studies. J Lipid Res. 2017 Jul;58(7):1267-1281. doi: 10.1194/jlr. R075796. Epub 2017 Apr 4. PMID: 28381441; PMCID: PMC5496044.

Shulman M, Rajagovindan R, Kong J, O'gorman J, Viollet L, Huang E, Hering H, Ratti E, Graham D, Haeberlein SB. Top-line results from TANGO, a phase 2 study of gosuranemab in participants with mild cognitive impairment due to Alzheimer's disease and mild Alzheimers disease. J Prev Alzheimers Dis. 2021;8(Suppl 1): S65.

Siddharthan V, Kim YV, Liu S, Kim KS. Human astrocytes/astrocyte-conditioned medium and shear stress enhance the barrier properties of human brain microvascular endothelial cells. Brain Res. 2007 May 25; 1147:39-50. doi:

10.1016/j.brainres.2007.02.029. Epub 2007 Feb 24. PMID: 17368578; PMCID: PMC2691862.

Simić G, Kostović I, Winblad B, Bogdanović N. Volume and number of neurons of the human hippocampal formation in normal aging and Alzheimer's disease. J Comp Neurol. 1997 Mar 24;379(4):482-94. doi: 10.1002/(sici)1096-9861(19970324)379:4<482: aid-cne2>3.0.co;2-z. PMID: 9067838.

Simonen PP, Gylling HK, Miettinen TA. Diabetes contributes to cholesterol metabolism regardless of obesity. Diabetes Care. 2002 Sep;25(9):1511-5. doi: 10.2337/diacare.25.9.1511. PMID: 12196419.

Singhal G, Kumar G, Chan S, Fisher FM, Ma Y, Vardeh HG, Nasser IA, Flier JS, Maratos-Flier E. Deficiency of fibroblast growth factor 21 (FGF21) promotes hepatocellular carcinoma (HCC) in mice on a long-term obesogenic diet. Mol Metab. 2018 Jul;13: 56-66. doi: 10.1016/j.molmet.2018.03.002. Epub 2018 Mar 8. PMID: 29753678; PMCID: PMC6026320.

Sisodia SS, St George-Hyslop PH. gamma-Secretase, Notch, Abeta and Alzheimer's disease: where do the presenilins fit in? Nat Rev Neurosci. 2002 Apr;3(4):281-90. doi: 10.1038/nrn785. PMID: 11967558.

Skaper SD, Facci L, Zusso M, Giusti P. An Inflammation-Centric View of Neurological Disease: Beyond the Neuron. Front Cell Neurosci. 2018 Mar 21; 12:72. doi: 10.3389/fncel.2018.00072. Erratum in: Front Cell Neurosci. 2020 Feb 03; 13:578. PMID: 29618972; PMCID: PMC5871676.

Skrzypski M, Kołodziejski PA, Pruszyńska-Oszmałek E, Wojciechowicz T, Janicka P, Krążek M, Małek E, Strowski MZ, Nowak KW. Daily Treatment of Mice with Type 2 Diabetes with Adropin for Four Weeks Improves Glucolipid Profile, Reduces Hepatic Lipid Content and Restores Elevated Hepatic Enzymes in Serum. Int J Mol Sci. 2022 Aug 29;23(17):9807. doi: 10.3390/ijms23179807. PMID: 36077198; PMCID: PMC9456344.

Slomski A. Anti-Tau Antibody Semorinemab Fails to Slow Alzheimer Disease. JAMA. 2022 Aug 2;328(5):415. doi: 10.1001/jama.2022.12727. PMID: 35916858.

So WY, Cheng Q, Chen L, Evans-Molina C, Xu A, Lam KS, Leung PS. High glucose represses β-klotho expression and impairs fibroblast growth factor 21 action in

mouse pancreatic islets: involvement of peroxisome proliferator-activated receptor γ signaling. Diabetes. 2013 Nov;62(11):3751-9. doi: 10.2337/db13-0645. Epub 2013 Jul 29. PMID: 23897951; PMCID: PMC3806592.

Solini A, Rossi C, Mazzanti CM, Proietti A, Koepsell H, Ferrannini E. Sodium-glucose co-transporter (SGLT)2 and SGLT1 renal expression in patients with type 2 diabetes. Diabetes Obes Metab. 2017 Sep;19(9):1289-1294. doi: 10.1111/dom.12970. Epub 2017 May 22. PMID: 28419670.

Sookoian S, Castaño GO, Scian R, Fernández Gianotti T, Dopazo H, Rohr C, Gaj G, San Martino J, Sevic I, Flichman D, Pirola CJ. Serum aminotransferases in non-alcoholic fatty liver disease are a signature of liver metabolic perturbations at the amino acid and Krebs cycle level. Am J Clin Nutr. 2016 Feb;103(2):422-34. doi: 10.3945/ajcn.115.118695. Epub 2016 Jan 20. PMID: 26791191.

Sookoian S, Pirola CJ. Alanine and aspartate aminotransferase and glutamine-cycling pathway: their roles in pathogenesis of metabolic syndrome. World J Gastroenterol. 2012 Aug 7;18(29):3775-81. doi: 10.3748/wjg. v18.i29.3775. PMID: 22876026; PMCID: PMC3413046.

Spanswick D, Smith MA, Mirshamsi S, Routh VH, Ashford ML. Insulin activates ATP-sensitive K+ channels in hypothalamic neurons of lean, but not obese rats. Nat Neurosci. 2000 Aug;3(8):757-8. doi: 10.1038/77660. PMID: 10903566.

Sperling RA, Aisen PS, Beckett LA, Bennett DA, Craft S, Fagan AM, Iwatsubo T, Jack CR Jr, Kaye J, Montine TJ, Park DC, Reiman EM, Rowe CC, Siemers E, Stern Y, Yaffe K, Carrillo MC, Thies B, Morrison-Bogorad M, Wagster MV, Phelps CH. Toward defining the preclinical stages of Alzheimer's disease: recommendations from the National Institute on Aging-Alzheimer's Association workgroups on diagnostic guidelines for Alzheimer's disease. Alzheimers Dement. 2011 May;7(3):280-92. doi: 10.1016/j.jalz.2011.03.003. Epub 2011 Apr 21. PMID: 21514248; PMCID: PMC3220946.

Spires-Jones TL, Hyman BT. The intersection of amyloid beta and tau at synapses in Alzheimer's disease. Neuron. 2014 May 21;82(4):756-71. doi: 10.1016/j.neuron.2014.05.004. PMID: 24853936; PMCID: PMC4135182

St George-Hyslop PH, Tanzi RE, Polinsky RJ, Haines JL, Nee L, Watkins PC, Myers RH, Feldman RG, Pollen D, Drachman D, et al. The genetic defect causing familial Alzheimer's disease maps on chromosome 21. Science. 1987 Feb 20;235(4791):885-90. doi: 10.1126/science.2880399. PMID: 2880399.

Stamouli EC, Politis AM. [Pro-inflammatory cytokines in Alzheimer's disease]. Psychiatriki. 2016 Oct-Dec;27(4):264-275. Greek, Modern. doi: 10.22365/jpsych.2016.274.264. PMID: 28114090.

Standeven KF, Hess K, Carter AM, Rice GI, Cordell PA, Balmforth AJ, Lu B, Scott DJ, Turner AJ, Hooper NM, Grant PJ. Neprilysin, obesity and the metabolic syndrome. Int J Obes (Lond). 2011 Aug;35(8):1031-40. doi: 10.1038/ijo.2010.227. Epub 2010 Nov 2. PMID: 21042321; PMCID: PMC3040694.

Stanley M, Macauley SL, Caesar EE, Koscal LJ, Moritz W, Robinson GO, Roh J, Keyser J, Jiang H, Holtzman DM. The Effects of Peripheral and Central High Insulin on Brain Insulin Signaling and Amyloid-β in Young and Old APP/PS1 Mice. J Neurosci. 2016 Nov 16;36(46):11704-11715. doi: K10.1523/JNEUROSCI.2119-16.2016. PMID: 27852778; PMCID: PMC5125227.

Steen E, Terry BM, Rivera EJ, Cannon JL, Neely TR, Tavares R, Xu XJ, Wands JR, de la Monte SM. Impaired insulin and insulin-like growth factor expression and signaling mechanisms in Alzheimer's disease--is this type 3 diabetes? J Alzheimers Dis. 2005 Feb;7(1):63-80. doi: 10.3233/jad-2005-7107. PMID: 15750215.

Stern Y. Cognitive reserve in ageing and Alzheimer's disease. Lancet Neurol. 2012 Nov;11(11):1006-12. doi: 10.1016/S1474-4422(12)70191-6. PMID: 23079557; PMCID: PMC3507991.

Storck SE, Hartz AMS, Bernard J, Wolf A, Kachlmeier A, Mahringer A, Weggen S, Pahnke J, Pietrzik CU. The concerted amyloid-beta clearance of LRP1 and ABCB1/P-gp across the blood-brain barrier is linked by PICALM. Brain Behav Immun. 2018 Oct; 73:21-33. doi: 10.1016/j.bbi.2018.07.017. Epub 2018 Jul 21. PMID: 30041013; PMCID: PMC7748946.

Storck SE, Kurtyka M, Pietrzik CU. Brain endothelial LRP1 maintains blood-brain barrier integrity. Fluids Barriers CNS. 2021 Jun 19;18(1):27. doi: 10.1186/s12987-021-00260-5. PMID: 34147102; PMCID: PMC8214794.

Storck SE, Meister S, Nahrath J, Meißner JN, Schubert N, Di Spiezio A, Baches S, Vandenbroucke RE, Bouter Y, Prikulis I, Korth C, Weggen S, Heimann A, Schwaninger M, Bayer TA, Pietrzik CU. Endothelial LRP1 transports amyloid-β(1-42) across the blood-brain barrier. J Clin Invest. 2016 Jan;126(1):123-36. doi: 10.1172/JCI81108. Epub 2015 Nov 30. PMID: 26619118; PMCID: PMC4701557

Stumvoll M, Goldstein BJ, van Haeften TW. Type 2 diabetes: principles of pathogenesis and therapy. Lancet. 2005 Apr 9-15;365(9467):1333-46. doi: 10.1016/S0140-6736(05)61032-X. PMID: 15823385

Summers WK, Majovski LV, Marsh GM, Tachiki K, Kling A. Oral tetrahydroaminoacridine in long-term treatment of senile dementia, Alzheimer type. N Engl J Med. 1986 Nov 13;315(20):1241-5. doi: 10.1056/NEJM198611133152001. PMID: 2430180.

Summers WK, Viesselman JO, Marsh GM, Candelora K. Use of THA in treatment of Alzheimer-like dementia: pilot study in twelve patients. Biol Psychiatry. 1981 Feb;16(2):145-53. PMID: 7225483

Swanson CJ, Zhang Y, Dhadda S, Wang J, Kaplow J, Lai RYK, Lannfelt L, Bradley H, Rabe M, Koyama A, Reyderman L, Berry DA, Berry S, Gordon R, Kramer LD, Cummings JL. A randomized, double-blind, phase 2b proof-of-concept clinical trial in early Alzheimer's disease with lecanemab, an anti-Aβ protofibril antibody. Alzheimers Res Ther. 2021 Apr 17;13(1):80. doi: 10.1186/s13195-021-00813-8. Erratum in: Alzheimers Res Ther. 2022 May 21;14(1):70. PMID: 33865446; PMCID: PMC8053280.

Takeyama K, Kodera Y, Suzawa M, Kato S. [Peroxisome proliferator-activated receptor (PPAR)--structure, function, tissue distribution, gene expression]. Nihon Rinsho. 2000 Feb;58(2):357-63. Japanese. PMID: 10707558.

Talbot K, Wang HY, Kazi H, Han LY, Bakshi KP, Stucky A, Fuino RL, Kawaguchi KR, Samoyedny AJ, Wilson RS, Arvanitakis Z, Schneider JA, Wolf BA, Bennett DA, Trojanowski JQ, Arnold SE. Demonstrated brain insulin resistance in Alzheimer's disease patients is associated with IGF-1 resistance, IRS-1 dysregulation, and cognitive decline. J Clin Invest. 2012 Apr;122(4):1316-38. doi: 10.1172/JCI59903. PMID: 22476197; PMCID: PMC3314463.

Tamaki C, Ohtsuki S, Iwatsubo T, Hashimoto T, Yamada K, Yabuki C, Terasaki T. Major involvement of low-density lipoprotein receptor-related protein 1 in the clearance of plasma free amyloid beta-peptide by the liver. Pharm Res. 2006 Jul;23(7):1407-16. doi: 10.1007/s11095-006-0208-7. Epub 2006 Jun 21. PMID: 16779710.

Tammineni P, Ye X, Feng T, Aikal D, Cai Q. Impaired retrograde transport of axonal autophagosomes contributes to autophagic stress in Alzheimer's disease neurons. Elife. 2017 Jan 13;6:e21776. doi: 10.7554/eLife.21776. PMID: 28085665; PMCID: PMC5235353.

Tang C, Kanter JE, Bornfeldt KE, Leboeuf RC, Oram JF. Diabetes reduces the cholesterol exporter ABCA1 in mouse macrophages and kidneys. J Lipid Res. 2010 Jul;51(7):1719-28. doi: 10.1194/jlr.M003525. Epub 2009 Nov 23. PMID: 19965614; PMCID: PMC2882721.

Tanida I, Minematsu-Ikeguchi N, Ueno T, Kominami E. Lysosomal turnover, but not a cellular level, of endogenous LC3 is a marker for autophagy. Autophagy. 2005 Jul;1(2):84-91. doi: 10.4161/auto.1.2.1697. Epub 2005 Jul 31. PMID: 16874052.

Tekirian TL, Saido TC, Markesbery WR, Russell MJ, Wekstein DR, Patel E, Geddes JW. N-terminal heterogeneity of parenchymal and cerebrovascular Abeta deposits. J Neuropathol Exp Neurol. 1998 Jan;57(1):76-94. doi: 10.1097/00005072-199801000-00009. PMID: 9600199

Tensil M, Hessler JB, Gutsmiedl M, Riedl L, Grimmer T, Diehl-Schmid J. Sex Differences in Neuropsychological Test Performance in Alzheimer's Disease and the Influence of the ApoE Genotype. Alzheimer Dis Assoc Disord. 2018 Apr-Jun;32(2):145-149. doi: 10.1097/WAD.0000000000000229. PMID: 29189302.

Terry RD, Masliah E, Salmon DP, Butters N, DeTeresa R, Hill R, Hansen LA, Katzman R. Physical basis of cognitive alterations in Alzheimer's disease: synapse loss is the major correlate of cognitive impairment. Ann Neurol. 1991 Oct;30(4):572-80. doi: 10.1002/ana.410300410. PMID: 1789684.

Thibault O, Anderson KL, DeMoll C, Brewer LD, Landfield PW, Porter NM. Hippocampal calcium dysregulation at the nexus of diabetes and brain aging. Eur J Pharmacol. 2013 Nov 5;719(1-3):34-43. doi: 10.1016/j.ejphar.2013.07.024. Epub 2013 Jul 17. PMID: 23872402; PMCID: PMC3838483.

Tietz S, Engelhardt B. Brain barriers: Crosstalk between complex tight junctions and adherens junctions. J Cell Biol. 2015 May 25;209(4):493-506. doi: 10.1083/jcb.201412147. PMID: 26008742; PMCID: PMC4442813.

Todd S, Barr S, Roberts M, Passmore AP. Survival in dementia and predictors of mortality: a review. Int J Geriatr Psychiatry. 2013 Nov;28(11):1109-24. doi: 10.1002/gps.3946. Epub 2013 Mar 22. PMID: 23526458

Tom SE, Hubbard RA, Crane PK, Haneuse SJ, Bowen J, McCormick WC, McCurry S, Larson EB. Characterization of dementia and Alzheimer's disease in an older population: updated incidence and life expectancy with and without dementia. Am J Public Health. 2015 Feb;105(2):408-13. doi: 10.2105/AJPH.2014.301935. PMID: 25033130; PMCID: PMC4318311.

Tomiyama T, Asano S, Furiya Y, Shirasawa T, Endo N, Mori H. Racemization of Asp23 residue affects the aggregation properties of Alzheimer amyloid beta protein analogues. J Biol Chem. 1994 Apr 8;269(14):10205-8. PMID: 8144598.

Toro CA, Zhang L, Cao J, Cai D. Sex differences in Alzheimer's disease: Understanding the molecular impact. Brain Res. 2019 Sep 15; 1719:194-207. doi: 10.1016/j.brainres.2019.05.031. Epub 2019 May 23. PMID: 31129153; PMCID: PMC6750802.

Toro CA, Zhang L, Cao J, Cai D. Sex differences in Alzheimer's disease: Understanding the molecular impact. Brain Res. 2019 Sep 15; 1719:194-207. doi: 10.1016/j.brainres.2019.05.031. Epub 2019 May 23. PMID: 31129153; PMCID: PMC6750802.

Towns R, Kabeya Y, Yoshimori T, Guo C, Shangguan Y, Hong S, Kaplan M, Klionsky DJ, Wiley JW. Sera from patients with type 2 diabetes and neuropathy induce autophagy and colocalization with mitochondria in SY5Y cells. Autophagy. 2005 Oct-Dec;1(3):163-70. doi: 10.4161/auto.1.3.2068. Epub 2005 Oct 2. PMID: 16874076.

Tremblay C, Choudhury P, Belden CM, Goldfarb D, Lorenzini I, Beach TG, Serrano GE. The role of sex differences in depression in pathologically defined Alzheimer's disease. Front Aging Neurosci. 2023 May 10; 15:1156764. doi: 10.3389/fnagi.2023.1156764. PMID: 37234269; PMCID: PMC10206015.

Tronson NC, Collette KM. (Putative) sex differences in neuroimmune modulation of memory. J Neurosci Res. 2017 Jan 2;95(1-2):472-486. doi: 10.1002/jnr.23921. PMID: 27870428; PMCID: PMC5120654.

Tsai CL, Pan CY, Chen FC, Huang TH, Tsai MC, Chuang CY. Differences in neurocognitive performance and metabolic and inflammatory indices in male adults with obesity as a function of regular exercise. Exp Physiol. 2019 Nov;104(11):1650-1660. doi: 10.1113/EP087862. Epub 2019 Oct 14. PMID: 31609518

Turtzo LC, Lescher J, Janes L, Dean DD, Budde MD, Frank JA. Macrophagic and microglial responses after focal traumatic brain injury in the female rat. J Neuroinflammation. 2014 Apr 24; 11:82. doi: 10.1186/1742-2094-11-82. PMID: 24761998; PMCID: PMC4022366.

Ulland TK, Song WM, Huang SC, Ulrich JD, Sergushichev A, Beatty WL, Loboda AA, Zhou Y, Cairns NJ, Kambal A, Loginicheva E, Gilfillan S, Cella M, Virgin HW, Unanue ER, Wang Y, Artyomov MN, Holtzman DM, Colonna M. TREM2 Maintains Microglial Metabolic Fitness in Alzheimer's Disease. Cell. 2017 Aug 10;170(4):649-663.e13. doi: 10.1016/j.cell.2017.07.023. PMID: 28802038; PMCID: PMC5573224.

Ulrich JD, Finn MB, Wang Y, Shen A, Mahan TE, Jiang H, Stewart FR, Piccio L, Colonna M, Holtzman DM. Altered microglial response to Aβ plaques in APPPS1-21 mice heterozygous for TREM2. Mol Neurodegener. 2014 Jun 3; 9:20. doi: 10.1186/1750-1326-9-20. PMID: 24893973; PMCID: PMC4049806.

Van Acker ZP, Bretou M, Annaert W. Endo-lysosomal dysregulations and late-onset Alzheimer's disease: impact of genetic risk factors. Mol Neurodegener. 2019 Jun 3;14(1):20. doi: 10.1186/s13024-019-0323-7. PMID: 31159836; PMCID: PMC6547588.

van der Flier WM, Scheltens P. Epidemiology and risk factors of dementia. J Neurol Neurosurg Psychiatry. 2005 Dec;76 Suppl 5(Suppl 5):v2-7. doi: 10.1136/jnnp.2005.082867. PMID: 16291918; PMCID: PMC1765715.

van Dijk EJ, Prins ND, Vrooman HA, Hofman A, Koudstaal PJ, Breteler MM. Progression of cerebral small vessel disease in relation to risk factors and cognitive consequences: Rotterdam Scan study. Stroke. 2008 Oct;39(10):2712-9. doi: 10.1161/STROKEAHA.107.513176. Epub 2008 Jul 17. PMID: 18635849.

Van Gool B, Storck SE, Reekmans SM, Lechat B, Gordts PLSM, Pradier L, Pietrzik CU, Roebroek AJM. LRP1 Has a Predominant Role in Production over Clearance of Aβ in a Mouse Model of Alzheimer's Disease. Mol Neurobiol. 2019 Oct;56(10):7234-7245. doi: 10.1007/s12035-019-1594-2. Epub 2019 Apr 19. PMID: 31004319; PMCID: PMC6728278.

Vance JE, Hayashi H. Formation and function of apolipoprotein E-containing lipoproteins in the nervous system. Biochim Biophys Acta. 2010 Aug;1801(8):806-18. doi: 10.1016/j.bbalip.2010.02.007. Epub 2010 Feb 17. PMID: 20170744.

Vandal M, Bourassa P, Calon F. Can insulin signaling pathways be targeted to transport Aβ out of the brain? Front Aging Neurosci. 2015 Jun 16; 7:114. doi: 10.3389/fnagi.2015.00114. PMID: 26136681; PMCID: PMC4468380.

Vandal M, White PJ, Chevrier G, Tremblay C, St-Amour I, Planel E, Marette A, Calon F. Age-dependent impairment of glucose tolerance in the 3xTg-AD mouse model of Alzheimer's disease. FASEB J. 2015 Oct;29(10):4273-84. doi: 10.1096/fj.14-268482. Epub 2015 Jun 24. PMID: 26108977.

Vandal M, White PJ, Tremblay C, St-Amour I, Chevrier G, Emond V, Lefrançois D, Virgili J, Planel E, Giguere Y, Marette A, Calon F. Insulin reverses the high-fat diet-induced increase in brain Aβ and improves memory in an animal model of Alzheimer disease. Diabetes. 2014 Dec;63(12):4291-301. doi: 10.2337/db14-0375. Epub 2014 Jul 9. PMID: 25008180.

Vander Haar E, Lee SI, Bandhakavi S, Griffin TJ, Kim DH. Insulin signalling to mTOR mediated by the Akt/PKB substrate PRAS40. Nat Cell Biol. 2007 Mar;9(3):316-23. doi: 10.1038/ncb1547. Epub 2007 Feb 4. PMID: 17277771.

Vermunt L, Sikkes SAM, van den Hout A, Handels R, Bos I, van der Flier WM, Kern S, Ousset PJ, Maruff P, Skoog I, Verhey FRJ, Freund-Levi Y, Tsolaki M, Wallin ÅK, Olde Rikkert M, Soininen H, Spiru L, Zetterberg H, Blennow K, Scheltens P, Muniz-Terrera G, Visser PJ; Alzheimer Disease Neuroimaging Initiative; AIBL Research Group; ICTUS/DSA study groups. Duration of preclinical, prodromal, and dementia stages of Alzheimer's disease in relation to age, sex, and APOE genotype. Alzheimers Dement. 2019 Jul;15(7):888-898. doi: 10.1016/j.jalz.2019.04.001. Epub 2019 Jun 1. PMID: 31164314; PMCID: PMC6646097.

Villavicencio-Tejo F, Flores-Bastías O, Marambio-Ruiz L, Pérez-Reytor D, Karahanian E. Fenofibrate (a PPAR-α Agonist) Administered During Ethanol Withdrawal Reverts Ethanol-Induced Astrogliosis and Restores the Levels of Glutamate Transporter in Ethanol-Administered Adolescent Rats. Front Pharmacol. 2021 Apr 20;12: 653175. doi: 10.3389/fphar.2021.653175. PMID: 33959021; PMCID: PMC8093785.

Villemagne VL, Burnham S, Bourgeat P, Brown B, Ellis KA, Salvado O, Szoeke C, Macaulay SL, Martins R, Maruff P, Ames D, Rowe CC, Masters CL; Australian Imaging Biomarkers and Lifestyle (AIBL) Research Group. Amyloid β deposition, neurodegeneration, and cognitive decline in sporadic Alzheimer's disease: a prospective cohort study. Lancet Neurol. 2013 Apr;12(4):357-67. doi: 10.1016/S1474-4422(13)70044-9. Epub 2013 Mar 8. PMID: 23477989.

Villena JA. New insights into PGC-1 coactivators: redefining their role in the regulation of mitochondrial function and beyond. FEBS J. 2015 Feb;282(4):647-72. doi: 10.1111/febs.13175. Epub 2015 Jan 12. PMID: 25495651.

Vitek MP, Bhattacharya K, Glendening JM, Stopa E, Vlassara H, Bucala R, Manogue K, Cerami A. Advanced glycation end products contribute to amyloidosis in Alzheimer disease. Proc Natl Acad Sci U S A. 1994 May 24;91(11):4766-70. doi: 10.1073/pnas.91.11.4766. PMID: 8197133; PMCID: PMC43869.

Wada M, Yano S, Hamano T, Nabika T, Kumakura S. Effect of Serum Cholesterol on Insulin Secretory Capacity: Shimane CoHRE Study. PLoS One. 2016 Feb 16;11(2): e0149452. doi: 10.1371/journal.pone.0149452. PMID: 26881755; PMCID: PMC4755542.

Walker JM, Dixit S, Saulsberry AC, May JM, Harrison FE. Reversal of high fat diet-induced obesity improves glucose tolerance, inflammatory response, β-amyloid accumulation and cognitive decline in the APP/PSEN1 mouse model of Alzheimer's disease. Neurobiol Dis. 2017 Apr; 100:87-98. doi: 10.1016/j.nbd.2017.01.004. Epub 2017 Jan 17. PMID: 28108292; PMCID: PMC5316363.

Walker LC, Rosen RF, Levine H 3rd. Diversity of Abeta deposits in the aged brain: a window on molecular heterogeneity? Rom J Morphol Embryol. 2008;49(1):5-11. PMID: 18273496.

Waller AP, George M, Kalyanasundaram A, Kang C, Periasamy M, Hu K, Lacombe VA. GLUT12 functions as a basal and insulin-independent glucose transporter in the heart. Biochim Biophys Acta. 2013 Jan;1832(1):121-7. doi: 10.1016/j.bbadis.2012.09.013. Epub 2012 Oct 4. PMID: 23041416.

Walsh CT, Garneau-Tsodikova S, Gatto GJ Jr. Protein posttranslational modifications: the chemistry of proteome diversifications. Angew Chem Int Ed Engl. 2005 Dec 1;44(45):7342-72. doi: 10.1002/anie.200501023. PMID: 16267872.

Wang G, Zhang X, Lu X, Liu J, Zhang Z, Wei Z, Wu Z, Wang J. Fish oil supplementation attenuates cognitive impairment by inhibiting neuroinflammation in STZ-induced diabetic rats. Aging (Albany NY). 2020 Aug 4;12(15):15281-15289. doi: 10.18632/aging.103426. Epub 2020 Aug 4. PMID: 32756005; PMCID: PMC7467369.

Wang J, Dickson DW, Trojanowski JQ, Lee VM. The levels of soluble versus insoluble brain Abeta distinguish Alzheimer's disease from normal and pathologic aging. Exp Neurol. 1999 Aug;158(2):328-37. doi: 10.1006/exnr.1999.7085. PMID: 10415140.

Wang L, Klionsky DJ, Shen HM. The emerging mechanisms and functions of microautophagy. Nat Rev Mol Cell Biol. 2023 Mar;24(3):186-203. doi: 10.1038/s41580-022-00529-z. Epub 2022 Sep 12. PMID: 36097284.

Wang Q, Xie C. Microglia activation linking amyloid-β drive tau spatial propagation in Alzheimer's disease. Front Neurosci. 2022 Aug 12; 16:951128. doi: 10.3389/fnins.2022.951128. PMID: 36033617; PMCID: PMC9417618.

Wang Q, Yuan J, Yu Z, Lin L, Jiang Y, Cao Z, Zhuang P, Whalen MJ, Song B, Wang XJ, Li X, Lo EH, Xu Y, Wang X. FGF21 Attenuates High-Fat Diet-Induced Cognitive Impairment via Metabolic Regulation and Anti-inflammation of Obese Mice. Mol Neurobiol. 2018 Jun;55(6):4702-4717. doi: 10.1007/s12035-017-0663-7. Epub 2017 Jul 15. PMID: 28712011; PMCID: PMC5971086.

Wang WY, Tan MS, Yu JT, Tan L. Role of pro-inflammatory cytokines released from microglia in Alzheimer's disease. Ann Transl Med. 2015 Jun;3(10):136. doi: 10.3978/j.issn.2305-5839.2015.03.49. PMID: 26207229; PMCID: PMC4486922

Wang Y, Cella M, Mallinson K, Ulrich JD, Young KL, Robinette ML, Gilfillan S, Krishnan GM, Sudhakar S, Zinselmeyer BH, Holtzman DM, Cirrito JR, Colonna M.

TREM2 lipid sensing sustains the microglial response in an Alzheimer's disease model. Cell. 2015 Mar 12;160(6):1061-71. doi: 10.1016/j.cell.2015.01.049. Epub 2015 Feb 26. PMID: 25728668; PMCID: PMC4477963.

Wang YL, Koh WP, Yuan JM, Pan A. Association between liver enzymes and incident type 2 diabetes in Singapore Chinese men and women. BMJ Open Diabetes Res Care. 2016 Sep 19;4(1): e000296. doi: 10.1136/bmjdrc-2016-000296. PMID: 27738514; PMCID: PMC5030569.

Wani A, Al Rihani SB, Sharma A, Weadick B, Govindarajan R, Khan SU, Sharma PR, Dogra A, Nandi U, Reddy CN, Bharate SS, Singh G, Bharate SB, Vishwakarma RA, Kaddoumi A, Kumar A. Crocetin promotes clearance of amyloid-β by inducing autophagy via the STK11/LKB1-mediated AMPK pathway. Autophagy. 2021 Nov;17(11):3813-3832. doi: 10.1080/15548627.2021.1872187. Epub 2021 Jan 19. PMID: 33404280; PMCID: PMC8632093.

Waring SC, Doody RS, Pavlik VN, Massman PJ, Chan W. Survival among patients with dementia from a large multi-ethnic population. Alzheimer Dis Assoc Disord. 2005 Oct-Dec;19(4):178-83. doi: 10.1097/01.wad.0000189033.35579.2d. PMID: 16327343.

Wellington CL, Walker EK, Suarez A, Kwok A, Bissada N, Singaraja R, Yang YZ, Zhang LH, James E, Wilson JE, Francone O, McManus BM, Hayden MR. ABCA1 mRNA and protein distribution patterns predict multiple different roles and levels of regulation. Lab Invest. 2002 Mar;82(3):273-83. doi: 10.1038/labinvest.3780421. PMID: 11896206.

Wen X, Xiao L, Zhong Z, Wang L, Li Z, Pan X, Liu Z. Astaxanthin acts via LRP1 to inhibit inflammation and reverse lipopolysaccharide-induced M1/M2 polarization of microglial cells. Oncotarget. 2017 Sep 3;8(41):69370-69385. doi: 10.18632/oncotarget.20628. PMID: 29050210; PMCID: PMC5642485.

West MJ, Coleman PD, Flood DG, Troncoso JC. Differences in the pattern of hippocampal neuronal loss in normal ageing and Alzheimer's disease. Lancet. 1994 Sep 17;344(8925):769-72. doi: 10.1016/s0140-6736(94)92338-8. PMID: 7916070.

Westerbacka J, Kolak M, Kiviluoto T, Arkkila P, Sirén J, Hamsten A, Fisher RM, Yki-Järvinen H. Genes involved in fatty acid partitioning and binding, lipolysis,

monocyte/macrophage recruitment, and inflammation are overexpressed in the human fatty liver of insulin-resistant subjects. Diabetes. 2007 Nov;56(11):2759-65. doi: 10.2337/db07-0156. Epub 2007 Aug 17. PMID: 17704301.

Westermark P, Wernstedt C, O'Brien TD, Hayden DW, Johnson KH. Islet amyloid in type 2 human diabetes mellitus and adult diabetic cats contains a novel putative polypeptide hormone. Am J Pathol. 1987 Jun;127(3):414-7. PMID: 3296768; PMCID: PMC1899776.

Whitmer RA, Gustafson DR, Barrett-Connor E, Haan MN, Gunderson EP, Yaffe K. Central obesity and increased risk of dementia more than three decades later. Neurology. 2008 Sep 30;71(14):1057-64. doi: 10.1212/01.wnl.0000306313. 89165.ef. Epub 2008 Mar 26. PMID: 18367704

Wildsmith KR, Holley M, Savage JC, Skerrett R, Landreth GE. Evidence for impaired amyloid β clearance in Alzheimer's disease. Alzheimers Res Ther. 2013 Jul 12;5(4):33. doi: 10.1186/alzrt187. PMID: 23849219; PMCID: PMC3978761.

Wilhelm I, Fazakas C, Krizbai IA. In vitro models of the blood-brain barrier. Acta Neurobiol Exp (Wars). 2011;71(1):113-28. PMID: 21499332.

Willard JR, Barrow BM, Zraika S. Improved glycaemia in high-fat-fed neprilysin-deficient mice is associated with reduced DPP-4 activity and increased active GLP-1 levels. Diabetologia. 2017 Apr;60(4):701-708. doi: 10.1007/s00125-016-4172-4. Epub 2016 Dec 8. PMID: 27933334; PMCID: PMC5342915.

Wirths O, Breyhan H, Cynis H, Schilling S, Demuth HU, Bayer TA. Intraneuronal pyroglutamate-Abeta 3-42 triggers neurodegeneration and lethal neurological deficits in a transgenic mouse model. Acta Neuropathol. 2009 Oct;118(4):487-96. doi: 10.1007/s00401-009-0557-5. Epub 2009 Jun 23. PMID: 19547991; PMCID: PMC2737116.

Wisniewski KE, Dalton AJ, McLachlan C, Wen GY, Wisniewski HM. Alzheimer's disease in Down's syndrome: clinicopathologic studies. Neurology. 1985 Jul;35(7):957-61. doi: 10.1212/wnl.35.7.957. PMID: 3159974.

Wolf A, Bauer B, Hartz AM. ABC Transporters and the Alzheimer's Disease Enigma. Front Psychiatry. 2012 Jun 4; 3:54. doi: 10.3389/fpsyt.2012.00054. PMID: 22675311; PMCID: PMC3366330.

Wu D, Chen Q, Chen X, Han F, Chen Z, Wang Y. The blood-brain barrier: structure, regulation, and drug delivery. Signal Transduct Target Ther. 2023 May 25;8(1):217. doi: 10.1038/s41392-023-01481-w. PMID: 37231000; PMCID: PMC10212980

Wullschleger S, Loewith R, Oppliger W, Hall MN. Molecular organization of target of rapamycin complex 2. J Biol Chem. 2005 Sep 2;280(35):30697-704. doi: 10.1074/jbc.M505553200. Epub 2005 Jul 7. PMID: 16002396.

Xie J, Brayne C, Matthews FE; Medical Research Council Cognitive Function and Ageing Study collaborators. Survival times in people with dementia: analysis from population-based cohort study with 14-year follow-up. BMJ. 2008 Feb 2;336(7638):258-62. doi: 10.1136/bmj.39433.616678.25. Epub 2008 Jan 10. PMID: 18187696; PMCID: PMC2223023.

Xu L, Zhu J, Yin W, Ding X. Astaxanthin improves cognitive deficits from oxidative stress, nitric oxide synthase and inflammation through upregulation of PI3K/Akt in diabetes rat. Int J Clin Exp Pathol. 2015 Jun 1;8(6):6083-94. PMID: 26261486; PMCID: PMC4525820.

Xu WL, Qiu CX, Wahlin A, Winblad B, Fratiglioni L. Diabetes mellitus and risk of dementia in the Kungsholmen project: a 6-year follow-up study. Neurology. 2004 Oct 12;63(7):1181-6. doi: 10.1212/01.wnl.0000140291. 86406.d1. PMID: 15477535.

Yamaguchi H, Ishiguro K, Uchida T, Takashima A, Lemere CA, Imahori K. Preferential labeling of Alzheimer neurofibrillary tangles with antisera for tau protein kinase (TPK) I/glycogen synthase kinase-3 beta and cyclin-dependent kinase 5, a component of TPK II. Acta Neuropathol. 1996 Sep;92(3):232-41. doi: 10.1007/s004010050513. PMID: 8870824.

Yamamoto H, Matsui T. Molecular mechanisms of macroautophagy, microautophagy, and chaperone-mediated autophagy. J Nippon Med Sch. 2023 Jun 2. doi: 10.1272/jnms.JNMS.2024_91-102. Epub ahead of print. PMID: 37271546.

Yang BT, Dayeh TA, Volkov PA, Kirkpatrick CL, Malmgren S, Jing X, Renström E, Wollheim CB, Nitert MD, Ling C. Increased DNA methylation and decreased expression of PDX-1 in pancreatic islets from patients with type 2 diabetes. Mol Endocrinol. 2012 Jul;26(7):1203-12. doi: 10.1210/me.2012-1004. Epub 2012 May 8. PMID: 22570331; PMCID: PMC5416998.

Yang T, Guo R, Zhang F. Brain perivascular macrophages: Recent advances and implications in health and diseases. CNS Neurosci Ther. 2019 Dec;25(12):1318-1328. doi: 10.1111/cns.13263. Epub 2019 Nov 20. PMID: 31749316; PMCID: PMC7154594.

Yang Y, Wu Y, Zhang S, Song W. High glucose promotes Aβ production by inhibiting APP degradation. PLoS One. 2013 Jul 23;8(7): e69824. doi: 10.1371/journal.pone.0069824. PMID: 23894546; PMCID: PMC3720941

Ye R, Gordillo R, Shao M, Onodera T, Chen Z, Chen S, Lin X, SoRelle JA, Li X, Tang M, Keller MP, Kuliawat R, Attie AD, Gupta RK, Holland WL, Beutler B, Herz J, Scherer PE. Intracellular lipid metabolism impairs β cell compensation during diet-induced obesity. J Clin Invest. 2018 Mar 1;128(3):1178-1189. doi: 10.1172/JCI97702. Epub 2018 Feb 19. PMID: 29457786; PMCID: PMC5824868.

Yeh CW, Yeh SH, Shie FS, Lai WS, Liu HK, Tzeng TT, Tsay HJ, Shiao YJ. Impaired cognition and cerebral glucose regulation are associated with astrocyte activation in the parenchyma of metabolically stressed APPswe/PS1dE9 mice. Neurobiol Aging. 2015 Nov;36(11):2984-2994. doi: 10.1016/j.neurobiolaging.2015.07.022. Epub 2015 Jul 18. PMID: 26264859.

Yeh FL, Hansen DV, Sheng M. TREM2, Microglia, and Neurodegenerative Diseases. Trends Mol Med. 2017 Jun;23(6):512-533. doi: 10.1016/j.molmed.2017.03.008. Epub 2017 Apr 22. PMID: 28442216.

Yin ZG, Wang QS, Yu K, Wang WW, Lin H, Yang ZH. Sex differences in associations between blood lipids and cerebral small vessel disease. Nutr Metab Cardiovasc Dis. 2018 Jan;28(1):28-34. doi: 10.1016/j.numecd.2017.10.001. Epub 2017 Oct 10. PMID: 29162363.

Yoo J, Jeong IK, Ahn KJ, Chung HY, Hwang YC. Fenofibrate, a PPARα agonist, reduces hepatic fat accumulation through the upregulation of TFEB-mediated lipophagy. Metabolism. 2021 Jul; 120:154798. doi: 10.1016/j.metabol.2021.154798. Epub 2021 May 11. PMID: 33984335.

Yook JS, Okamoto M, Rakwal R, Shibato J, Lee MC, Matsui T, Chang H, Cho JY, Soya H. Astaxanthin supplementation enhances adult hippocampal neurogenesis and spatial memory in mice. Mol Nutr Food Res. 2016 Mar;60(3):589-99. doi: 10.1002/mnfr.201500634. Epub 2016 Jan 7. PMID: 26643409.

You D, Nilsson E, Tenen DE, Lyubetskaya A, Lo JC, Jiang R, Deng J, Dawes BA, Vaag A, Ling C, Rosen ED, Kang S. Dnmt3a is an epigenetic mediator of adipose insulin resistance. Elife. 2017 Nov 1;6: e30766. doi: 10.7554/eLife.30766. PMID: 29091029; PMCID: PMC5730374.

Zandi PP, Carlson MC, Plassman BL, Welsh-Bohmer KA, Mayer LS, Steffens DC, Breitner JC; Cache County Memory Study Investigators. Hormone replacement therapy and incidence of Alzheimer disease in older women: the Cache County Study. JAMA. 2002 Nov 6;288(17):2123-9. doi: 10.1001/jama.288.17.2123. PMID: 12413371.

Zandl-Lang M, Fanaee-Danesh E, Sun Y, Albrecher NM, Gali CC, Čančar I, Kober A, Tam-Amersdorfer C, Stracke A, Storck SM, Saeed A, Stefulj J, Pietrzik CU, Wilson MR, Björkhem I, Panzenboeck U. Regulatory effects of simvastatin and apoJ on APP processing and amyloid-β clearance in blood-brain barrier endothelial cells. Biochim Biophys Acta Mol Cell Biol Lipids. 2018 Jan;1863(1):40-60. doi: 10.1016/j.bbalip.2017.09.008. Epub 2017 Sep 20. PMID: 28941799.

Zenaro E, Piacentino G, Constantin G. The blood-brain barrier in Alzheimer's disease. Neurobiol Dis. 2017 Nov; 107:41-56. doi: 10.1016/j.nbd.2016.07.007. Epub 2016 Jul 15. PMID: 27425887; PMCID: PMC5600438.

Zhang B, Gaiteri C, Bodea LG, Wang Z, McElwee J, Podtelezhnikov AA, Zhang C, Xie T, Tran L, Dobrin R, Fluder E, Clurman B, Melquist S, Narayanan M, Suver C, Shah H, Mahajan M, Gillis T, Mysore J, MacDonald ME, Lamb JR, Bennett DA, Molony C, Stone DJ, Gudnason V, Myers AJ, Schadt EE, Neumann H, Zhu J, Emilsson V. Integrated systems approach identifies genetic nodes and networks in late-onset Alzheimer's disease. Cell. 2013 Apr 25;153(3):707-20. doi: 10.1016/j.cell.2013.03.030. PMID: 23622250; PMCID: PMC3677161.

Zhang B, Wei YZ, Wang GQ, Li DD, Shi JS, Zhang F. Targeting MAPK Pathways by Naringenin Modulates Microglia M1/M2 Polarization in Lipopolysaccharide-Stimulated Cultures. Front Cell Neurosci. 2019 Jan 11;12: 531. doi: 10.3389/fncel.2018.00531. PMID: 30687017; PMCID: PMC6336899.

Zhang HH, Huang J, Düvel K, Boback B, Wu S, Squillace RM, Wu CL, Manning BD. Insulin stimulates adipogenesis through the Akt-TSC2-mTORC1 pathway. PLoS One.

2009 Jul 10;4(7): e6189. doi: 10.1371/journal.pone.0006189. PMID: 19593385; PMCID: PMC2703782.

Zhang M, Li J, Guo X, Wang X, Shi D, Cui L, Zhou Y. Co-administration of berberine/gypenosides/bifendate ameliorates metabolic disturbance but not memory impairment in type 2 diabetic mice. Heliyon. 2021 Jan 22;7(1): e06004. doi: 10.101/ j. heliyon. 2021.e06004. PMID: 33537476; PMCID: PMC7840859.

Zhang Q, Bian G, Chen P, Liu L, Yu C, Liu F, Xue Q, Chung SK, Song B, Ju G, Wang J. Aldose Reductase Regulates Microglia/Macrophages Polarization Through the cAMP Response Element-Binding Protein After Spinal Cord Injury in Mice. Mol Neurobiol. 2016 Jan;53(1):662-676. doi: 10.1007/s12035-014-9035-8. Epub 2014 Dec 19. PMID: 25520004.

Zhang TT, Li W, Meng G, Wang P, Liao W. Strategies for transporting nanoparticles across the blood-brain barrier. Biomater Sci. 2016 Feb;4(2):219-29. doi: 10.1039/c5bm00383k. PMID: 26646694.

Zhang XS, Zhang X, Wu Q, Li W, Wang CX, Xie GB, Zhou XM, Shi JX, Zhou ML. Astaxanthin offers neuroprotection and reduces neuroinflammation in experimental subarachnoid hemorrhage. J Surg Res. 2014 Nov;192(1):206-13. doi: 10.1016/j.jss.2014.05.029. Epub 2014 May 21. PMID: 24948541.

Zhang XS, Zhang X, Wu Q, Li W, Zhang QR, Wang CX, Zhou XM, Li H, Shi JX, Zhou ML. Astaxanthin alleviates early brain injury following subarachnoid hemorrhage in rats: possible involvement of Akt/bad signaling. Mar Drugs. 2014 Jul 28;12(8):4291-310. doi: 10.3390/md12084291. PMID: 25072152; PMCID: PMC4145317.

Zhang Y, Hu W. NFκB signaling regulates embryonic and adult neurogenesis. Front Biol (Beijing). 2012 Aug;7(4):10.1007/s11515-012-1233-z. doi: 10.1007/s11515-012-1233-z. PMID: 24324484; PMCID: PMC3855406.

Zhao WQ, Alkon DL. Role of insulin and insulin receptor in learning and memory. Mol Cell Endocrinol. 2001 May 25;177(1-2):125-34. doi: 10.1016/s0303-7207(01)00455-5. PMID: 11377828.

Zhao Y, Liu Y, Xu Y, Li K, Zhou L, Qiao H, Xu Q, Zhao J. The Role of Ferroptosis in Blood-Brain Barrier Injury. Cell Mol Neurobiol. 2023 Jan;43(1):223-236. doi: 10.1007/s10571-022-01197-5. Epub 2022 Feb 1. PMID: 35106665.

Zhou X, Zhang F, Hu X, Chen J, Wen X, Sun Y, Liu Y, Tang R, Zheng K, Song Y. Inhibition of inflammation by astaxanthin alleviates cognition deficits in diabetic mice. Physiol Behav. 2015 Nov 1; 151:412-20. doi: 10.1016/j.physbeh.2015.08.015. Epub 2015 Aug 10. PMID: 26272354.

Zhu D, Montagne A, Zhao Z. Alzheimer's pathogenic mechanisms and underlying sex difference. Cell Mol Life Sci. 2021 Jun;78(11):4907-4920. doi: 10.1007/s00018-021-03830-w. Epub 2021 Apr 12. PMID: 33844047; PMCID: PMC8720296.

Zhu DY, Lu J, Xu R, Yang JZ, Meng XR, Ou-Yang XN, Yan QY, Nie RF, Zhao T, Chen YD, Lu Y, Zhang YN, Li WJ, Shen X. FX5, a non-steroidal glucocorticoid receptor antagonist, ameliorates diabetic cognitive impairment in mice. Acta Pharmacol Sin. 2022 Oct;43(10):2495-2510. doi: 10.1038/s41401-022-00884-9. Epub 2022 Mar 8. PMID: 35260821; PMCID: PMC9525278.

Zhu Y, Wang X, Zhou X, Ding L, Liu D, Xu H. DNMT1-mediated PPARα methylation aggravates damage of retinal tissues in diabetic retinopathy mice. Biol Res. 2021 Aug 6;54(1):25. doi: 10.1186/s40659-021-00347-1. PMID: 34362460; PMCID: PMC8348846.

Zlokovic BV, Deane R, Sagare AP, Bell RD, Winkler EA. Low-density lipoprotein receptor-related protein-1: a serial clearance homeostatic mechanism controlling Alzheimer's amyloid β-peptide elimination from the brain. J Neurochem. 2010 Dec;115(5):1077-89. doi: 10.1111/j.1471-4159.2010.07002. x. Epub 2010 Oct 5. PMID: 20854368; PMCID: PMC2972355.

Zlokovic BV. Neurodegeneration and the neurovascular unit. Nat Med. 2010 Dec;16(12):1370-1. doi: 10.1038/nm1210-1370. PMID: 21135839.

Zlokovic BV. Neurovascular mechanisms of Alzheimer's neurodegeneration. Trends Neurosci. 2005 Apr;28(4):202-8. doi: 10.1016/j.tins.2005.02.001. PMID: 15808355.

Zlokovic BV. The blood-brain barrier in health and chronic neurodegenerative disorders. Neuron. 2008 Jan 24;57(2):178-201. doi: 10.1016/j.neuron.2008.01.003. PMID: 18215617.